11-14-2013

Improved Dynamic Headspace Sampling and Detection using Capillary Microextraction of Volatiles Coupled to Gas Chromatography Mass Spectrometry

Wen Fan
wfan001@fiu.edu

FLORIDA INTERNATIONAL UNIVERSITY

Miami, Florida

IMPROVED DYNAMIC HEADSPACE SAMPLING AND DETECTION USING CAPILLARY MICROEXTRACTION OF VOLATILES COUPLED TO GAS CHROMATOGRAPHY MASS SPECTROMETRY

A dissertation submitted in partial fulfillment of

the requirements for the degree of

DOCTOR OF PHILOSOPHY

in

CHEMISTRY

by

Wen Fan

2013

To: Dean Kenneth G. Furton
College of Arts and Sciences

This dissertation, written by Wen Fan, and entitled Improved Dynamic Headspace Sampling and Detection using Capillary Microextraction of Volatiles Coupled to Gas Chromatography Mass Spectrometry, having been approved in respect to style and intellectual content, is referred to you for judgment.

We have read this dissertation and recommend that it be approved.

_____
William Anderson

_____
Yong Cai

_____
Piero Gardinali

_____
Jeffrey Joens

_____
José Almirall, Major Professor

Date of Defense: November 14, 2013

The dissertation of Wen Fan is approved.

_____
Dean Kenneth G. Furton
College of Arts and Sciences

_____
Dean Lakshmi N. Reddi
University Graduate School

Florida International University, 2013

DEDICATION

I would like to dedicate this dissertation to my parents, Linye Fan and Jing Tao, who love me unconditionally.

ACKNOWLEDGMENTS

First, I would like to express my deepest appreciation to my major professor, Dr. José Almirall for providing me the opportunity to work on such an amazing project. His strong work ethic always inspires me to learn more and work harder and his endless support guided me through the barriers in this project

I would like to thank all my committee members as well for taking their valuable time to provide insightful contributions to this project. Dr. William Anderson, Dr. Yong Cai, Dr. Piero Gardinali, and Dr. Jeffrey Joens guided me to see different perspectives of the project and challenged me to my best with their expertise.

I also want to thank Mimy Young, my closest friend in Miami who showed me what a true friend means. Without her presence, my time in Miami would be less entertaining.

I want to express my appreciation to Dr. Eiceman and Dr. Oxley for being so kind to allow me conducting experiments and learning new knowledge in their laboratories. Their students were really appreciated for all their help in the experiment setup and sample preparation. Dr. Mathee, Dr. Furton and their students were also greatly appreciated for providing the samples need for the experiments

I would like to show my appreciation to Matthew Staymates from NIST, and Shane Addleman from PNNL for their help in visualizing the flow of CMV and determining the surface area of PSPME. I also want to thank Armando from the Chemistry Department scientific receiving for letting me use the area to conduct my experiments as well as the local shipping facility for letting me using their facility for headspace sampling.

I would like to acknowledge the FIU University Graduate School for awarding me both the Presidential Fellowship and the Dissertation Evidence Acquisition Fellowship. I also

would like to thank Journal of Analytical and Bioanalytical Chemistry for permitting the re-use the contents in my publications for this dissertation.

I want to say a big thank you to all the past and present A-Team members for their friendship and professionalism. The time we spent together will always be a part of the beautiful memory. In particular, I want to show my appreciation to Howard Holness for all the help he has provided no matter if it is technical difficulties encountered or general chemistry questions. He is always willing to help without any complaints.

Finally, I would like to thank all my family and friends. Without your support and love, I wouldn't have made it this far.

ABSTRACT OF THE DISSERTATION

IMPROVED DYNAMIC HEADSPACE SAMPLING AND DETECTION USING CAPILLARY MICROEXTRACTION OF VOLATILES COUPLED TO GAS CHROMATOGRAPHY MASS SPECTROMETRY

by

Wen Fan

Florida International University, 2013

Miami, Florida

Professor José Almirall, Major Professor

Sampling and preconcentration techniques play a critical role in headspace analysis in analytical chemistry. My dissertation presents a novel sampling design, capillary microextraction of volatiles (CMV), that improves the preconcentration of volatiles and semivolatiles in a headspace with high throughput, near quantitative analysis, high recovery and unambiguous identification of compounds when coupled to mass spectrometry. The CMV devices use sol-gel polydimethylsiloxane (PDMS) coated microglass fibers as the sampling/preconcentration sorbent when these fibers are stacked into open-ended capillary tubes. The design allows for dynamic headspace sampling by connecting the device to a hand-held vacuum pump. The inexpensive device can be fitted into a thermal desorption probe for thermal desorption of the extracted volatile compounds into a gas chromatography-mass spectrometer (GC-MS). The performance of the CMV devices was compared with two other existing preconcentration techniques, solid phase microextraction (SPME) and planar solid phase microextraction (PSPME). Compared to SPME fibers, the CMV devices have an improved surface area and phase

volume of 5000 times and 80 times, respectively. One (1) minute dynamic CMV air sampling resulted in similar performance as a 30 min static extraction using a SPME fiber. The PSPME devices have been fashioned to easily interface with ion mobility spectrometers (IMS) for explosives or drugs detection. The CMV devices are shown to offer dynamic sampling and can now be coupled to COTS GC-MS instruments. Several compound classes representing explosives have been analyzed with minimum breakthrough even after a 60 min. sampling time. The extracted volatile compounds were retained in the CMV devices when preserved in aluminum foils after sampling. Finally, the CMV sampling device were used for several different headspace profiling applications which involved sampling a shipping facility, six illicit drugs, seven military explosives and eighteen different bacteria strains. Successful detection of the target analytes at ng levels of the target signature volatile compounds in these applications suggests that the CMV devices can provide high throughput qualitative and quantitative analysis with high recovery and unambiguous identification of analytes.

TABLE OF CONTENTS

CHAPTER PAGE

Chapter 1 Introduction to the Problem....1
1.1 Project Motivation and Significance....1
1.2 Current Challenges....2
1.3 Research hypothesis and Project Goals....3
1.3.1 Hypothesis....3
1.3.2 Project Goals....3

Chapter 2 Introduction to Explosives....5
2.1 History of Explosives....5
2.2 Classification of explosives....5
2.2.1 Military explosives....7
2.2.2 Improvised explosives....7
2.2.2.1 Smokeless powder....8
2.2.2.2 Peroxide explosives....12
2.2.2.3 Terrorist attacks....13
2.3 Detection of explosives....15
2.3.1 Bulk Detection....16
2.3.2 Trace Detection....17
2.3.2.1 Chemical Signatures....17
2.3.2.2 Sampling of Trace Amount of Explosives....18
2.3.2.3 Detection with Trace Detectors....18

Chapter 3 Instrumentation Background....20
3.1 Gas Chromatography – Mass Spectrometry (GC-MS)....20
3.1.1 Sample Introduction....21
3.1.1.1 Headspace Samplers....22
3.1.1.2 Thermal Desorption Devices....23
3.1.2 Types of Detectors....24
3.1.2.1 Mass Spectrometers....24
3.2 Ion Mobility Spectrometry (IMS)....25
3.2.1 Radioactive Ionization Sources....26
3.2.2 Gas-phase Ions (^{63}Ni Source)....28
3.2.2.1 Formation of Reactant Ions....28
3.2.2.2 Formations of Product Ions....29
3.2.3 Drift Tube Design....30
3.2.3.1 Single drift tube....30
3.2.3.2 Dual drift tubes....33
3.2.4 Detection and Chemical Identification....34
3.2.4.1 Reduced Mobility Coefficient (K_0)....34
3.2.4.2 Standard Compounds....36
3.2.5 Applications....36

Chapter 4 Evolution of headspace analysis 38
4.1 Gas-tight syringe direct injection 40
4.2 Purge and Trap 41
4.3 Solid Phase Microextraction (SPME) 43
4.3.1 Principles 44
4.3.2 Coatings 44
4.3.3 Dynamic headspace analysis 45
4.3.4 Coupling to Ion Mobility Spectrometers 48
4.3.5 Summary 49
4.4 PSPME 50
4.4.1 PSPME Preparation 50
4.4.2 Fabrication of PSPME 51
4.4.3 Static Sampling 52
4.4.4 Dynamic Sampling 53

Chapter 5 Headspace Analysis of Smokeless Powders Using SPME-GC-MS and PSPME-IMS 54
5.1 SPME-GC-MS Performance Evaluation using Smokeless Powders 54
5.1.1 Instrumentation 54
5.1.2 Materials 55
5.1.3 Methods 56
5.1.4 Results 57
5.1.4.1 Extraction Profiles for Four Different Scenarios 57
5.1.4.2 Extraction from plastic boxes 62
5.1.4.3 Extraction for cardboard boxes 64
5.1.5 Summary 65
5.2 Headspace Profile of Twenty-four Different Smokeless Powders 65
5.2.1 Instrumentation 66
5.2.2 Materials 66
5.2.3 Methods 68
5.2.4 Results 69
5.2.5 Summary 72

Chapter 6 Headspace Analysis of Peroxide Explosives using SPME-GC-MS and PSPME-IMS 74
6.1 Instrumentation 74
6.2 Chemicals 76
6.3 Methods 77
6.4 Results 80
6.4.1 Surface Area Analysis for PSPME devices 80
6.4.2 Detection of Solid TATP 82
6.4.3 Detection of Standard Solutions of TATP 85
6.4.4 Absolute mass calibration of TATP in PSPME filters 87
6.4.5 Headspace extraction recovery comparison of PSPME and SPME 88
6.4.6 Field Sampling of TATP 90

6.4.7 Detection of HMTD 93
6.5 Summary 95

Chapter 7 Double Blind Study to Evaluate the Performance of PSPME-IMS 97
7.1 Instrumentation.... 97
7.2 Materials.... 97
7.3 Methods.... 99
7.4 Results 100
7.5 Summary 104

Chapter 8 Invention of Capillary Microextraction of Volatiles (CMV) Devices 105
8.1 Preparation of Capillary Microectraction of Volatiles (CMV) Devices 105
8.2 Theory of CMV 107
8.3 Method Development to Couple CMV to GC-MS 110
8.3.1 Instrumentation....110
8.3.2 Materials....113
8.3.3 Methods....113
8.4 Results 115
8.4.1 Method Optimization....115
8.4.1.1 Split vs. Splitless.... 116
8.4.1.2 Injection Port Temperature 117
8.4.1.3 Regular Split/Splitless Injection Port vs. Multi-Mode Inlet 118
8.4.2 Calibration Curves Generated by Spiking Standard Solutions on CMV Devices 120
8.4.3 Dynamic Headspace Sampling Method Development....121
8.4.3.1 Equilibrium Study.... 121
8.4.3.2 Flow Rate.... 122
8.4.3.3 Preconcentration Material Comparison 123
8.4.3.4 Recovery in the Headspace.... 126
8.4.3.5 Retention Capability of CMV.... 128
8.4.3.6 Extended Sampling Time.... 131
8.4.4 SPME vs. CMV....134
8.4.5 Open System vs. Closed System 136
8.5 Summary 139

Chapter 9 CMV-GC-MS Forensic Applications....141
9.1 Detection of Smokeless Powders 141
9.2 Headspace Analysis in a Shipping Facility 142
9.2.1 Introduction of Sampling in Shipping Facility....142
9.2.2 Materials and Methods 143
9.2.3 Results 144
9.3 Headspace Analysis of Military Explosives.... 146
9.3.1 Introduction of Military Explosives 146
9.3.1.1 NG, EGDN and ETN 147
9.3.1.2 PETN.... 147
9.3.1.3 RDX and HMX.... 148

9.3.1.4 TNT 148
9.3.1.5 Plastic explosives 150
9.3.2 Materials and Methods 151
9.3.3 Results 152
9.3.3.1 NG, EGDN and ETN 152
9.3.3.2 PETN and RDX 157
9.3.3.3 TNT and C4 Wrappers 158
9.4 Headspace Analysis of Illicit Drugs using CMV-GC-MS 160
9.4.1 Introduction of Illicit Drugs 160
9.4.1.1 Cocaine-Base and Cocaine-HCl 161
9.4.1.2 Methamphetamine and MDMA 163
9.4.1.3 Heroin 165
9.4.1.4 Marijuana 165
9.4.2 Materials and Methods 167
9.4.3 Results 167
9.4.3.1 Cocaine-Base 168
9.4.3.2 Cocaine-HCl 169
9.4.3.3 Methamphetamine 170
9.4.3.4 MDMA 172
9.4.3.5 Heroin 173
9.4.3.6 Marijuana 174
9.5 Summary 176

Chapter 10 CMV-GC-MS Biomedical Application 178
10.1 Introduction of *Pseudomonas aeruginosa* (*P. aeruginosa*) 178
10.2 Materials and Methods 180
10.3 Results 183
10.3.1 Identification of Volatile Compounds in the Headspace of P. aeruginosa 183
10.3.2 Blind Study to Differentiate Pseudomonas from Other Bacteria 186
10.4 Summary 189

Chapter 11 Conclusions 190
11.1 SPME-GC-MS 190
11.2 PSPME-IMS 190
11.3 CMV-GC-MS 192
11.4 Future Directions 194

List of References 196

Appendices 206

VITA 210

LIST OF TABLES

TABLE PAGE

Table 2-1 Structures and vapor pressures of TATP and HMTD 8

Table 2-2 Representative compositions for smokeless powders [31].....10

Table 2-3 List of well-known world-wide explosive attacks.....15

Table 3-1 Summary of ionization techniques used in ion mobility spectrometry [67] 27

Table 4-1 List of major development of headspace analysis.....38

Table 4-2 Commercially available SPME fibers for different applications [82,33].....45

Table 5-1 GC-MS conditions used for SPME sampling over the headspace of smokeless powders.....54

Table 5-2 Four different containers were used in the study to represent four different real life scenarios.....56

Table 5-3 Extraction profile for All Unique Smokeless Powder.....60

Table 5-4 Extraction profile for IMR 4198 Smokeless Powder 61

Table 5-5 Extraction Profile for Red Dot Smokeless Powder 61

Table 5-6 Optimized extraction time and sample amount for SPME GC-MS 61

Table 5-7 IMS conditions used for sampling larger containers and profiling twenty-four different smokeless powders 66

Table 5-8 Twenty-four different smokeless powders' headspace were profiled using PSPME-IMS 67

Table 6-1 Conditions for the IMS instruments used as detectors for both SPME and PSPME sampling/preconcentration 75

Table 6-2 GC-MS conditions for SPME headspace mass quantitation 76

Table 6-3 Percent recovery comparison of PSPME and SPME by 5 minutes static extraction of different amount of TATP 90

Table 6-4 Field sampling of TATP with varied distance and varied extraction times 92

Table 7-1 One hundred solutions prepared for double blind study 97

Table 7-2 Double blind study results for 2,4-DNT, NG, DPA, TATP and EC 103

Table 8-1 Surface area and phase volume comparison among SPME, PSPME and CMV 107

Table 8-2 GC-MS conditions for smokeless powder headspace analysis using CMV and SPME 112

Table 8-3 Recovery calculated for dynamic sampling using standard mixtures 127

Table 8-4 Recovered mass (as %) of NG, DNT and DPA after a 1 min. dynamic extraction using CMV devices and compared with 30 min. and 10 min. static extractions using SPME fibers.....135

Table 9-1 Compounds detected in the shipping facility from 30 samples taken 145

Table 9-2 Structures and vapor pressures of military explosives [94,95].....146

Table 9-3 Structure of cocaine, methamphetamine and MDMA and their signature volatile compounds in the headspace.....161

Table 9-4 Headspace volatiles detected in the headspace of MDMA [101].....164

Table 9-5 Headspace compounds detected in heroin and pseudo heroin samples [101].....165

Table 9-6 Comparison of the composition of headspace vapors of Marijuana with the composition of essential oil of Marijuana [103] 166

Table 9-7 Volatile compounds detected in the headspace of cocaine-base 168

Table 9-8 Compounds detected in the headspace of Cocaine-HCl.....170

Table 9-9 Volatile compounds detected in the headspace of methamphetamine 171

Table 9-10 Volatile compounds detected in the headspace of MDMA tablets 173

Table 9-11 Volatile compounds detected in the headspace of Heroin.....173

Table 9-12 Volatile compounds in the headspace of Marijuana.....176

Table 9-13 Potential biomarkers for *Pseudomonas aeruginosa* 179

Table 9-14 Bacteria strains used in headspace analysis of *Pseudomonas aeruginosa* 180

Table 9-15 Volatile compounds detected in the headspace of different cultural plates right after the plates were obtained.....187

Table 9-16 Volatile compounds detected in the headspace of different cultural plates after 24 hours 187

Table 9-17 Volatile compounds detected in the headspace of 13 different bacteria with triplicates.....188

LIST OF FIGURES

FIGURES PAGE

Figure 2-1 DPA functions as a stabilizer in smokeless powders to convert the energetic gases into stable compounds: (1) DPA, (2) *N*-nitroso-diphenylamine (*N*-NODPA), (3) 2-nitrodiphenylamine (2-NDPA), (4) 4-nitroso-diphenylamine (4-NODPA), (5) 4-nitrodiphenylamine (4-NDPA), (6) *N*-nitroso-2-nitrodiphenylamine (*N*-NO-2-NDPA, (7) 2,4-dinitrodephenylamine (2,4-NDPA), (8) 2,4'-dinitrodephenylamine (2,4'-NDPA) [37] 11

Figure 3-1 Schematic diagram of a typical gas chromatography system 21

Figure 3-2 A commercially available thermal desorption device that can be coupled to a GC-MS 23

Figure 3-3 Flow diagram in a thermal desorption device in split mode [66] 24

Figure 3-4 Schematic diagram of an IMS 26

Figure 3-5 Reagent gases can be introduced: (A) directly into the ionization region, (B) into the carrier gas stream, (C) throughout the entire drift tube. [67] 31

Figure 4-1 Principles of static headspace – gas chromatography. (A) Equilibration and (B) sample transfer. CG = carrier gas, SV = sample vial, TH = thermostat, COL = GC column, D=detector [64] 40

Figure 4-2 Schematic diagram of a dynamic headspace system, purge and trap [29] 41

Figure 4-3 Commercial SPME device. (a) SPME fiber holder; (b) section view of SPME holder and fiber assembly [81] 43

Figure 4-4 The stainless steel hollow needle with a piece of GC capillary column (A) and carbon coating (B) used in the INCAT device [73] 46

Figure 4-5 Diagram of dynamic sampling using the INCAT device [73] 47

Figure 4-6 Schematic diagram of the SPME device (a) and the SPDE device (b) [83] 48

Figure 4-7 Schematic diagram of the SPME-IMS interface [71] 49

Figure 4-8 Three different sizes dynamic PSPME devices (a) that can be fabricated into different shapes (b) and combined with a holder (c) to be used in a dynamic sampler (d) for thermal desorption into a commercial IMS system (e) 52

Figure 5-1 Chromatograph comparison of PDMS (Red) and PDMS/DVB (Green) SPME fibers on All Unique smokeless powder extraction....58

Figure 5-2 Calibration curves of (a) NG, (b) 2,4-DNT and (c) DPA in GC-MS. All calibration standards were prepared in ACN. The limits of detection were 3.0 ng for NG, 2.4 ng for 2,4-DNT and 9.9 ng for DPA....58

Figure 5-3 Background comparison between gallon cans (blue) and plastic boxes (red)....63

Figure 5-4 Black dotted line marked interference in the plastic boxes (red) compared to 2,4-DNT detection from 2 h extraction of 500 mg of IMR 4198 (blue)....63

Figure 5-5 Detection of 1 g of smokeless powder in cardboard boxes....64

Figure 5-6 Morphology of twenty-four different smokeless powders....68

Figure 5-7 Smokeless powders headspace profiling using PSPME and quart cans....69

Figure 5-8 Volatile compounds distribution in twenty-four smokeless powders....69

Figure 5-9 Headspace profile of twenty-four smokeless powders using PSPME static extractions....71

Figure 5-10 Headspace profile of twenty-four smokeless powders using PSPME static extractions....72

Figure 6-1 Three different commercial IMS systems (a) GE IonTrack (b) Smiths Detection IONSCAN (c) Morpho Detection Hardened MobileTrace....75

Figure 6-2 PSPME were placed inside a cardboard box at different distances from the TATP source....80

Figure 6-3 Microscope images of the surface and cross-section of an uncoated glass filter, (a) and (b) respectively, and images of the surface and cross-section of a coated PSPME devices, (c) and (d) respectively....82

Figure 6-4 Signal observed at 4.3 ms at different static extraction times of 10 mg of TATP at different temperature profiles....83

Figure 6-5 IMS plasmagram of static PSPME TATP extractions performed at 20 °C with varying extraction times (10 s – 2 min). Confirmation of TATP was performed by manually spiking 1000 ng μL^{-1} unto the PSPME device followed by detection via IMS....84

Figure 6-6 Detection for TATP was achieved within 10 seconds of static extractions at 40 °C....84

Figure 6-7 Dynamic extractions using the PSPME devices produced greater IMS signals with only 5 s extraxtion time 85

Figure 6-8 3D Plasmagram and 2D Plasmagram show detection of TATP in the Smiths IMS where reactant ion peak (RIP) was consumed during the ionization.....86

Figure 6-9 TATP calibration by spiking 2 μL TATP of the following concentrations: 0.5, 1.0, 1.5, 2.0, 2.5, 3.0, 5.0 ng μL^{-1} onto a PSPME device detected at 6.7 ms.....86

Figure 6-10 TATP headspace calibration obtained from 5 minute static PSPME headspace extraction of TATP (spiking 5 μL of solutions of the following concentrations: 5, 10, 15, 20, 25, 30 ng μL^{-1}).....88

Figure 6-11 Percent recovery comparison of PSPME and SPME by different static extraction time (0.5 – 30 minutes) of 100 ng TATP.....89

Figure 6-12 Field sampling of TATP in a cardboard box with 5 PSPME devices placed at different distances from the TATP solid explosives. All the devices showed detection of TATP which were preconcentrated from the headspace. 91

Figure 6-13 TATP detection in different extraction time at a distance of 10 inches from the explosive source 92

Figure 6-14 TATP detection with only 30 s dynamic extraction over the headspace of the cardboard box 93

Figure 6-15 SPME extraction of HMTD and the following detection in GE Itemizer 2 in (a) negative mode and (b) positive mode.....94

Figure 6-16 PSPME extraction of HMTD and the following detection in portable IMS Hardened MobileTrace 94

Figure 7-1 3D plasmagram of headspace analysis of 3 ppm TATP in 1-butanol showed no detection of TATP because of the competitive ionization from 1-butanol ...101

Figure 7-2 3D plasmagram of headspace analysis of 56 ppm 2,4-DNT in 1-butanol and showed detection of 2,4-DNT 101

Figure 8-1 (a) The picture has shown the dimension of a CMV device. The inner diameter is ~2 mm and the glass tube is about 2 cm long and packed with sol-gel coated glass filters. (b) An enlarged image of one end of the CMV device. 106

Figure 8-2 CMV device was connected to the hand-held dynamic sampling pump 106

Figure 8-3 Pluming diagram for the two-way splitter with makeup gas [91].....111

Figure 8-4 Flow ratio of the MSD to the μ-ECD is controlled by using restrictors [91] 112

Figure 8-5 (a) Sampling in a closed system with only 1 small opening where CMV is placed above opening without any movement (b) Sampling in a closed system with two small openings where CMV is placed above one of the openings without any movement; (c) Sampling by moving the tip of the hose in a circular motion over the area of the open area. 115

Figure 8-6 Split and splitless mode comparison in GC-MS using blank CMV devices 116

Figure 8-7 Split and splitless mode comparison in GC-MS using CMV devices sampling over the headspace of 10 mg of IMR 4198 117

Figure 8-8 Optimized injection port temperature was set at 180 °C for efficient thermal desorption without thermal decomposition 118

Figure 8-9 Three points calibration for NG, DNT and DPA using a multi-mode inlet 119

Figure 8-10 Three points calibration for NG, DNT and DPA using a regular split/splitless inlet 120

Figure 8-11 GC-MS Chromatograph of direct spike of a 1 μL of standard solution mixture 120

Figure 8-12 Calibration curves of (a) NG (b) 2,4-DNT (c) DPA (d) EC by directly spiking standard solution mixtures on CMV devices 121

Figure 8-13 Equilibrium time study in a quart can using standard solution mixtures 122

Figure 8-14 Extracted amount of DPA was higher at a lower flow rate with various extraction times in a large container (cardboard box) 123

Figure 8-15 Different preconcentration materials comparison using standard solution mixtures 124

Figure 8-16 GC-MS Chromatograph comparison of (a) DPA and (b) NG between PSPME and uncoated glass filters packed in capillary tubes 124

Figure 8-17 PDMS and PDMS/DVB coating comparison in CMV devices when doing (a) direct spike and (b) dynamic headspace analysis of NG 126

Figure 8-18 Dynamic headspace extraction curves for (a) NG (b) 2,4-DNT (c) DPA using CMV devices 127

Figure 8-19 CMV blank after sealing the device in parafilm which showed strong background....129

Figure 8-20 After dynamic sampling 10 mg of All Unique smokeless powders, NG and DPA was retained after sealed in parafilm....129

Figure 8-21 Blank CMV device after sealed in aluminum foil 130

Figure 8-22 2,4-DNT and DPA were retained in the CMV device after 67 hours sealed in aluminum foil....131

Figure 8-23 After 67 hours, about 70 % of (a) 2,4-DNT and (b) DPA were still remaining in the CMV devices 131

Figure 8-24 Dynamic sampling of the headspace of 500 ng, 800 ng, and 1500 ng of NG with various extraction times 132

Figure 8-25 Extended dynamic headspace extraction suggesting quantitative results. (a) NG (b) 2, 4-DNT (c) DPA....133

Figure 8-26 Two CMV devices were connected back to back to evaluate the preconcentration efficiency....134

Figure 8-27 Calibration curves generated for NG (a), 2, 4-DNT (c) and DPA (e) by using both CMV (red square) and GC autosampler (blue triangle). Headspace extractions with 1 min dynamic sampling time using CMV device (red square) and 30 min static sampling time using SPME fiber (blue triangle) show comparable quantitative analysis results. (b) NG (d) 2,4-DNT (f) DPA....136

Figure 8-28 Flow visualization setup (a, b, and c) and results (d, e, and f) of dynamic sampling of CMV devices over the headspace of a container. (a and d) one hole on the lid, (b and e) two holes on the lid, (c and f) open system....138

Figure 8-29 Dynamic headspace sampling using CMV with (a) an open system and (b) a semi-closed system....138

Figure 9-1 Detection of NG and DPA in a cardboard box with only one minute dynamic extraction time....142

Figure 9-2 Different scenarios in the shipping facility (a) an empty LD8 container (b) a fully packed LD3 container (c) a heavy taped cardboard box (d) a half packed LD8 container (e) a fully loaded LD8 container ready for shipping (f) a cardboard box with clear wrap (g) a red plastic bag (h) a regular cardboard box (i) a wood box....144

Figure 9-3 Vapor signature of 1966 military-grade TNT as determined by GC-ECD [97]....149

Figure 9-4 Military explosives sampling using dynamic CMV devices (a) NG in a plastic bottle in a 3 quart plastic container (b) ETN on a watch glass in a 3 quart plastic container (c) TNT wrappers sealed in a Ziploc bag (d) C4 wrappers sealed in a Ziploc bag....152

Figure 9-5 Chromatogram of GC-MS after thermally desorbing a CMV device that was used to sample the headspace of NG for 1 min....153

Figure 9-6 Chromatogram of GC-ECD for 1 min dynamic sampling of the headspace of NG with a CMV device....154

Figure 9-7 Nitroglycerin mass spectrum obtained from the headspace of NG (up) compared to the mass spectrum in the library (down)....154

Figure 9-8 1,3-propanediol, dinitrate mass spectrum obtained from the headspace of NG (up) compared to the mass spectrum in the library (down)....155

Figure 9-9 GC-MS Chromatogram of EGDN headspace after 1 min dynamic sampling....156

Figure 9-10 GC-MS Chromatogram of ETN after 3 min dynamic extraction using a CMV device....157

Figure 9-11 Chromatogram of 1 min dynamic headspace of TNT wrappers using GC-MS....158

Figure 9-12 Detection of 2,4-DNT in TNT wrappers in GC-μECD after 1 min dynamic headspace sampling using a CMV device....159

Figure 9-13 Chromatogram of 1 min dynamic headspace of C4 wrappers using GC-MS....159

Figure 9-14 Detection of DMNB and RDX in GC-μECD after 1 min dynamic headspace sampling using a CMV device....160

Figure 9-15 Two different SPME fibers were compared for 90 min sampling the headspace of 50 g of Coc-HCl followed by detection in GC-MS [100]....162

Figure 9-16 Different synthesis pathways of MDMA [19]....164

Figure 9-17 GC-MS Chromatogram of 3 g of Cocaine-Base sampled by a CMV device for 3 min in a quart can....169

Figure 9-18 GC-MS Chromatogram of 3 min dynamic headspace sampling of 3 g of Cocaine-HCl in a quart can....170

Figure 9-19 GC-MS Chromatogram of 3 min dynamic headspace sampling of 25 g Methamphetamine using a CMV device.....171

Figure 9-20 GC-MS Chromatogram of 3 min dynamic headspace sampling of 3 g of MDMA in a quart can.....172

Figure 9-21 GC-MS Chromatogram of open air sampling of Heroin headspace for 1 min using a CMV device.....174

Figure 9-22 GC-MS Chromatogram of 25 g of Marijuana in a quart can sampled with a CMV device for 3 min.....175

Figure 9-23 The pictures show the three different bacteria used in the study (a) *Pseudomonas aerugenosa*, (b) *Chromobacterium violaceum*, and (c) *Escherichia coli*. Two different methods were used for dynamic sampling with a CMV device over the headspace of (d) a solid LB agar plate, (f) liquid LB medium in a test tube, and (g) liquid Saline medium in a container.....183

Figure 9-24 1 min dynamic sampling of LB plate, DH5α, PA, CV cultural plate using a CMV device showed detection of Undecene and 2-AA only in the headspace of PA.....184

Figure 9-25 Detection of Limonene in PA and CV plate in the second day sampling....184

Figure 9-26 1 min dynamic headspace sampling of LB, DH5α, PA, CV and Saline in the liquid cultural solutions in a test tube showed less intensity in headspace volatiles.....185

Figure 9-27 Calibration curve for 2-AA.....186

ABBREVIATIONS AND ACRONYMS

2,4-Dinitrotoluene	2,4-DNT
2-Aminoacetophenone	2-AA
Autosampler	ALS
Alliant Unique smokeless powder	AU
Chromobacterium violaceum	*C. violaceum*
Cystic Fibrosis	CF
Capillary Microextraction of Volatiles	CMV
Commercial off-the-shelf	COTS
Diacetone Diperoxide	DADP
Dichloromethane	DCM
2,3-Dimethyl-2,3-dinitrobutane	DMNB
Diphenylamine	DPA
Divinylbenzene	DVB
Escherichia coli	*E. coli*
Ethyl centralite	EC
Electron Capture Detector	ECD
Ethylene glycol dinitrate	EDGN
Erythritol tetranitrate	ETN
Florida International University	FIU
Gas chromatography	GC
Hexamethylene triperoxide diamine	HMTD

IMR Powder Co. 4198	IMR 4198
Ion mobility spectrometry	IMS
Luria-Bertani	LB
Load device	LD
Methyl Centralite	MC
3,4-Methylenedioxy-N-methylamphetamine	MDMA
1-(3,4-methylenedioxyphenyl)-2-propanone	MD-P2P
Multi-mode Inlet	MMI
Mass spectrometry	MS
Methyltrimethoxysiloxane	MTMOS
Nitroglycerin	NG
National Institute of Standards and Technology	NIST
Pseudomonas aeruginosa	*P. aeruginosa*
Polydimethylsiloxane	PDMS
Pentaerythritol tetranitrate	PETN
Poly(methylhydrosiloxane)	PMHS
Pacific Northwest National Laboratory	PNNL
Planar solid phase microextraction	PSPME
Red Dot smokeless powder	RD
1,3,5-Trinitro-1,3,5-triazacyclohexane	RDX
Solid phase microextraction	SPME
Triacetone triperoxide	TATP

Trifluoroacetic acid	TFA
2,4,6-Trinitrotoluene	TNT
Volatile inorganic compound	VIC
Vinyl-terminated polydimethylsiloxane	vt-PDMS
Volatile organic compound	VOC

Chapter 1 Introduction to the Problem

1.1 Project Motivation and Significance

Odors, also known as scents, are a composition of one or more volatile organic compounds (VOCs) and volatile inorganic compounds (VICs) that can stimulate the olfactory cells in humans and/or other animals [1]. Among odors, volatile organic compounds (VOCs) are those in the gas phase emitted from certain solids and/or liquids [1] which have unique headspace profiles. Thus, analysis of those headspace profiles can be used to identify the origin of the odor and the cause of its emission. In the past decades, headspace analysis has been widely applied in various fields which include environmental monitoring [2-4], food analysis [5-7], biomedical analysis [8-10], and forensic analysis [2,11,12]. Tracing odors has been applied in various forensic applications, not only with the use of cadaver canines in guiding to a missing person or body [13-15] and detection canines for alarms of illicit substances [16,17], but also with extremely sensitive instruments where sources of illicit or toxic substances can be identified [18,19] from trace amounts of VOCs in the headspace. Biomedical analysis has shown that the most accurate diagnostic is performed using an invasive technique where a small tissue sample or fluid sample is obtained from a patient; however, some of the lung diseases can be diagnosed through breath analysis with a non-invasive technique that could significantly reduce the cost of patient treatment while maintaining the accuracy requisite for medical research [20,21]. Consequently, there are special needs in this research area with practical applications to develop an efficient and accurate method for headspace analysis where quantitation can be achieved with high sensitivity in a short period of time.

1.2 Current Challenges

The current challenges of headspace analysis are associated with two main aspects of the approach. First, there are not enough compounds present over the headspace for analysis, in which some cases involve compounds that are semi-volatile to non-volatile which are rarely observed in the headspace and other cases volatile compounds are found in small concentrations in the headspace because of the large headspace volume and/or limited volatile sources. Thus, the compounds in the headspace need to be preconcentrated onto a matrix material before introduction into an instrument to improve sensitivity. Second, because of the complexity in the gas phase (ranging from polar compounds to non-polar compounds), many challenges are perceived in the preconcentration and identification of all the compounds in the headspace over a certain matrix. So far, many preconcentration devices [22,23] have been developed to overcome the first challenge in headspace analysis and coupling the sampling devices to a gas chromatography – mass spectrometer (GC-MS) can help with the second challenge; however, restricted by the GC-MS injection port, the devices are limited in their shape, and therefore, surface area and phase volume. In the past few years, a novel preconcentration device was developed in the Almirall research group, planar solid phase microextraction (PSPME) [24,25], to achieve a larger surface area and phase volume [26], thus increasing the sampling throughput. A planar solid phase microextraction (PSPME) device has enlarged surface area and phase volume compared to the solid phase microextraction (SPME) fiber resulted from the well-designed, but flexible geometry configuration. The devices are used for dynamic sampling by allowing air flow through the device to assist larger volume analysis [24] which have been shown to provide faster preconcentration with improved recovery [26].

The only disadvantage with a PSPME device is the geometry design only allows using ion mobility spectrometers (IMS) as detectors, resulting in unresolved peaks and misinterpreted conclusions, without identification unless the compounds have been programmed in the system previously. Applications were also limited. Therefore, a device similar to PSPME that provides a large surface area and phase volume is needed to fit in the GC-MS injection port in order to improve the sampling process.

1.3 Research hypothesis and Project Goals

1.3.1 Hypothesis

Solid phase microextraction (SPME) is a thin fiber that functions on a syringe-like holder which can be injected into a GC injection port directly; however, the GC injection port is not limited to liquid injection where it can be replaced with a thermal separation probe in which allows for analysis of the contents in a micro vial and then thermally desorbed into the GC-MS instrument [27]. A new preconcentration device using the micro vial used in thermal separation probe can be designed to hold PSPME strips with open ends to allow for the device to be used for dynamic sampling using a vacuum pump. Using PSPME as the matrix in the preconcentration devices, the new design can maintain the improved surface area and phase volume for more efficient preconcentration results. In addition to better preconcentration performance, the compounds accumulated on the devices can be further identified in the GC-MS with quantitative capabilities.

1.3.2 Project Goals

There are three main goals to be achieved in this project. The first goal is to evaluate previously developed preconcentration devices, including solid phase microextraction

(SPME) and planar solid phase microextraction (PSPME) for their performances in headspace analysis using low explosives (smokeless powders) and peroxide explosives (triacetone triperoxide). The second goal is to develop capillary microextraction of volatiles (CMV) and couple it to a GC-MS to achieve the ultimate goal in headspace analysis which can overcome the two current challenges. The preconcentration performances of CMV are then determined and compared to both SPME and PSPME. The last goal is to take the CMV sampling device for real life scenarios which include sampling a shipping facility, illicit drugs, military explosives, and different bacteria strains.

Chapter 2 Introduction to Explosives

2.1 History of Explosives

The early history of explosives is closely connected with the discovery of saltpeter which is also known as potassium nitrate (KNO_3) [28], but the definition of explosives was unclear during that time. The use of gunpowder, the only explosive known until the middle of the nineteenth century, was initially confined to warfare and there has not been any use for blasting purposes for several hundred years since its invention [29]. Manufacturing of gunpowder had been adjusted from the early stage to prevent separation from the turbulence in the transportation and in sixteenth century, further improvement was made to keep the gunpowder consistent in the composition. A major milestone in history of explosives was the first time nitroglycerin (NG) was put to use safely by Nobel in 1875 and by the end of 1918, the explosives have expanded the categories to nitrate mixtures, nitro compounds and chlorate mixtures [30]. The explosive list continues to expand as more and more improvised explosive devices continue to be synthesized by scientists and terrorists.

2.2 Classification of explosives

One way to classify explosives is according to the type and velocity of the reaction involved, categorizing them as either high or low explosives. Primarily used as detonation charges, high explosives function unconfined (exhibiting shattering effects); although most readily burn, high explosives generally need a shock wave to initiate the explosion [28]. High explosives can be subdivided into two groups, primary explosives and secondary explosives, defined by their function in the explosion. Primary explosives

are used to start an explosion and secondary explosives are used as the main charge [31]. On the other hand, low explosives require confinement to be effective and are often used as propellants for firearms or rockets, rather than blasting. Low explosives are more sensitive than high explosives; they can be easily initiated from flame, spark and friction. Low explosives deflagrate rapidly with propagation from particle to particle [28].

Another way to classify explosives is through their applications which include commercial, military, or improvised explosives [28]. Commercial explosives are used in blasting devices for coal mining, steel industry, building transcontinental railroad and many other applications. Since the mid-1970s, the use of commercial explosives has changed toward using high explosives with low sensitivity for both economic and safety considerations. Because of the strict requirements, such as ease of processing and fabrication of munitions, low sensitivity to shock initiation on the battlefield, and good long-term stability, limited high explosives are suitable for military applications and some of them will be discussed in Chapter 10.3. Improvised explosives are very different from commercial blasting devices and military explosives. They are often nonhomogeneous mixtures of one or more oxidizers with suitable fuels typically developed by terrorists. The variety of improvised explosives is still increasing since the initial reactants can be materials commonly seen in the daily life such as flour, peroxide, and other over-the-counter products. The most commonly encountered improvised explosive devices in the United States are pipe bombs which are packed with commercially available black or smokeless powder or other improvised explosive mixtures. No matter what the source or type of filler used, an explosive confined in a

container and fitted with an initiation system is considered as an improvised explosive device (IED) [32].

2.2.1 Military explosives

Most military explosives are organic high explosives and they can be further separated into three categories based on the chemistry structure which include aromatic nitro (C-NO_2), nitrate esters(C-O-NO_2), and nitramines (C-N-NO_2). The compound 2,4,6-Trinitrotoluene (TNT), the most important explosive for blasting purposes of various weapons in military applications, is one of the aromatic nitro explosives. Nitroglycerin (NG), ethylene glycol dinitrate (EGDN), and pentaerythritol tetranitrate (PETN) can represent the group of nitrate ester explosives. The compound 1,3,5-Trinitro-1,3,5-triazacyclohexane (RDX) and 1,3,5,7-Tetranitro-1,3,5,7-tetrazazyclooctane (HMX), currently the most important high-brisance military explosives in use, fall into the nitramine explosives category [33]. Further introduction of military explosives will be included in Chapter 9.3.3.

2.2.2 Improvised explosives

An improvised explosive device (IED) is defined as "a criminally fabricated device incorporating destructive, lethal, noxious, pyrotechnic or incendiary chemicals, and designed to destroy, disfigure, distract, or harass. It may incorporate military stores but normally is designed from commercial or homemade components" (Department of Defense Joint Publication 1-02 [2011]) [34]. In another words, IEDs are non-licensed explosives usually fabricated by individuals for destructive and often lethal purposes and are commonly seen in terrorist attacks. In most cases, IEDs have not been described in

literatures before, but have only been manufactured in clandestine laboratories in which most can be synthesized from commercially available materials. Examples of such explosives are urea nitrate (a mixture of fertilizer and nitric acid), triacetone triperoxide (TATP), and hexamethylenetriperoxidediamine (HMTD) [34]. Table 2-1 shows the structure of TATP and HMTD and their reported vapor pressures.

Table 2-1 Structures and vapor pressures of TATP and HMTD

Chemical Name	Structure Formula	Vapor Pressure (Torr)
Triacetone Triperoxide (TATP)	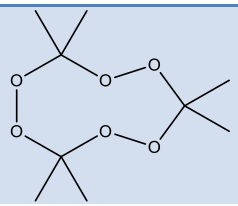	5×10^{-2} at 25 °C [35]
Hexamethylenetriperoxidediamine (HMTD)	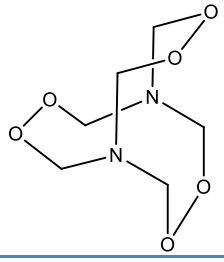	-- [36]

-- HMTD vapor pressure can not be determined due to formation of decomposition products at a higher temperature

2.2.2.1 Smokeless powder

Smokeless powders are categorized as low explosives and are used as propellants which are designed to accelerate a projectile from its rest position to full velocity. Smokeless powders are normally used as the propellant in military weapons; however, because it is easily accessible in the market, smokeless powders can be often found in pipe bombs or other IEDs that are related to criminal and terrorist attacks.

Propellants originated from black powder with the combination of charcoal, sulfur and potassium nitrate in different mass ratios to produce desired effects. The drawback of black powder is that the propellant produces a solid reaction product, producing a dense black cloud upon ignition, making it unfavorable for military use as a result. The dense cloud resulted in exposure of the position upon firing a weapon and lead to confusion and general chaos, thus developing "smokeless" powders in government's weapons laboratory [34].

Smokeless powders, also known as gunpowders, are commonly used in ammunition. There are three different types of smokeless powders depending on the major components: single-based, double-based and triple-based smokeless powders. Nitrocellulose (NC) was the first nitrated material to be tried as a replacement for black powder, but it has high nitrogen content (13.35 % - 13.45 %) which was prone to accidents. In order to lower the nitrogen content and prevent explosive accidents, alcohol was mixed with NC, kneaded in a breadmaking type machine, rolled out into thin sheets, and then cut into small squares and dried to produce the first "single-based" smokeless powder. Single-based smokeless powder only contains nitrocellulose as the energetic material in the composition. In 1888, Nobel invented a powder which was a low-nitrated NC gelatinized with nitroglycerin, known today as double-based smokeless powder. Triple-based powders contain nitroguanidine as the most frequent encountered component. Unlike single-base and double-base powders, triple-base powders were cooler-burning and were mainly used in large-caliber weapons [34,37]. Representative compositions for the three types of smokeless powders are listed in Table 2-2 [31].

Table 2-2 Representative compositions for smokeless powders [31]

Single-base powder
(a) NC + diphenylamine (DPA) + DNT + Dibutyl phthalate (DBP)
(b) NC + potassium sulfate (K_2SO_4) + DPA
(c) NC + potassium sulfate + DPA + DNT
Double-base powder
(a) NC + NG + potassium nitrate (KNO3) + ethyl centralite (EC) + graphite
(b) NC + NG + potassium nitrate + EC + diethyl phthalate (DEP)
(c) NC + NG + EC + triacetin + lead salicylate + lead stearate
(d) NC + NG + DEP + 2-nitrodiphenylamine (2-NDPA) + lead salts + wax
Triple-base powder
(a) NC + NG + nitroguanidine [$H_2NC(NH)NHNO_2$] + EC + sodium aluminum fluoride
(b) NC + NG + nitroguanidine + sodium aluminum fluoride + DBP + 2-NDPA

Identification of smokeless powder can rely on the detection of the energetic materials; however, the detection of NC and NG are not strong conclusive evidence in forensic analysis because wide use of nitrocellulose in varnishes celluloid films [38] and pharmaceutical industry as well as the use of nitroglycerin in pharmaceutical preparation for heart diseases [39] and insulin and glucose regulation [40]. In addition to the energetic materials, organic additives are also present in smokeless powders which include stabilizers, plasticizers and coatings [31]. Dinitrotoluene (DNT) isomers are used as a flash suppresser; dibutyl phthalate (DBP) is used as a plasticizer; methyl and ethyl centralite (MC and EC) and diphenylamine (DPA) are used as stabilizers [37]. And

detection any organic additives in additional to the energetic materials can help make a conclusive decision in the presence of smokeless powders.

Diphenylamine (DPA) is one of the most popular additives in smokeless powders; although, similarly to NC and NG, detection of only DPA cannot be used as a conclusive evidence of presence of gunpowder because it is also commonly used in the dye manufacture, perfumery [41], food industry [42] and as an antioxidant in the rubber and elastomer industry [43]. Diphenylamine acts as a stabilizer in smokeless powders and binds to nitrous oxide gases formed from NC decomposition to form stable compounds following the process shown in Figure 2-1 [37]. The detection of the nitrous oxidized stabilized compounds confirms the presence of gunpowder; however, the DPA derivatives have relatively low vapor pressure which complicate the detection process[37].

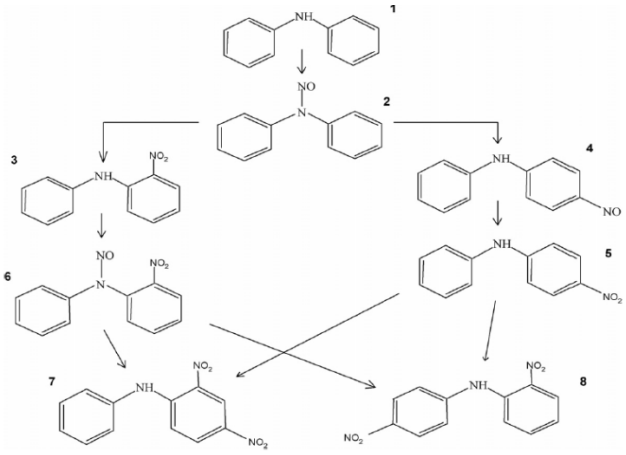

Figure 2-1 DPA functions as a stabilizer in smokeless powders to convert the energetic gases into stable compounds: (1) DPA, (2) *N*-nitroso-diphenylamine (*N*-NODPA), (3) 2-nitrodiphenylamine (2-NDPA), (4) 4-nitroso-diphenylamine (4-NODPA), (5) 4-nitrodiphenylamine (4-NDPA), (6) *N*-nitroso-2-nitrodiphenylamine (*N*-NO-2-NDPA, (7) 2,4-dinitrodephenylamine (2,4-NDPA), (8) 2,4'-dinitrodephenylamine (2,4'-NDPA) [37]

2.2.2.2 Peroxide explosives

Peroxide explosives are generated from decomposition from peroxides or a mixture of peroxides and other organic compounds. Easy access of the reactants has increased the popularity of peroxide explosives as IEDs. Peroxides are widely used commercially, such as bleaching agents and polymerization catalysts. The weak O-O bond undergoes exothermic thermal decomposition to produce radicals, causing peroxides to be sensitive to shock and friction, thus handling has to be extremely cautious. Some peroxides, such as dibenzoyl peroxide (used as an acne treatment) or di-t-butyl peroxide (used as a radical initiator in organic synthesis and polymer chemistry), contain too much carbon to be considered as true explosives; however, the energy released in explosion is still equivalent to 25 % and 30 % of the energy released by the same amount of TNT, respectively. Over the past couple years, an increasing number of incidents regarding the use of triacetone triperoxide (TATP), diacetone diperoxide (DADP) and hexamethylene triperoxide diamine (HMTD) were reported; thus, the three peroxide explosives will be the primary focus in this research [44].

Triacetone triperoxide was first prepared by Wolffenstein in the 19th century [45]. The dimer of acetone peroxide, also known as DADP, is a byproduct in the synthesis of TATP, especially when sulfuric acid is used as the catalyst in the reaction. As an explosive, TATP is almost as powerful as TNT, but extremely sensitive to shock, friction, and temperature changes, especially if stored as a dry product. Because of its extreme sensitivity, it is not safe to be used in either commercial or military applications [46].

The explosive HMTD was first synthesized by Legler in 1881 [47] and initial studies only focused on its synthesis and structure determination. It is not as sensitive to impact as TATP, so HMTD was used as a military explosive between 1940s and 1960s; nevertheless, the applications in commercial and military were terminated because of its sensitivity. Recently, it has found use in terrorist attacks because of ease of synthesis and availability of starting materials. The thermal decomposition of pure HMTD was examined over the temperature range 100 °C and 180 °C and it was found up to 150 °C, the decomposition products are mainly CO_2, but also trimethylamine and ammonia. Above 150 °C, the decomposition became nearly instantaneous and instead of carbon dioxide, carbon monoxide was the main product with no observation of trimethylamine [48].

These two peroxide explosives are not fluorescent and they do not have significant adsorption in the UV spectrum which makes the detection difficult compared to the other explosives. Today, the methods most frequently used for identification of TATP and HMTD are infrared (IR) spectroscopy and chemical ionization mass spectrometry. The compound TATP can also be analyzed in a GC-MS or IMS; on the other hand, no sensitive methods are currently available for trace analysis of HMTD explosive [46].

2.2.2.3 Terrorist attacks

Numbers of terrorist attacks have increased dramatically in the past 40 years [49]. A few well-known terrorist attacks involved explosives are listed in Table 2-3. As shown in the table, terrorist attacks are not limited in the United States, but have become a world-wide issue. Furthermore, the explosions can happen through different transportation systems.

In the wake of 9/11, the massive deployment of security technology resulted in sophisticated, effective explosives detection capability in aviation security. To a certain extent, the increased security in aviation has resulted in terrorists shifting their focus from aviation to other targets, such as cargo, mass transportation, and public monuments and some cases involving suicide bombings, whereby explosives are carried on the person, rather than in a packages or luggage [34]. Thus, the detection of explosives is important at different checkpoints to ensure international securities.

Additionally, more than one kind of explosives has been used in terrorist attacks. Terrorist plots involving explosives have migrated from the use of commercial and military explosives (Pan Am Flight 103) to a wide range of homemade explosives (Boston marathon bombing, London bombing, Oklahoma City bombing), formulated from common industrial chemicals [50-52]. The proliferation of homemade explosives has resulted in changes in detection strategy to include detection of many combinations of explosive/oxidizer-fuel formulations based upon raw materials that are available to bomb makers. The need to detect a growing variety of explosives that may be hidden in increasingly numbers of ways have never been greater [34]. Consequently, the method that used for detection of explosives should be universal for all different formulas including the improvised explosive devices which compositions change all the time.

Table 2-3 List of well-known world-wide explosive attacks

Year	Country	Explosives	Death/Injuries	Reference
2013	Boston Marathon United States	Low explosives mixture	3/264	[50,53]
2005	London United Kingdom	Homemade organic peroxide explosives	52/>700	[51]
1995	Oklahoma City United States	Agricultural fertilizer, diesel fuel	167/684	[54,52]
1993	World Trade Center United States	Urea nitrate, hydrogen gas	6/>1000	[55]
1988	Pan Am Flight 103 Scotland	RDX, PETN	270/--	[56,57]

2.3 Detection of explosives

The fundamentals of explosives detection can be summarized into the following three primary goals: sensitivity, specificity and throughput. Sensitivity is defined as a minimum detectable mass for various threat materials. The presence of fast expanded threat materials meant that a detection list can not be effectively used by agencies. Programming the new combinations of alarm threats in a timely manner may still miss a newly synthesized homemade explosive which would lead to a national catastrophe. Besides, because of the development of all the advanced technologies, terrorists made the improvised devices harder to be identified from improvements in concealments which requires the detection system to be able to perform with appropriate sensitivity when the targeted compounds are only on the trace level [34]. Specificity relies on the minimized

false alarm rate. False positive alarms are economically costly and bothersome to customers because additional investigations are required to higher level of security examinations. False negative alarms have to be avoided to prevent national tragic incidents; however, the false negative alarm potential is increasing as the list of energetic materials are expanding in such a fast rate [34]. The third goal is to maximize the operation throughput, in which the screening must be in a high speed to not delay on the progress of reaching the destination regardless of whether it is a checkpoint for cargoes transportation, or it is a security check for passengers in the airport. The modern techniques that applied in the field should achieve the three primary goals at the same time to ensure efficient detection.

2.3.1 Bulk Detection

Bulk explosives detection refers to the detection of large amounts of energetic materials through the interaction of explosive material with energy, such as those in the electromagnetic spectrum (ultrasound, infrared, terahertz, gigahertz, millimeter, microwaves and radio waves), the X-ray spectrum and neutron interrogation techniques [34]. For examining small objects such as a bottle, the appropriate techniques that may be applied include the following: ultrasound; Raman scattering; X-ray fluorescence; neutron activation analysis and many other approaches. For larger objects, such as a briefcase, purse, or luggage which typically contains a wider variety of materials, imaging technologies (X-ray, neutron, and magnetic resonance imaging (MRI)) or non-imaging element-specific techniques such as nuclear quadrupole resonance (NQR) may be applicable which enables the visualization of the contents without opening the

concealments. For even larger objects, such as boxes or crates used in air cargo, variants of X-ray and neutron imaging are applicable [34].

The throughput of bulk detection technologies is generally speaking high; however, there is not one technique can meet all the detection requirements. Additionally different bulk detection technologies suffer from specific disadvantages, which include not suitable for liquid detection, low resolution or lacking of specificity [58].

2.3.2 Trace Detection

Trace explosives detection uses a chemical analysis of explosive residues resulting from building or concealing explosive devices. Trace detection has well-established applications to aviation security, particularly aviation checkpoints, for screening of people, carry-on baggage, and checked baggage; however, some applications including personnel, small and large cargo items, and vehicle screening cannot be addressed with existing trace explosives detection equipment as a result of difficult technology requirements such as higher throughput or increased screening complexity. In contrast to bulk explosive detection, trace explosives detection technologies are generally more complicated involving three major components: signatures, sampling, and detection [34].

2.3.2.1 Chemical Signatures

The detection of explosives with trace technology relies on the determination of unique chemical signatures that can be exploited for detection, especially in vapor form detection. Since the vapor pressures of some explosives are very low and nonhomogeneous mixture in the IEDs, detection of parent compounds can not be relied on; instead, identification of the signature volatile compounds in the headspace either from the volatile portion or the

decomposition products is critical in determination of the presence of the explosives. The instruments used should adequately detect a wide range of particulate and vapor trace threat signatures, which may involve increasing sampling capability, instrumental resolution, and improving methods of detection [34].

2.3.2.2 Sampling of Trace Amount of Explosives

Even if a given trace explosives detector has sufficient detection sensitivity, a poor sampling approach will diminish the detection performance of the entire system because of the inability of the system to effectively deliver samples to the detectors for analysis. The sampling process includes the harvesting the explosives residues from a person or item of interest efficiently and transferring the collected materials to a suitable detector for analysis [34]. Trace detection can be in particulate or vapor forms, where particle detection relies on the swabs to pick up the particulate matter that was left on the surface whereas vapor detection relies on a relative high concentration of the explosive in the headspace.

Improvements in the sampling process are active areas of research and development, and may benefit from improvements in sample media, better introduction of the sample to the detector, and effective collection of both particles and vapor samples across the range of detection scenarios.

2.3.2.3 Detection with Trace Detectors

Ion mobility chemistry is the foundation of a class of explosive trace detectors that demonstrates unique specificity for explosives by virtue of the high electron affinity typically expressed in explosives. Ion mobility spectrometers (IMS) are trace detectors

analyzing both vapor and particulate explosives, though not all models can perform both functions. The IMS, which are widely used at airports, can be used with two different sample protocols including swabbing with or without the assistance of hand held wands, and automated detection with a single or series of forced air vents to pass the vapor or particles to a sample trap. Sensitivity and throughput are extremely high for IMS trace detectors, but specificity is sometimes compromised when the surrounding environment has contaminated chemicals.

Mass spectrometer explosive trace detectors can use a quadrupole, a time-of-flight or an ion trap analyzer coupled to a variety of front end sampling systems [34]; however these detectors are currently limited in deployment and undergoing active development. The analyzers used in this type of detectors allow for a much higher specificity compared to IMS; however, throughput is the limited factor for deploying MS-based detectors in the checkpoints.

Chapter 3 Instrumentation Background

3.1 Gas Chromatography – Mass Spectrometry (GC-MS)

Gas chromatography is an analytical technique using solid or liquid stationary phase and gas as the mobile phase to separate complex samples [59]. The typical process for a GC analysis includes five steps: sampling (collection and storage), sample preparation (extraction, fractionation, concentration and derivatization), GC analysis (separation), data handling (identification and quantification) and reporting the data [60]; among these, sampling and sample preparation are the most time-consuming, error-prone and contamination prone steps [60]. A typical gas chromatograph system is shown in Figure 3-1. Normally, the samples (solid and liquid samples need to be diluted in organic solvents before injected into the system) are injected into a thermally heated port to vaporize all the compounds present in the solution and then the compounds are further moved through a packed column or an open tubular column with the assistance of the gas mobile phase. Depending on the chemical structure, different compounds have different polarity which could change their interaction with the stationary phase and inert gas phase, thus separating the individual compounds in the column. Upon separation, the compounds will be eluted from the column one by one in the order of retention time to the detectors in which the compounds are analyzed for identification and quantitation. The most common used detectors coupled to GC systems are mass spectrometers, which is defined as any instrument capable of producing ions from neutral species and provides a means of determining the mass of those ions, on the basis of the mass-to-charge ratio (m/z, where z is the number of elemental charges) and/or the number of ions. A mass spectrometer is composed of an ion source, analyzer(s), and detector(s) [61]. The

exceptional performance have raised it to an outstanding position among analytical methods providing unequalled sensitivity, detection limits, speed and diversity of its applications, which include biochemical analysis, pollution control, food control, natural products or process monitoring, and forensic analysis and so on [62].

Many factors could affect the separation and detection results obtained from a gas chromatography analysis, which include injection methods, types of columns, detectors and the coupling to the detectors [59]. Detailed explanation can be found elsewhere [63-65] and only the most recent development that is used in the dissertation will be discussed in the following contents.

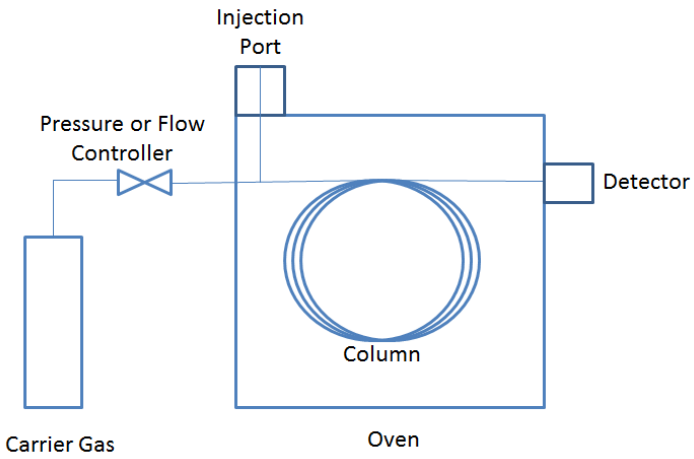

Figure 3-1 Schematic diagram of a typical gas chromatography system

3.1.1 Sample Introduction

Sample introduction is one of the critical steps in GC where it must be instantaneous to minimize the sample vapor band introduced into the column which already has a significant width. The injection port, or the GC inlet, must receive the sample, evaporate

it rapidly and deliver accurate, reproducible and predictable amount of materials to the column as a narrow band. Generally speaking, thermal decomposition should be limited to keep the composition of the transferred material unchanged upon entering the column; however, there are some techniques such as purge and trap, and pyrolysis GC in which finish the sample introduction the opposite way [59,60].

For a capillary column, multi inlets have been developed to improve the sample introduction which include the most commonly used split/splitless mode, programmed temperature vaporizer, cool-on-column injection and other auxiliary sample introduction devices such as headspace, purge and trap, thermal desorption devices and gas and liquid sampling valves [60].

Except the general use of GC syringes as the injection method to introduce liquid samples, there are other inlets that allow introduction of gas, liquid or solid samples directly into the GC without dissolving the samples in organic solvents as previously discussed.

3.1.1.1 Headspace Samplers

Headspace samplers are used to introduce a portion of the headspace gas present over the sample confined in a closed system. Any type of samples, gas, liquid or solid, can be sealed in a vial. The vial can be left at room temperature or heated to a certain temperature to let all the volatiles equilibrate in the vial. The advantage of headspace sampler is to selectively sample the species of interest while leaving the complex matrix in the vial without causing any contamination [60]. When the gas phase is in equilibrium, a portion of the headspace will be purged into the column using gas syringes, loop systems or balanced pressure system [64]. Overall, headspace is very useful for analysis

of samples with complicated matrix such as soil, water, food and drinks; however, as a result of the low concentration in the headspace and small sample volume, the detection of trace compounds could be problematic.

3.1.1.2 Thermal Desorption Devices

Thermal desorption devices are very much alike split/splitless inlets with the only difference that instead of using a GC syringe, a micro-vial is used to contain the and the injection is accomplished using a probe.

Figure 3-2 shows an example of a commercially available thermal desorption device that is able to be easily coupled to GC systems. By using the micro-vial, liquid and solid samples can be both analyzed in the GC-MS as shown in Figure 3-3 with the flow diagram of the thermal desorption device in split mode [66]. It simplifies the sample preparation with the elimination of the step of dissolving the sample in organic solvents. The advantage of thermal desorption devices over headspace samplers is instead of taking a portion of the gas phase, the sample matrix is heated and the entire volatile gas phase is transferred into the column which could significantly improve sensitivity.

Figure 3-2 A commercially available thermal desorption device that can be coupled to a GC-MS

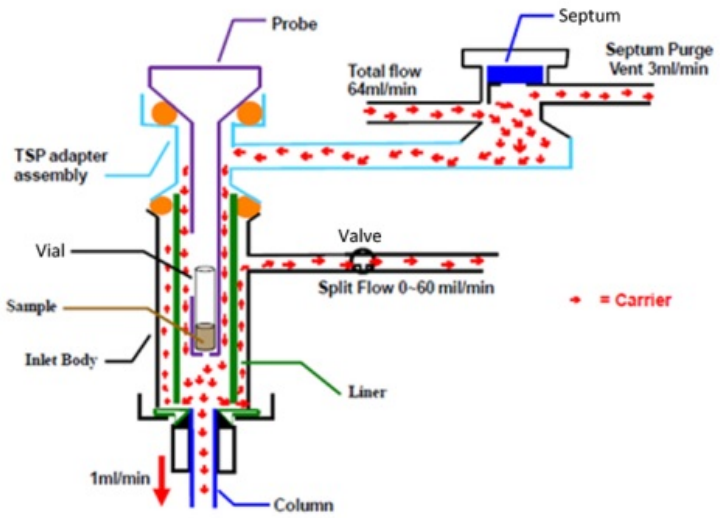

Figure 3-3 Flow diagram in a thermal desorption device in split mode [66]

3.1.2 Types of Detectors

Two different types of detectors are the ones that only respond to certain type of compounds, considered as to be selective or element-specific detectors, and the detectors that do not show any selectivity towards certain type of compounds, known as universal detectors or non-specific detectors. While selective detectors can greatly simplify the chromatogram when analyzing complex mixtures, universal detectors have great advantages in identification of an unknown. Both types of detectors can be coupled to a GC system and the combination of a selective with a universal detector can not only provide information on the entire sample, but also give greater quantitative sensitivity on specific components [59].

3.1.2.1 Mass Spectrometers

The selective detectors like electron capture detector (ECD) allow for detection of a certain type of compounds, but they do not provide enough information to identify the

eluting solutes. Therefore, most of the GC detection systems rely on spectroscopic detectors that allow selective recognition of the separated compounds, such as GC-fourier transform infrared spectroscopy (GC-FTIR), GC-atomic emission detection (GC-AED) and GC-mass spectrometry (GC-MS). These systems can provide sensitive and selective quantitation of eluted solutes with structural information for unknown identification [61]. Among these techniques, mass spectrometry has the widest applications and is the detector used in my dissertation. Mass spectrometry theory has been well explained in different textbooks and won't be described further [62,61].

3.2 Ion Mobility Spectrometry (IMS)

Ion mobility spectrometry is an analytical technique used to separate and identify ions on the basis of their ion mobility in an electric field [67]. A schematic displaying the process of IMS can be seen in Figure 3-4 [68,37]. Even though different ionization sources, including laser ionization, corona discharge and electrospray ionization, can all be coupled to IMS drift tubes, IMS systems that use radioactive ionization sources still take the greatest part in the currently deployed IMS instruments. Solid particles on a swab or a small amount of solutions on a swab can be thermally desorbed into the IMS drift tube where all the compounds were present in the gas-phase and then further ionized in the ionization chamber. The swarm of ions formed in the reaction region is then pulsed into the drift region through an ion shutter which functions like a gate. In the drift region, the ions are moved by the applied electric field (E) of several hundred V/cm over a fixed distance (drift tube length L), usually 5 – 8 cm long [69]. As the ions travel through the drift tube, they are slowed down by collisions with the drift gas molecules

travelling in the opposite direction. Depending upon the ion size and shape (collision cross section, Ω_D), different constant velocities (v_d) are attained. Ions with lower mass, smaller collision cross section, and higher charge reach the detector at a faster rate since they are less affected by the drift gas molecules and more affected by the electric field. Upon separation, ions collide with a faraday detector, in the order of the smallest ions to the largest ions, causing them to become neutralized which in turn generates a current flow of 10 to 100 pA that is then amplified and converted into a voltage signal of 0 to 10 V [67]. The voltage signal, along with the drift time (t_d), are plotted against each other in a mobility spectrum.

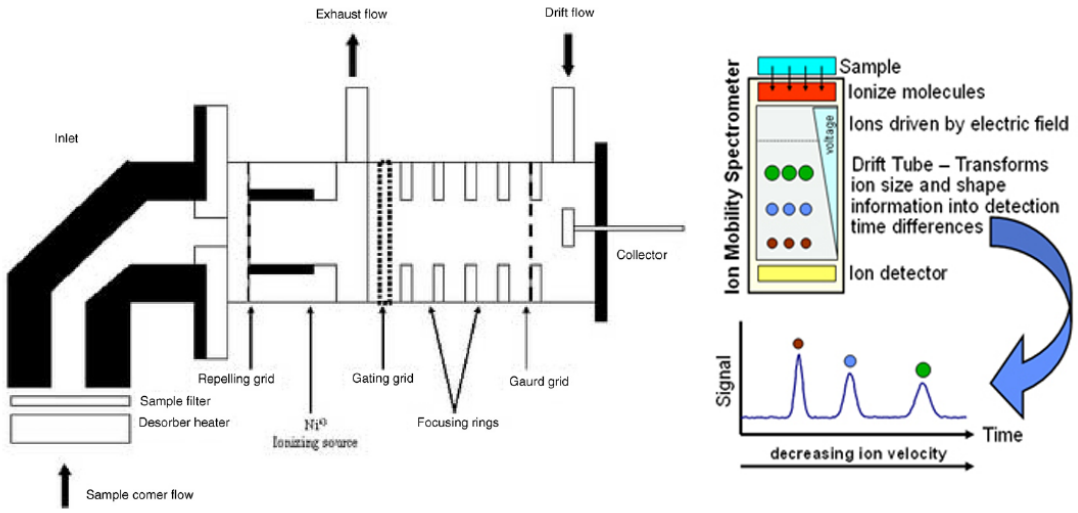

Figure 3-4 Schematic diagram of an IMS

3.2.1 Radioactive Ionization Sources

Ionization in IMS instruments occur under atmospheric pressure where the ion production mechanism must be able to operate with the levels of moisture and oxygen in the ambient air. There are several ionization methods that can be used in IMS systems

which include radioactive sources, photo-discharge lamps, lasers, electrospray ion sources, flames, corona discharges, and other surface ionization sources. A summary of these ionization techniques are listed in Table 3-1. Among the techniques, radioactive sources are the most popular because of the stability and reliability with the ionization chemistry in the applications of IMS [67].

Table 3-1 Summary of ionization techniques used in ion mobility spectrometry [67]

Source	Type of Chemicals	Maintenance	Cost	Comments
Radioactive	Universal	Low	Medium/Low	Licensing required
Corona discharge	Universal	High	Medium	Maintenance required
Photoionization	Selective (IP)	Medium	Medium	Low efficiency
Surface ionization	Nitrogen bases	High	Medium	Complex
Electrospray	Liquids	Medium	Medium	Long clearance
MALDI	Solids	High	High	Laboratory use
Flame	Selective	Medium	Low	Molecular structure lost

Radioactive sources that can be used in IMS include an alpha-emitting isotope, ^{241}Am (Americium) and two beta-emitting sources, ^{75}T (Tritium) and ^{63}Ni (Nickel). ^{241}Am source emits highly energetic alpha particles (5.4 MeV) that have a short effective range in air; ^{75}T source produces less radiation hazards than ^{63}Ni and has been used in environmental study for monitoring toxic compounds in air. ^{63}Ni is the most widely used

and best understood of the three radioactive sources or all ionization sources, typically in the shape of a thin layer of 10 mCi of ^{63}Ni coated on a metal strip, generally nickel or gold. The β electrons emitted from a ^{63}Ni source has the energy distribution ranges from 0 to 67 keV with an average value of 17 keV. As listed in Table 3-1, radioactive source does not need an external power supply and requires minimum maintenance and combined with the easy operation and well understood ionization chemistry, ^{63}Ni is the most favored ionization source in IMS systems; however, the use of ^{63}Ni is discouraged because of the potential radioactive hazards [67].

3.2.2 Gas-phase Ions (^{63}Ni Source)

3.2.2.1 Formation of Reactant Ions

Ionization in IMS relies on gas-phase ion chemistry where sample molecules (M) are ionized by collisions with reactant ions. Reactant ions are formed from the supporting atmosphere in the ionization region by colliding with high-energy primary electrons emitted from a ^{63}Ni source. When the primary electrons collide with nitrogen molecules in the atmosphere, N_2^+ ions are formed and the primary electrons lose some energy as shown in Equation 3-1. Determined by the amount energy remaining, the electron can still be a primary electron or a secondary ion and the electron can keep ionizing nitrogen molecules until its energy is below the ionization potential of air (35 eV) which are known as thermalized electrons.

$$N_2 + e^-(\text{primary}) \rightarrow N_2^+ + e^-(\text{primary or secondary}) \qquad \textbf{Equation 3-1}$$

The N_2^+ ions will undergo collisions with the atmospheric molecules that lead to a series of reactions as shown in Equation 3-2 to Equation 3-5 to form positive reactant ions.

Depending on the moisture level in the drift tube, the water molecules number (n) in the positive reactant ions could fluctuate dependent on moisture level, thus, affecting the performance of IMS instruments.

$$N_2^+ + 2N_2 \rightarrow N_4^+ + N_2 \qquad \textbf{Equation 3-2}$$

$$N_4^+ + H_2O \rightarrow 2N_2 + H_2O^+ \qquad \textbf{Equation 3-3}$$

$$H_2O^+ + H_2O \rightarrow H_3O^+ + OH \qquad \textbf{Equation 3-4}$$

$$H_3O^+ + (n-1)H_2O + N_2 \leftrightarrow H^+(H_2O)_n + N_2 \qquad \textbf{Equation 3-5}$$

The formation of negative reactant ions is different, where thermalized electrons attached to oxygen molecules in the atmosphere through three-body collisions to form O_2^- and the hydrates (Equation 3-6 and Equation 3-7) where M stands for the third body which can be O_2, H_2O, or another neutral molecule.

$$M + O_2 + e^- \rightarrow O_2^- + M \qquad \textbf{Equation 3-6}$$

$$M + (n)H_2O + O_2^- \leftrightarrow O_2^-(H_2O)_n + M \qquad \textbf{Equation 3-7}$$

3.2.2.2 Formations of Product Ions

Reactant ions are continuously produced in the ionization region and are forced to the reaction region under the electric field force. Without the presence of analytes, the reactant ions pass through the drift tube and collide with the detector forming the reactant ion peak as detected in the IMS instrument. When analyte molecules (M) are introduced into the reaction region, they will collide with the reactant ions and yield product ions and water. Equation 3-8 and Equation 3-9 show the product ions formed in both positive

mode and negative mode, respectively. In positive mode, dimer or trimer of the analytes could form as product ions as well (Equation 3-10).

$$M + H^+(H_2O)_n \leftrightarrow MH^+(H_2O)_n \rightarrow MH^+(H_2O)_{n-x} + xH_2O \quad \textbf{Equation 3-8}$$

$$M + O_2^-(H_2O)_n \rightarrow MO_2^-(H_2O)_{n-x} + xH_2O \quad \textbf{Equation 3-9}$$

$$MH^+(H_2O)_n + M \rightarrow M_2H^+(H_2O)_{n-x} + xH_2O \quad \textbf{Equation 3-10}$$

3.2.3 Drift Tube Design

3.2.3.1 Single drift tube

Over 30 years of ion mobility spectrometry development, there is little uniformity in the design of drift tubes. Many include some or all of the common components, which are the inlet, ion source, reaction region, shutter controller, drift region, temperature controller, high voltage supply, signal amplifier and detector system.

3.2.3.1.1 Inlets and Reagent Gases

Since ion mobility spectrometers are designed to separate ions in the gas phase, the inlet system has to deliver sample to the drift tube in the gas form. Using ^{63}Ni as the ionization source, the common inlet is by thermally desorbing the samples from the substrate. A membrane is applied in the inlet system where moisture, dust, and other interfering chemicals are blocked from entering the reaction region; thus, the background noise is reduced and sensitivity is improved. When using other ionization sources, different inlets have to be used to allow efficient transfer of ions into the drift tubes.

The inlet is not a passive element in an ion mobility spectrometer. It is often used in conjunction with reagent gases to improve selectivity of the instruments. In positive

mode, the common reagent gases are acetone, ammonia, dimethylsulfoxide (DMSO), nicotinamide, and nonylamine. In negative mode, small chlorocarbons such as dichloromethane are primarily used to produce chloride ions. The purpose of using reagent gases is to enhance the specificity of response by discriminating against molecules with low proton affinity in the positive mode and control of anion attachment reactions in negative mode which is described in detail in Chapter 3.2.2. There are different patterns used to introduce reagent gases into the drift tube, shown in Figure 3-5 which could lead to more efficient separation in the drift tube.

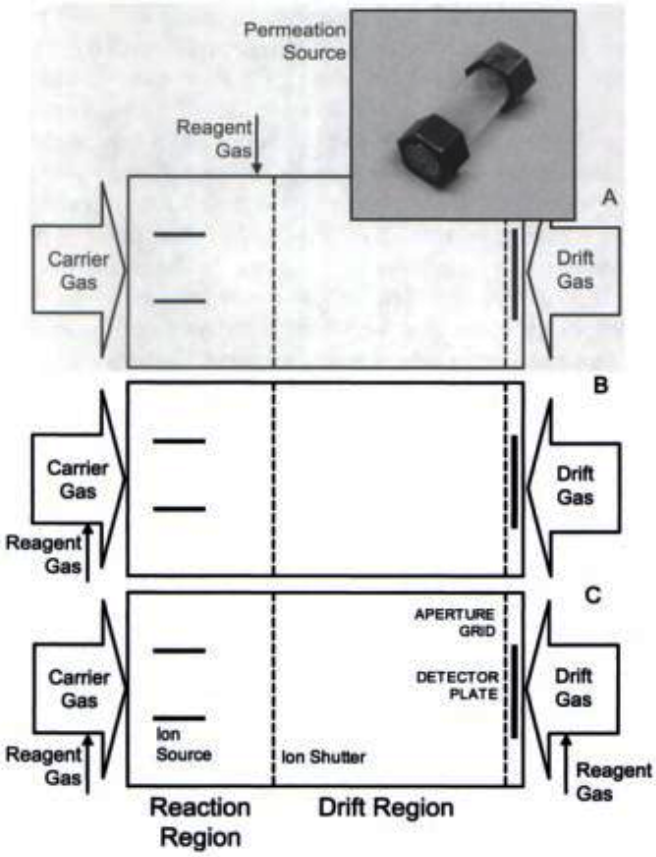

Figure 3-5 Reagent gases can be introduced: (A) directly into the ionization region, (B) into the carrier gas stream, (C) throughout the entire drift tube. [67]

3.2.3.1.2 Drift tubes

The drift tube is the most important component of an IMS and there are two basic designs that are well recognized: the linear electric field (DC) drift tube and the field asymmetric design (AC or RF) drift tube. My dissertation will only discuss the linear electric field drift tube.

A drift tube is constructed with conductive rings, insulated rings, two ion shutters and a high voltage supply with a total length ranging from 6 to 12 cm. The conductive rings are compressed with a spring and each of the conductive rings is insulated by the insulated rings. The conductive rings are applied with different biased voltages to maintain an electric field from 200 to 300 V/cm along the central axis of the drift tube where the ions are forced to move towards the detector. There are two ion shutters along the drift tube, the first one is close to the inlet which is also known as the gate which allows a fraction of the ions formed in the source to be introduced into the drift region and the second one is close to the faraday plate and it is open at a time that was delayed relative to the closing of the first shutter. As a result, only ions with drift times that equal to the delay time can pass the second shutter and cause an impact with the detector. A mobility spectrum is obtained by changing the delay time, and creating a plot of signal intensity vs. delay (or drift) time.

3.2.3.1.3 Gas Flow

Two main gas flows in an IMS are the carrier gas and the drift gas. The carrier gas is introduced from the inlet and used to transport sample molecules in the gas phase to the reaction region, which also serves as the supporting atmosphere where ionization

occurred. The drift gas is introduced from the detector-end of the instrument in counter-flow with the carrier gas. It is used to maintain the clean environment in the drift tube from contaminations. The supply of the two gases can be provided from compressed gas cylinders or through the use of air pumps which collect the surrounding air, pump through filters (molecular sieves or adsorbent traps) and are then used as carrier gas and drift gas.

3.2.3.2 Dual drift tubes

Single drift tubes used in commercially available IMS have been proven to be reliable and since temperature can be precisely controlled, the measurements are reproducible over hours, days, and/or months; however, applications focused on illicit substances detection requires dual polarity detection. Narcotics are commonly detected in the positive polarity; while explosives are normally found in the negative polarity. In addition, explosives have large variations in vapor pressures and ionization properties, which are temperature-dependent. Thus, neither a single temperature nor a particular polarity is effective or optimum for the determination of all explosives and narcotics by IMS. One approach to solve the dilemma is to use two drift tubes in one IMS system. One of the most recent developments in IMS technology is the introduction of an IMS analyzer with authentic twin drift tubes where the sample is ionized in a single reaction region and positive and negative ions are extracted and characterized in two separated drift tubes placed at appropriate polarity. Using this design, temperature of the two drift tubes can be controlled separately although the ion source is common to both drift tubes.

The only issue with dual drift tubes is loss of sensitivity since the sample is separated into two parts after ionization [67].

3.2.4 Detection and Chemical Identification

3.2.4.1 Reduced Mobility Coefficient (K_0)

Since the electric field in the drift tube is weak and uniform (200 to 300 V/cm), the ion swarm will drift along the field lines in which the drift velocity of the ions (v_d) is proportional to the magnitude of the electric field (E) as shown in Equation 3-11 [70] where V is the high voltage applied on the drift tube.

$$\boldsymbol{v_d = KE = K \cdot \frac{V}{L}} \qquad \textbf{Equation 3-11}$$

Since the velocities are constant, v_d can be calculated with the drift tube length (L) and the ion drift time (t_d) Equation 3-12 [70].

$$\boldsymbol{v_d = L/t_d} \qquad \textbf{Equation 3-12}$$

The term mobility coefficient (K) is a unique value specific to the ion molecule based on a given combination of an ion and neutral-gas molecules of the supporting atmosphere at a fixed temperature and can be calculated using Equation 3-13 [70]. Since air is commonly used in ion mobility spectrometers, the K value depends mostly on the temperature and the introduced compounds.

$$\boldsymbol{K\,(T) = \frac{v_d}{E} = \frac{L^2}{t_d V}} \qquad \textbf{Equation 3-13}$$

Since the drift tube length L cannot be measured accurately, the mobility coefficient can be also determined by using a standard (an ion of known mobility) Equation 3-14.

$$\frac{K\ (\text{Unknown})}{K\ (\text{Standard})} = \frac{t_d\ (\text{Unknown})}{t_d\ (\text{Standard})} \qquad \textbf{Equation 3-14}$$

To have a universal standard, the mobility coefficient K is normalized at 273 K and 760 torr based on Equation 3-15, establishing a reduced mobility coefficient, K_0, which is used for chemical identifications.

$$K_0 = K\left(\frac{273}{T}\right)\left(\frac{P}{760}\right) \qquad \textbf{Equation 3-15}$$

At a certain temperature and pressure, $\boldsymbol{K}$ ($\boldsymbol{T}$) is proportional to $\boldsymbol{K_0}$ and hence the reduced mobility of an ion can be obtained using the similar formula as Equation 3-14, shown as Equation 3-16.

$$\frac{\boldsymbol{K_0}\ (\text{Unknown})}{\boldsymbol{K_0}\ (\text{Standard})} = \frac{\boldsymbol{t_d}\ (\text{Unknown})}{\boldsymbol{t_d}\ (\text{Standard})} \qquad \textbf{Equation 3-16}$$

Even though K_0 can be used for chemical identifications, downfalls are associated with using the reduced mobility for identification purposes. First, the sample concentration can affect the clusters formed in the drift tube where monomers, dimers or even trimers could be present at the same time. Second, thermal decomposition of the analytes is possible from the thermal desorption and clusters formed from the decomposition products in the drift tube would present a different drift time. Third, the use of different reagent gases could significantly affect what clusters are formed. Fourth, as mentioned earlier in the chapter, moisture level in the IMS system is critical in forming reactant ions; thus, it will further affect the product ions formed in the analyzer. As a result, the reduce mobility coefficient relies on the operating conditions used in the IMS instruments and daily calibrations are required for the instrument to ensure proper function.

3.2.4.2 Standard Compounds

It is difficult to compare the reduced mobility coefficient in different IMS systems, especially with instruments of different physical constructions. It is still important to obtain the reduced mobility coefficient accurately where a good standard has to be used to provide K_0 (Standard) for calculation. A universal standard for an IMS has to have the following properties: a relatively high proton affinity for competitive ionization, readily obtainable in sufficient purity to avoid extraneous ions, thermally stable up to the maximum operating temperature, minimum tendency to form dimers and trimmers, sufficient resolution at all temperatures from the reactant ion peak and minimum tendency to form hydrates [70]. 2,4-Dimethylpyridine (2,4-DMP, commonly called 2,4-lutidine) and 2,6-di-t-butyl pyridine (2,6-D*t*BP) are two proposed standard compounds worth trying in ambient air [70]. In my dissertation, cocaine and trinitrotoluene (TNT) are used as standard compounds in positive polarity and negative polarity, respectively.

3.2.5 Applications

Ion mobility spectrometry (IMS) has high sensitivity toward high electronegativity compounds (explosives and chemical warfare agents (CWAs)) and compounds with high proton affinity (some illicit drugs and CWAs). Ion mobility spectrometers have been made into handheld devices, portable instruments, walk-through portals and systems for luggage screening. They are one of the most successful technologies for chemical trace detection of explosives and drugs at security checkpoints because of the following reasons: operation at atmospheric pressure, simplistic ion characterization, rapid analysis

(on the order of seconds), high sensitivity (sub nano-gram detection for many organic compounds), field portability, ease of use and relatively low-cost [68,67,24].

Applications of IMS have been expanded beyond the measurements of volatiles and semivolatile compounds of illicit substances and CWAs since the introduction of electrospray ionization (ESI) for aqueous samples and matrix-assisted laser desorption and ionization (MALDI) for solid samples. Peptides, proteins and carbohydrates have also been explored during the past decade; thus a new door has been open for biological and medical research with IMS [67].

Chapter 4 Evolution of headspace analysis

Volatile compounds in liquid or solid mixtures vaporize partially from the sample into the gas phase above it and back again into the sample. The process continues until it reaches equilibrium, where the concentration of the volatile compound in the gas phase remains the same. The equilibrium can be predicted by distribution constant, partition coefficient and Henry's law constant. Generally speaking, the gas phase formed from the sample is referred as headspace (HS) and the investigation of the headspace is known as headspace analysis (HSA) [64]. Headspace analysis has received a wide interest in the analytical chemistry field due to its ability to avoid complex non-volatile liquid and/or solid matrices while resulting in less solvent waste during the sample preparation [26,71,10,72,22,73]. The idea of headspace analysis existed before the development of gas chromatography [74]; however, since the emerging of the GC technique, headspace analysis quickly evolved [75-79]. The milestones that reflect the major development of headspace analysis are listed in Table 4-1.

Table 4-1 List of major development of headspace analysis

Year	Milestones	Reference
1939	First time using dynamic headspace analysis to determine the alcohol content in water and body fluids	[74]
1958	First document on combination of GC and static headspace analysis	[75]
1973	Development of purge and trap as dynamic headspace analysis to couple to GC	[77]
1990	First report on solid phase microextraction (SPME) as a preconcentration device coupled to GC	[76]

2001	Single drop microextraction (SDME) as static headspace analysis to couple to GC	[78]
2008	First publication on combination of Planar solid phase microextraction (PSPME) with Ion Mobility Spectrometer (IMS)	[79]

One of the biggest challenges of headspace analysis is the lack of compounds present in the headspace which leads to less sensitivity in detection [3]. First, non-volatile and semi-volatile compounds in a mixture are less likely to be present in the headspace which results in an incomplete profile of the composition of the mixture. Second, for volatile compounds confined in a large headspace volume, the concentration in the headspace will be dramatically reduced which is difficult to detect even with the most sensitive detectors. As a result, preconcentration of compounds of interest in the headspace has become a critical step in the sample preparation. As shown in Table 4-1, the major developments for headspace analysis have been focused on the preconcentration of compounds in the headspace. Several preconcentration devices have shown superior performance and are discussed in this chapter.

There are two different types of headspace analysis: static and dynamic analysis. Static or equilibrium headspace analysis takes an aliquot of the gas phase and the volatile compounds can be analyzed without interferences from the matrix. In doing so, the gas phase and liquid/solid phase in the system are not disturbed and sample transfer is normally carried out after the equilibrium is reached. In contrast, dynamic headspace analysis is a continuous sample transfer by using air or other inert gas as mobile phase

above a liquid or solid sample to separate volatile sample constituents from the matrix [64].

4.1 Gas-tight syringe direct injection

Gas-tight syringe direct injection is the traditional static headspace analysis. Two steps involved in static headspace analysis are equilibration and sample transfer, shown in Figure 4-1 [64]. First, the sample, no matter if it is a liquid or a solid, is placed in a sealed container controlled under a constant temperature until equilibrium is reached between the gas phase and liquid/solid phase. An aliquot of the gas phase in the container is introduced into the carrier gas stream which flows into a GC column where the gas phase analytes are analyzed. Sample transfer can be carried out manually using as gas-tight syringe, or automatically using pressure, time or volume controlled module to transfer a certain amount of the gas phase into a GC column [64].

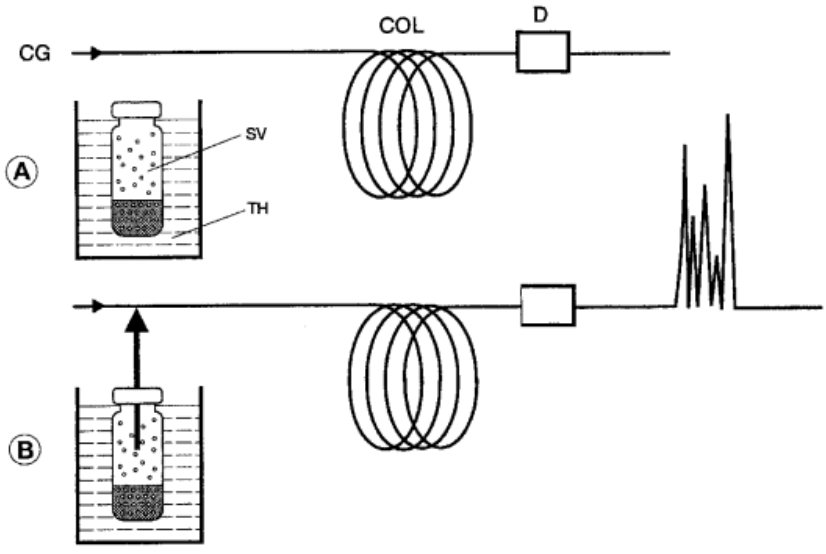

Figure 4-1 Principles of static headspace – gas chromatography. (A) Equilibration and (B) sample transfer. CG = carrier gas, SV = sample vial, TH = thermostat, COL = GC column, D=detector [64]

4.2 Purge and Trap

The well-known dynamic headspace technique is purge and trap (P&T) for the analysis of volatile organic compounds (VOCs) which consists of three steps, shown in Figure 4-2. The first step is to let a carrier gas purge through an aqueous sample to remove the volatile compounds from the matrix followed by the collection of these volatile compounds by using a cold or a sorbent trap where Tenax is the most commonly used adsorbent. The final step is to release the trapped compounds by thermal desorption and transfer them into the column using the carrier gas. The purpose of the purge and trap is not to collect a small portion of the headspace, but to completely separate the volatiles from the sample in order to have a complete profile of the headspace for quantitative analysis. Despite the preconcentration adsorbent trap applied in the system, purge and trap headspace analysis technique suffers from the water, the flow and the time problems which make this technique not ideal for dynamic headspace analysis [64].

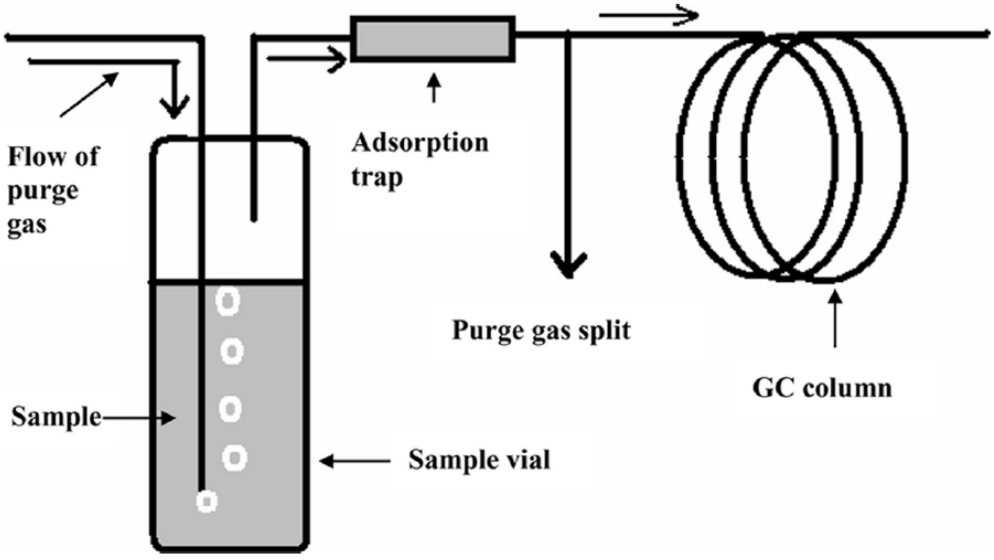

Figure 4-2 Schematic diagram of a dynamic headspace system, purge and trap [29]

The water problem is caused by the large amount of water vapor that comes from an aqueous sample. Even though the adsorbent used in purge and trap are hydrophobic (Tenax, Carbopack, Carbotrap, Carboxen, etc.) where the excess of water vapors passes through, some water may still be trapped in the sorbent tube by capillary condensation in the micropores of the adsorbent. The residual amount of water will degrade the column and further hinder the MS analysis [64].

A high flow rate of the purge gas assists the exhaustive extraction to finish in a reasonable time; however, the high purge flow rate (20-40 mL/min) can cause breakthrough of volatile compounds in the adsorbent tube, especially with the weak adsorbent Tenax [64]. During the thermal desorption step, a lower flow rate (10-20 mL/min) is used; however, it is still too high for the flow requirement in a capillary column which is around (1-4 mL/min), depending on the column diameter and other chromatographic parameters where cryogenic focusing is required to transfer a tight plug to the head of a chromatographic column [14]. Another way to reduce the flow rate through the capillary column is using a splitter to provide the correct flow rate, causing lower sensitivity because most of the headspace analytes go to waste and only a small portion of the gas phase analytes are analyzed in the column [64].

Another problem encountered in purge and trap is the time issue in which the capillary columns requires a small concentration profile of the sample at the beginning of the chromatographic separation process to achieve high resolution. Since the desorption step in purge and trap is assisted by the flow, the analytes take longer to be introduced to the inlet of the instrument, preventing the instantaneous introduction into a capillary column

and causing broadened peaks with poor sensitivity. The gas analytes can be refocused with technique, such as cryogenic focusing (-70 °C), but this complicates the entire technique [64].

4.3 Solid Phase Microextraction (SPME)

Solid phase microextraction (SPME) is one of the greatest inventions in the field of analytical chemistry and has been described thoroughly elsewhere [22,80]. A SPME is basically composed of a short thin fiber of fused silica coated with an immobilized stationary phase and mounted on a modified GC syringe, shown in Figure 4-3. It can be either immersed in a liquid sample or in the headspace above a liquid or solid sample. The volatile compounds in the headspace or in the liquid sample will absorb or adsorb in or on the fiber coating and the fiber is subsequently desorbed in the heated injection port of the gas chromatograph [64].

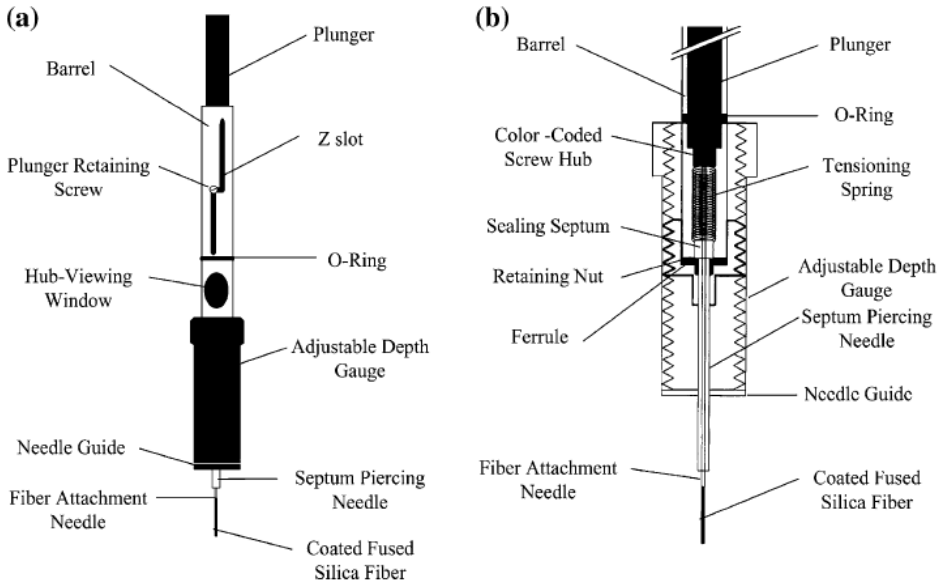

Figure 4-3 Commercial SPME device. (a) SPME fiber holder; (b) section view of SPME holder and fiber assembly [81]

4.3.1 Principles

In SPME, besides the equilibrium between the gas phase and the liquid/solid phase, there is also partitioning of analytes between the stationary phase on the fiber coating and the gas phase. When the coated fiber is exposed to the sample or its headspace, the target analytes starts to partition from the sample matrix into the coating.

The mass accumulated on the fiber (n) can by calculated using Equation 4-1 where K_{fs} is the fiber/coating matrix distribution constant, V_f is the volume of the fiber coating, V_s is the sample volume, and C_0 is the initial concentration of the targeted compounds in the sample.

$$n = \frac{K_{fs} V_f V_s C_0}{K_{fs} V_f + V_s} \qquad \textbf{Equation 4-1}$$

When the sample volume (V_s) is significantly larger than $K_{fs}V_f$, Equation 4-1 can be simplified to Equation 4-2 where a direct proportional relationship is indicated between initial concentration in the sample and the extracted amount on the fiber. Equation 4-2 is the foundation for quantitative analysis for SPME preconcentration.

$$n = K_{fs} V_f C_0 \qquad \textbf{Equation 4-2}$$

4.3.2 Coatings

Using Equation 4-2, the amount extracted onto a SPME fiber is dependent on the fiber/coating matrix distribution constant (K_{fs}) and the volume of the fiber coating (V_f). The volume of the fiber coating mainly relies on the thickness of the coating and the fiber/coating matrix distribution constant depends on the chemistry of the coating,

affecting the selectivity of the compounds towards the coated phase or the sample matrix. Coating design for SPME fiber is similar to building a chromatography column where "like dissolves like" theory is applied. There is a wide range of commercially available fibers for different applications (Table 4-2) [33,82] where PDMS and PDMS/DVB fibers are the most commonly used for forensic applications because most of the targeted compounds are semi-volatiles to volatiles, amines and nitroaromatics.

Table 4-2 Commercially available SPME fibers for different applications [82,33]

Fiber Coating	Coating Type	Application
7-µm PDMS	Absorbent	Non-polar high molecular weight compounds
30-µm PDMS	Absorbent	Non-polar semi-volatiles
100-µm PDMS	Absorbent	Non-polar volatiles
85-µm PA	Absorbent	Polar and semi-volatiles
PDMS-DVB	Adsorbent	Volatiles, amines and nitroaromatic compounds
CW-DVB	Adsorbent	Alcohols and polar compounds
DVB-Carboxen-PDMS	Adsorbent	Volatile and semi-volatile flavorings and odorants
Carboxen-PDMS	Adsorbent	Gases and low molecular weight compounds

PDMS polydimethylsiloxane, PA polyacrylate, DVB divinylbenzene, CW carbowax

4.3.3 Dynamic headspace analysis

The SPME devices generally require long extraction times to achieve detection in the instruments; however, in most forensic explosive analysis cases, fast on-site detection is critical. As a result, improvement of the sampling throughput for the SPME devices needs to be achieved by developing dynamic headspace analysis mode. Some

modifications have been made to achieve dynamic headspace sampling with SPME fibers which include inside needle capillary adsorption trap (INCAT) [73] and solid phase dynamic extraction (SPDE) [83].

The INCAT setup, first reported in 1997, is composed of a hollow needle with either a short piece of GC column placed inside it, or an internal coating of carbon as the preconcentration matrix [73]. Figure 4-5 shows the mechanism of the technique. By pulling and pushing the syringe holder, gas or liquid sample was transported through the device and the targeted compounds can be accumulated on either the GC column or the internal coated carbon layer within the needle. The INCAT device then can be introduced into a GC injection port to desorb the preconcentrated materials into the column [73].

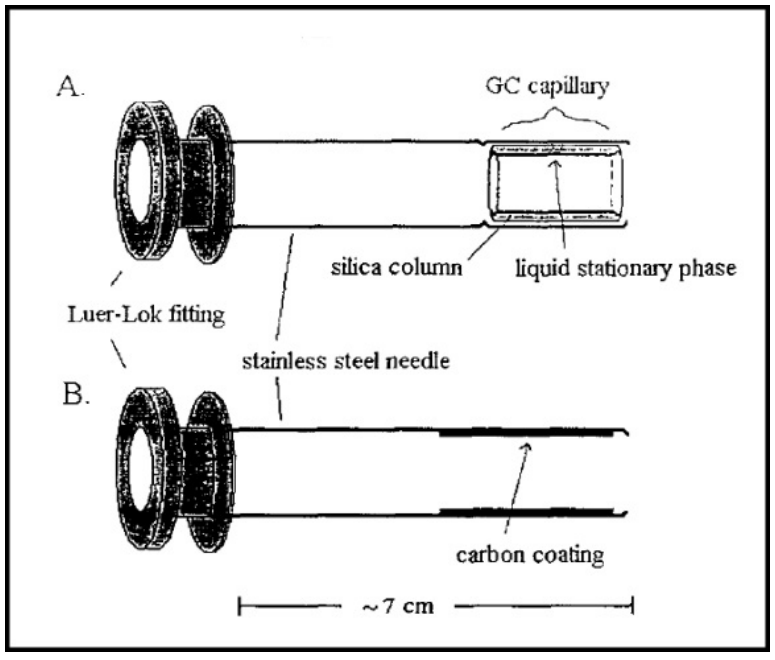

Figure 4-4 The stainless steel hollow needle with a piece of GC capillary column (A) and carbon coating (B) used in the INCAT device [73]

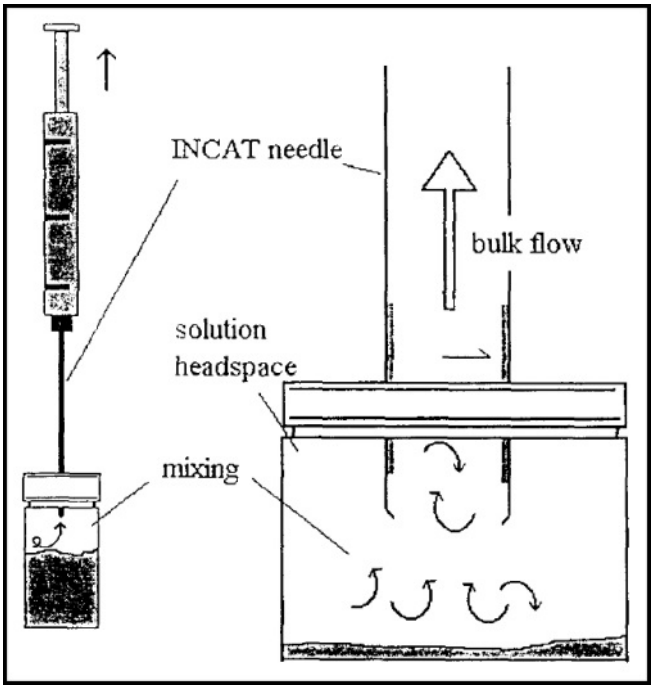

Figure 4-5 Diagram of dynamic sampling using the INCAT device [73]

The SPDE was first developed in 2002 for the detection of amphetamines and synthetic designer dugs in hair samples [83]. Similar to the INCAT device, the SPDE used a hollow needle as well, but the inside was coated with PDMS as the preconcentration matrix (Figure 4-6). The extraction mechanism is the same as the INCAT device. Pulling the syringe allows gas through the device and the extracted compounds are further desorbed into the GC column.

With the two different designs on the needle part, dynamic sampling can be achieved with the SPME-like devices; however, due to the limited sampling surface area and phase volume and the restricted sampling volume with the syringe shape, the dynamic sampling is not very efficient.

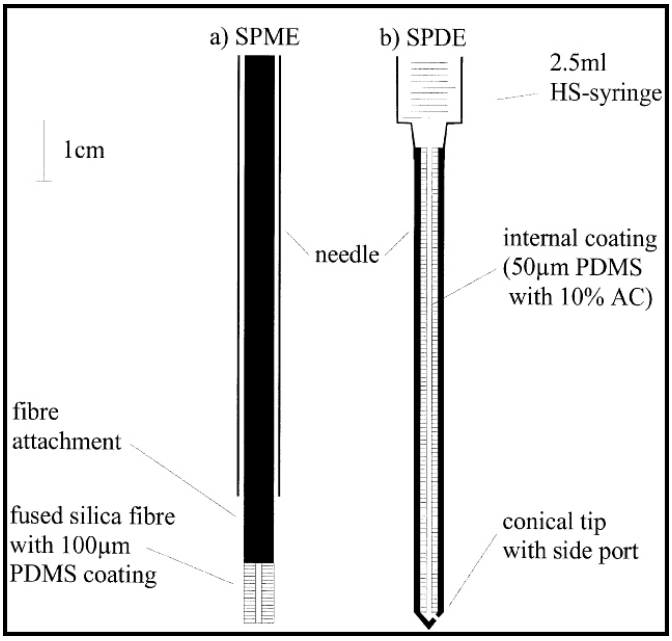

Figure 4-6 Schematic diagram of the SPME device (a) and the SPDE device (b) [83]

4.3.4 Coupling to Ion Mobility Spectrometers

Besides developing dynamic headspace analysis, another way to minimize the entire sampling and detection time is to apply a faster detector system. As introduced in Chapter 3.2, IMS can be operated at atmospheric pressure with high throughput (on the order of seconds) and high sensitivity with sub nano-gram detection for many organic compounds [68,67,24], which makes it an ideal detector to reduce the sampling time. Solid phase microextraction (SPME) was first coupled to IMS analysis by the development of a SPME-IMS interface in 2005 as shown in Figure 4-7 [71]. The inlet surface was deactivated and can be heated using a resistor to desorb the SPME fibers. The interface was evaluated for the detection of three taggants: 2-nitrotoluene (2-NT), 4-nitrotoluene (4-NT), and 2,3-dimethyl-2,3-dinitrobutane (DMNB) and the following common explosives: smokeless powder (nitrocellulose, NC), 2,4-dinitrotoluene (2,4-

DNT), 2,6-dinitrotoluene (2,6-DNT), 2,4,6-trinitrotoluene (2,4,6-TNT), hexahydro-1,3,5-trinitro-s-triazine (RDX), and pentaerythritol tetranitrate (PETN). The resulting limits of detection showed significant improvements in sensitivity [71]. The interface also enabled preconcentration of volatile odor compounds from different commercial smokeless powders, identifying the presence of diphenylamine (DPA) and ethyl centralite (EC) as potential signature odors [84]. By using the IMS as a detector, the detection was shortened from 30 min to a couple of seconds; however, the IMS still suffered from unidentifiable peaks, particularly in unknown matrices, caused by the instrument limitations.

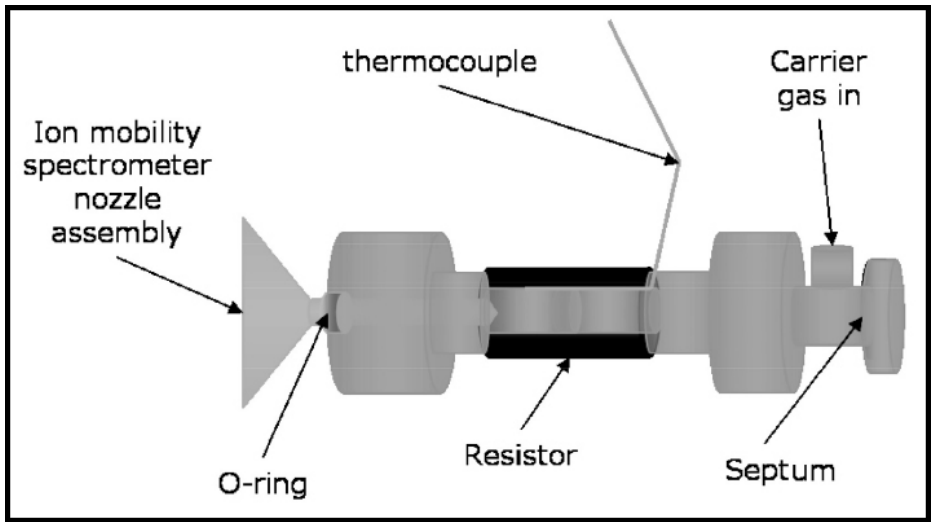

Figure 4-7 Schematic diagram of the SPME-IMS interface [71]

4.3.5 Summary

The SPME fibers have several advantages compared to other preconcentration techniques which include quantitative results from very low concentrations of analytes and almost no sample losses during extraction, concentration and desorption; however, it does suffer

from two main drawbacks which are the limited surface area and phase volume and simple static sampling mode.

4.4 PSPME

To overcome the two major drawbacks of SPME fibers, planar solid phase microextraction (PSPME) was invented by changing the geometry of SPME fibers into planar surfaces and coupled to existing ion mobility spectrometers for detection [79,24,25].

4.4.1 PSPME Preparation

The PSPME preparation was described with details elsewhere [24]; however, some small modifications were made to reduce the background noise in the IMS system in the preparation procedures. Three different glass fiber filter circles with diameters of 4.25 cm, 3.3 cm and 2.4 cm (G6, Fisherbrand, Pittsburgh, PA) were used for fabricating into different commercial IMS instruments. The glass fiber filter circles were prepared with a similar activation procedure in the literature. The glass fiber filters were placed into a 2:1 mixture of concentrated sulfuric acid (Fisher Scientific, Fair Lawn, NJ) and 30% hydrogen peroxide (Fisher Scientific, Fair Lawn, NJ) at room temperature for 10 min. The solution was decanted and the substrates were rinsed with deionized water until all the acidic molecules were neutralized. The filters were then submerged into 1 M NaOH solution for 1 h to expose the silanols on the glass fibers and followed by thorough rinsing with deionized water until the litmus papers didn't change color. The cleaned filters were placed in an oven at 80 °C for 2 h to dry with the compact side facing down the matte side of the aluminum foil to avoid breakage of the filter. While waiting the

glass filters to dry, a sol-gel PDMS solution was prepared in the following quantities: 2.060 g vt-PDMS was dissolved in 8 mL of DCM; then 1.10 mL of MTMOS and 0.535 g PMHS were added, followed by 0.875 mL of TFA (Acros) (5% water v/v). The solution was vortexed and allowed to react for 30 min. To evenly coat the filters, the prepared glass fiber filter circle was placed on top of a cut glass slide held by vacuum on the chuck of a spin-coater (Laurell Technologies, North Wales, PA). The coating solution of 1.2, 1.0 and 0.8 mL was deposited on the glass fiber filter circle 4.25 cm, 3.3 cm and 2.4 cm diameter, respectively and coated with the spin coater programmed at 1000 rpm for 60 s. The newly coated PSPME device was placed in the vacuum desiccator for 1 h, dipped for 5 min in DCM, and gelated in an oven at 40 °C overnight. The PSPME device was then placed in a GC oven in a nitrogen atmosphere at 120 °C for 1 h, 240 °C for 1 h, and 300 °C for 3 h for final curing. After the final curing process, the PSPME device was cooled in the oven in a controlled program about 8 °C/min to prevent cracking of the coating.

4.4.2 Fabrication of PSPME

Figure 4-8 (a) shows three different sizes of PSPME devices and in Figure 4-8 (b), the 4.25 cm PSPME filters can be fabricated into the same shape as the trap supplied by Morpho Detection used for Hardened MobileTrace IMS and the 2.4 cm PSPME devices can be placed in a holder shown in Figure 4-8 (c) to be used in Smiths IONSCAN IMS (Figure 4-8 (e)). All the PSPME devices can be fitted in the air vacuum pump shown in Figure 4-8 (d) and then thermally desorbed into commercially available IMS instruments from different manufactures without further modifications.

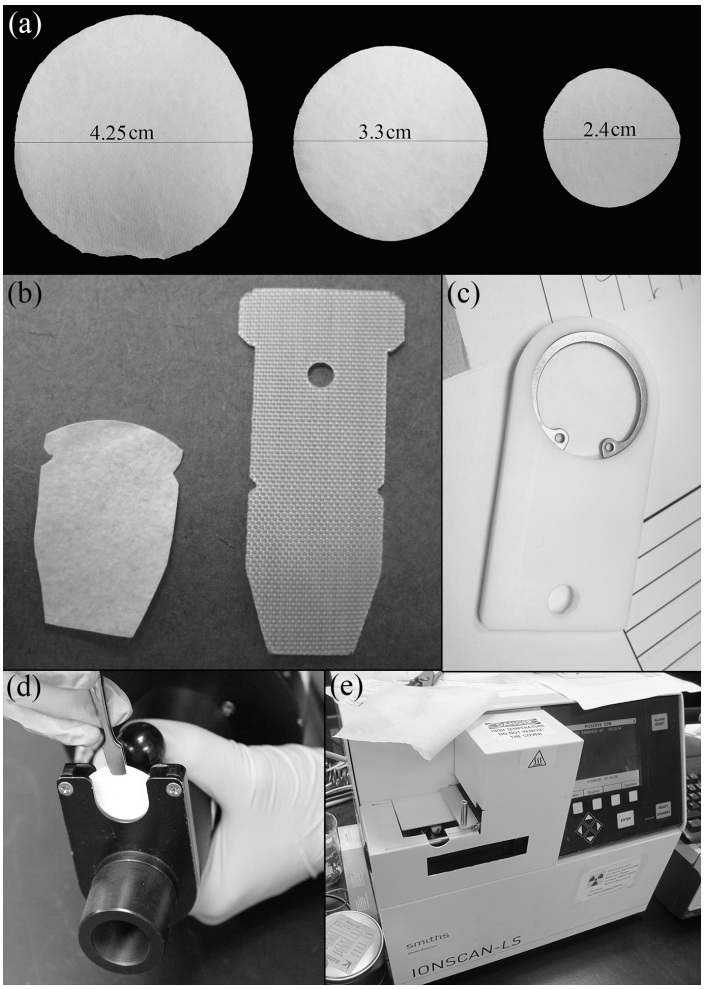

Figure 4-8 Three different sizes dynamic PSPME devices (a) that can be fabricated into different shapes (b) and combined with a holder (c) to be used in a dynamic sampler (d) for thermal desorption into a commercial IMS system (e)

4.4.3 Static Sampling

The first generation of PSPME devices was first reported in 2008 using microscope slides as the planar surfaces which are coated with PDMS and sol-gel PDMS as the preconcentration materials for fast screening cargo containers [79]. The second generation of PSPME devices was developed in 2010 using glass filters instead of microscope slides as the planar surfaces [24]. Both generations can be used for static

sampling in a concealed container in which the devices can be placed for preconcentration.

4.4.4 Dynamic Sampling

The second generation PSPME using glass filters as the planar surfaces allowed air pumping through for dynamic analysis. With the assistance of a hand-held vacuum with an average air speed measured at the head of the nozzle of 0.5 m s^{-1} (0.35 L s^{-1}), the dynamic PSPME devices were reported with high extraction efficiency resulted from the increased surface area and phase volume, resulting in absolute mass detection of less than a nanogram in 10 s dynamic extractions [24].

Chapter 5 Headspace Analysis of Smokeless Powders Using SPME-GC-MS and PSPME-IMS

5.1 SPME-GC-MS Performance Evaluation using Smokeless Powders

Solid phase microextraction (SPME) is used as a gold standard in headspace analysis and its performance is evaluated in this study for preconcentration of volatiles over the headspace of smokeless powders in various containers.

5.1.1 Instrumentation

After sampling the smokeless powders, the SPME fibers were analyzed using a Varian (Palo Alto, CA) CP 3800 gas chromatograph coupled to a Saturn 2000 ion trap mass spectrometer and equipped with an CP 8400 autosampler (Varian Inc., Walnut Creek, CA). The GC-MS conditions are listed in Table 5-1.

Table 5-1 GC-MS conditions used for SPME sampling over the headspace of smokeless powders

Column type	Agilent Tech nologies 30 m x 0.25 mm ID x 0.25 µm DB – 5MS UI
Carrier gas	Helium at a flow rate of 2.0 mL min^{-1}
Split ratio	5:1
Injector Temperature	180 °C
Column oven parameters	40 °C, hold for 1 min. 200 °C at 15 °C min^{-1}, hold for 1 mins. 240 °C at 15 °C min^{-1}, hold for 6.5 mins. 270 °C at 25 °C min^{-1}, hold for 0 mins. 280 °C at 5 °C min^{-1}, hold for 4 mins.
MS Transfer Line temperature	280 °C

MS Ion Trap Temperature	180 °C
Running Time	29.33 min
Run Cycle	35 min

5.1.2 Materials

Using GC-MS as the analyzer and detector, PDMS and PDMS/DVB SPME fibers (SUPELCO, Bellefonte, PA, USA) were both used for headspace preconcentration of volatile organic compounds (VOCs) emitted from three different smokeless powders which are Alliant Unique (Alliant Powder, Radford, VA), IMR 4198 (IMR Powder Co., Shawnee Mission, KS) and Red Dot (Alliant Powder, Radford, VA).

To mimic real life scenario, four different containers were used in this study. Quart-size metal cans (All-American Containers, Miami, FL, USA) have similar volumes as medium size handbags. Gallon-size metal can (All-American Containers, Miami, FL, USA) has similar volume to a backpack. For larger container, plastic boxes (The Container Store, USA) and cardboard boxes (Lowe's, USA) are used which can represent a half packed carry-on luggage or a half full car trunk. The detailed information on the containers used in the study is listed in Table 5-2. For the metal cans and cardboard boxes, a hole was punctured on the top of each container and sealed with a red rubber sleeve stopper which can be punctured through with a SPME fiber and hold the SPME fiber for headspace extraction.

Table 5-2 Four different containers were used in the study to represent four different real life scenarios

Container	Volume (L)	Dimensions (inches)	Distributor Information
Metal quart can	0.94	2 1/8 (radius) x 4 3/4 (height)	All-American Containers (Miami, FL, USA)
Metal gallon can	3.8	3 1/4 (radius) x 7 1/2 (height)	
Cardboard box	38	16 x 12 x 12	Lowe's (USA)
Polypropylene Plastic container	45	15-5/8 x 13 1/8 x 13 1/4	The Container Store (USA)

Calibrations for the GC-MS instrument were performed using standard solutions of nitroglycerin (NG) (Cerilliant Corporation, Round Rock, TX), 2,4-dinitrotoluene (2,4-DNT) (Alfa Aesar, Heysham, Lancs), and diphenylamine (DPA) (Acros Organics, New Jersey, USA) diluted using Optima grade methanol (Fisher Scientific, fair Lawn, NJ, USA) to concentrations ranging from 2 – 50 µg mL^{-1}.

5.1.3 Methods

For Alliant Unique (AU) smokeless powders, 10 mg, 50 mg, and 100 mg were scattered at the bottom of quart-size cans and gallon-size cans. One hundred (100) mg and 500 mg of AU were weighted in petri-dishes and then placed in plastic containers. One (1) g of AU were weighted in petri-dishes and then put in cardboard boxes. The IMR 4198 smokeless powders were prepared in the same manner as AU; the only difference was that only 10 mg and 100 mg were placed in quart-size cans and gallon-size cans. All the containers were prepared in triplicates.

After calibration curves were established, preliminary extractions were performed using both PDMS and PDMS/DVB SPME fibers and all the following extractions were accomplished only using PDMS/DVB SPME fibers. Five (5) min, 10 min and 30 min extraction times were performed in the quart cans. Five (5) min, 10 min, 30 min and 60 min extraction times were used over the headspace of the gallon cans. For larger containers, plastic boxes and cardboard boxes, longer extraction times were used to achieve detection in GC-MS. Plastic containers were sampled with SPME for 30 min, 1 h and 2 h and cardboard boxes were sampled for 30 min, 1 h, 2 h and 3 h.

Red Dot smokeless powders were also prepared for the detection of ethyl centralite (EC). 100 mg and 500 mg of smokeless powders were placed in quart-size cans and a wide range of extraction times (5 min – 60 min) were used after the headspace reached equilibrium after 48 hours.

5.1.4 Results

5.1.4.1 Extraction Profiles for Four Different Scenarios

For the preliminary study, PDMS and PDMS/DVB SPME fibers were both tested for the headspace preconcentration of 10 mg of AU and they show very similar results in the interested volatile compounds (NG and DPA). As PDMS/DVB SPME fibers showed slightly higher integrated area in chromatograms (Figure 5-1), they were chosen for the following studies.

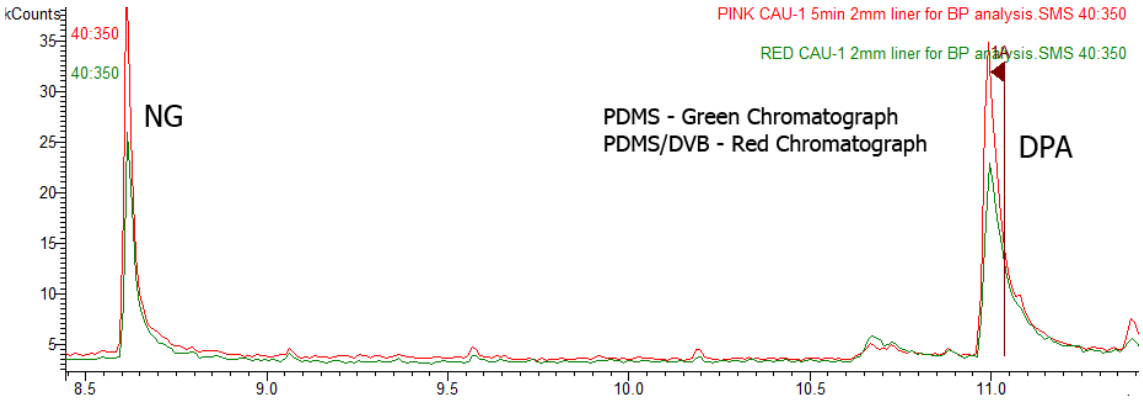

Figure 5-1 Chromatograph comparison of PDMS (Red) and PDMS/DVB (Green) SPME fibers on All Unique smokeless powder extraction

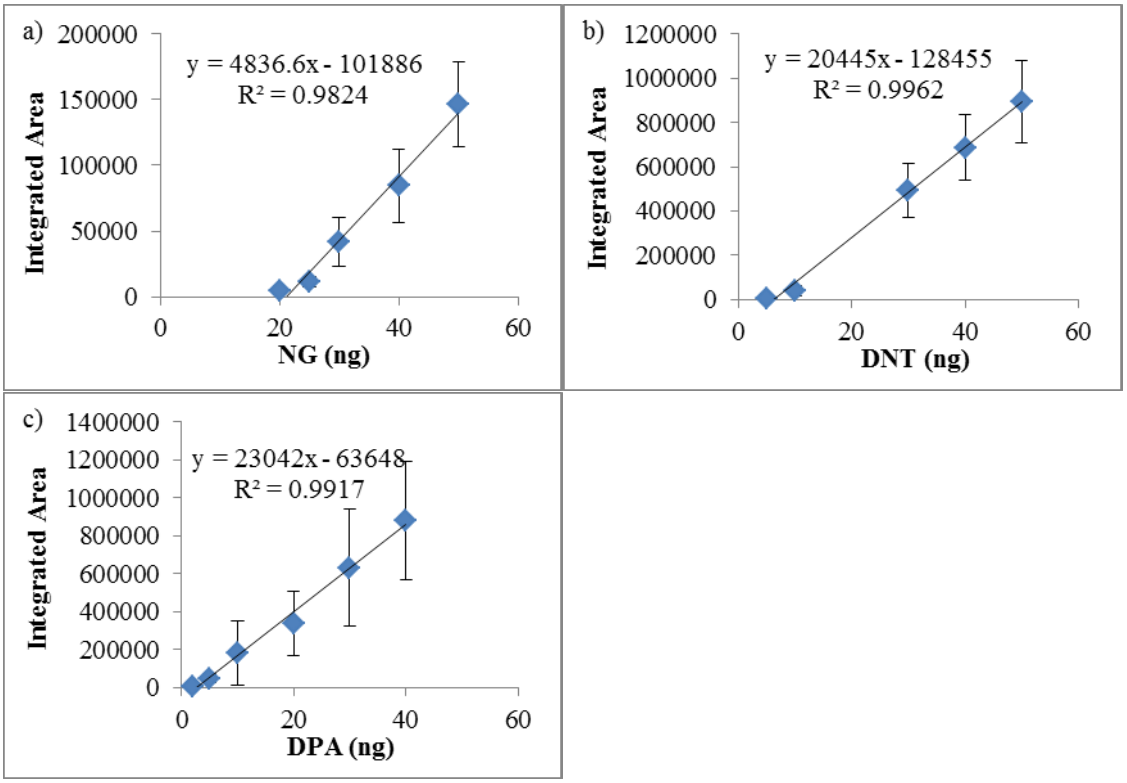

Figure 5-2 Calibration curves of (a) NG, (b) 2,4-DNT and (c) DPA in GC-MS. All calibration standards were prepared in ACN. The limits of detection were 3.0 ng for NG, 2.4 ng for 2,4-DNT and 9.9 ng for DPA

Calibration curves for NG (Figure 5-2 (a)), 2,4-DNT (Figure 5-2 (b)) and DPA (Figure 5-2 (c)) were generated based on 1 μL direct injection in GC-MS. For DNT and DPA, 1, 2, 5, 10, 20 and 30 ng μL^{-1} was used; while 5, 10, 15, 20, 25 and 30 ng μL^{-1} was used for NG. All the standard solutions were prepared in acetonitrile. As shown in Figure 5-2, DNT and DPA have good linear ranges for the selected concentrations; however, NG has a narrow dynamic range.

The SPME fibers have been used for the extractions of NG and DPA from All Unique, 2,4-DNT and DPA from IMR 4198 and NG, DPA and EC from Red Dot smokeless powders [85]. The extraction profile for the three smokeless powders in this study was shown in Table 5-3, Table 5-4, and Table 5-5, respectively.

On the basis of the results shown in Table 5-3 to Table 5-5, the optimized extraction times and the optimized amount of smokeless powders were summarized in Table 5-6 for the four different scenarios. With amounts as small as 10 mg of smokeless powders in both quart cans and gallon cans, NG was easily detected within 10 min extraction for All Unique and Red Dot smokeless powders and 2,4-DNT was successfully detected in IMR 4198 smokeless powders. When the amount of smokeless powders increased to 50 mg, DPA detection was easily achieved. As mentioned in Chapter 2.2.2, detection of both energetic materials and additives can provide conclusive determination of presence of smokeless powders; thus, two different amounts of smokeless powders were chosen for the small containers. As for plastic boxes and cardboard boxes, longer extraction times were used because of the increased headspace volume. Thirty (30) min for plastic box and 60 min for cardboard box extractions showed confident detection of NG and 2,4-

DNT in the GC-MS, while decreased extraction time resulted in reduced true positive rate. As NG, DPA, 2,4-DNT, and EC have very different composition percentage in smokeless powders, not all the compounds can be successfully detected within short period of extraction times. Diphenylamine (DPA) in AU and IMR 4198 smokeless powders needed longer extraction times to be detected in the GC-MS. And EC was even harder to be detected using the smokeless powders currently available in the lab. With a large amount (500 mg) of Red Dot in the smallest volume container (quart cans), at least 30 min extraction time was needed to show a very weak detection in the GC-MS (Table 5-5).

Table 5-3 Extraction profile for All Unique Smokeless Powder

			5 min	10 min	30 min	60 min	120 min	180 min
AU	Quart Can	10 mg	NG	NG	NG			
		50 mg	NG, DPA	NG, DPA	NG, DPA			
		100 mg	NG, DPA	NG, DPA	NG, DPA			
	Gallon Can	10 mg	NG	NG	NG	NG, DPA		
		50 mg	NG, DPA	NG, DPA	NG, DPA	NG, DPA		
		100 mg	NG, DPA	NG, DPA	NG, DPA	NG, DPA		
	Plastic Box	100 mg			NG	NG, DPA	NG, DPA	
		500 mg			NG, DPA	NG, DPA	NG, DPA	
	Cardboard Box	1 g				NG, DPA	NG, DPA	NG, DPA

Table 5-4 Extraction profile for IMR 4198 Smokeless Powder

			5 min	10 min	30 min	60 min	120 min	180 min
IMR	Quart Can	10 mg	DNT	DNT, DPA	DNT, DPA			
		100 mg	DNT, DPA	DNT, DPA	DNT, DPA			
	Gallon Can	10 mg	DNT	DNT	DNT	DNT		
		100 mg	DNT	DNT, DPA	DNT, DPA	DNT, DPA		
	Plastic Box	100 mg			DNT	DNT	DNT	
		500 mg			DNT	DNT	DNT	
	Cardboard Box	1 g			DNT	DNT	DNT, DPA	DNT, DPA

Table 5-5 Extraction Profile for Red Dot Smokeless Powder

			5 min	10 min	30 min	60 min
Red Dot	Quart Can	100 mg	NG, DPA	NG, DPA	NG, DPA	NG, DPA
		500 mg	NG, DPA	NG, DPA	NG, DPA, EC	NG, DPA, EC

Table 5-6 Optimized extraction time and sample amount for SPME GC-MS

	Optimized Extraction Time	Optimized Sample Amount
Quart Can	10 min	10 mg, 50 mg
Gallon Can	10 min	10 mg, 50 mg
Plastic Box	30 min	500 mg
Cardboard Box	60 min	1 g

The experiments were also carried in a cluttered environment to determine the false positive rate. First, these experiments were attempted at a shipping facility at the Florida International University (FIU) Chemistry Department. A couple of clean quart cans were left in the shipping facility open for 24 h and then sealed and sampled for 10 min statically using SPME. No interference peaks were observed in the chromatograms analyzed by GC-MS from 10 replicates.

5.1.4.2 Extraction from plastic boxes

The study in plastic boxes was carried in the container without any pre-treatment. It is hard to use heat to remove the organic compounds and using soap to clean the container was not very effective in removing interference. As a result, a very noisy background was observed in the plastic boxes compared to the baked cans as shown in Figure 5-3. Barely any compounds were eluted from the extractions in the blank gallon cans, only a couple of peaks caused from column bleeding; while in plastic boxes, long chains of alkanes, alkenes and alcohols were detected in the mass spectrometer. The interference in the plastic boxes can only be neglected when a sufficient amount of targeted compounds were preconcentrated on the SPME fibers. As shown in Figure 5-4, when the plastic box was analyzed by a SPME fiber for 2 hours (green chromatograph), there was a peak eluted at 10.277 min which was identifies as a long chain alcohol; however, in the 2 hours headspace extraction of 500 mg of IMR 4198 smokeless powders (red chromatograph), the peak eluted at the same retention time was identified as 2,4-DNT which is one of the targeted compounds. Thus, the interferences from the plastic boxes

may cause false alarms in reality by just comparing the chromatograms which is why mass spectrometer is critical for identification purposes.

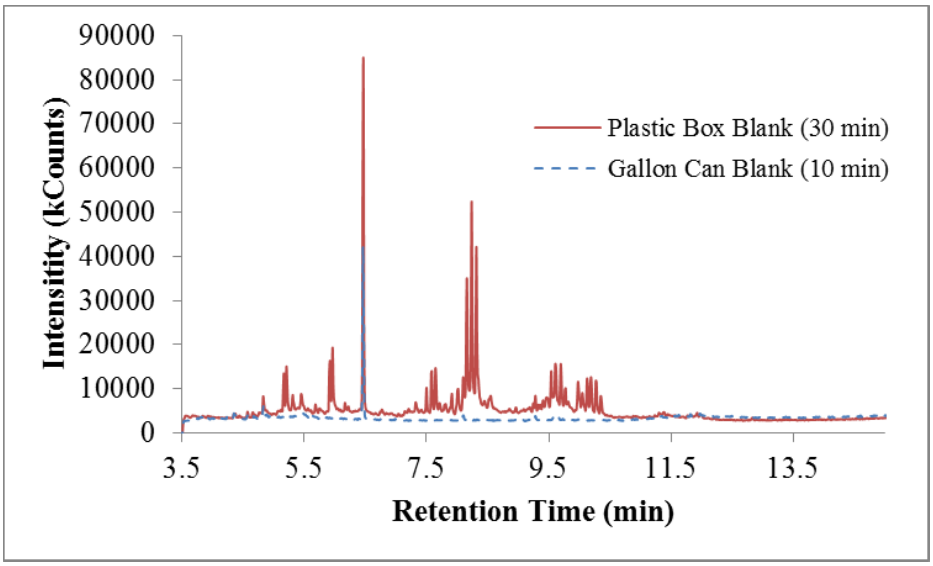

Figure 5-3 Background comparison between gallon cans (blue) and plastic boxes (red)

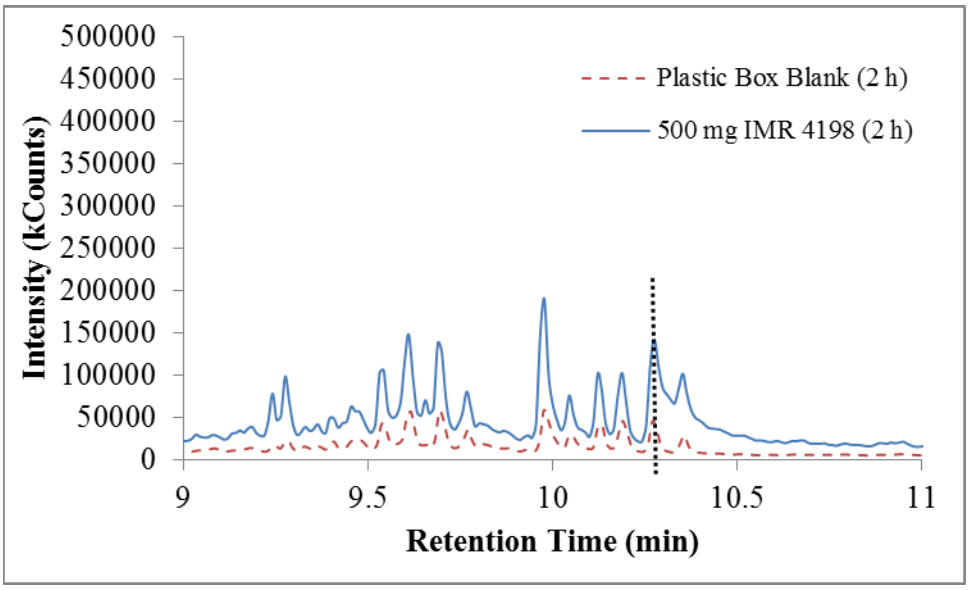

Figure 5-4 Black dotted line marked interference in the plastic boxes (red) compared to 2,4-DNT detection from 2 h extraction of 500 mg of IMR 4198 (blue)

5.1.4.3 Extraction for cardboard boxes

Different from plastic boxes, cardboard boxes did not have a large background; however, the signal intensity was also significantly reduced which could be caused by the strong adsorption of the volatile compounds with the cardboard materials. Even though a cardboard box is slightly smaller than a plastic box, it took a much longer extraction time to achieve the similar detection. The detection of DPA from both All Unique and IMR 4198 was only at the level of limit of detection (Figure 5-5) which cannot be used as a confirmation for the presence of smokeless powders. The detections of NG and 2,4-DNT were also much lower than the other containers.

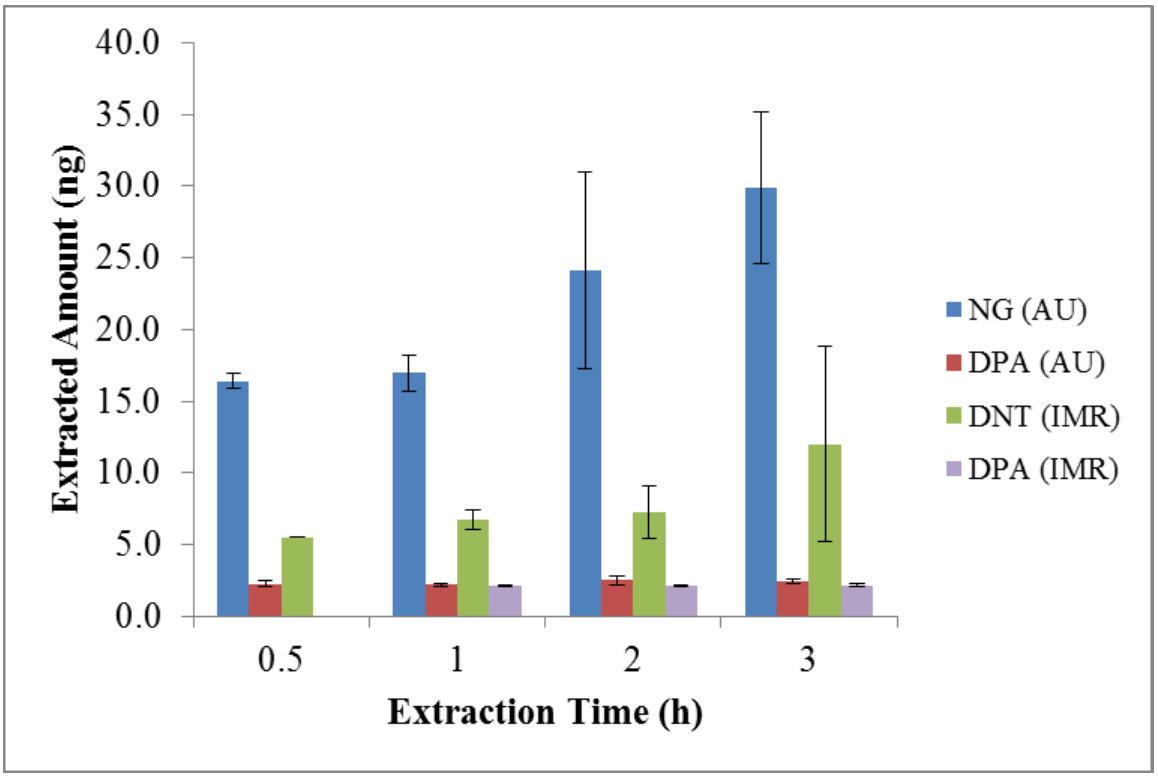

Figure 5-5 Detection of 1 g of smokeless powder in cardboard boxes

5.1.5 Summary

The SPME-GC-MS technique was successfully applied for headspace analysis of three different smokeless powders in four different scenarios. The results showed detection of NG and DPA in Alliant Unique, 2,4-DNT and DPA in IMR 4198, and NG, DPA, and EC in Red Dot which were consistent with the previously reported results [85]. In the four different scenarios, SPME extraction was only efficient in the baked metal cans which were the small size containers; with 10 min static extraction time, the targeted compounds can be extracted and detected in the GC-MS. In contrast to the small containers, preconcentraion in plastic boxes and cardboard boxes encountered different difficulties: plastic boxes were high in the background noise which caused interferences for 2,4-DNT detection and cardboard boxes had strong adsorption of the interested volatile compounds in the headspace resulting in low intensity signal. Because of these difficulties and the increased headspace volume, even with 500 mg of smokeless powders in plastic boxes and 1 g of smokeless powders in cardboard boxes, the extraction times were still too long (30 min in plastic boxes and 1 h for cardboard boxes) for forensic applications. Consequently, preconcentration techniques with high throughput need to be explored.

5.2 Headspace Profile of Twenty-four Different Smokeless Powders

Headspace profiling various smokeless powders has been accomplished using SPME fibers; however, under the laboratory setup reported (100 mg of smokeless powder sealed in 15 mL vials), the extraction times were still long considering applying into field studies [85]. Planar solid phase microextraction (PSPME) devices were reported with

increased sampling throughput [24], thus used to profile the headspace of twenty-four different smokeless powders in quart-sized cans.

5.2.1 Instrumentation

The profile of twenty-four smokeless powders were achieved using IONSCAN®-LS (Smiths Detection, Warren, NJ) for the positive mode analysis and Barringer IONSCAN® 400 IMS for the negative mode analysis. The conditions of the IMS were listed in Table 5-7.

Table 5-7 IMS conditions used for sampling larger containers and profiling twenty-four different smokeless powders

IMS operating conditions	Smiths IONSCAN®-LS	Barringer IONSCAN® 400
Polarity	Positive (+)	Negative (-)
Desorber Temperature (°C)	250	300
Drift Tube Temperature (°C)	235	115
Sample Flow (mL min^{-1})	200	500
Drift Flow (mL min^{-1})	300	350
Reagent Gas	Nicotinamide	Hexachloroethane
Compound of Interest	DPA, EC, MC	NG, TNT, 2,4-DNT

5.2.2 Materials

The smokeless powder samples were provided by a law enforcement laboratory as part of a larger study of the bulk composition of the smokeless powders. Twenty four different samples representing eight powder distributors from around the world were included in

the sample set. Table 5-8 lists the powders by the manufacture name and the smokeless powder name. The morphology of each smokeless powder was also presented in Figure 5-6, classified as rod-like, granular and flake shaped among the 24 different kinds of smokeless powder. It is important to note that both the Alliant and Hercules brand names and the Dupont and IMR brand names are from the same distributor [85]. The PSPME devices were prepared in the same manner described in Chapter 4.4.1.

Table 5-8 Twenty-four different smokeless powders' headspace were profiled using PSPME-IMS

Manufacturer	Number of powders	Smokeless Powder name
Alliant	8	Alliant 2400, Alliant Unique, Alliant American Select, Alliant Red Dot, Alliant Power Pistol, Alliant Blue Dot, Alliant Herco, Alliant Greent Dot
Hodgdon	2	Hodgdon H322, Hodgdon Trap 100
Accurate	2	Accurate 2495BR, Accurate Nitro 100
IMR	2	IMR 4198, IMR 4320
Winchester	2	Winchester 452AA, Winchester 748
Hercules	2	Hercules Herco, Hercules Blue Dot
Dupont	2	Dupont 700X, Dupont PB
Norma	2	Norma R-1, Norma N-201
Vihta Vuori	1	Vihta Vuori N133
Scot Royal Scot	1	Scot Royal Scot

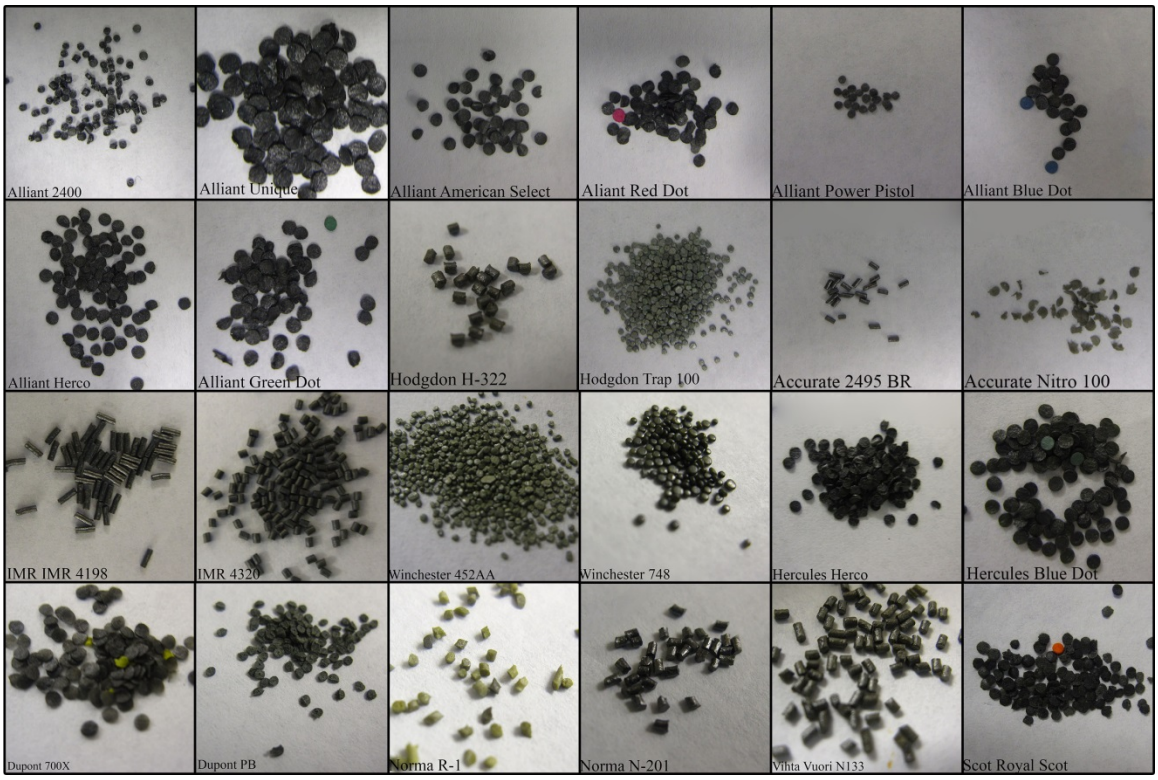

Figure 5-6 Morphology of twenty-four different smokeless powders

5.2.3 Methods

Each of the different smokeless powder were weighed to 100 mg and placed in quart-size cans in triplicates for 24 hours to allow volatile organic compounds reach equilibrium in the headspace, shown in Figure 5-7. Five (5) min static PSPME extractions were followed by IONSCAN®- LS 400 B (Smiths Detection, Warren, NJ) detection in positive mode and IONSCAN® 400 (Barringer Instruments, New Providence, NJ) detection in negative mode. Dynamic, 30 sec. extractions were also performed using a pump air sampler (Barringer) to allow air to flow through the PSPME device (0.17 L/s) followed by IMS detection.

Figure 5-7 Smokeless powders headspace profiling using PSPME and quart cans

5.2.4 Results

Volatile compounds 2,4-dinitrotoluene (2,4-DNT), nitroglycerin (NG), ethyl centralite (EC), methyl centralite (MC) and diphenylamine (DPA) were successfully detected from the twenty-four smokeless powders using PSPME devices in both static and dynamic mode (Figure 5-8).

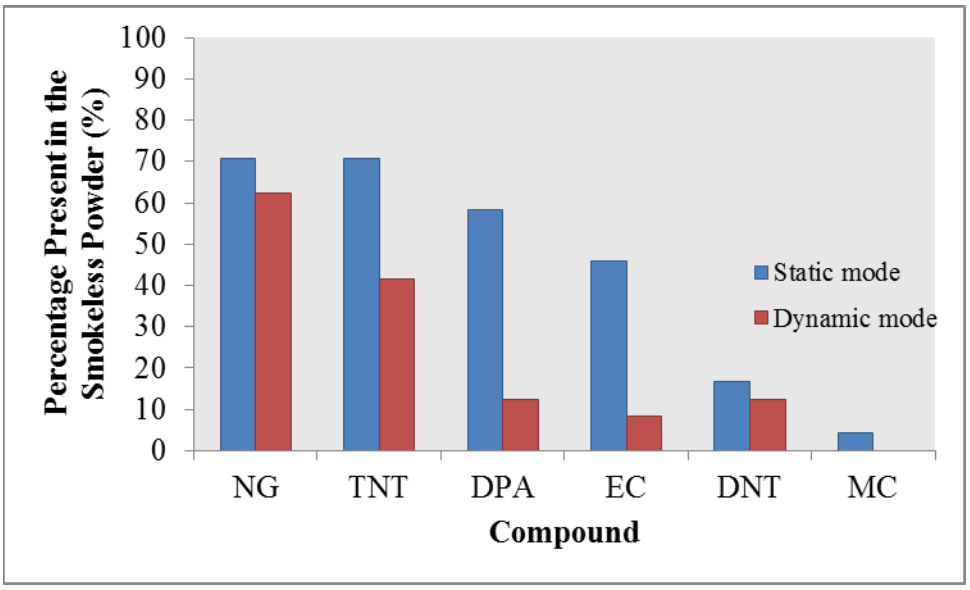

Figure 5-8 Volatile compounds distribution in twenty-four smokeless powders

The resulted profiles have shown smokeless powders from different manufacturers released different volatile compounds to the headspace based upon their differences in composition (i.e., single-based or double-based) while smokeless powders from the same manufacturer (e.g., Alliant) were determined to produce similar volatile compounds (NG, DPA, and/or EC) with different intensities.

In static mode extractions, nothing was detected in 3 out of the 24 smokeless powders and only one compound was found in 4 smokeless powders. For the 17 other smokeless powders, at least 4 different volatile compounds were found in the headspace and the presence of NG was in all 17 smokeless powders.

Dynamic extractions resulted in similar volatile compound profiles (Figure 5-9) as static extractions; however, the signal intensities observed for dynamic extractions were significant lower than that of the static extractions and the most volatile compound, NG, was dominant in the headspace profile (Figure 5-10). Breakthrough was observed since dynamic extractions resulted in detection of nothing for 1/3 of the 24 smokeless powders and most of the rest only showed detection of NG.

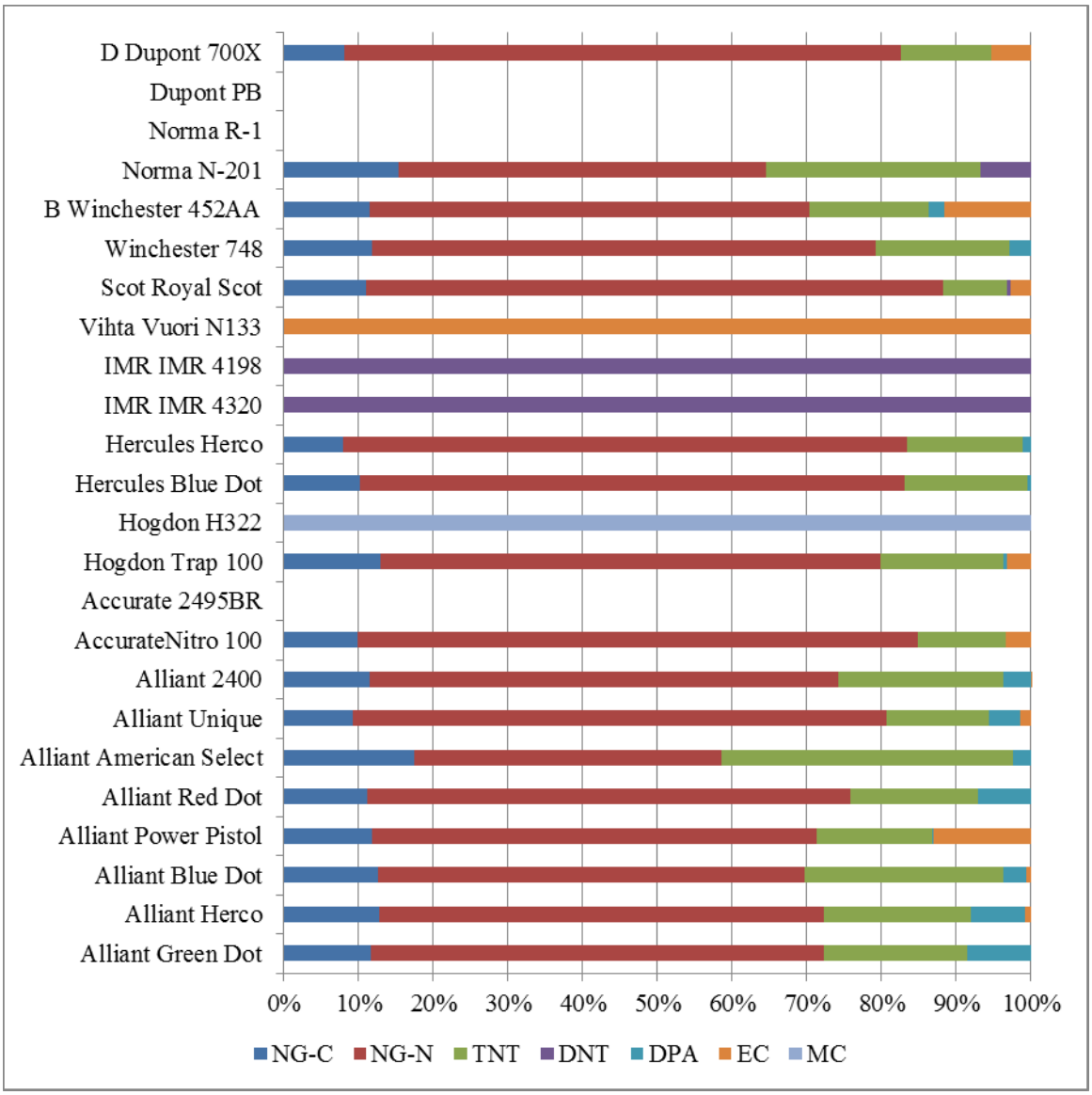

Figure 5-9 Headspace profile of twenty-four smokeless powders using PSPME static extractions

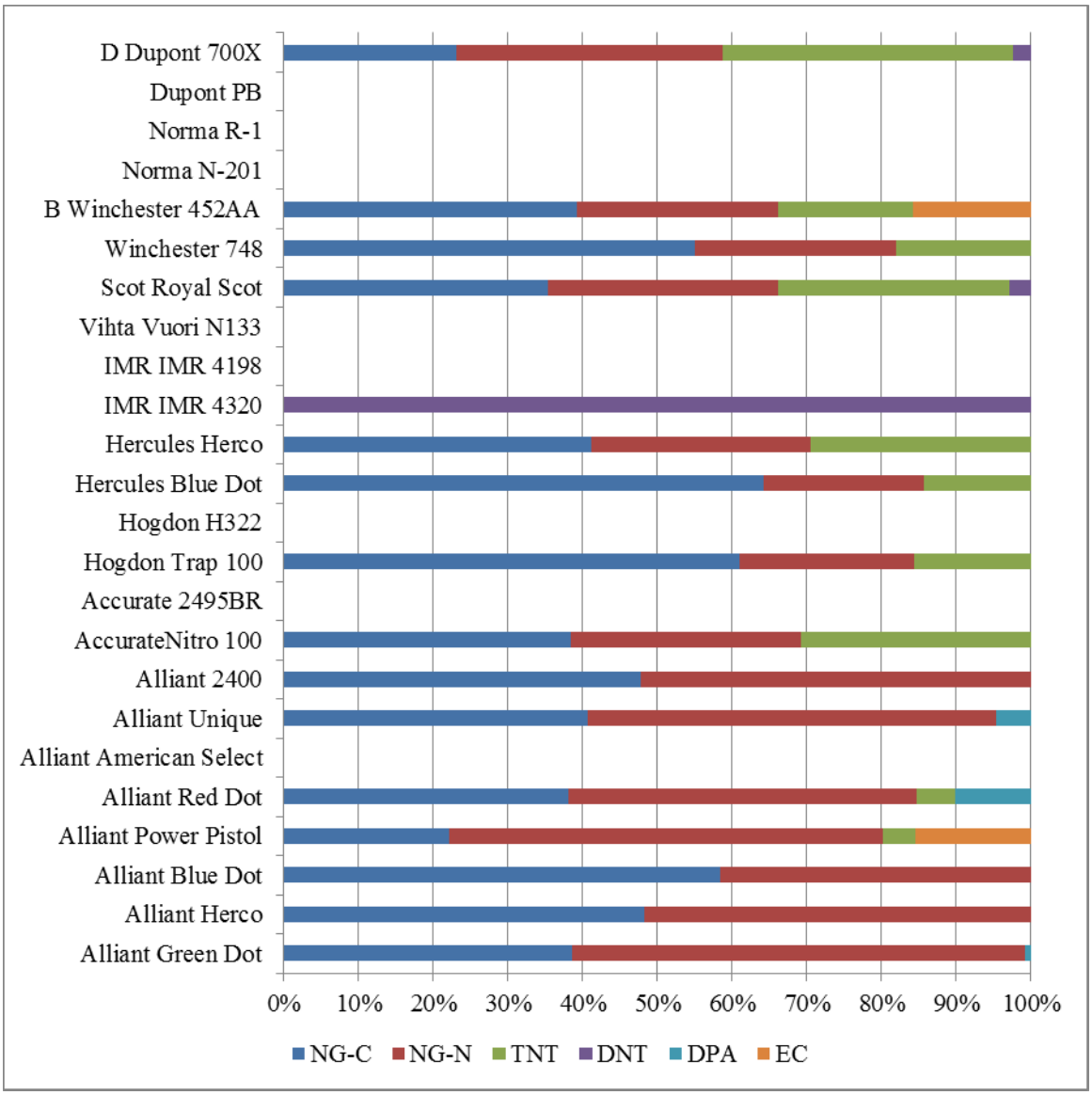

Figure 5-10 Headspace profile of twenty-four smokeless powders using PSPME static extractions

5.2.5 Summary

Headspace profiling of 24 different smokeless powders were successful using PSPME devices in both static and dynamic sampling mode, volatile compounds 2,4-dinitrotoluene (2,4-DNT), nitroglycerin (NG), ethyl centralite (EC), methyl centralite (MC) and

diphenylamine (DPA) were found in the headspace. The profiling results showed that smokeless powders from different manufacturers had different volatile compounds in the headspace resulted from differences in the compositions, while smokeless powders from the same manufacturer (e.g., Alliant) were observed to produce similar volatile compounds (NG, DPA, and/or EC) with different intensities according to individual compositions.

Static and dynamic extractions resulted in similar volatile compound profiles; however, signal intensities observed for dynamic extractions were significantly lower than that of the static extractions and breakthrough was observed in dynamic sampling mode. Accordingly, modifications still need to be made for dynamic PSPME devices to avoid breakthrough.

Chapter 6 Headspace Analysis of Peroxide Explosives using SPME-GC-MS and PSPME-IMS

In the previous chapter, results have shown improved sampling throughput with PSPME compared to SPME fibers because of the increase in surface area and phase volume along with the application of dynamic sampling mode in PSPME devices; however, the two different setup experiments couldn't compare the performance side by side. In this chapter, analysis of peroxide of explosives was achieved using both SPME-GC-MS and PSPME-IMS under the same sampling conditions which can provide the comparison of the two preconcentration techniques.

6.1 Instrumentation

Headspace sampling of solid TATP and HMTD was carried using SPME and PSPME devices and coupled to a commercial GE Ion Track (Wilmington, MA) ITEMIZER 2 IMS instrument (Figure 6-1 (a)) containing a radioactive ^{63}Ni source (10.0 mCi). The GE Itemizer 2 used the original manufactured thermal desorber as well as SPME interface setup that has been reported elsewhere [71] to couple SPME with the IMS system (Figure 4-7). Narcotics-mode (positive mode) calibration traps (GE, Wilmington, MA) containing cocaine were used to calibrate the instrument. Further TATP detection experiments were performed using the Smiths Detection IONSCAN®-LS (Smiths Detection, Warren, NJ) IMS, shown in Figure 6-1 (b), and Morpho Detection Hardened MobileTrace as shown in Figure 6-1 (c) (Morpho Detection, Wilmington, MA). The Smiths Detection IMS used two different dopants, nicotinamide (original dopant in the positive mode) and isobutyramide purchased from Smiths Detection (Warren, NJ) [86].

The Hardened MobileTrace was used as a portable IMS system and operated in the Explosives Particle Mode with dichloromethane (VICI Metronics, Inc., Poulsbo, WA, USA) and ammonia (Real Sensors, Inc., Hayward, CA, USA) dopants. Experiments performed in all IMS instruments used the default manufacture settings and are shown in Table 6-1.

Figure 6-1 Three different commercial IMS systems (a) GE IonTrack (b) Smiths Detection IONSCAN (c) Morpho Detection Hardened MobileTrace

Table 6-1 Conditions for the IMS instruments used as detectors for both SPME and PSPME sampling/preconcentration

IMS operating conditions	GE Ion Track ITEMIZER	Smiths Detection IONSCAN®-LS	Morpho Detection Hardened MobileTrace
Polarity	Positive (+)	Positive (+)	Positive (+)/ Negative (-)
Desorber Temperature (°C)	175	250	235
Drift Tube Temperature (°C)	195	235	162
Sample Flow (mL min^{-1})	500	200	*
Drift Flow (mL min^{-1})	350	351	*
Reagent Gas	Ammonia	Nicotinamide Isobutyramide	Ammonia (+) Dichloromethane (-)

* Unit was not specified in the manufacture settings

Absolute mass quantitation with SPME was analyzed using a Varian (Palo Alto, CA) CP 3800 gas chromatograph coupled to a Saturn 2000 ion trap mass spectrometer and equipped with an CP 8400 autosampler (Varian Inc., Walnut Creek, CA). The GC-MS conditions are listed in Table 6-2. The MS was operated in electron ionization mode (-70 eV) with a scan range of 40-450 m/z and a delay of 3.5 minutes.

Table 6-2 GC-MS conditions for SPME headspace mass quantitation

Column type	Restek 15 m x 0.25 mm ID x 0.25 µm Rxt-5 fused silica
Carrier gas	Helium at a flow rate of 1.0 mL min^{-1}
Split ratio	5:1
Injector Temperature	180 °C
Column oven parameters	40 °C, hold for 1 min. 100 °C at 5 °C min^{-1}, hold for 6 mins. 250 °C at 10 °C min^{-1}, hold for 5 mins.
MS Transfer Line temperature	280 °C
MS Ion Trap Temperature	180 °C

6.2 Chemicals

The TATP and HMTD explosives were synthesized and prepared in the University of Rhode Island laboratory [44]. Two different HMTD solid explosives were provided in this research which were crude HMTD and crystalized HMTD. Crude HMTD has a small amount of solvent residues and impurities left in the solid explosives which could cause more degradation compared to crystallized, clean HMTD. Cocaine standards were purchased from Cerilliant (Round Rock, TX) for the positive mode IMS calibration.

Further headspace static extraction studies were conducted using certified TATP standards of 0.1 mg mL^{-1} (AccuStandard, New Haven, CT) in acetonitrile. The TATP stock solution was diluted to concentrations 5, 10, 15, 20, 25 and 30 ng μL^{-1} using methanol or acetonitrile of optima grade (Fisher Scientific, Fair Lawn, NJ) for absolute mass quantitation in the SPME-GC-MS and PSPME-IMS sampling/detector configurations.

6.3 Methods

The PSPME sampling devices were used for both static and dynamic extractions. Approximately 10 mg of solid TATP explosive was placed in a half gallon glass jar and was allowed to equilibrate for 30 minutes. Static extractions were performed by suspending the PSPME devices over the solid TATP sample at the opening of the jar. Various sampling times (10 s, 30 s, 1 min, 2 min, 5 min) and temperatures (20 °C, 25 °C and 40 °C) were tested in triplicates to determine the minimum amount of time required for the detection of TATP using the PSPME devices. For dynamic extractions, the PSPME device was inserted into a nozzle of a handheld vacuum sampler (Barringer) in order to allow the air sample to flow through the PSPME device at a rate of 0.17 L s^{-1}. All static extractions were equilibrated at different temperatures; however, all dynamic sampling was performed at room temperature (20 °C).

The studies involving HMTD was prepared by placing approximately 100 mg of solid explosives in a half gallon glass jar and was allowed to equilibrate for 24 hours. The PSPME devices were suspended over the solid HMTD sample at the opening of the jar and vapors were extracted statically with various sampling times (1 h, 2 h, 4 h, 6 h, 16 h)

and two different temperatures (25 °C and 40 °C) to achieve headspace preconcentration of volatile compounds over the headspace of HMTD using the PSPME devices. In order to identify the volatile compounds in the headspace, standards of several reported odors [36], such as hexamine, dimethylformamide (DMF), trimethylamine (TMA) and ethanol, were directly spiked on the PSPME devices and the spectrum was compared to the headspace spectrum of HMTD solid explosives. All the solutions were obtained at University of Rhode Island and because of the strong odor emitted by TMA, a dilution of 5 % of TMA/ethanol was sealed in a 15 mL vial with a headspace crimp cap and PTFE/silicone septa.

Further static extractions using TATP standards were performed in the research laboratory prepared in a similar manner in which a quart can was spiked with 10 μL of varying concentrations of TATP solutions (5 – 40 ng μL^{-1}) in which the PSPME device was suspended over the TATP sample for different extraction times (0.5 to 10 minutes). Calibration of the IMS instrument was conducted by directly spiking 2 μL of standard TATP solutions of varying concentration. Calibration and confirmation of TATP in the GC-MS was performed by spiking 1 μL TATP solutions in the instrument with the CP 8400 autosampler.

The optimum equilibrium time was obtained by conducting the static extractions at different elapsed times after spiking the solutions at the bottom of the cans in triplicates. Once the optimized equilibrium time was achieved, 5 μL of standard solutions of known concentration ranging from 5 to 30 ng μL^{-1} were spiked into a quart-sized can containing a suspended PSPME filter and sealed immediately for 5 min static extractions. The

signals were recorded and plotted to give a quantitative mass calibration of TATP in the PSPME devices.

Evaluation of the extraction recovery of SPME and PSPME was achieved by spiking the desired amount of TATP on a quart can and extracting immediately without headspace equilibrium development. Detection of TATP extracted by SPME was performed using the Varian GC-MS, using the conditions described in Table 6-2. Detection of TATP extracted by PSPME was analyzed with Smiths Detection IONSCAN®-LS IMS without further modification.

Field sampling was also done for TATP using the portable Hardened MobileTrace IMS system. Five hundred (500.1) mg of solid TATP which is used for canine training was placed in a petri-dish and placed at the bottom of a cardboard box (0.6 m × 0.6 m × 0.9 m). Five (5) PSPME were taped round the cardboard box the same time as the TATP was placed in the box as shown in Figure 6-2 where the PSPME devices were at different distances from the TATP source. The box was set in the parking lot of the chemistry building of University of Rhode Island. The weather conditions were windy with temperatures of ~ 10 °C, harsher conditions than the ideal laboratory environment. After equilibrium/extraction time 1 hour, the PSPME devices were taken out from the box and analyzed by the IMS. The sampling was also achieved in a different way where the distance from the TATP source was fixed as 10 inches and 15 min, 30 min and 60 min extraction times were used to test how efficient the PSPME devices are when they are relatively close to the source. At the end of the field sampling, one PSPME device was used for dynamic sampling of headspace of the whole cardboard box for only 30 seconds.

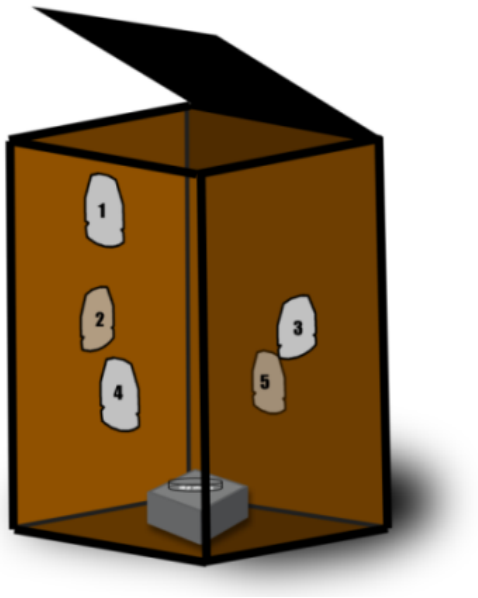

Figure 6-2 PSPME were placed inside a cardboard box at different distances from the TATP source

6.4 Results

6.4.1 Surface Area Analysis for PSPME devices

The PSPME devices have shown extraordinary performance in the headspace profiling of smokeless powders. To further evaluate the performance, first, surface area analysis of the dynamic PSPME devices was performed in the Pacific Northwest National Laboratory (Richland, WA) using a Quantachrome FloVac Degasser (Boynton Beach, FL) for degassing the sample and a Quantachrome Autosorb iQ_2 for nitrogen Brunauer-Emmett-Teller (BET). First, a PSPME filter and an uncoated glass filter were cut into ~ 6 × 9 mm strips and were placed into two large bulb 9 mm BET tubes separately. The Quantachrome FloVac Degasser was used for degrassing the samples for 3 hours at 150 °C. After degassing, nitrogen BET was performed on the samples using the Quantrachrome Autosorb iQ_2 by taking 40 adsorption and 40 desorption points. Surface

area calculations were then performed using a 5-point multipoint BET isotherm. Pore sizes and distributions were calculated using Barrett-Joyner-Halenda (BJH) adsorption isotherm.

For the PSPME devices with a 2.4 cm diameter, the surface area was determined as ~ 0.15 m^2 and the phase volume was calculated as 300 mm^3. In comparison to SPME fiber, PSPME has a ~ 2 x 10^4 fold increase in surface area than SPME fiber (~ 9.5 x 10^{-6} m^2) and the extraction phase volume of a PSPME disk is calculated to be greater than 500 times, compared to the commercial fiber SPME with a maximum phase volume of 0.6 mm^3 [80]. Digital microscope imaging (Keyence) was also performed to characterize the surface of the PSPME in comparison to the uncoated glass filter (Figure 6-3). The cross-section thickness of a PSPME device was determined to be ~ 324 μm (Figure 6-3 (d)) while an uncoated glass filters had a cross-section thickness of ~ 347 μm (Figure 6-3(b)). No increase in cross-sectional thickness indicates the sol-gel based PDMS is well incorporated into the glass-filter surface. Furthermore, surface images (Figure 6-3**Error! Reference source not found.** (a) and (c)) show increased thickness of the glass fibers by ~ 2 μm in PSPME, thus enhancing the capacity and phase volume. Further surface analysis studies show a decrease in glass filter surface area after coating, declining from 5.244 m^2/g (uncoated glass filter) to 2.196 m^2/g (coated glass filter), in agreement with the thickness measurements of the PSPME in Keyence digital microscope (Figure 6-3).

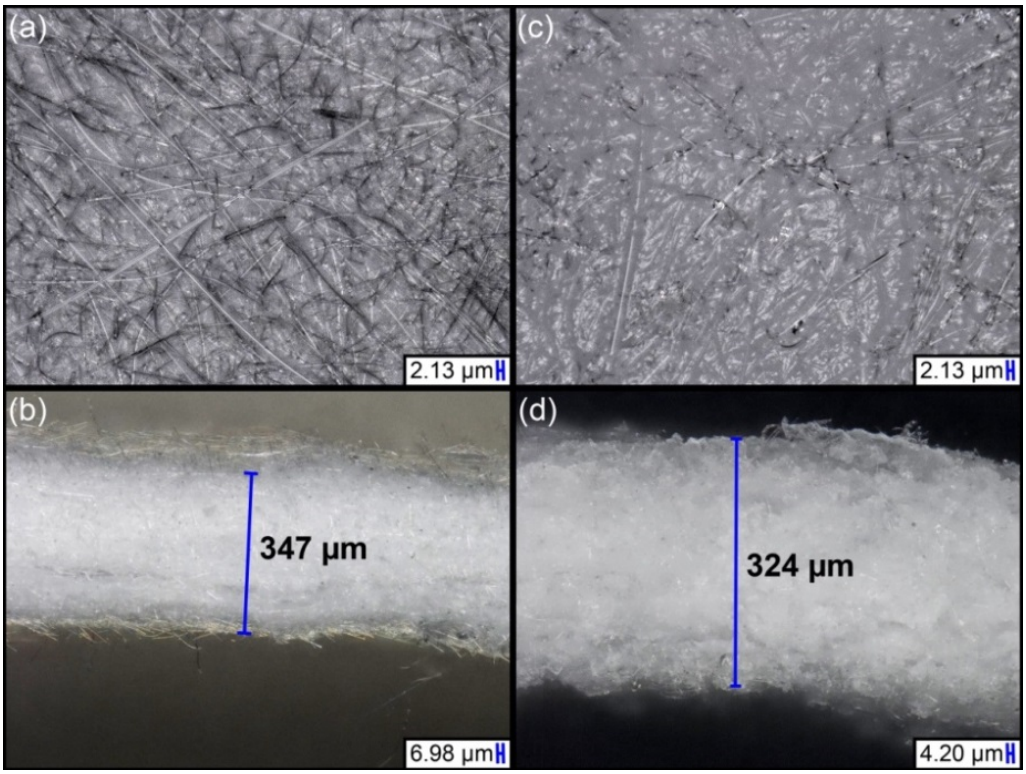

Figure 6-3 Microscope images of the surface and cross-section of an uncoated glass filter, (a) and (b) respectively, and images of the surface and cross-section of a coated PSPME devices, (c) and (d) respectively

6.4.2 Detection of Solid TATP

Various static extraction times were used at room temperature (20 °C), 25 °C and 40 °C to determine the shortest extraction times for the detection of a 10 mg TATP sample. Detection of TATP was achieved within a 1 minute static extraction of the headspace of a half-gallon glass container at room temperature (Figure 6-4). In fact, after a one-minute static extraction, the pool of protonated clusters associated as the reactant ion peak (RIP) in the IMS was completely depleted by the TATP on the PSPME device, giving two strong signals at 4.3 ms and 4.7 ms separately corresponding to reduced mobilities (K_0) of 2.13 $cm^2V^{-1}s^{-1}$ and 1.95 $cm^2V^{-1}s^{-1}$ in GE-IMS. The identity of the peak was confirmed

by direct spiking 2 µL 1000 ng μL^{-1} TATP in dichloromethane onto a PSPME device forming two peaks with the same drift time as shown in Figure 6-5 and the drift time agree with a previous publication under the same conditions [87]. Similar results were obtained at elevated temperatures with even shorter extraction times and greater signals. Detection for TATP was achieved within 10 seconds of static extractions at 40 °C (Figure 6-6).

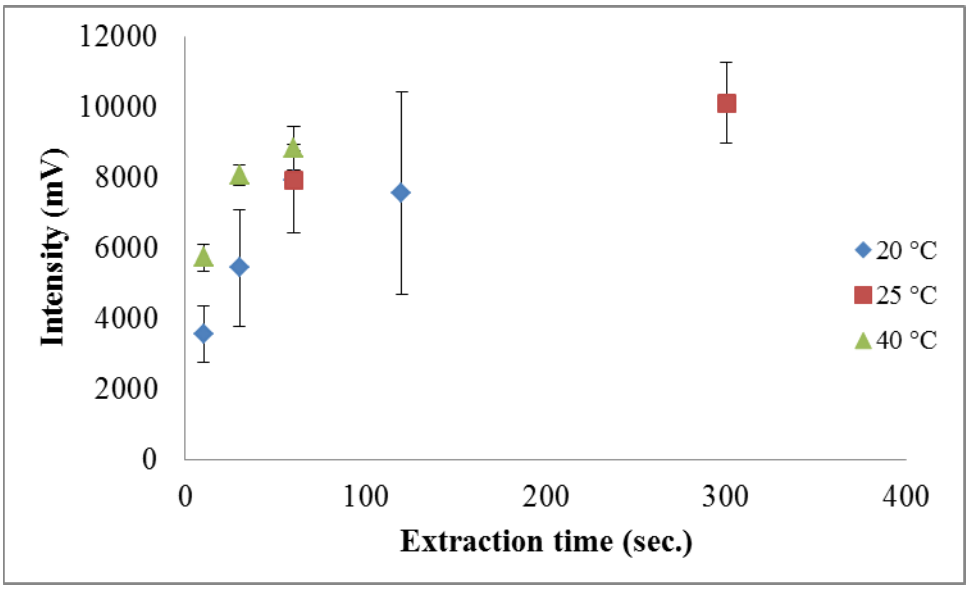

Figure 6-4 Signal observed at 4.3 ms at different static extraction times of 10 mg of TATP at different temperature profiles

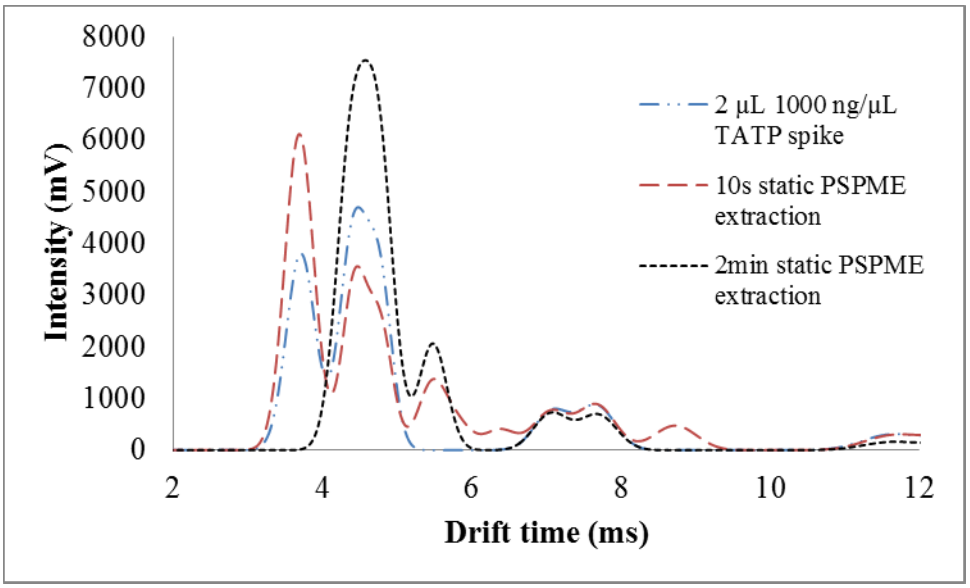

Figure 6-5 IMS plasmagram of static PSPME TATP extractions performed at 20 °C with varying extraction times (10 s – 2 min). Confirmation of TATP was performed by manually spiking 1000 ng µL^{-1} unto the PSPME device followed by detection via IMS.

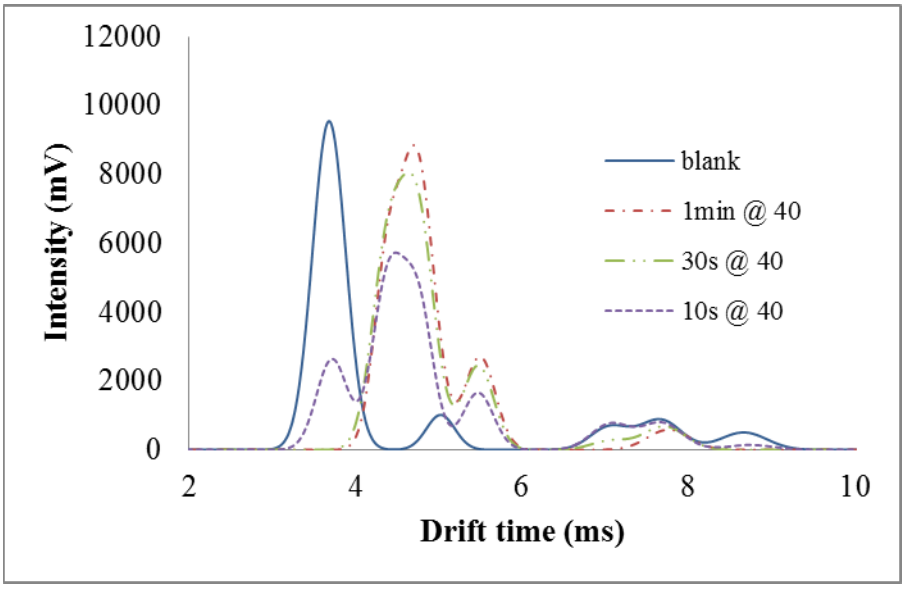

Figure 6-6 Detection for TATP was achieved within 10 seconds of static extractions at 40 °C

Dynamic extractions using the PSPME devices produced greater IMS signals with shorter extraction times. A 5 second extraction at room temperature (20 °C) produced a strong signal of TATP (4.3 ms and 4.7 ms peaks in the plasmagram), completely depleting the RIP (3.7 ms) by the saturated amount of TATP present in the PSPME device, after sampling a total volume of 0.85 L (Figure 6-7).

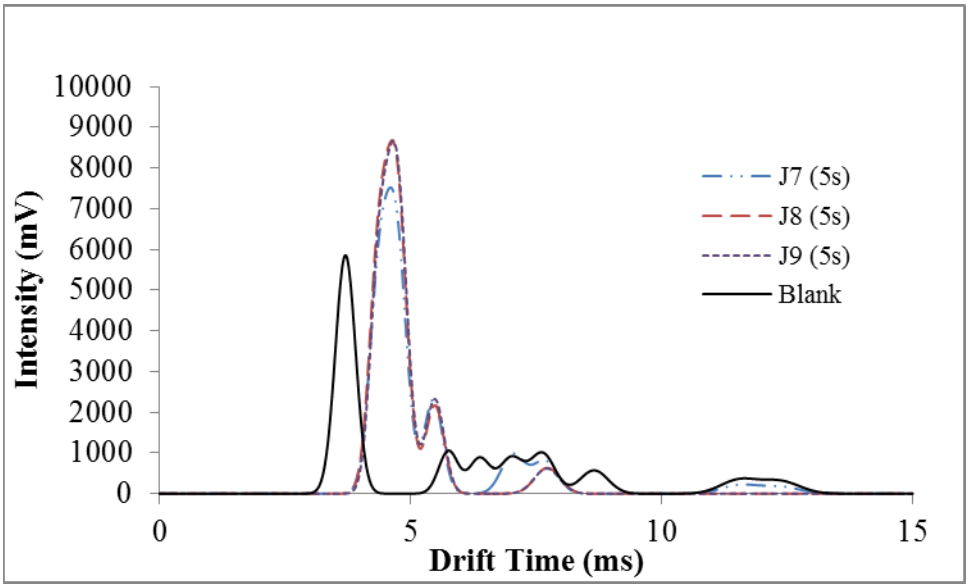

Figure 6-7 Dynamic extractions using the PSPME devices produced greater IMS signals with only 5 s extraxtion time

6.4.3 Detection of Standard Solutions of TATP

Detection of TATP in the Smiths IMS was observed within 1 minute of static extraction with 0.5 µg spike of a TATP standard in the quart container, generating a peak with a drift time of 6.7 ms and a reduced mobility (K_0) of 2.57 $cm^2V^{-1}s^{-1}$ in close agreement with previously stated reduced mobility of TATP [88] (Figure 6-8). The reduced mobility (2.57 $cm^2V^{-1}s^{-1}$) is different from other reported values [89,90] and could be caused by decomposition of TATP at an increased temperature and/or formation of

different adducts with different dopants applied. Additional identification and quantitation of the TATP was conducted by directly spiking 2 µL of certified standard solutions diluted to concentrations ranging from 0.5-5.0 ng μL^{-1} (Figure 6-9).

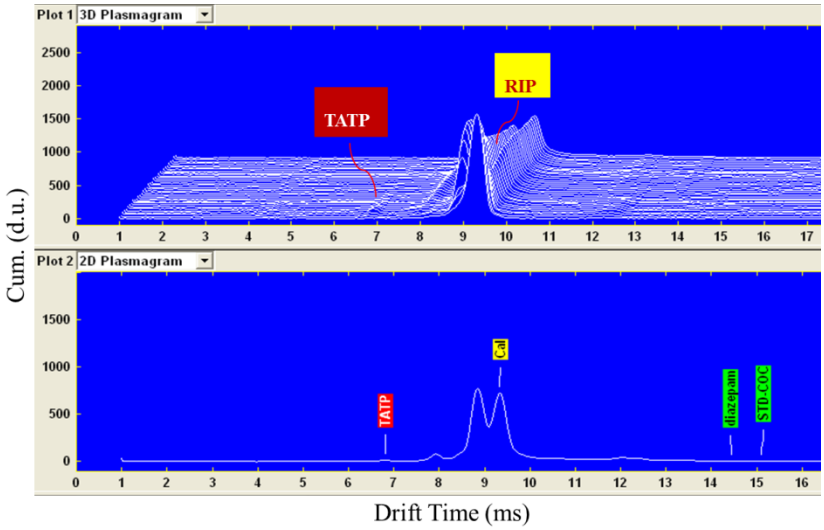

Figure 6-8 3D Plasmagram and 2D Plasmagram show detection of TATP in the Smiths IMS where reactant ion peak (RIP) was consumed during the ionization

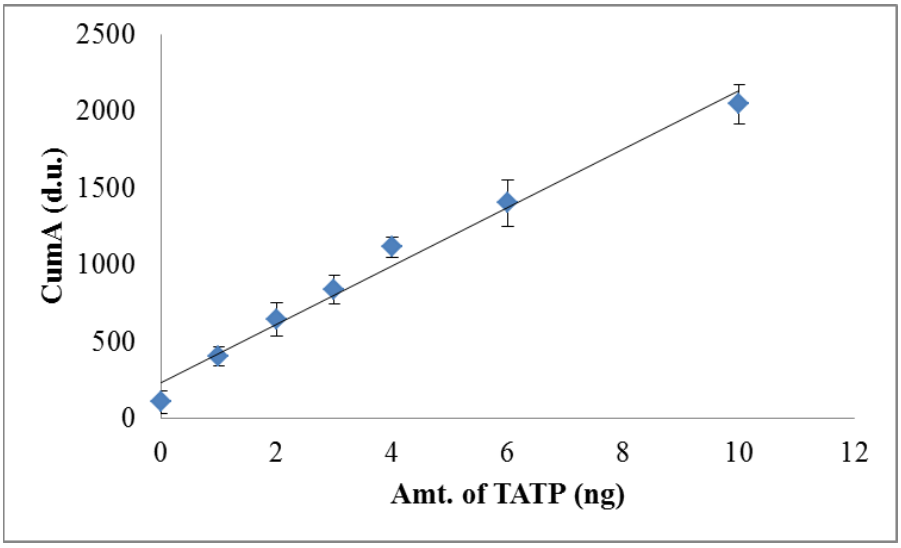

Figure 6-9 TATP calibration by spiking 2 µL TATP of the following concentrations: 0.5, 1.0, 1.5, 2.0, 2.5, 3.0, 5.0 ng μL^{-1} onto a PSPME device detected at 6.7 ms

6.4.4 Absolute mass calibration of TATP in PSPME filters

A response curve was generated using the observed maximum amplitude (d.u.) from the Smiths IONSCAN resulting in the following linear regression line Equation 6-1:

$$y = 190.05\ x - 229.72,\ r^2 = 0.984 \qquad \textbf{Equation 6-1}$$

From this method, the minimum detectable amount of TATP in the IMS instrument was determined to be 1.4 ng.

Since a PSPME extraction is an equilibrium technique similar as a SPME, this technique can be used for quantitative analysis. Headspace calibration was achieved by spiking a known amount of TATP into a closed system and headspace sampling using PSPME at the equilibrium time of 5 minutes (Figure 6-10). Dopant selection is essential for optimal instrument performance in order to form stable and identifiable analyte ions and suppressing ionization of unwanted analytes. Isobutyramide was used for calibration of TATP due to its reported more accurate detection on peroxide-based explosives [86]. Response curves from the Smiths IONSCAN using the nicotinamide and isobutyramide are given in Equation 6-2 and Equation 6-3 respectively:

$$y = 20.04\ x - 272.3,\ r^2 = 0.986 \qquad \textbf{Equation 6-2}$$

$$y = 22.58\ x - 384.5,\ r^2 = 0.986 \qquad \textbf{Equation 6-3}$$

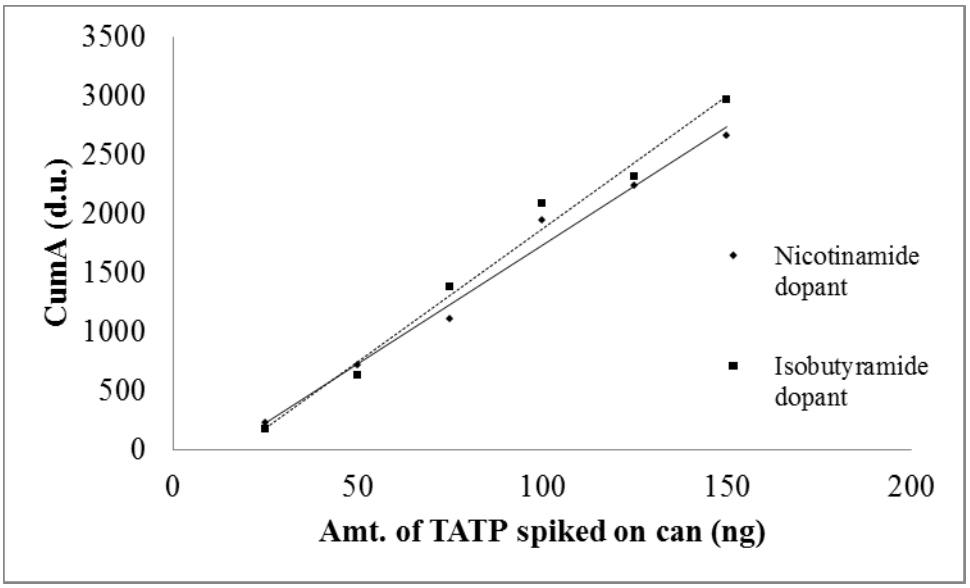

Figure 6-10 TATP headspace calibration obtained from 5 minute static PSPME headspace extraction of TATP (spiking 5 µL of solutions of the following concentrations: 5, 10, 15, 20, 25, 30 ng µL^{-1})

The response signals observed in the IMS were similar using either the nicotinamide or the isobutyramide dopant, thus majority of the experiments were performed using the initially installed nicotinamide dopant. After 5 minutes of static PSPME extractions, the minimum amount of detectable TATP vapors when spiked and extracted in the can using both dopants was determined to be approximately 19 ng, as shown in Figure 6-10.

6.4.5 Headspace extraction recovery comparison of PSPME and SPME

Minimum amount of extraction time for detection of 100 ng of TATP for PSPME was observed to be 0.5 minutes in comparison to 5 minutes using SPME (Figure 6-11). Comparison of the extraction recovery by varying concentration of TATP was performed by spiking different nanogram-level of TATP standard and extracting for five minutes. Minimum amount of TATP required to be spiked into the cans in order for detection of

TATP was 100 ng. The amount of TATP recovered using PSPME was calculated by using an external calibration curve with the regression line in Equation 6-1. For SPME analysis on the GC-MS, the following linear regression curve Equation 6-4 was used:

$$y = 2539\ x - 3592,\ r^2 = 0.988 \qquad \textbf{Equation 6-4}$$

Recovery of TATP on PSPME and SPME was determined to be approximately 15% and 5% respectively as shown in Table 6-3. Thus, the increased surface area and phase volume of PSPME offers much greater recovery rate and faster detection in comparison to the commercially available fiber-based SPME.

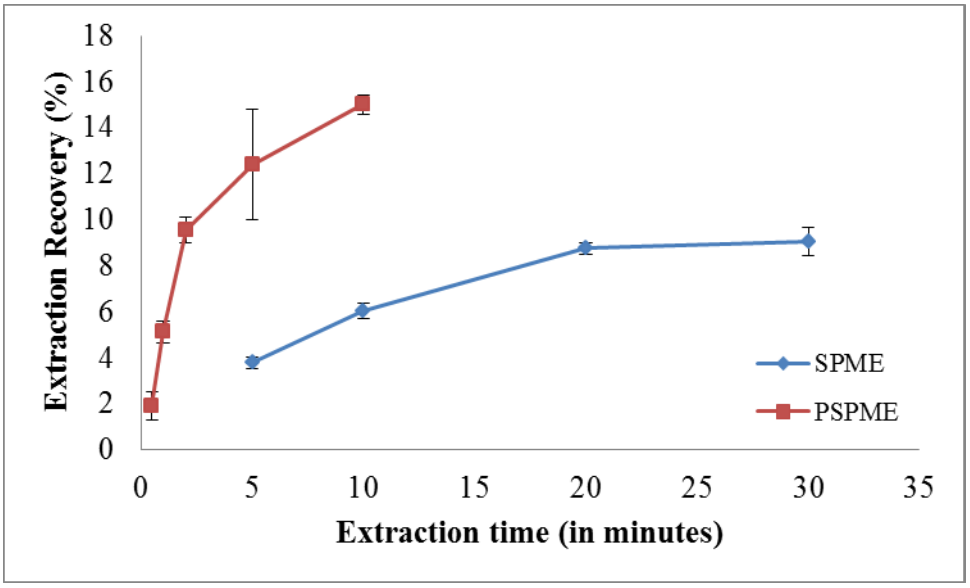

Figure 6-11 Percent recovery comparison of PSPME and SPME by different static extraction time (0.5 – 30 minutes) of 100 ng TATP

Table 6-3 Percent recovery comparison of PSPME and SPME by 5 minutes static extraction of different amount of TATP

	PSPME		SPME	
Amt. spiked in can (ng)	Amt. of TATP recovered (ng)	Recovery %	Amt. of TATP recovered (ng)	Recovery %
50.0	2.58	5.2%	2.63	5.3%
75.0	4.63	6.2%	4.26	5.7%
100.	9.00	9.0%	3.45	3.5%
150.	21.0	14. %	7.03	4.7%
200.	35.1	18.%	9.35	4.7%
300.	61.8	21.%	13.2	4.4%
400.	79.2	20.%	16.9	4.3%

6.4.6 Field Sampling of TATP

Besides laboratory work, the headspace analysis method was also tested in the field sampling with harsh conditions where the temperature was low and the surroundings were highly clustered. The portable IMS instrument had a significant peak in the background sampling which proved the environment tested had contaminations; however, the background peak did not interfere with the TATP detection peak as shown in Figure 6-12. For all the scenarios for static extractions using PSPME devices in the large container, TATP was detected within one hour equilibrium/extraction time regardless of the distance of the PSPME device from the explosive source; the closer the distance was to the source, the greater the signal intensity because of the high concentration of vapors close to the source (Figure 6-12). When the device was fixed at a certain distance close

to the explosives with varying extraction times (15 min – 60 min), 15 min extraction time was sufficient to detect TATP in the headspace where longer the extraction time, corresponded to greater signal intensity (Figure 6-13). Detailed detection results were listed in Table 6-4. After all the static extractions were completed, the cardboard box was sampled with the dynamic sampler for 30 seconds over the headspace which was sufficient sampling to detect TATP in the IMS system (Figure 6-14).

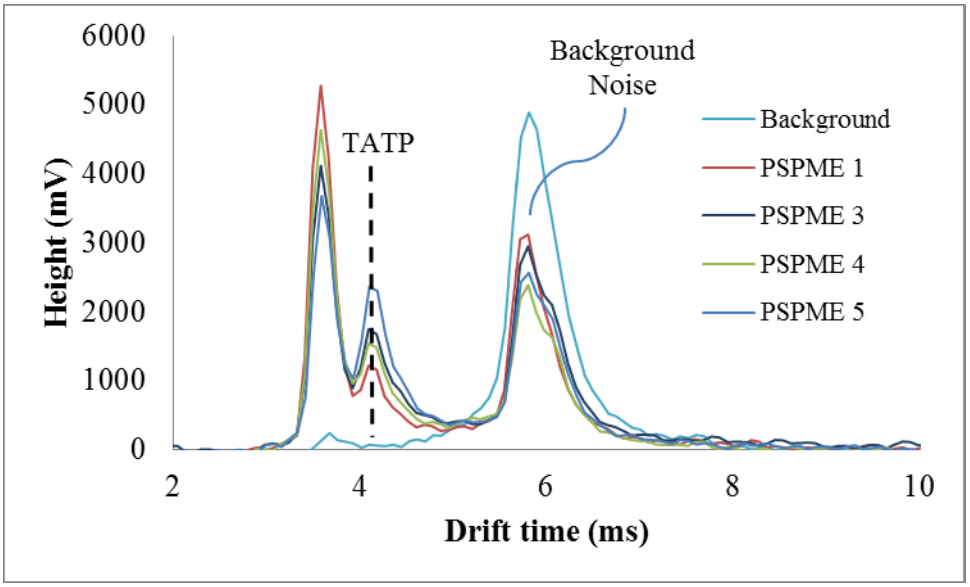

Figure 6-12 Field sampling of TATP in a cardboard box with 5 PSPME devices placed at different distances from the TATP solid explosives. All the devices showed detection of TATP which were preconcentrated from the headspace.

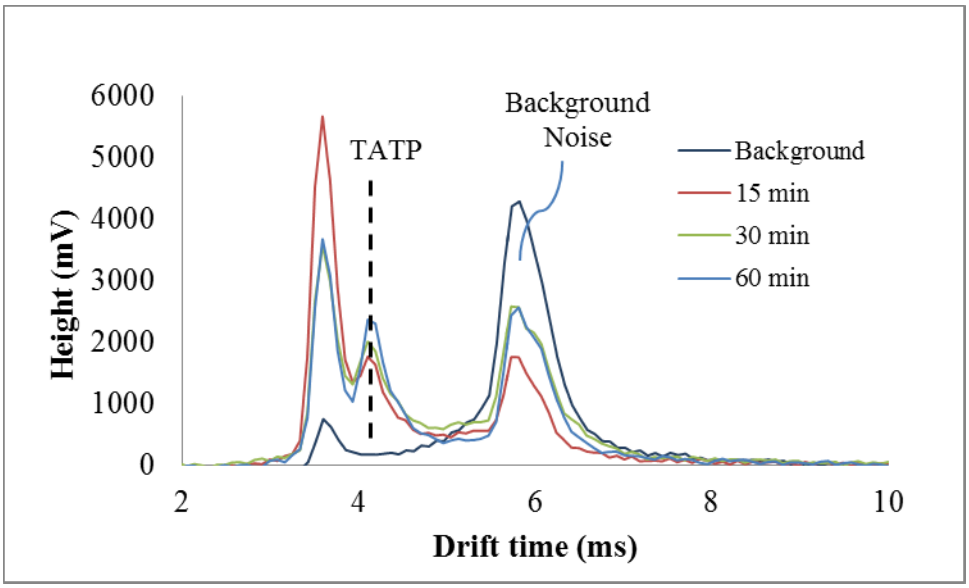

Figure 6-13 TATP detection in different extraction time at a distance of 10 inches from the explosive source

Table 6-4 Field sampling of TATP with varied distance and varied extraction times

		Distance (in.)		
		12	24	36
PSPME static extraction time (min.)	15	-		
	30	+	-	
	60	+	+	-

(-) no alarm for TATP (below alarm threshold)
(+) alarm for TATP

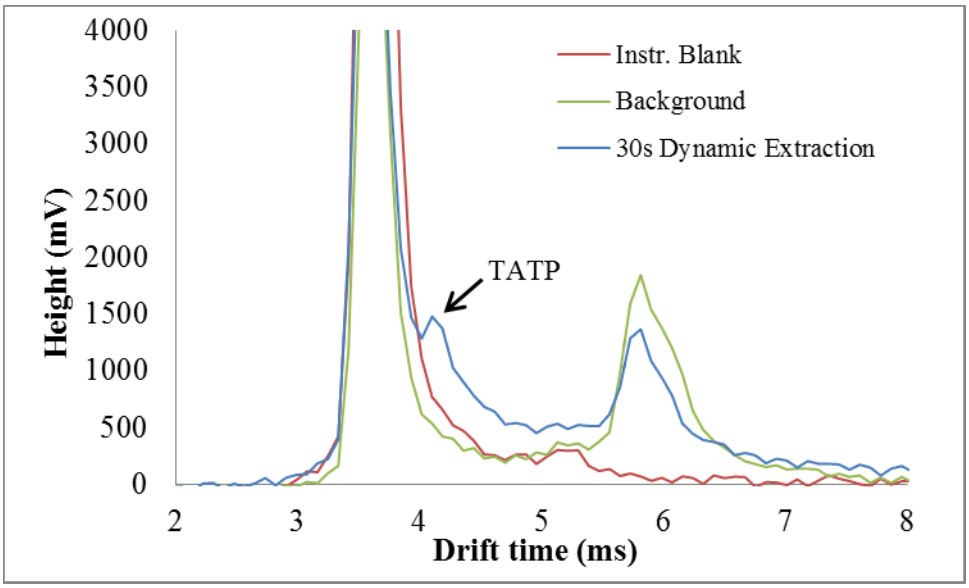

Figure 6-14 TATP detection with only 30 s dynamic extraction over the headspace of the cardboard box

6.4.7 Detection of HMTD

Because of low volatility, HMTD detection was much harder compared to TATP solid explosives. With longer extractions and elevated temperatures, more volatile compounds were released into the headspace. As shown in Figure 6-15, after heating in the oven at 40 °C for over 24 hours, the headspace was analyzed with SPME fibers for 2 hours and 16 hours. Within 2 hours extraction of crude HMTD, two peaks were observed with drift times of 5.59 ms and 6.19 ms in the negative mode. In 16 hours extraction of crystallized HMTD, two similar peaks were obtained with an addition peak at the drift time of 5.73 ms in negative mode; however, none of these peaks were identified without proper standard solutions. In positive mode, there was a small peak shown in the spectrum at the drift time of 10.18 ms which was consistent with 30 s extraction over the headspace of 5 % sealed TMA in a vial (Figure 6-15 (b)). Further confirmation was still needed for identification. With PSPME devices, 2 hours extraction time was able to detect the three

peaks shown in 16 h extraction using SPME and 16 hours extraction showed significant peaks in the spectrum (Figure 6-16). The peak at 4.5 ms was a decomposition product from HMTD which alarmed for urea nitrate in the IMS system and the other two peaks remained unconfirmed. The presence of TMA in positive mode was not confirmed since TMA extractions could not be achieved using PSPME in the sealed headspace vial.

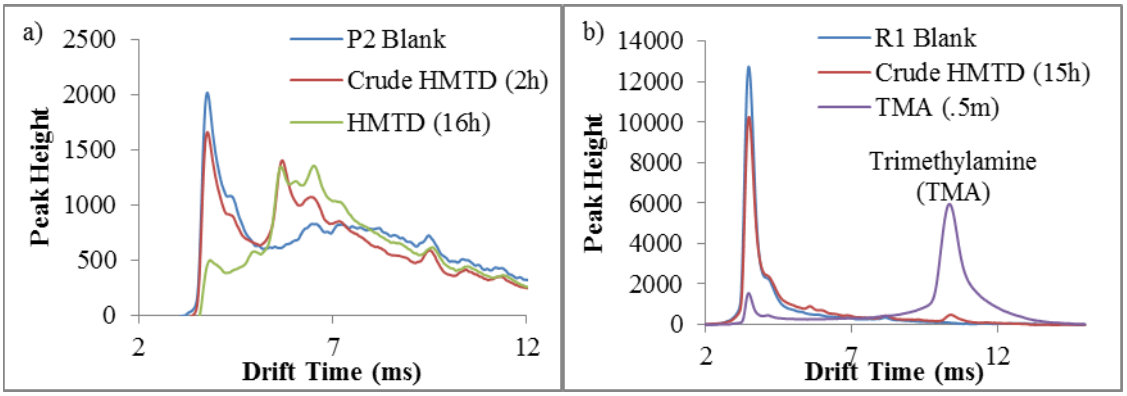

Figure 6-15 SPME extraction of HMTD and the following detection in GE Itemizer 2 in (a) negative mode and (b) positive mode

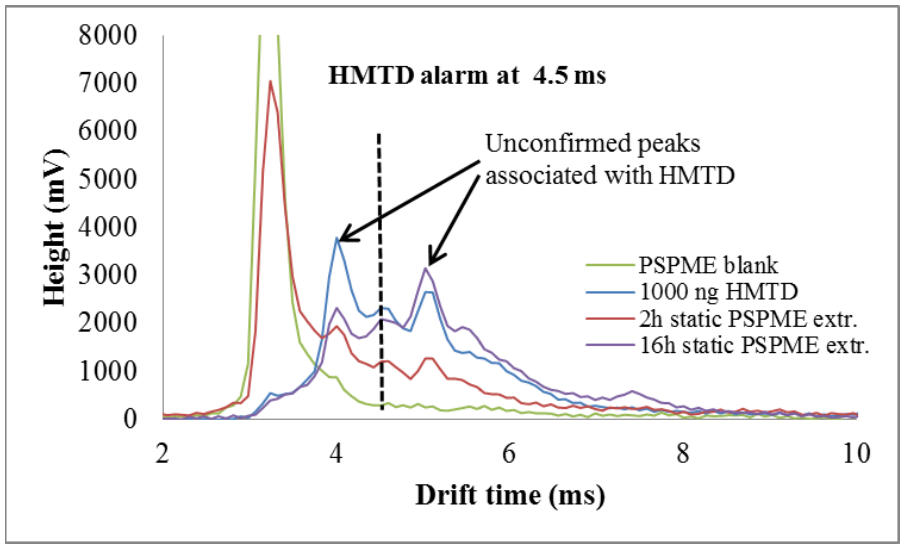

Figure 6-16 PSPME extraction of HMTD and the following detection in portable IMS Hardened MobileTrace

6.5 Summary

Two different peroxide explosives were analyzed in the headspace, TATP and HMTD. Solid TATP can be easily detected with PSPME in static sampling mode as fast as 1 min and in dynamic mode as fast as 5 s, both sampling method completely depleted the reactant ion peak in the IMS system. When standard solutions of TATP were used for headspace analysis, SPME-GC-MS and PSPME-IMS performances were compared side by side. PSPME improved the sampling throughput by introducing a higher surface area and phase volume along with the dynamic sampling option and the ruggedness of the devices allowed for portability for field sampling; however, the identification capability became a disadvantage when the devices were coupled to IMS systems.

Minimum amount of extraction time for detection of 100 ng of TATP spiked in the quart-size cans for static PSPME was observed to be 0.5 minutes in comparison to 5 minutes using SPME which showed the increased surface area allowed PSPME to reach equilibrium much faster than the conventional fiber geometry. Additionally, recovery of TATP on SPME remained at 5 % no matter how much TATP solutions were originally spiked into the containers, while the recovery on PSPME and SPME increased from 5 % to 15% when the original amount spiked into the containers increased. The recovery results showed the increased phase volume of PSPME improved the preconcentration capacities. Unfortunately, HMTD explosives have very low vapor pressure in the headspace and the preconcentration was not a success using either SPME or PSPME. At least 16 hours was needed for SPME and 4 hours for PSPME to accumulate two unidentified decomposition products over the headspace of 100 mg of solid HMTD at an

elevated temperature (40 °C). Even though the PSPME devices shortened the preconcentration time for almost 12 hours, the detection using an IMS system couldn't provide identification information for the compounds accumulated on the device.

Upon finishing the laboratory experiment, only PSPME-IMS was taken to the field for headspace analysis of TATP because SPME fibers are too fragile for field sampling. The harsher environmental conditions did not impede the performance of PSPME-IMS; with one hour equilibrium/extraction time, all the PSPME devices at difference distances from the TATP explosive source showed detection in the IMS.

Chapter 7 Double Blind Study to Evaluate the Performance of PSPME-IMS

As stated in the last chapter, using IMS as a detector can be a disadvantage because lacking of identification capability; thus, in this chapter, the performance of PSPME-IMS was further evaluated using double blind study.

7.1 Instrumentation

All the double blind study experiments were completed using the Morpho Detection Hardened MobileTrace, because this IMS system can achieve detection ions in both positive mode and negative mode at the same time. The dual drift tubes in the same IMS system have a lower sensitivity, but significantly improve the throughput without switching detection modes. The condition used in the instrument was the same as shown in Table 6-1.

7.2 Materials

Table 7-1 shows the solutions prepared by a lab researcher which included blanks and dilutions of compounds of interest and interferences ranging 0.5 – 2000 ng μL^{-1} concentration and PSPME devices were prepared as described in Chapter 4.4.1.

Table 7-1 One hundred solutions prepared for double blind study

	1	2	3	4	5
A	66 ppm MB in MeOH	3 ppm TATP in 1-BuOH	8ppm 2,4-DNT + 16ppm 3,4-DNT in MeOH	20ppm TNT + 28ppm 2,4-DNT in ACN	0.66% DMF + 0.22% TMA in MeOH
B	30ppm Quinine + Cocaine (ACN)	2 ppm 2N-DPA in ACN	67ppm Piperonal + MB in 1-BuOH	10 ppm NG in 1-BuOH	100ppm α + β-Pinene in MeOH

C	4 ppm DPA + EC in MeOH	80 ppm Caffeine in MeOH	2ppm TATP in 50/50 MeOH/ Acetone	1:100 RD in MeOH	40 ppm DMF in Hexane
D	CS_2	10 ppm DEP in ACN	20 ppm m-Xylene in MeOH	80 ppm DPA + 1 ppm TATP in MeOH	10ppm Cocaine + 2,4-Lutidine in ACN
E	ACN	15 ppm HMX in ACN	50/50 2-Propanol & ACN	5 ppm 2N- + 4N- + NN-DPA in ACN	1:300 IMR 4198 in Hexane
F	1:1500 IMR 4198 + RD + AU in ACN	4 ppm EC in 1-BuOH	56 ppm 2,4-DNT in 1-BuOH	1:500 IMR 4198 in ACN	98 ppm 2,4-DNT in DCM
G	60ppm MB + 20ppm Cocaine in MeOH	1:100 AU + IMR in MeOH	0.5 ppm DPA in HEX	1:10000 Gasoline in MeOH	60ppm 2,4-Lutidine in ACN
H	50/50 2-ProOH/BuOH	0.22% TMA in MeOH	67ppm α-Pinene + MB in MeOH	80ppm DMF + 3,4-DNT in ACN	10ppm HMTD in ACN
J	2 ppm TNT in ACN	9ppm Acetone + 2ppm TATP in MeOH	42ppm 2,4-DNT + 40ppm EC in 1-BuOH	1:500 RD in Hexane	Hexane
K	25 ppm 4N-DPA in MeOH	56ppm EC + 3,4-DNT in Hexane	2000ppm MB in MeOH	100 ppm α-Pinene in ACN	30 ppm Diazepam in MeOH
	6	7	8	9	0
A	2ppm 2,4-DNT in MeOH	100 ppm DPA in CS_2	40 ppm PETN in DCM	J2-40-1 (40) 1:150 diluted w/MeOH	40ppm DPA + 2ppm TATP in MeOH
B	4 ppm EC in MeOH	MeOH	1% Acetone & DMF in MeOH	1 ppm TATP + 10 ppm DNT in ACN	50ppm 2,4-DNT + 100ppm EC in 1-BuOH
C	1:750 RD + IMR 4198 in ACN	10ppm 2N-DPA + N,N-DPA in DCM	1:250 IMR 4198 in Hexane	10ppm RDX + TNT in 1-BuOH	Meth-HCl ACS (1:1000) in MeOH
D	1:1:1 1-BuOH + MeOH + ACN	8 ppm MC in 2-Propanol	20ppm 3,4-DNT + 20ppm DMF in ACN	67ppm α-Pinene in Hexane	2ppm TATP + 200ppm Acetone in CS_2

E	50ppm Artesunate + Quinine in ACN	1:1500 IMR + 1:150000 Gasoline in MeOH	5 ppm HMTD in ACN	1:100 IMR 4198 in MeOH	24ppm EC in 50/50 MeOH/BuOH
F	1:10^4 Gasoline + 10ppm 3,4-DNT in ACN	80ppm DPA + 40ppm 2,4-DNT in Hexane	60 ppm Lutidine in ACN	48ppm 3,4-DNT in MeOH	2ppm HMTD in CS_2
G	5ppm HMTD + 100ppm 3,4-DNT in ACN	60ppm SS-Pseudoephedrine in ACN	1:1500 IMR 4198 in ACN	12ppm TNT + RDX + 2,4-DNT in 1-BuOH	8ppm 3,4-DNT in CS_2
H	1:500 AU in ACN	5ppm TATP + 50ppm Cocaine in ACN	2-Propanol	30 ppm N,N-DPA in MeOH	100 ppm DPA in 1-BuOH
J	1 ppm TATP + HMTD in DCM	60ppm DPA + EC in Hexane	56 ppm 3,4-DNT + 2,4-DNT in Hexane	12 ppm DMF in MeOH	1 ppm HMTD + TATP in ACN
K	50ppm Artesunate/Artemisinin (MeOH)	Acetone	4ppm HMTD + 40ppm 2,4-DNT in MeOH	1 ppm TATP + 0.1% Acetone in MeOH	22ppm Indene + Benzonitrile (ACN)

7.3 Methods

To ensure the double blind study is not biased, all the solutions were numbered using the alphabetic character and the number combination (as shown in Table 7-1). The GC vials that contained the solutions were also wrapped with red tape to ensure the confidentially of the identity of the compound. Solutions were randomly picked and spiked into the bottom of a can (10 μL) and the can was sealed with a PSPME device taped on the lid for 30 min. After 30 min extraction time, the PSPME device was taken from the can and analyzed using the Hardened MobileTrace IMS. The solution spiking step and the analyzing step were accomplished by two different persons to avoid any biased judgments.

7.4 Results

Most of the compounds of interest were not detected in the IMS system; however, the various solvents used in the study caused a lot of interferences which included 1-butanol, CS_2, 2-propanol, and hexane. The spectrum of A2 solution (3 ppm TATP in 1-butanol) was shown in the 3D plasmagram (Figure 7-1) and in positive mode, the reactant ion peak shifted dramatically and the shifted region covered the region of detection of TATP in which caused a false negative alarm; however, in negative mode, the 1-butanol solution did not interfere with the detection of 2,4-DNT (F3 solution, 56 ppm 2,4-DNT in 1-butanol) as shown in Figure 7-2. Similar to 1-butanol, 2-propanol, CS_2, and hexane all caused significant shift of the reactant ion peak in both positive mode and negative mode; and the detection of interested compounds can only be achieved if the concentration was high and the shifted region was not interfering with the drift time. One thing that being noticed was that in the negative mode, the shift of reactant ion peak was simple and caused less interferences and in positive mode, the shift was more complicated and normally muted the signal from the targeted compounds; thus, a lower true positive rate was observed in the positive mode detection.

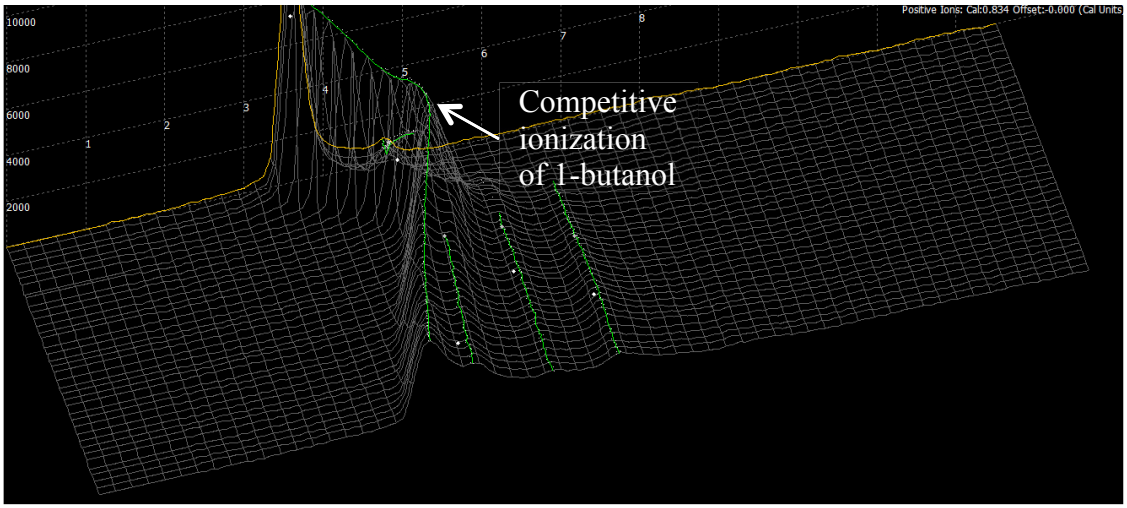

Figure 7-1 3D plasmagram of headspace analysis of 3 ppm TATP in 1-butanol showed no detection of TATP because of the competitive ionization from 1-butanol

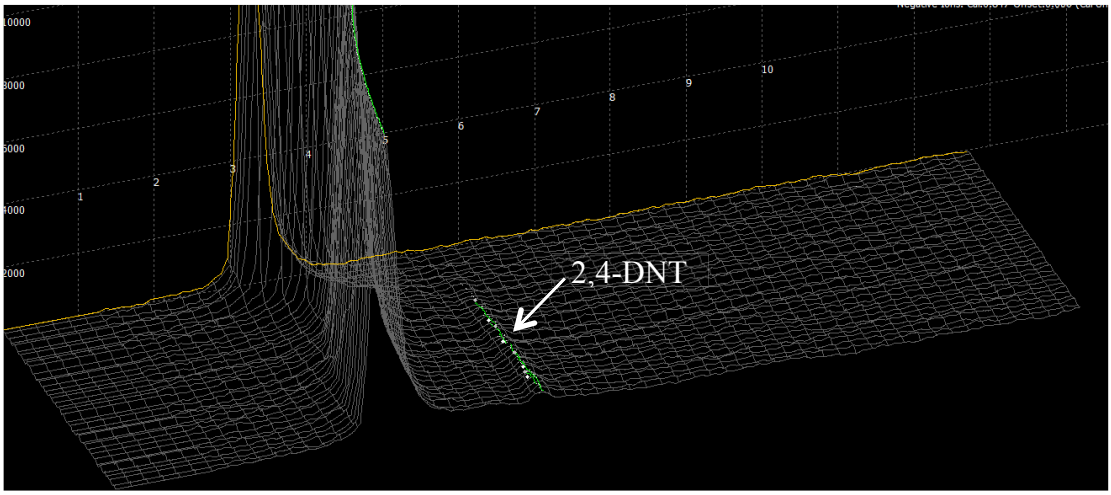

Figure 7-2 3D plasmagram of headspace analysis of 56 ppm 2,4-DNT in 1-butanol and showed detection of 2,4-DNT

In total, 300 samples were analyzed in the IMS system. When a compound was present in the solution, it was called solution positive and vice versa, when the compound was not present in the solution, it was solution negative. After preconcentration on the PSPME devices, the headspace was analyzed in the IMS system and if an alarm was

triggered, it was an instrument positive and when the system was not alarmed, it was an instrument negative. As name indicated, true positive means when the instrument alarmed for one compound, the compound was in the solution (solution positive) and false positive means when the instrument alarmed for one compounds, the compound was not in the solution (solution negative). Similarly, we can define true negative and false negative. In reality applications, the true positive rate and true negative rate should be as high as possible while the false positive rate and false negative rate should be minimized. False positive hindered fast detection and could cause inconvenience with innocent civilians which false negative could cause drastic tragic; thus it is important to reduce the false rate. As shown in Table 7-2, true positive rate, false positive rate, true negative rate and false negative rate were listed for 2,4-DNT, NG, DPA, TATP and EC. 2,4-DNT and NG both have relatively high vapor pressure and the IMS system is sensitive to their detection which lead to a very high true positive rate and relative high true negative rate. The few false negative was caused by the solvent interferences. In the positive mode detection, the results are not ideal; the solvents caused significant interferences in the detection of DPA and TATP. Especially in TATP detection, about 70 % of the positive alarms were caused by the reactant ion peak shift from the solvent. Due to low volatility, EC was not successfully detected in the headspace and had a high false negative rate.

In this research, double blind study was only a preliminary study where not all the solution positives and solution negatives were balanced. The true negative rate can not reflect the true performance of the IMS system since the solution negative took a large number in the 300 samples. In the future design of the experiments, three

recommendations can be noted. First, the interested compounds should be evenly distributed in the 100 samples where about 50 of the solutions should contain the interested compounds and the other 50 solutions do not contain. This could prevent the over large data for solution negatives. Second, more interferences should be introduced into the study which can be commonly encountered in real life that have strong odors such as coffee and perfume. Third, certain solvents were concluded to interfere with the detection of explosives; the next step would be to determine the threshold of the solvent amount that will affect the results. If very small amount of the solvent will still cause the interference, they should be banned from using in making explosives and the smell of the solvent should be trained to the dogs to be prevented in the checkpoints.

Table 7-2 Double blind study results for 2,4-DNT, NG, DPA, TATP and EC

2,4-DNT	**Instrument Positive**	**Instrument Negative**				
Solution Positive	48	36	True Positive Rate	1	False Positive Rate	0
Solution Negative	0	216	True Negative Rate	0.86	False Negative Rate	0.14
NG	Instrument Positive	Instrument Negative				
Solution Positive	14	7	True Positive Rate	0.93	False Positive Rate	0.07
Solution Negative	1	278	True Negative Rate	0.98	False Negative Rate	0.02
DPA	Instrument Positive	Instrument Negative				
Solution Positive	21	54	True Positive Rate	0.6	False Positive Rate	0.4
Solution Negative	9	216	True Negative Rate	0.84	False Negative Rate	0.16
TATP	Instrument	Instrument				

	Positive	Negative				
Solution Positive	2	37	True Positive Rate	0.29	False Positive Rate	0.71
Solution Negative	5	256	True Negative Rate	0.87	False Negative Rate	0.13
EC	Instrument Positive	Instrument Negative				
Solution Positive	1	32	True Positive Rate	1	False Positive Rate	0
Solution Negative	0	267	True Negative Rate	0.89	False Negative Rate	0.11

7.5 Summary

The performance of PSPME-IMS was further evaluated when the complex matrices were encountered. The results showed some organic solvents caused a lot of interferences which included 1-butanol, CS_2, 2-propanol, and hexane. In the positive mode, the effects are more significant where the false positive rates for DPA and TATP were as high as 0.4 and 0.71, respectively. The negative mode was not strongly affected; however, the interferences from the solvents mentioned above resulted in some false negative results. Because of the large number in solution negatives and the small number in solution positives, this study reached a very high true negative rate and low false negative rate, and this study can be further optimized to achieve a receiver operating characteristic (ROC) curve when the solution positives and solution negatives are evenly distributed.

The double blind study results showed the introduction of interferences caused misclassified detection alarms in the IMS because of the instrument has limited resolution and lacks identification capability. Thus, for complex matrix, a detector that allows selective recognition of the separated compounds is needed.

Chapter 8 Invention of Capillary Microextraction of Volatiles (CMV) Devices

As stated before, the PSPME devices can provide a significant increase in surface area and phase volume with capability of dynamic headspace sampling mode to allow faster air sampling; however, coupling to IMS as a detector, the detection of compounds is limited to the pre-programmed compounds and the IMS is not a detector for identification of unknown compounds. Therefore, in this dissertation, the geometry of PSPME devices is further modified to be applied in a GC-MS instrument which is the gold standard for headspace analysis.

8.1 Preparation of Capillary Microectraction of Volatiles (CMV) Devices

Sorbent-coated glass filters were prepared using the method described in Chapter for the PSPME extraction disks and then the filters were fabricated into ~ 2 mm by rectangular pieces. A glass capillary (Wiretrol II, Broomall, PA) with an inner of 2 mm can be fabricated into different length to fit into the thermal desorption probe (

Figure 3-2 and Figure 3-3) and for this project, the capillary was cut into 2 cm long and filled with seven of the ~ 2 mm-wide and 2 cm long strips of the sorbent-coated strips. The packed capillary glass tubes are named capillary microextraction of volatiles (CMV) devices (Figure 8-1).

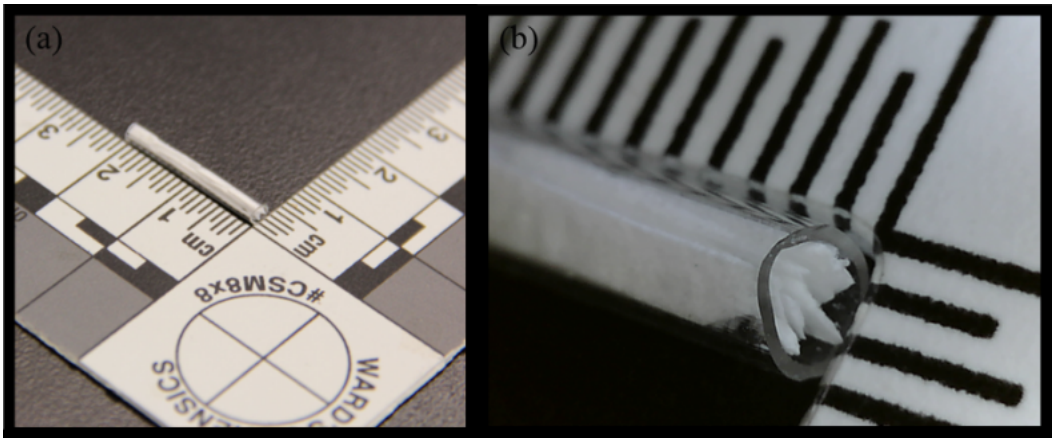

Figure 8-1 (a) The picture has shown the dimension of a CMV device. The inner diameter is ~2 mm and the glass tube is about 2 cm long and packed with sol-gel coated glass filters. (b) An enlarged image of one end of the CMV device.

Figure 8-2 CMV device was connected to the hand-held dynamic sampling pump

The CMV devices have both ends open and one end can be connected to a hand-held vacuum pump that operated at the flow rate 1.5 liters per minute (LPM) which allows airflow through the CMV device and compounds can be extracted onto the sol-gel PDMS coated glass fiber filters. The CMV devices were then placed into a commercial thermal

desorption unit (Agilent Techonologies, Santa Clara, CA) to desorb all the accumulated compounds into GC column for separation and identification with mass spectrum.

With a length of 2 cm, the CMV device contains about 0.230 g of coated glass filters. The ~ 0.05 m^2 PDMS coated surface is calculated to contain a phase volume of 50 mm^3, which is significantly greater than a single SPME fiber (9.4×10^{-6} m^2 surface area and 0.612 mm^3 phase volume) [72]. The surface area and phase volume comparison of SPME, PSPME and CMV devices is listed in Table 8-1.

Table 8-1 Surface area and phase volume comparison among SPME, PSPME and CMV

	SPME	PSPME	CMV
Surface Area (m^2)	9.4×10^{-6}	0.15	0.05
Phase Volume (mm^3)	0.612	300	50

8.2 Theory of CMV

The CMV devices function similarly to a packed GC column at room temperature. When the CMV devices are connected to a vacuum pump, an air flow is pulled through the device and compounds in the headspace partition in and out of the sol-gel PDMS preconcentration coating.

Based on gas chromatography theory, the distribution constant (K_D) can be used to define the interaction between the two phases (stationary phase and mobile phase) as shown in **Equation 8-1** [63].

$$K_D = \frac{\text{concentration per unit volume stationary phase}}{\text{concentraction per unit volume mobile phase}} = \frac{c_S}{c_M} \quad \textbf{Equation 8-1}$$

The distribution constant (K_D) is an equilibrium constant which depends on the compound, stationary phase and the temperature. Referring back to Equation 8-1, the distribution constant K_D can also be defined as shown in Equation 8-2 to Equation 8-4 [63].

$$K_D = \frac{\text{amount in stationary phase/volume of stationary phase}}{\text{amount in mobile phase/volume of mobile phase}} \quad \textbf{Equation 8-2}$$

$$K_D = \frac{\text{amount in stationary phase}}{\text{amount in mobile phase}} \times \frac{\text{volume of mobile phase}}{\text{volume of stationary phase}} \quad \textbf{Equation 8-3}$$

$$K_D = \frac{m_S}{m_M} \times \frac{V_S}{V_M} = k\beta \quad \textbf{Equation 8-4}$$

In Equation 8-4, the latter fraction is also defined as the phase ratio (β), and the former is known as the partition ratio (k). The phase ratio is a measure of the "openness of the column" where for the packed column the number is larger since the mobile phase is limited and the support area is larger. Thus, for the CMV device, the amount of compounds extracted in the stationary phase (m_S), in this case onto the CMV device, can be calculated as Equation 8-5.

$$m_S = \frac{K_D}{\beta} m_M \quad \textbf{Equation 8-5}$$

The partition ratio can also be calculated using retention times in the gas chromatogram (Equation 8-6).

$$k = \frac{t_R - t_0}{t_0} \qquad \textbf{Equation 8-6}$$

The retention time of a compound in GC can be related to the retention time (t_R) in the CMV devices when the compounds migrate from one end of the device to the other end. From Equation 8-6, **Equation 8-7** can be deducted where L is the length of the CMV device and μ is the flow rate of the vacuum pump (linear velocity).

$$t_R = t_0(1 + k) = t_0\left(1 + \frac{K_D}{\beta}\right) = \frac{L}{\mu}\left(1 + \frac{K_D}{\beta}\right) \qquad \textbf{Equation 8-7}$$

Combine Equation 8-5 and **Equation 8-7**, the amount extracted onto the CMV device can be calculated using **Equation 8-8** where t represents the extraction time, F is the dynamic sampling flow rate, and C_h stands for the concentration of the sample in the headspace.

$$m_S = \left(\frac{t_R\mu}{L} - 1\right) m_M = \left(\frac{t_R\mu}{L} - 1\right) tFC_h \qquad \textbf{Equation 8-8}$$

The concentration of the sample in the headspace (C_h) can also be calculated as **Equation 8-9**, where C_0 is the initial concentration in the sample, V_0 is the initial sample volume, m_{loss} is the sample loss during the sampling process, and V_h is the headspace volume over the sample. Thus Equation 8-8 can be further expressed as **Equation 8-10**.

$$C_h = \frac{C_0V_0 - m_{loss}}{V_h} \qquad \textbf{Equation 8-9}$$

$$m_S = \left(\frac{t_R\mu}{L} - 1\right) tF\left(\frac{C_0V_0 - m_{loss}}{V_h}\right) \qquad \textbf{Equation 8-10}$$

Based upon **Equation 8-10**, it is clear that the preconcentrated amount in the CMV devices depends on the extraction time, initial concentration, and the retention time;

while the retention time relies on the distribution constant which is specific to the compounds of interest. Additionally, if m_{loss} is significantly smaller than the initial amount C_0V_0, its value can be neglected and the preconcentrated amount is directly proportional to the extraction time and initial concentration as shown in **Equation 8-11**.

$$m_S = \left(\frac{t_R\mu}{L} - 1\right) tF \frac{C_0V_0}{V_h} \qquad \textbf{Equation 8-11}$$

When the extraction time (t) equals to the retention time (t_R), the amount extracted should reach the maximum where plateau should be observed in the extraction time graph. If the distribution constant between the mobile phase (air) and the stationary phase (PDMS) is low, the elution time is faster which means the compounds get saturated in the CMV devices easily and the extraction can reach plateau in a short time; whereas a high distribution constant means the elution from the dynamic sampling device is much slower and it is not easily saturated in the device.

8.3 Method Development to Couple CMV to GC-MS

8.3.1 Instrumentation

An Agilent Technologies 7890A GC system was coupled to a 5975C inert XL mass spectrometry detector (MSD) and a micro-electron capture detector (μ-ECD) by using a two-way splitter with makeup gas connections controlled by a pneumatics control module (PCM), shown in Figure 8-3 [91]. The flow ratio of the MSD to the μ-ECD is controlled at 5 to 1 by using restrictors as shown in Figure 8-4 [91]. Since MSD requires vacuum and μ-ECD is operated under atmospheric pressure, the restrictor should limit the flow goes into the MSD either by increase the length or using a thinner restrictor. In this setup, the restrictor used for μ-ECD is a 0.405 m restrictor with an inner diameter of 0.10 mm

and the restrictor used for MSD is 1.113 m with an inner diameter of 0.15 mm. The GC front injector was a regular split/splitless port used for direct liquid injection using an autosampler and SPME analysis and the back injector was replaced with a thermal separation probe adapter which was used to thermally desorb the CMV devices at 180 °C. The thermal separation probe used in this research was previously described in Chapter 3.1.1. The GC-MS conditions used in this study are listed in

Table 8-2.

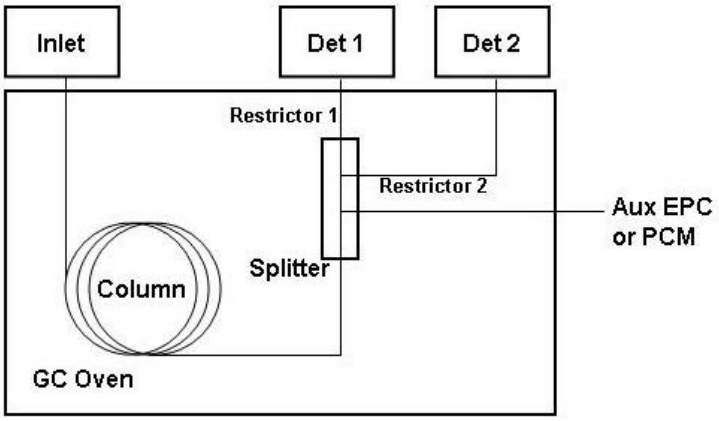

Figure 8-3 Pluming diagram for the two-way splitter with makeup gas [91]

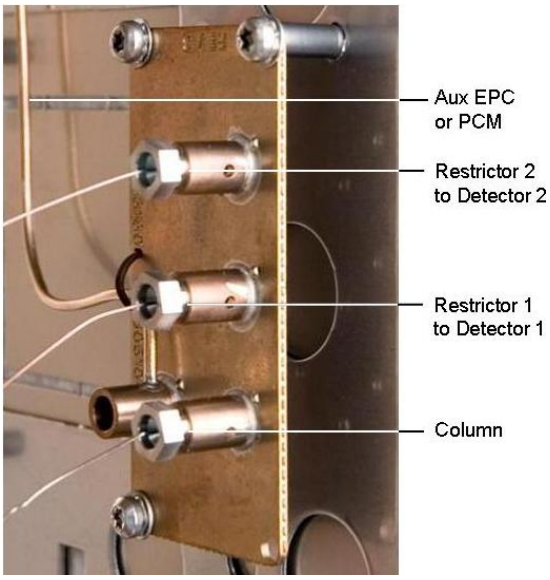

Figure 8-4 Flow ratio of the MSD to the µ-ECD is controlled by using restrictors [91]

Table 8-2 GC-MS conditions for smokeless powder headspace analysis using CMV and SPME

Column type	Agilent Technologies 8 m x 0.25 mm ID x 0.25 µm DB – 5MS UI
Carrier gas	Helium at a flow rate of 1.0 mL min^{-1}
Split ratio	5:1
Injector Temperature	180 °C
Column oven parameters	40 °C, hold for 1 min. 200 °C at 15 °C min^{-1}, hold for 1 mins. 240 °C at 15 °C min^{-1}, hold for 6.5 mins. 270 °C at 25 °C min^{-1}, hold for 0 mins. 280 °C at 5 °C min^{-1}, hold for 4 mins.
MS Transfer Line temperature	280 °C
MS Ion Trap Temperature	180 °C
Running Time	29.33 min

Run Cycle	35 min

8.3.2 Materials

Calibrations for the GC-MS instrument were performed using standard solutions of nitroglycerin (NG) (Cerilliant Corporation, Round Rock, TX), 2,4-dinitrotoluene (2,4-DNT) (Alfa Aesar, Heysham, Lancs), and diphenylamine (DPA) (Acros Organics, New Jersey, USA) diluted using Optima grade methanol (Fisher Scientific, Fair Lawn, NJ, USA) to concentrations ranging from 2 – 50 μg mL^{-1}. Headspace extraction studies were performed with standard solutions of volatile compounds found in the headspace of smokeless powder with concentrations ranging from 40 – 150 μg mL^{-1}. Small quantities of smokeless powders which included Alliant Unique (Alliant Powder, Radford, VA, USA) and IMR 4198 (IMR Powder CO., Shawnee Mission, KS, USA) were placed in quart-sized metal cans (All-American Containers, Miami, FL) and packing cardboard boxes (38 L) (Lowe's, Miami, FL) for headspace analysis. PDMS SPME fibers (SUPELCO, Bellefonte, PA, USA) were used in parallel studies in comparison to CMV devices.

8.3.3 Methods

The CMV devices were conditioned in an oven at 250 °C for 1 hour, allowed to cool to room temperature and connected to a hand-held air monitoring vacuum pump (Escort Elf Air Sampling Pump, Zefon International Inc., Ocala, FL) that provides a flow through the CMV device of 0.1 - 1.5 liters per min (LPM). After typical sampling times of between 30 s – 1 min, the CMV device was disconnected from the tubing and inserted into a probe

for thermal desorption in an Agilent Technologies 7890A GC injector. The thermal separation probe (Agilent Technologies Inc., Santa Clara, CA) can be coupled with the GC injector using a commercially available adapter.

Standard solutions containing the analytes were spiked into quart-size cans and sampled after 10 min equilibration between the spike and the headspace for the solution; smokeless powders were placed in either the quart cans or cardboard boxes and dynamically sampled after a 24 hour equilibration with the can lid open and the CMV was held at one end of the can opening (Figure 8-5 (c)). A different sampling configuration was used in which the headspace was sampled through a ~ 5 mm diameter hole on the lid of the can (Figure 8-5 (a)). The two setups along with the setup shown in Figure 8-5 (b) were visualized using Schlieren flow visualization at National Institute of Standards and Technology (NIST). The handle flap on the cardboard boxes was opened in order to have access for headspace sampling using the CMV device. In order to evaluate the retention performance of the CMV devices, the CMV devices were analyzed at different time intervals after sampling from 0 minutes up to 67 hours after sampling.

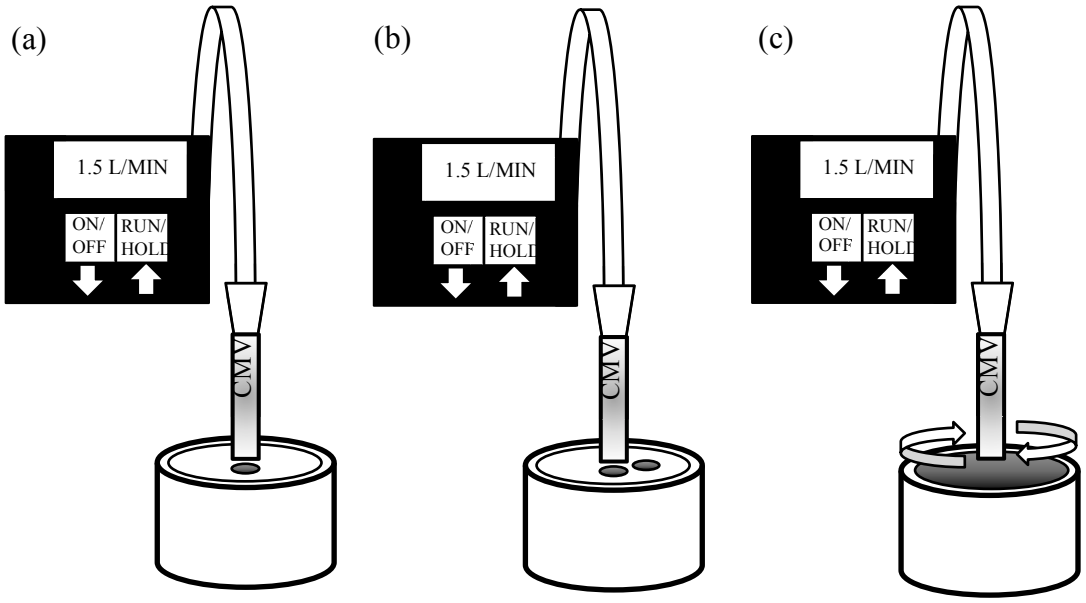

Figure 8-5 (a) Sampling in a closed system with only 1 small opening where CMV is placed above opening without any movement (b) Sampling in a closed system with two small openings where CMV is placed above one of the openings without any movement; (c) Sampling by moving the tip of the hose in a circular motion over the area of the open area.

8.4 Results

8.4.1 Method Optimization

Capillary microextraction of volatiles was first developed in this dissertation and the method development, method optimization and performance evaluation was accomplished using standard solution mixtures and small amount of smokeless powders.

In this dissertation, detection was mainly focused on explosives, so the electron capture detector was preferred in the detection system to compliment a mass spectrometer detector. The electron capture detectors shows high sensitivity to the explosives containing nitro groups, thus, the flow ratio between ECD and MS is not necessary to be 1 to 1. As a result, in this dissertation, the flow ratio between the two detectors was set at 1 to 5 as stated earlier as to not compromise the MS sensitivity.

8.4.1.1 Split vs. Splitless

Since vapor pressures of explosives are relatively low, especially in high explosives, samples have to be preconcentrated and the detector has to be sensitive to achieve detection. As stated in Chapter 5.1.2, splitless mode can allow introduction of all the desorbed compounds into the column for trace analysis; however, splitless mode showed higher background noise (Figure 8-6) compared to split mode. As shown in Figure 8-7, with a 10 to 1 split ratio, split mode still showed detection of 2,4-DNT within 1 min of extraction time over the headspace of 10 mg of IMR 4198 which was about 1/3 of the signal intensity detected in splitless mode.

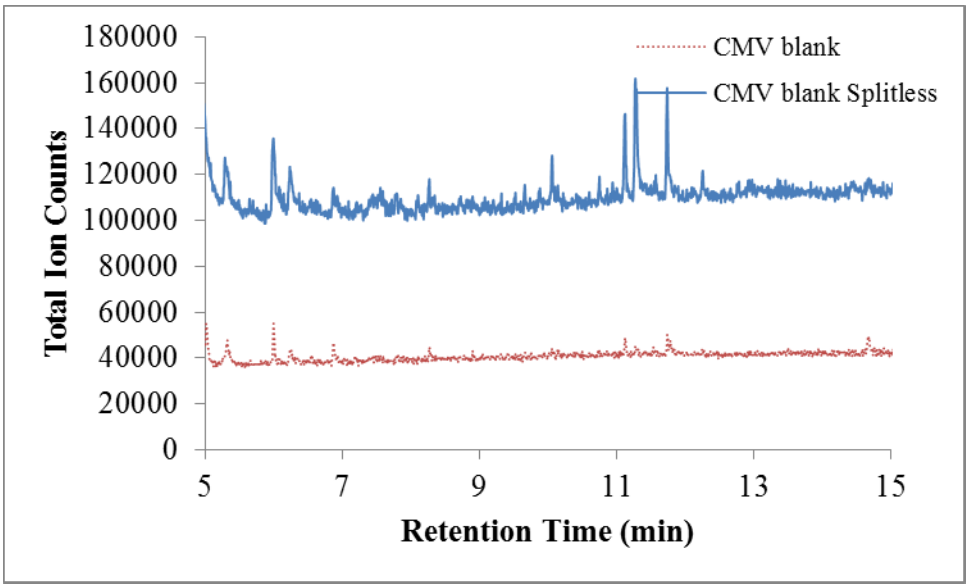

Figure 8-6 Split and splitless mode comparison in GC-MS using blank CMV devices

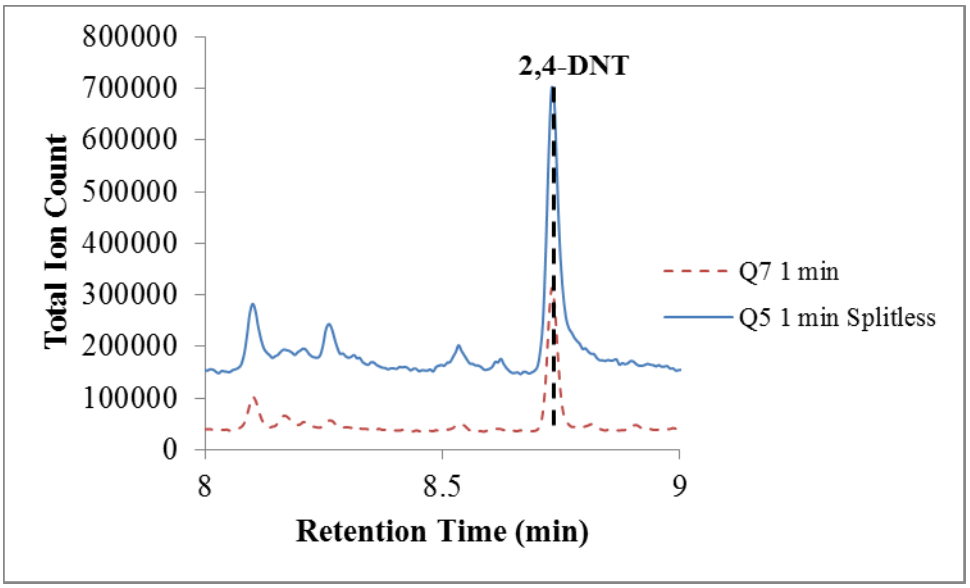

Figure 8-7 Split and splitless mode comparison in GC-MS using CMV devices sampling over the headspace of 10 mg of IMR 4198

8.4.1.2 Injection Port Temperature

The injection port temperature is also very important in the method development to make sure all the compounds preconcentrated on the device were desorbed without decomposing the thermally unstable compounds. As shown in Figure 8-8, when the desorption temperature is set as low as 150 °C, not all the compounds are desorbed into the column; however, when the injection port temperature is above 200 °C, a slight increase in signal for DPA was observed; however, nitroglycerin was not observed in the chromatograph which means the molecules decomposed prior to reaching the detector. As a result, the optimized temperature was set at 180 °C.

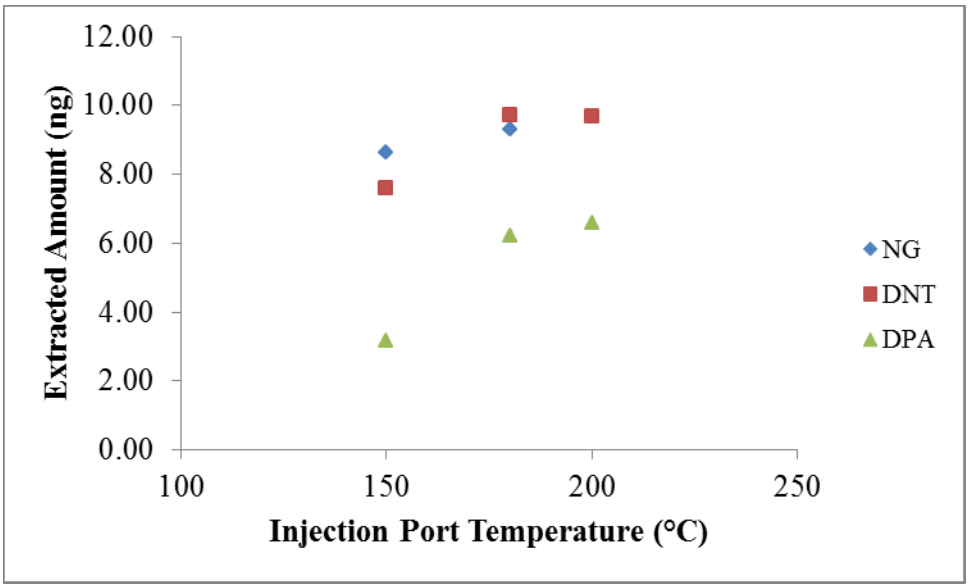

Figure 8-8 Optimized injection port temperature was set at 180 °C for efficient thermal desorption without thermal decomposition

8.4.1.3 Regular Split/Splitless Injection Port vs. Multi-Mode Inlet

Compared to regular split/splitless inlets which are set at a constant temperature, further prevention of thermal decomposition and sample loss during injection can be achieved using a multi-mode inlet (MMI) to heat the inlet at a flash speed from room temperature after injection and cool down the inlet after each use. Figure 8-9 showed the three points calibration for NG, DNT and DPA using a multi-mode inlet and Figure 8-10 showed the same calibration using a regular split/splitless inlet. Limits of detection and linearity are slightly better with the MMI, but there were no significant difference between the two types of inlets. Consequently, the multi-mode inlet was not used in the following experiments because of two reasons. First, MMI inlets required a separate gas tank for efficiently cooling down the inlet after each use which took longer compared to a constant temperature and was also cumbersome for field sampling. Second, the injection

port temperature was flash heated; however, the temperature can not be maintained at the pre-set temperature and the temperature kept increasing as the oven temperature increased.

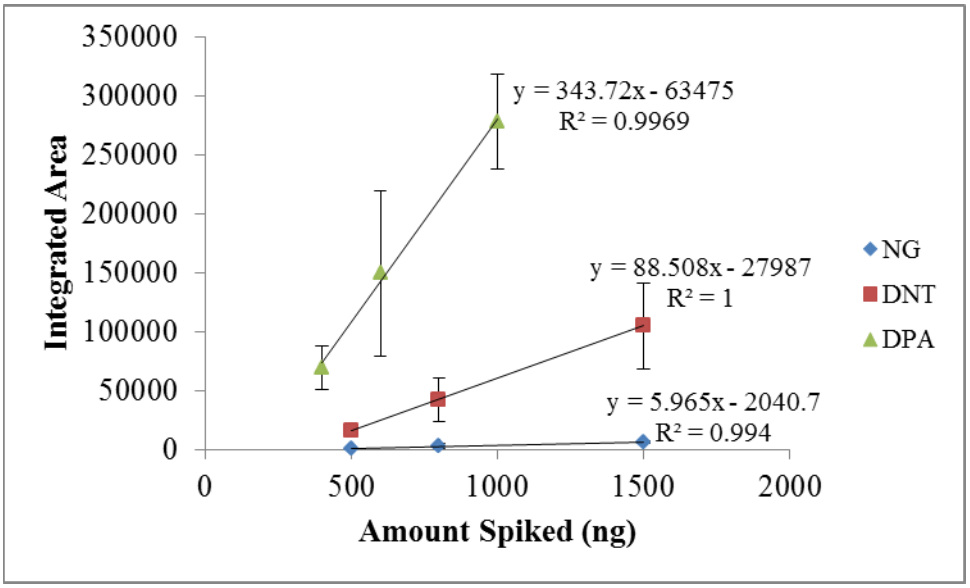

Figure 8-9 Three points calibration for NG, DNT and DPA using a multi-mode inlet

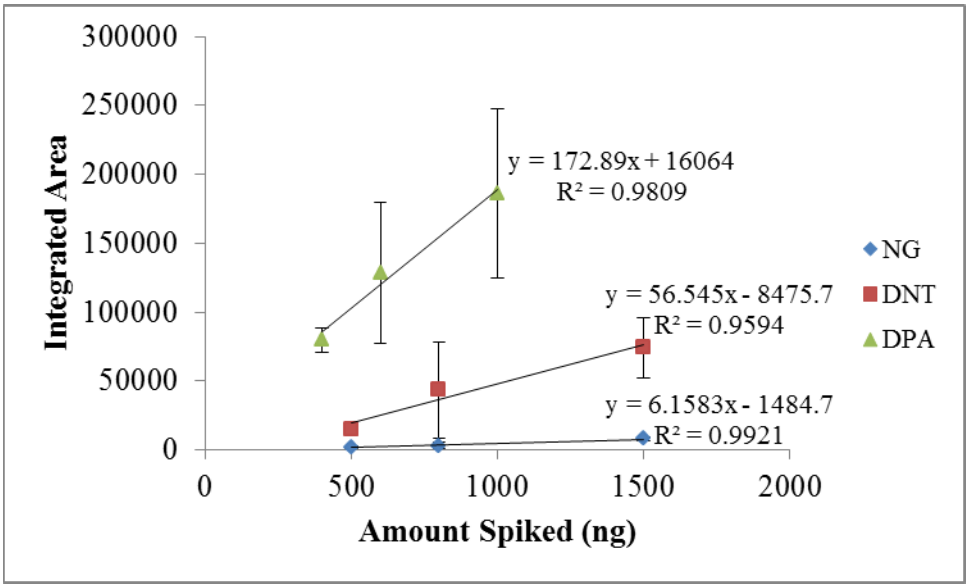

Figure 8-10 Three points calibration for NG, DNT and DPA using a regular split/splitless inlet

8.4.2 Calibration Curves Generated by Spiking Standard Solutions on CMV Devices

Apart from dynamic sampling, CMV devices can be calibrated by directly spiking standard solution on one end. Figure 8-11 showed the chromatograph of direct spike of a 1 µL of mixture of NG, DNT, DPA and EC. The peaks were sharp which provided good separation and showed great sensitivity. Figure 8-12 showed calibration curves of four major components, NG, 2,4-DNT, DPA, and EC, in smokeless powders (Figure 5-8). To ensure accurate quantitation analysis, the standard solutions were prepared every three months and the calibration curves were generated weekly.

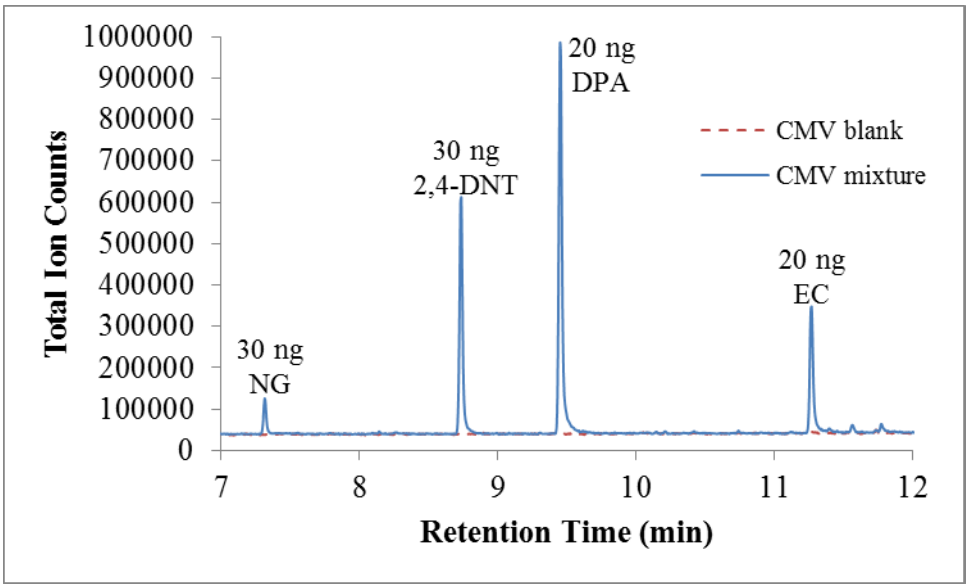

Figure 8-11 GC-MS Chromatograph of direct spike of a 1 µL of standard solution mixture

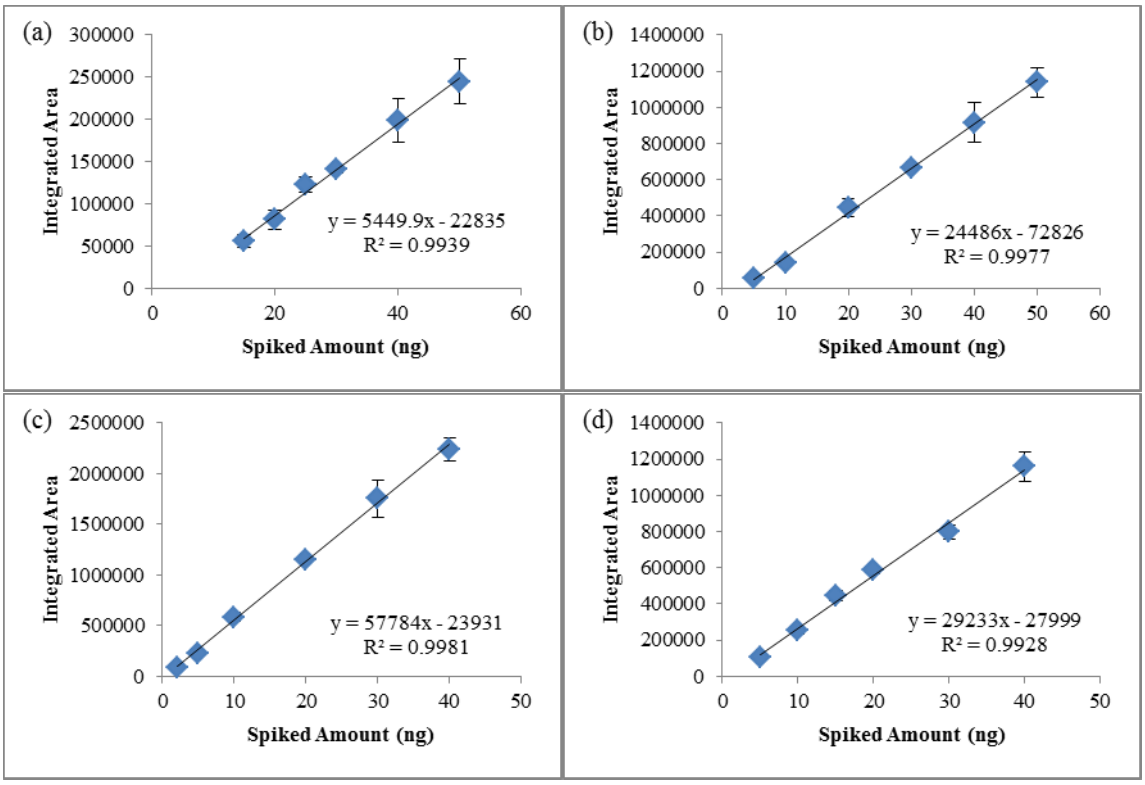

Figure 8-12 Calibration curves of (a) NG (b) 2,4-DNT (c) DPA (d) EC by directly spiking standard solution mixtures on CMV devices

8.4.3 Dynamic Headspace Sampling Method Development

8.4.3.1 Equilibrium Study

Equilibrium studies were performed before dynamic sampling optimization to determine the headspace development after the sample was spiked at the bottom of the can. 10 µL of a mixture solution was spiked in a quart can and then sealed with the lid on for 5 min, 10 min, 30 min, and 60 min to allow the volatile compounds to travel into the headspace. The results were shown in Figure 8-13 in which DNT and NG headspace concentration increased as the equilibrium time increase; however, DPA headspace concentration dropped dramatically after 10 min equilibrium time and EC did not successfully evolve

into the headspace because of its low volatility. For efficient preconcentration of all three compounds present in the same headspace, the 10 min equilibrium time was chosen for the future experiments.

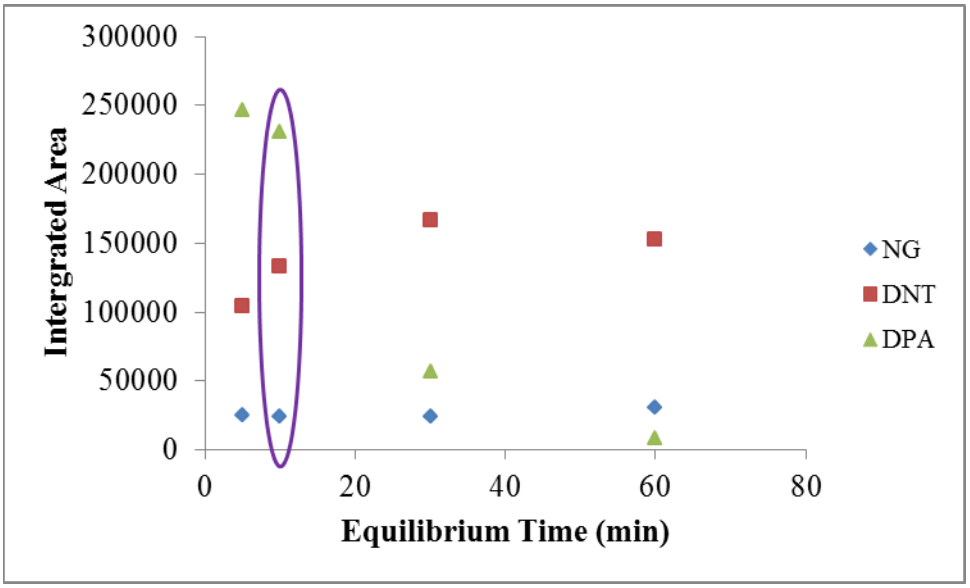

Figure 8-13 Equilibrium time study in a quart can using standard solution mixtures

8.4.3.2 Flow Rate

Upon establishing equilibrated headspace, flow rate of the dynamic sampler was optimized which controlled the volume of headspace passing through the CMV device; so to further optimize dynamic sampling, flow rate of the dynamic sampler was also tested. The recommended setting was 1-2 liters per minute (LPM), and the maximum flow rate achieved was 3 LPM; nevertheless, when the flow rate was set at 3 LPM, the back pressure caused by the CMV was too high which led to unstable flow rate and the maximum rate never reached 3 LPM. The results (Figure 8-14) showed a slightly higher recovery achieved using the lower flow rate 1.5 LPM despite the smaller volume of the

headspace in the container was sampled which meant that the partition between the preconcentration material and the air were relatively slow and when the flow rate increased, less partitioning happened during the dynamic sampling process.

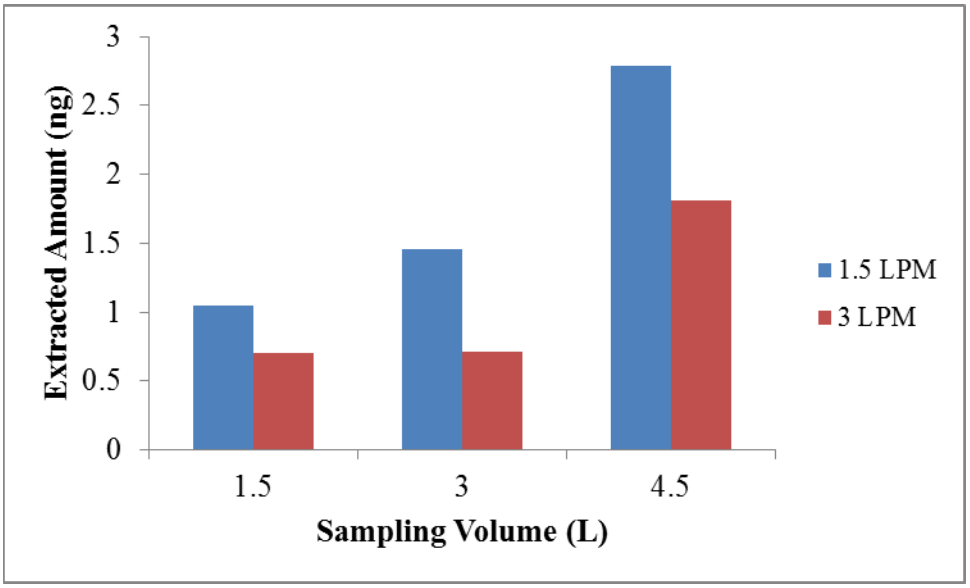

Figure 8-14 Extracted amount of DPA was higher at a lower flow rate with various extraction times in a large container (cardboard box)

8.4.3.3 Preconcentration Material Comparison

To evaluate the performance of the CMV devices, the preconcentration was determined using different materials and two different coatings. First, sol-gel coated PSPME devices were directly compared to the uncoated glass filters and the Teflon trap used for IMS. All three materials were cut into the same size strips (2 mm × 2 cm) and packed into capillary tubes as described in Chapter 7.3. With 1 min dynamic extraction of the headspace of standard solutions, the devices packed with different materials were desorbed in the thermal separation probe and the extracted amount of NG, 2,4-DNT and DPA were calculated using calibration curves generated as described in Chapter 11.2.2.

In Figure 8-15 and Figure 8-16, traps and uncoated glass filters showed no detection of NG and about half of the extracted amount of DNT and DPA compared to CMV devices.

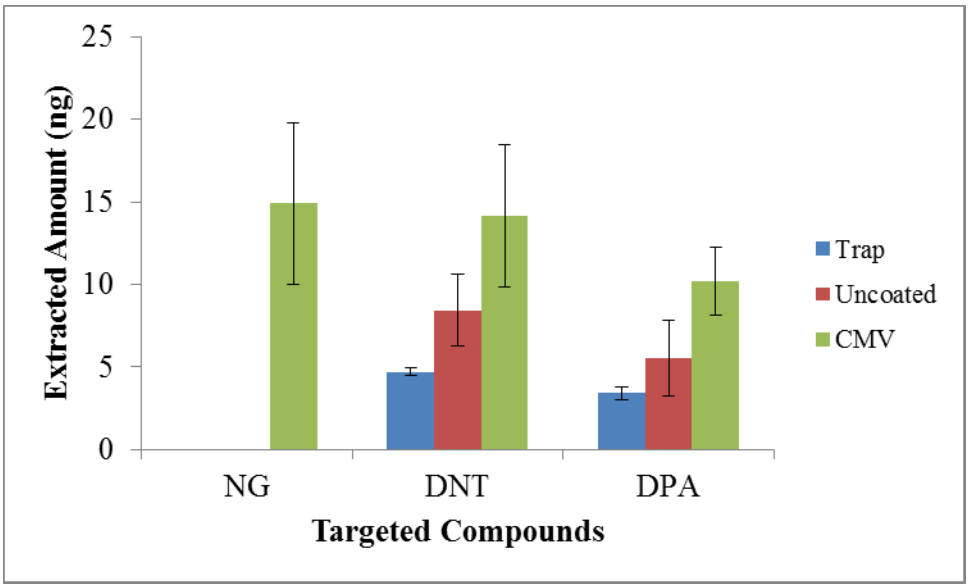

Figure 8-15 Different preconcentration materials comparison using standard solution mixtures

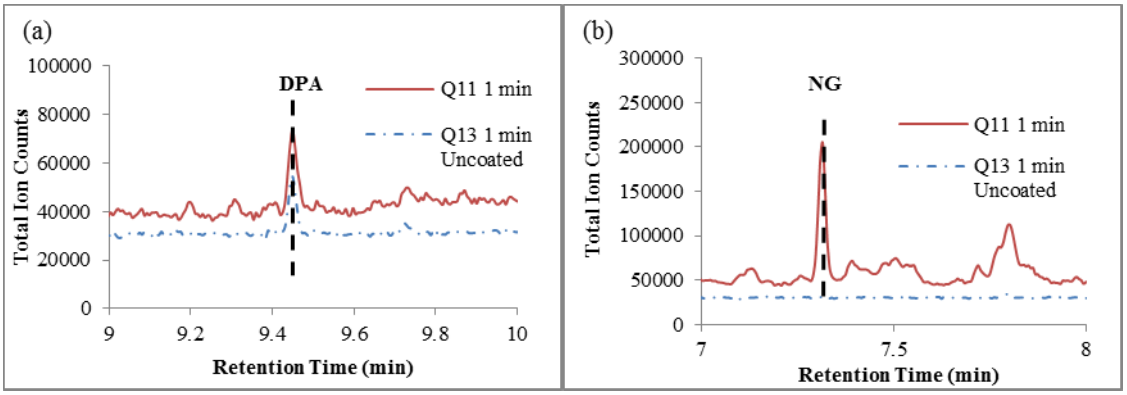

Figure 8-16 GC-MS Chromatograph comparison of (a) DPA and (b) NG between PSPME and uncoated glass filters packed in capillary tubes

In the original design of CMV devices, sol-gel PDMS coated glass fiber filters were used as the preconcentration material. In order to be able to preconcentrate a broader range of

compounds, the coating of PSPME can be modified to incorporate other linkers for polar compounds. Since the sol-gel chemistry coating was well developed, in this research, 10 % *v/v* of DVB was added to the *vt*-PDMS sol solution mixture and not modifying the remaining procedures as described in Chapter 4.4.1. Preliminary studies did not show much difference when NG, 2,4-DNT and DPA were sampled using two different sol-gel based coatings, PDMS and PDMS/DVB (Figure 8-17); yet, even in SPME fibers comparison, PDMS and PDMS/DVB fibers performed similarly in preconcentration NG and DPA (Figure 5-1). Thus, other compounds such as straight-chain alcohol compounds should be used to further test the difference between the two coatings and/or the preparation procedures of different coatings can be explored. If different coatings can be appropriately prepared, different coating glass filter strips can be packed into one capillary tube which allows CMV to incorporate more than two different coatings to achieve preconcentration of almost all compounds in the headspace.

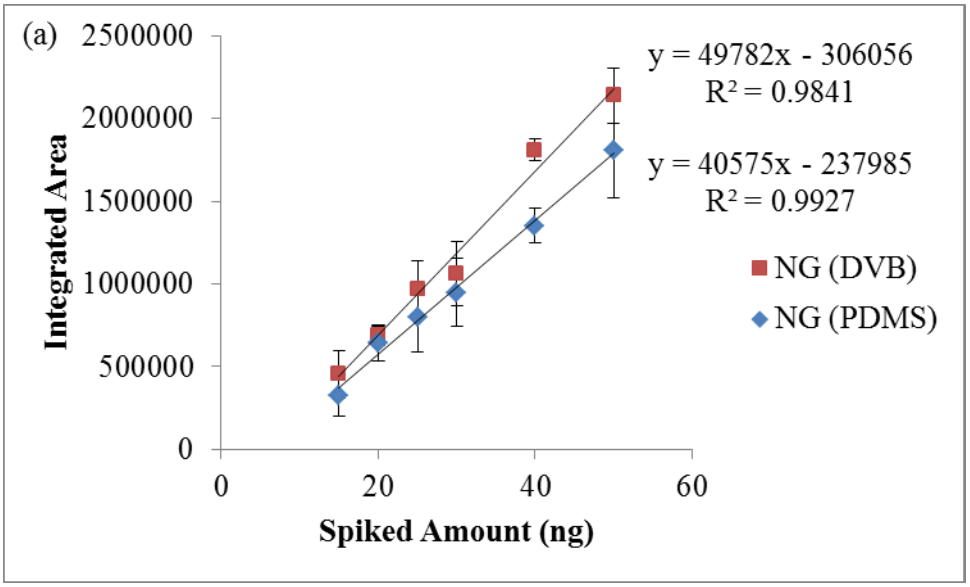

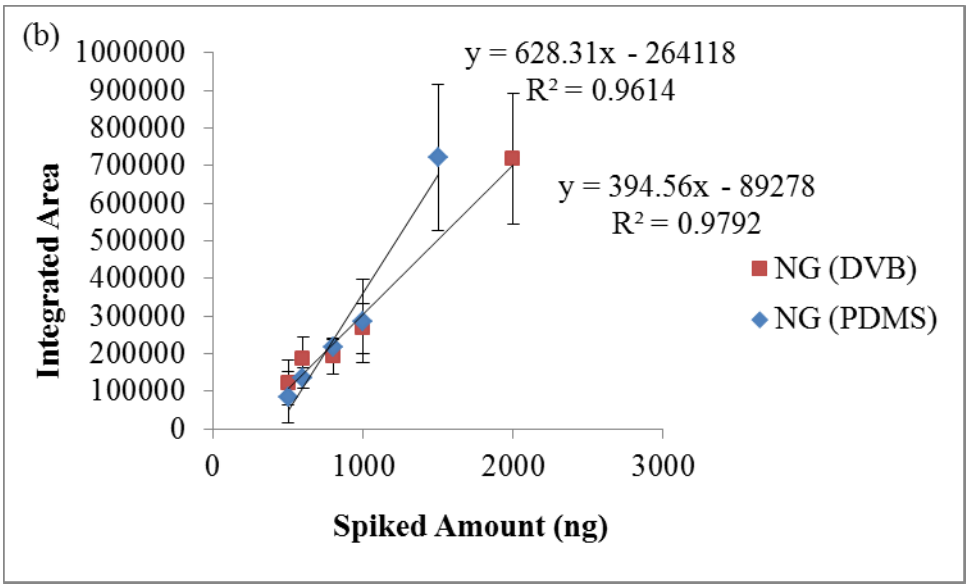

Figure 8-17 PDMS and PDMS/DVB coating comparison in CMV devices when doing (a) direct spike and (b) dynamic headspace analysis of NG

8.4.3.4 Recovery in the Headspace

With optimized dynamic sampling parameters (10 min equilibrium time, 1.5 LPM flow rate and 1 min extraction time), headspace extraction curves were completed using various concentration standard solution mixtures. As shown in the extraction profile (Figure 8-18), linearity was very good which would allow for quantitative analysis. By using the calibration curves generated as described in Chapter 8.3.2, the amount extracted in the headspace can be calculated; thus the recovery can be determined which was shown in Table 8-3.

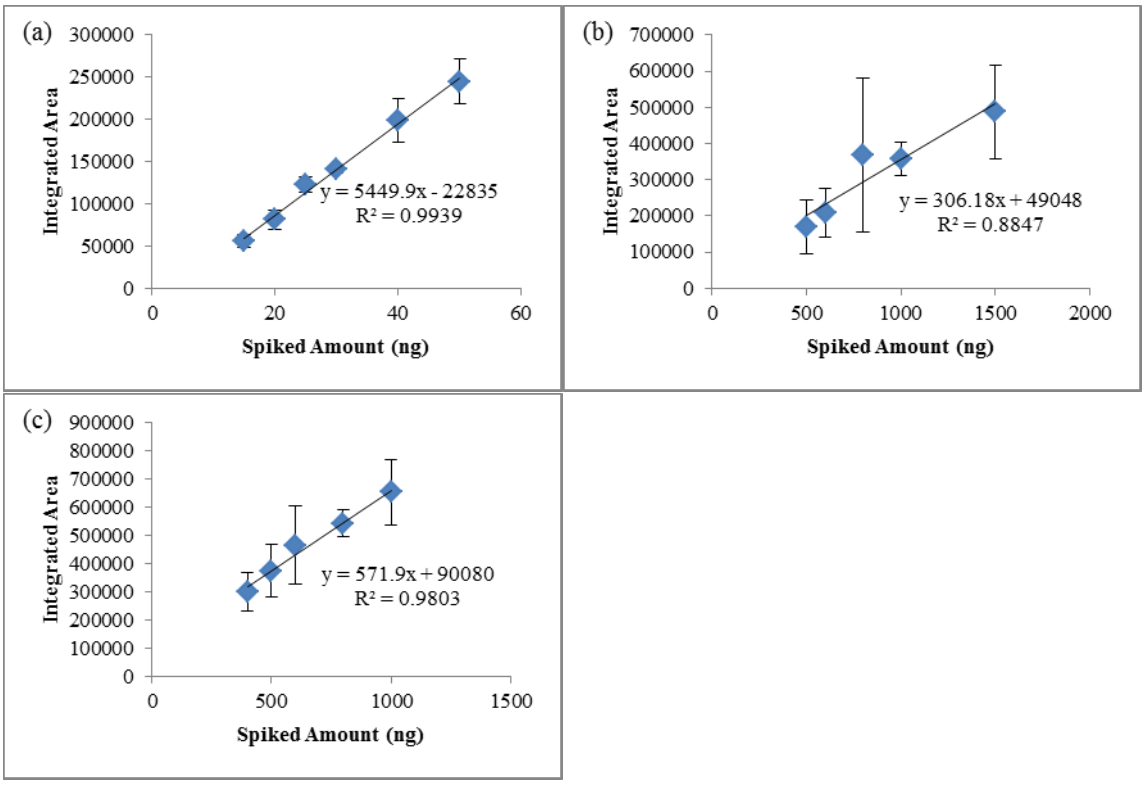

Figure 8-18 Dynamic headspace extraction curves for (a) NG (b) 2,4-DNT (c) DPA using CMV devices

Table 8-3 Recovery calculated for dynamic sampling using standard mixtures

	NG (ng)	Ave	Recovered Amount (ng)	Recovery Rate (%)
#20	500	33469.3	10.33	2.07
#21	600	33320.7	10.30	1.72
#22	800	59465.0	15.10	1.89
#23	1000	61751.3	15.52	1.55
#24	1500	93524.3	21.35	1.42
#25	2000	94205.3	21.48	1.07
	DNT (ng)	Ave	Recovered Amount (ng)	Recovery Rate (%)
#20	500	170520.3	9.94	1.99
#21	600	208431.7	11.49	1.91
#22	800	369036.7	18.05	2.26
#23	1000	357170.3	17.56	1.76
#24	1500	487258.7	22.87	1.52
#25	2000	426505.3	20.39	1.02

	DPA (ng)	Ave	Recovered Amount (ng)	Recovery Rate (%)
#20	400	299564.7	5.60	1.40
#21	500	374596.0	6.90	1.38
#22	600	465998.0	8.48	1.41
#23	800	543460.0	9.82	1.23
#24	1000	654054.7	11.73	1.17
#25	1500	706290.3	12.64	0.84

8.4.3.5 Retention Capability of CMV

To evaluate the retaining performance for CMV devices, both parafilm and aluminum foil were used to seal the CMV after dynamic sampling. The study was first performed using parafilm which can provide excellent seal; however, it left residues on the CMV devices that showed significant peaks in the background (Figure 8-19) because the parafilm was made out of Paraffin wax, a white or colorless soft solid, that is derived from petroleum and consists of a mixture of hydrocarbon molecules [92]. When using a CMV device to sample the headspace of 10 mg of All Unique smokeless powders and then sealed the device in parafilm, the compounds accumulated were retained and the background was not interfering with the detection of the targeted compounds (Figure 8-20).

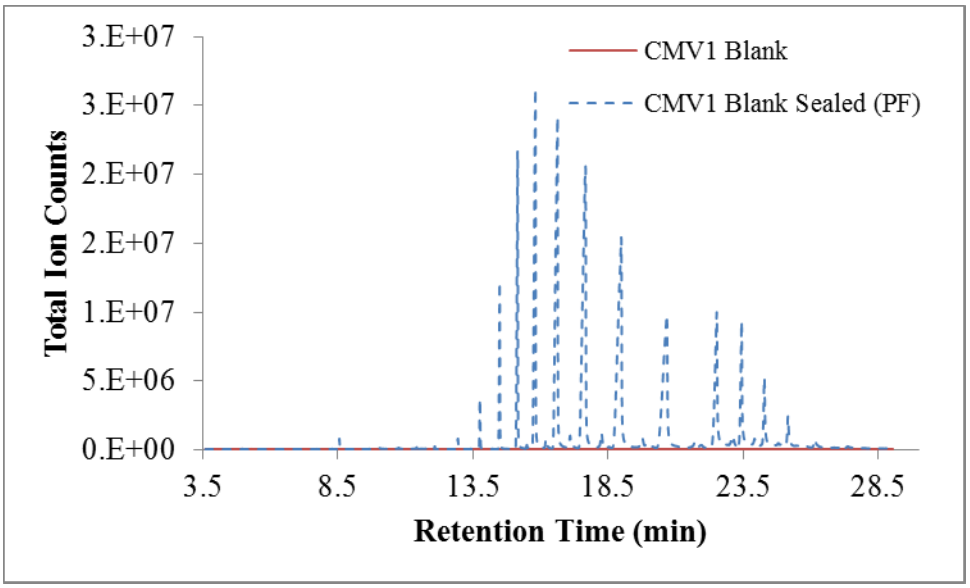

Figure 8-19 CMV blank after sealing the device in parafilm which showed strong background

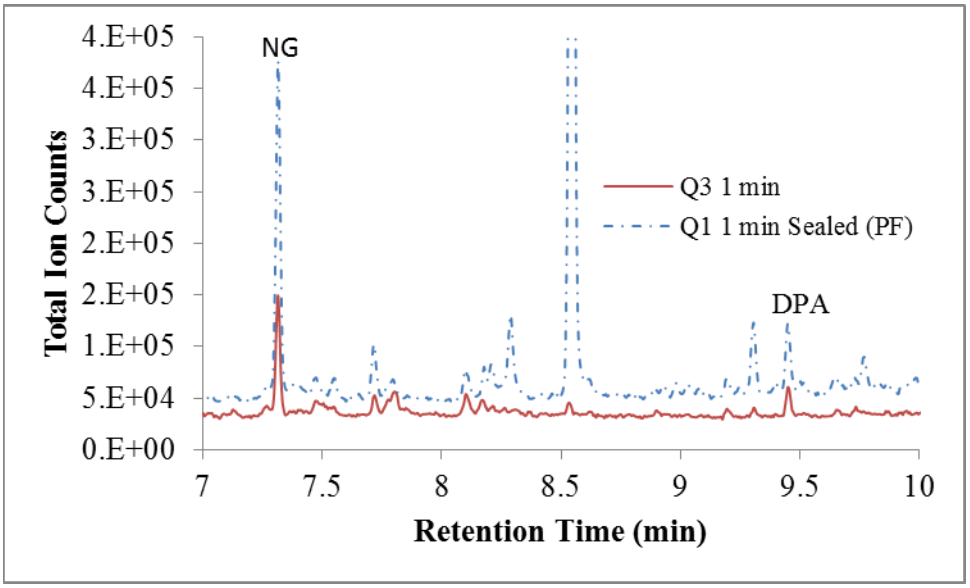

Figure 8-20 After dynamic sampling 10 mg of All Unique smokeless powders, NG and DPA was retained after sealed in parafilm

Different from parafilm, aluminum foil won't provide a perfect seal which means some of the compounds would get oxidized after long-time storage; however, the aluminum foil did not affect the blank CMV devices as shown in Figure 8-21. The seal kept moisture out of the device and no significant residue was observed in the blank after 68 h. After 30 s dynamic extraction of headspace over 100 mg of IMR 4198 smokeless powder, the CMV devices were sealed in aluminum foil for 67 hours. With 67 hours in the aluminum foil, about 70 % of the initial amount of compounds extracted was still retained in the CMV devices (Figure 8-22 and Figure 8-23). The amazing retaining performance of CMV devices in aluminum allowed for easy transportation of the devices when using CMV in the field analysis. The analysis can be completed either in a field portable instrument or brought back to the laboratory for thorough analysis on a bench top instrument.

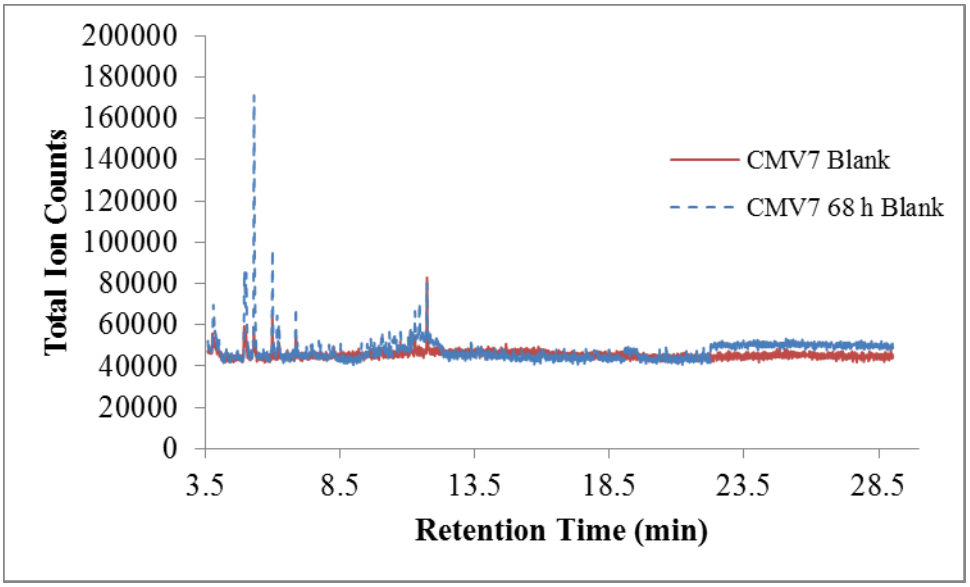

Figure 8-21 Blank CMV device after sealed in aluminum foil

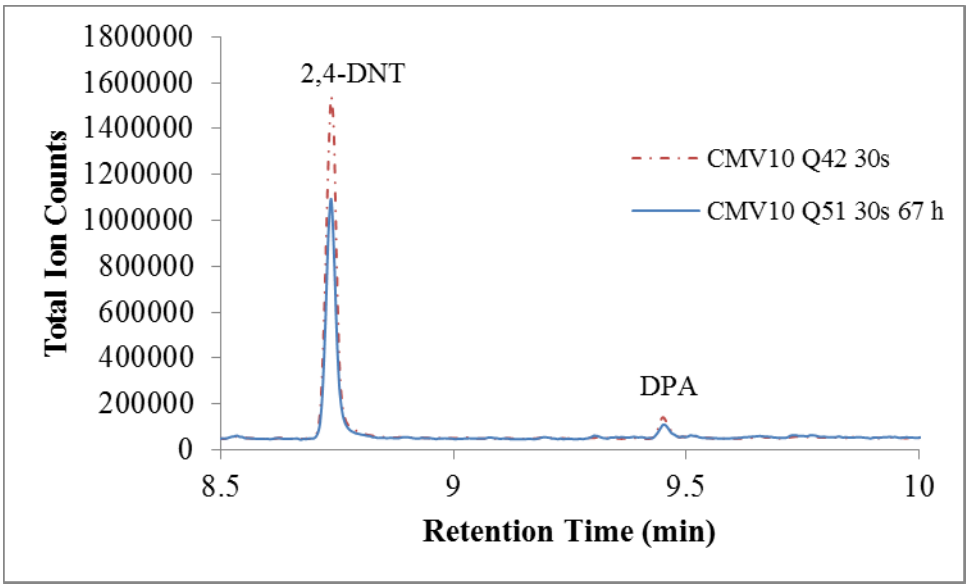

Figure 8-22 2,4-DNT and DPA were retained in the CMV device after 67 hours sealed in aluminum foil

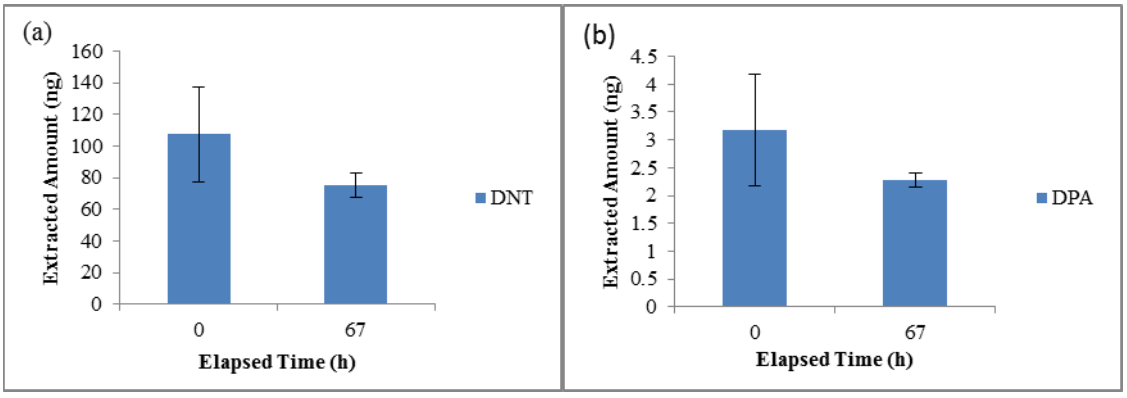

Figure 8-23 After 67 hours, about 70 % of (a) 2,4-DNT and (b) DPA were still remaining in the CMV devices

8.4.3.6 Extended Sampling Time

Besides the increased surface area, CMV also has an increased phase volume (Table 8-1) which allowed for a larger dynamic range that has been proven in the following experiments. Spiking a certain amount of NG into the quart can and equilibrium for 10

min as stated before, the can was sampled with extraction times varied from 30 s to 5 min. As shown in Figure 8-24, as the extraction time increased, the extracted amount of NG increased followed a linear curve which meant certain amount of compounds were extracted every minute and it can be used for quantitative analysis as well. To test the breakthrough volume for CMV, hour long extraction times were used. Breakthrough was not observed for all the compounds tested and Figure 8-25 (a) and (b) showed that even after a 60 min extraction the CMV devices have not been saturated for NG and 2,4-DNT and the recovery rate can reach as high as 20 % and 15 %, respectively. For DPA, the extracted amount plateaued (reached an equilibrium) after a 20 min extraction resulting in the familiar single fiber SPME extraction curve shown in Figure 8-25 (c).

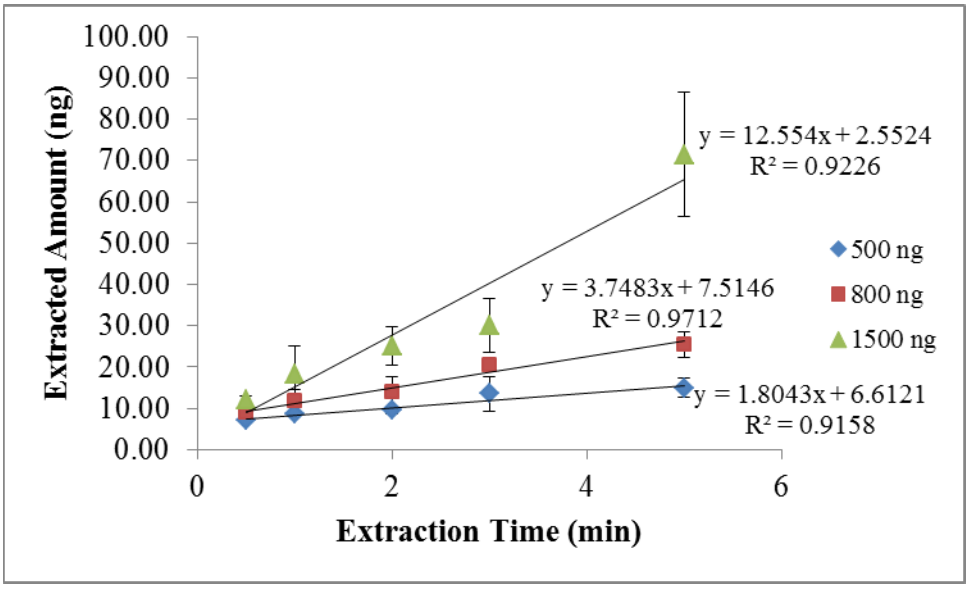

Figure 8-24 Dynamic sampling of the headspace of 500 ng, 800 ng, and 1500 ng of NG with various extraction times

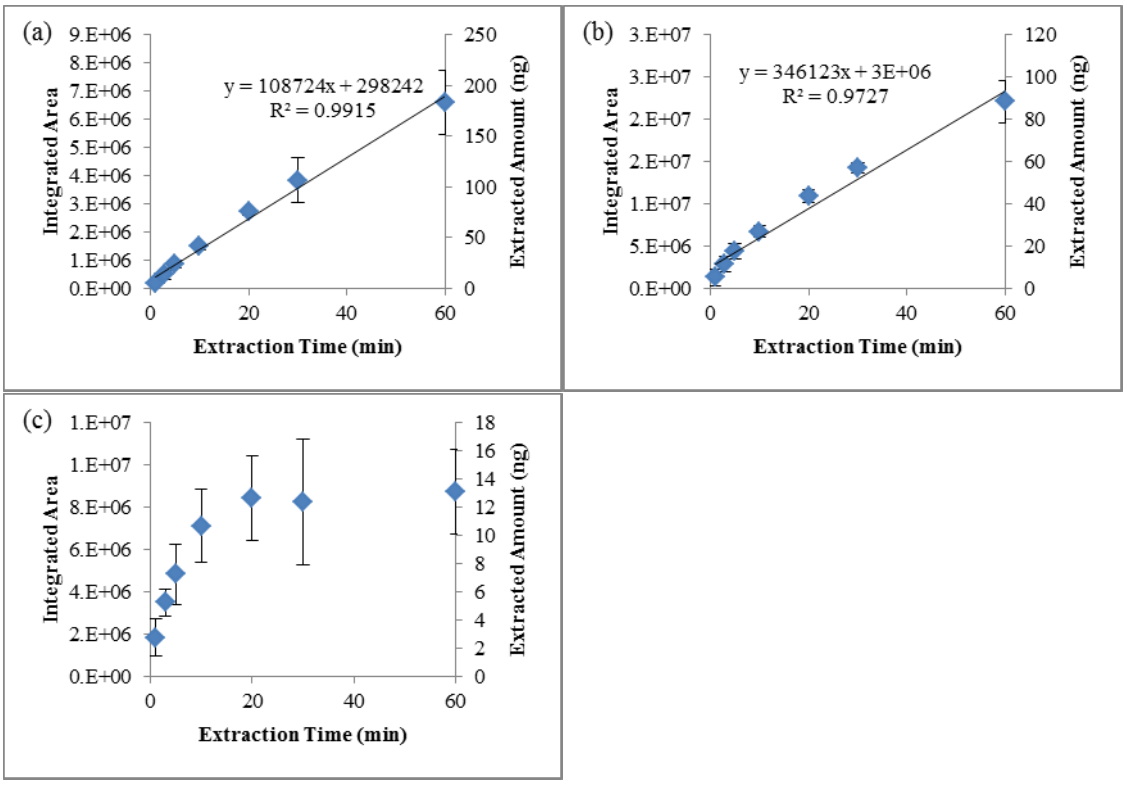

Figure 8-25 Extended dynamic headspace extraction suggesting quantitative results. (a) NG (b) 2, 4-DNT (c) DPA

To further evaluate the efficiency of the extraction, two CMV devices were connected back to back in front of the dynamic sampler. Consequently, the compounds were not preconcentrated on the first device would flow through it and be preconcentrated on the second device or lost into the atmosphere. As shown in Figure 8-26, there were small amount of NG preconcentrated on the second CMV device and with the extended extraction time, the amount of NG did increase. To conclude this experiment, the partitioning happened between the PDMS material and the air were sufficient to preconcentrated most of the compounds flew through; however, some analytes moved

faster with air in the CMV devices when the partition coefficient of PDMS/air is low which led to sample loss.

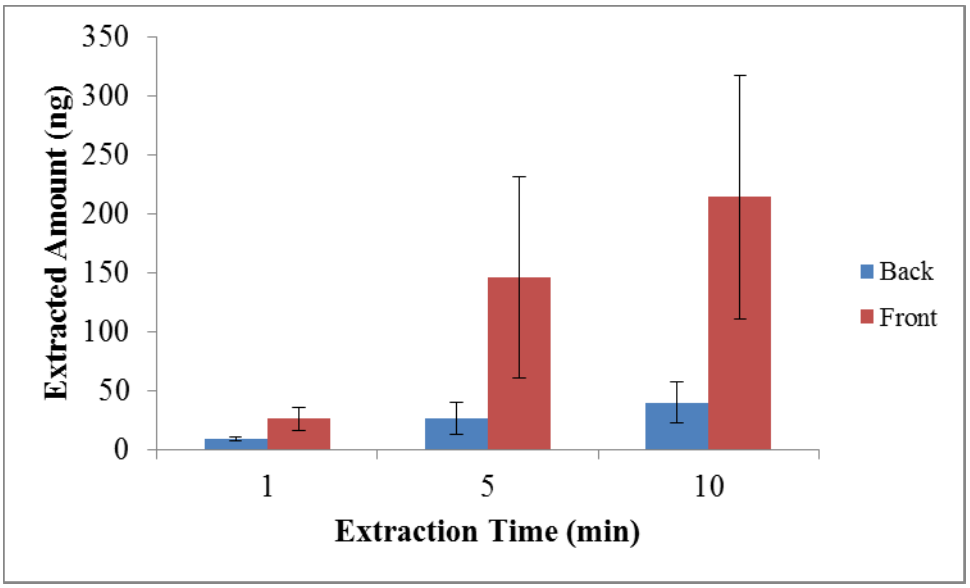

Figure 8-26 Two CMV devices were connected back to back to evaluate the preconcentration efficiency

8.4.4 SPME vs. CMV

The extraction performance of CMV was compared to SPME to prove the improved preconcentration ability. First, the direct injection was done using both CMV and an autosampler to obtain calibration curves for NG, 2,4-DNT and DPA. The integrated peak areas are comparable for both extraction methods for NG (Figure 8-27 (a)) and DPA (Figure 8-27 (e)) while CMV results in better overall sensitivity for DNT (Figure 8-27 (c)). Headspace extraction of mixtures containing the target volatiles in concentrations ranging from 40 – 150 µg mL^{-1} were conducted after a 10 min. equilibrium period at room temperature (23 °C). The CMV device was placed at the opening of the can, collecting the headspace in a circular motion for 1 min during dynamic extraction of the

headspace in the can at a flow rate of 1.5 L/min. A parallel study was done using static SPME extractions of the same mixture solutions for 10 min and 30 min extractions at 23 °C. Figure 8-27 (b, d, and f) showed the comparison of a 1 min. dynamic CMV extraction to a 30 min. static SPME extraction resulting in similar extraction/detection performance. The recovery of each analyte compound extracted on the CMV device can be calculated by using the calibration curves generated from the direct injection (Figure 8-27 (a, c, and e)). The recovery of a particular analyte was obtained by dividing the amount detected with the amount available and is summarized in Table 8-4. For a 1 min extraction with the CMV, the NG recovery is 1.4 % compared to the 0.5 % with a SPME 30 min extraction; while for DNT and DPA, the recovery percentages are 1.4 % and 1.3 % for CMV and 1.7 % and 1.3 % for SPME. Less extraction times with SPME fibers (10 min) resulted in significantly lower recovery of 0.5 %, 0.1 % and 0.5 % for NG, 2,4-DNT and DPA, respectively. This comparison experiment shows the improved extraction and recovery due to a higher surface area and phase volume even with significantly reduced sampling times.

Table 8-4 Recovered mass (as %) of NG, DNT and DPA after a 1 min. dynamic extraction using CMV devices and compared with 30 min. and 10 min. static extractions using SPME fibers

Recovery (%)	CMV (1 min)	SPME (30 min)	SPME (10 min)
NG	1.5	0.5	0.5
DNT	1.4	1.7	0.1
DPA	1.3	1.3	0.5

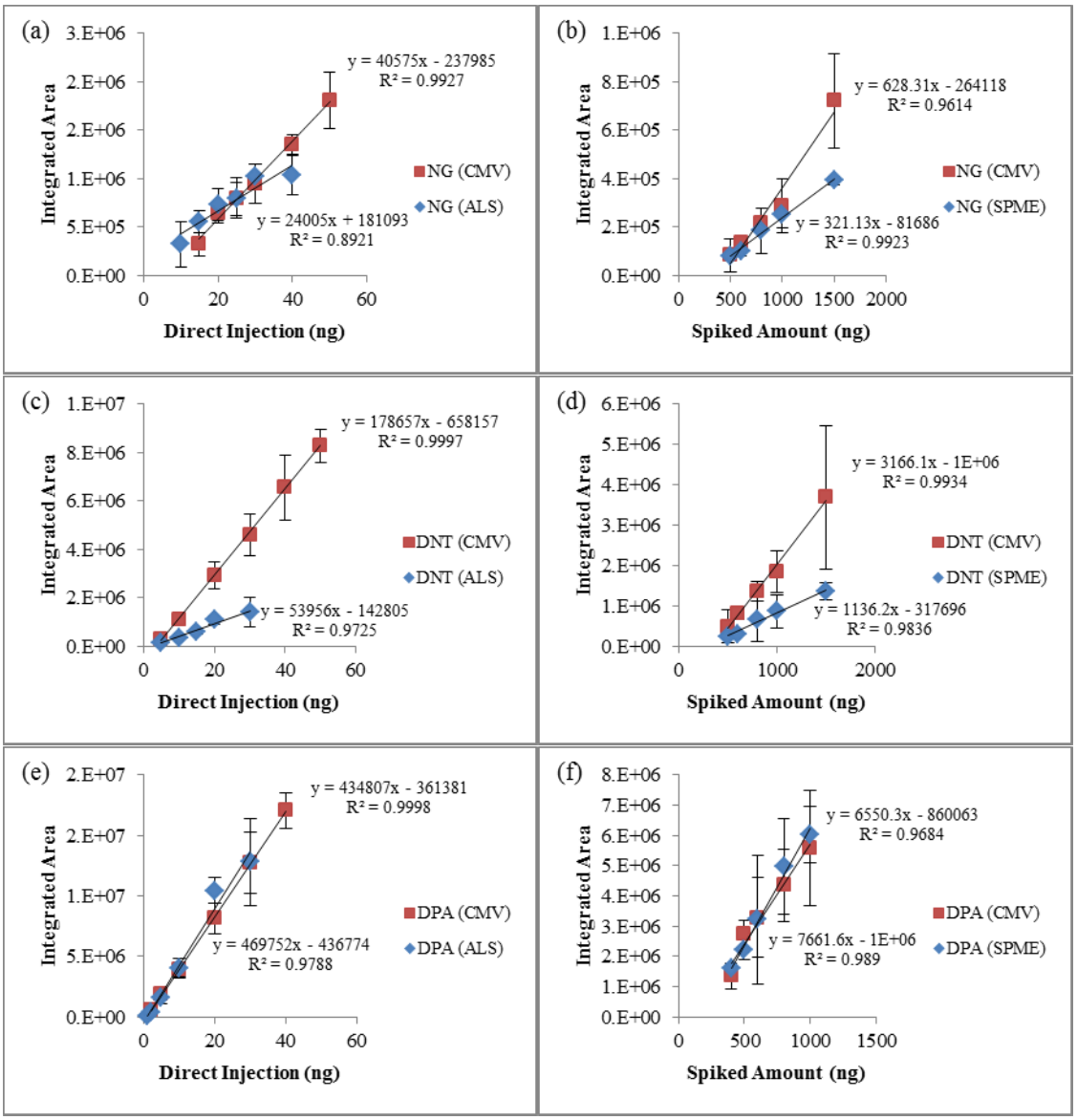

Figure 8-27 Calibration curves generated for NG (a), 2, 4-DNT (c) and DPA (e) by using both CMV (red square) and GC autosampler (blue triangle). Headspace extractions with 1 min dynamic sampling time using CMV device (red square) and 30 min static sampling time using SPME fiber (blue triangle) show comparable quantitative analysis results. (b) NG (d) 2,4-DNT (f) DPA

8.4.5 Open System vs. Closed System

When the extraction using CMV was compared to SPME, one major disadvantage of CMV is that sampling was done in an open system where sample loss would cause low

sensitivity. To prevent sample loss, instead of using open lid, a hole was punctured on the lid and the CMV can sample through the hole with the option to puncture another hole on the lid for introducing new air into the can. To visualize the sampling process, the CMV devices and the dynamic sampler were sent to Matthew Staymates at NIST for flow visualization using a Schlieren optical system. The experimental setup consisted of a 50mm can and a small piece of cotton cloth soaked with acetone and sampling was processed by applying three different setups which were one hole on the lid (Figure 8-28 (a)), two holes on the lid (Figure 8-28 (b)) and open system (Figure 8-28 (c)). The CMV devices were applied to sample each of the setup and the distance between the device and the opening was varied to observe the optimized sampling distance. The video footages of the flow visualization were edited and one clip was shown in Figure 8-28 (d, e, and f) for each setup. The CMV performed well in collecting vapor at a very small standoff distance (0 to 1 cm); however, the aerodynamic reach of the CMV is limited to about 2cm, and at 2cm even the slightest external breeze will perturb the inlet flow. As seen in Figure 8-28 (f), in the open system, the samples escaped from the container during the sampling process and in the single hole setup, the sample loss has been reduced. With two holes on the lid, the CMV were extracting from both holes which could cause some sample loss due to the distance between the second hole and the CMV device; thus, the semi-closed system with one hole on the lid should be used in the future experiments. Even though the system is not completely closed, it reduced the sample loss and the recovery of CMV has shown a 3-times increase (Figure 8-29).

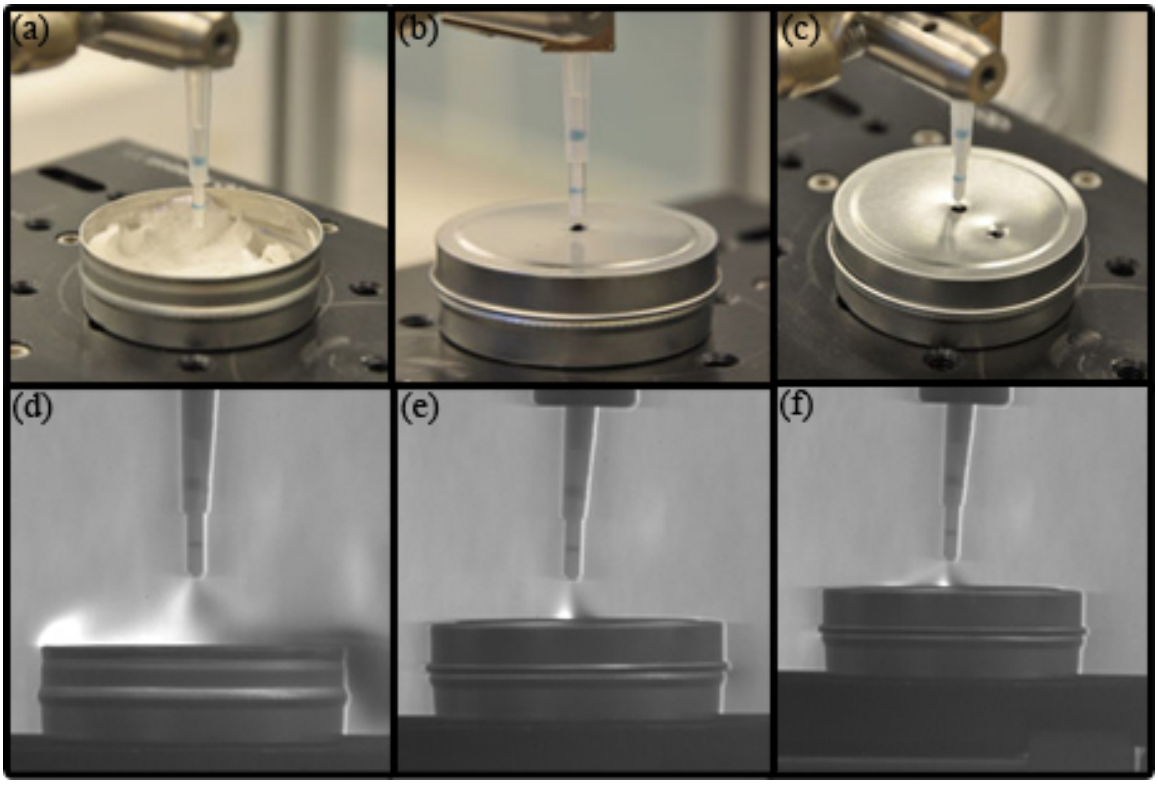

Figure 8-28 Flow visualization setup (a, b, and c) and results (d, e, and f) of dynamic sampling of CMV devices over the headspace of a container. (a and d) one hole on the lid, (b and e) two holes on the lid, (c and f) open system

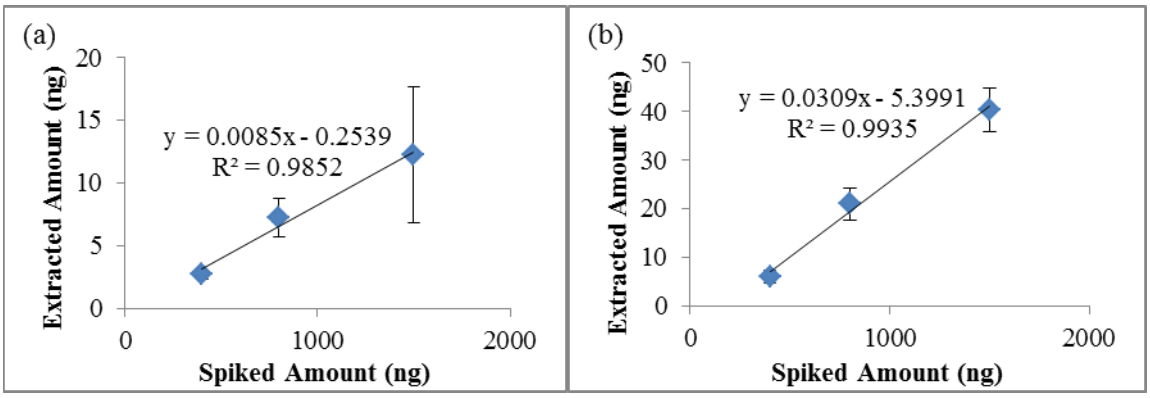

Figure 8-29 Dynamic headspace sampling using CMV with (a) an open system and (b) a semi-closed system

8.5 Summary

The newly invented preconcentration device, capillary microextraction of volatiles (CMV), was coupled to a GC-MS for compounds separation and detection. The CMV devices maintain a high surface are and phase volume from the PSPME devices which can provide high preconcentration capacities that is lacking from SPME fibers. Besides that, the modified geometry also allows dynamic headspace analysis that improves the sampling throughput, along with the increased preconcentration capacity, the extraction time was shortened from 30 min using a SPME fiber to only 1 min extraction with a CMV device to achieve the same recovery percentage.

As stated before, PSPME improved the sampling throughput and the ruggedness of the devices allowed for portability for field sampling; however, the fast flow rate caused breakthrough that led to significant sample loss and the identification capability was lacking since the devices can only be coupled to IMS systems. In contrast, CMV devices overcame both of the disadvantages: no breakthrough was observed in CMV devices even after 1 hour long extraction time that showed efficient preconcentration and retention capability of the technique and coupling to GC-MS as the detector, complex matrices can be analyzed with identification of individual compounds preconcentrated on the device.

The CMV devices were also proven to not only perform quantitative analysis in a semi-closed system with great precision, but also provide quantitative results in an open system which suggests that the method can be applied to sampling open environment. Additional benefit from CMV is the portability of the device that can be sealed in

aluminum foils for preservation and transportation back to the laboratory for further analysis.

Chapter 9 CMV-GC-MS Forensic Applications

The novel dynamic preconcentration technique was brought to real life scenarios for case studies after the CMV-GC-MS method was developed and optimized. The applications were accomplished with the generous offer from a local shipping facility, a local government facility, and one FIU research laboratories. Because of the limited resources, the headspace analysis for military explosives and illicit drugs can only be accomplished with limited replicates.

9.1 Detection of Smokeless Powders

Detection of smokeless powders using CMV-GC-MS has been shown above in the method optimization. In addition to efficient detection, the CMV devices with the air sampling tubing also allowed for flexible sampling where the devices can be used in the containers instead of outside the containers. As stated before, cardboard boxes showed adsorption of compounds emitted from smokeless powders; thus, long extraction time has to be applied for SPME to achieve detection in GC-MS (at least 2 to 3 hours). With the flow assisted sampling, CMV was used to sample inside of the box and will not get broken because of the housing provided protect for the preconcentration materials. 1 min dynamic extraction was used in a cardboard box and as shown in Figure 9-1, NG and DPA were detected.

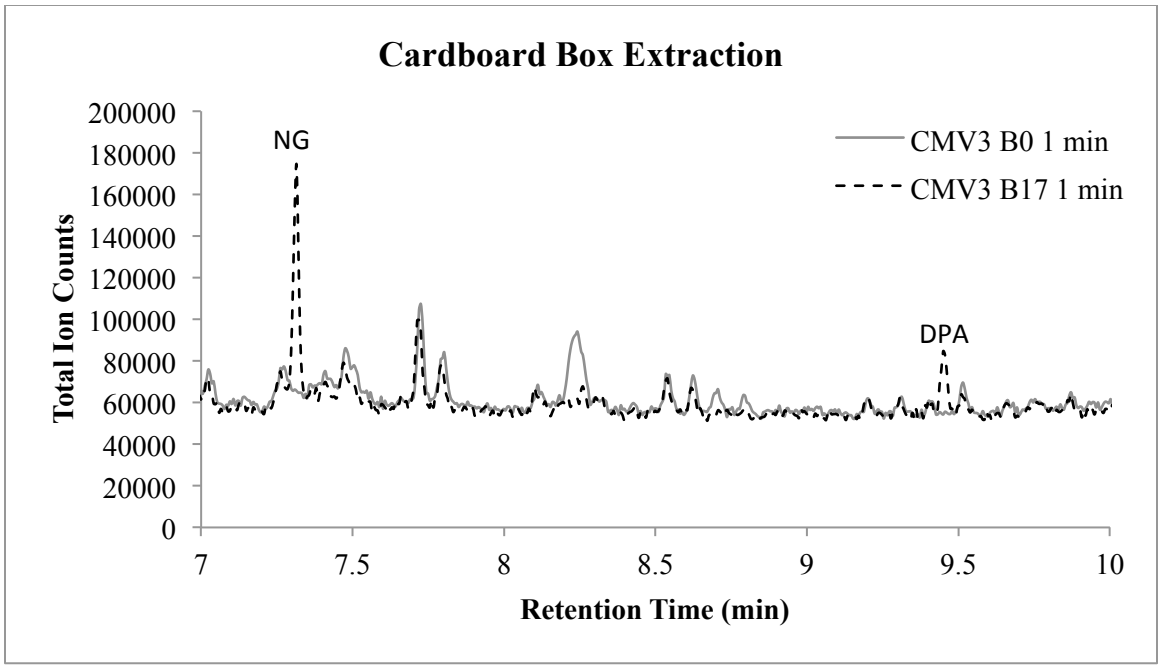

Figure 9-1 Detection of NG and DPA in a cardboard box with only one minute dynamic extraction time

9.2 Headspace Analysis in a Shipping Facility

9.2.1 Introduction of Sampling in Shipping Facility

There is a high volume and variety of cargo entering the United States from border checkpoints at land, seaports and airports every day. Screening the high volume of commercial cargos for illicit substances is always a challenging task for the US customs and Border Protection based on the high throughput requirements. Any delay caused by false positive alarm will result in high cost of time and money and any false negative alarm will put great threat to public safety. As a result, a high-throughput sampling and detection system with high accuracy is needed. Both bulk and trace detection are deployed at checkpoints to complement one another at this moment [58]. And for trace detection, particle swabbing using IMS as a detector is the most common method

encountered; however, using particle sampling could cause high background noise and great interferences which will lead to high false positive alarms [93]. Thus, the method developed here was tested for the application in the shipping facilities for fast preconcentration of the headspace of suspected packages.

9.2.2 Materials and Methods

The sampling process took place at a local shipping facility where massive amount of packages were present which were ready for delivery or shipping. Different packaging methods were also observed which involved LD3 (79 × 60.4 × 64 in), LD8 (125 × 60.4 × 64 in) shipping containers, cardboard boxes, plastic bags, and wooden boxes in different states (empty, half loaded, and fully loaded and closed for shipping) and some cardboard boxes were even wrapped with clear plastic tape to secure the packaging, summarized in Figure 9-2.

Since the CMV is a small rugged preconcentration device connected to a long tubing, it can be inserted into the container with just a small opening and thus easily access the inside of the container without opening the shipment. For the largest containers, LD8, 3 min and 5 min sampling time was used. For the large containers, LD3, 1 min and 3 min sampling time was used. One min dynamic sampling time was used for all the other size packages. After sampling, all the CMV devices were sealed in aluminum foil on site and transported back to the lab for GC-MS analysis.

Figure 9-2 Different scenarios in the shipping facility (a) an empty LD8 container (b) a fully packed LD3 container (c) a heavy taped cardboard box (d) a half packed LD8 container (e) a fully loaded LD8 container ready for shipping (f) a cardboard box with clear wrap (g) a red plastic bag (h) a regular cardboard box (i) a wood box

9.2.3 Results

A total of 30 different samples were taken and the detected compounds and their frequency of detection were listed in Table 9-1, negating compounds detected only once. Among these compounds detected at least twice, the majority compounds present were long chain alkanes and their isomers. The rest of the compounds also included some common fatty acid such as n-Hexadecanoic acid, octadecanoic acid and tetradecanoic acid and commonly used plasticizer such as benzyl butyl phthalate, 1,2-

benzenedicarboxylic acid, butyl 2-ethylhexyl ester and 1,2-benzenedicarboxylic acid, mono (2-ethylhexyl) ester. Most compounds detected were volatiles associated with common household products: squalene (cosmetics), homosalate (sunscreen), nonanal (flavors and perfume), naphthalene (mothballs).

In this study, no suspicious material were detected in the shipping facility, which largely avoided the false positive alarms by using headspace preconcentration.

Table 9-1 Compounds detected in the shipping facility from 30 samples taken

Compounds Detected	Frequency (n=30)
n-Hexadecanoic acid	16
Squalene	8
Dodecane	6
Benzyl butyl phthalate	6
1,2-Benzenedicarboxylic acid, butyl 2-ethylhexyl ester	5
Undecane	4
Dibutyl phthalate	4
Pentadecanoic acid	4
Nonanal	3
1,2-Benzenedicarboxylic acid, mono(2-ethylhexyl) ester	3
Octadecanoic acid	3
Naphthalene	2
2-Propenoic acid, 2-ethylhexyl ester	2
Homosalate	2
Decane	2
Dodecane, 3-methyl-	2
Decane, 2-methyl-	2
Tetradecane	2
Tetradecanoic acid	2

9.3 Headspace Analysis of Military Explosives

9.3.1 Introduction of Military Explosives

Seven military explosives will be discussed in this chapter individually. The structures and vapor pressures of these military explosives were listed in Table 9-2 [94].

Table 9-2 Structures and vapor pressures of military explosives [94,95]

Chemical Name	Structure Formula	Vapor Pressure (Torr)
2,4,6-Trinitrotoluene (TNT)	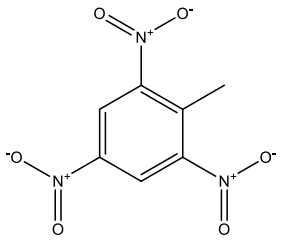	1.1×10^{-6} at 20 °C
Erythritol tetranitrate (ETN)	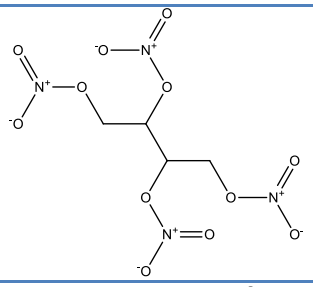	2.3×10^{-5} at 25 °C
Pentaerythritol Tetranitrate (PETN)	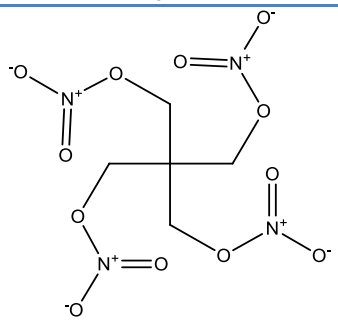	1.4×10^{-8} at 25 °C
Nitroglycerin (NG)	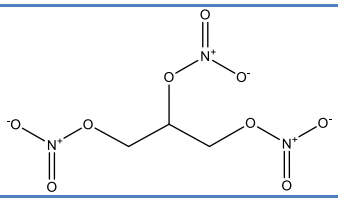	4.4×10^{-4} at 25 °C
Ethylene Glycol Dinitrate (EGDN)	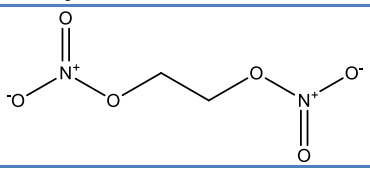	2.8×10^{-2} at 25 °C

1,3,5-Trinitro-1,3,5-triazacyclohexane (RDX)	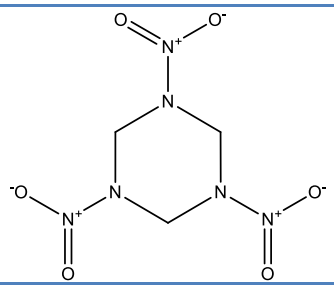	4.6×10^{-9} at 25 °C

9.3.1.1 NG, EGDN and ETN

Both nitroglycerin (NG) and ethylene glycol dinitrate (EGDN) are colorless liquid explosives. NG has been the main component in many dynamites and it is an ingredient in multi-base propellants. The sensitivity of NG is very high to shock impact and friction, and it can only be used when desensitized with other components. EGDN is more stable than NG, but it has a higher vapor pressure [31].

Erythritol tetranitrate (ETN), not used in the military applications, has a chemical structure that is similar to PETN; however, the high vapor pressure makes ETN easier to be detected in the headspace. The synthesis process of ETN has been known for a long time; yet, the erythritol precursor was not available until it was produced on an industrial scale using microbial techniques. With the increased market availability, recent reports have shown the use of ETN by juveniles, criminals and terrorists [95].

9.3.1.2 PETN

Pentaerythritol tetranitrate (PETN), also known as Penta, was first prepared in 1891 and became commercially available in the 1930s. It can be used as a base charge in blasting caps and detonators, or as the core explosive in detonating cord, booster charges, plastic explosives [31] and considered the most powerful and most brisant explosives. The

sensitivity of PETN is relatively high, but can be easily phlegmatized by adding a small amount of wax which does not affect the completeness of detonation. The stabilized PETN can also be used to produce boosters and fillings for smaller caliber projectiles. It is a component in many military explosives, most notably pentolite, where it may comprise 10 % - 60 % of a mixture with TNT [34]. It can also be used as industrial explosives when incorporated into gelatinous [96].

9.3.1.3 RDX and HMX

1,3,5-Trinitro-1,3,5-triazacyclohexane (RDX) and 1,3,5,7-Tetranitro-1,3,5,7-tetrazazyclooctane (HMX) were both used for military applications during and after World War II [96]. The two explosives are homologous where RDX is hexogen and HMX is octogen. They are currently the most important high-brisance military explosive in use. The high brisance power (greater than TNT) results from the high density and high detonation velocity. A vast number of explosives consisting of mixtures of various explosive compounds were developed in World War II and many of these combinations include HMX and RDX. A few important combinations are Composition B (60 % RDX/40 % TNT/plus wax), Cyclotol (60 % - 75 % RDX/25 % - 40 % TNT), Torpex 2 (42 % RDX/40 % TNT/18 % Al), and Composition C-4 (91 %) [96].

9.3.1.4 TNT

2,4,6-Trinitrotoluene (TNT) is still the most important explosive for blasting purposes of various weapons in military applications because it is very stable and shows low sensitivity to impact, friction and high temperature [31], and it can be applied pure or mixed with other components to improve the blasting performance or increase sensitivity.

Mixed with ammonium nitrate, aluminum powder and 1,3,5-Trinitro-1,3,5-triazacyclohexane (RDX) will produce Amatols, Tritonal and Composition B, respectively [34,96]. For military-grade TNT, 99.8% of the solid explosive was 2,4,6-trinitrotoluene and only 0.08% was 2,4-dinitrotoluene from manufacturing impurity; however, in the equilibrium vapor in the headspace over the explosive, TNT accounted for 58% and 2,4-DNT account for 35 % because the difference in the vapor pressure. Besides 2,4-DNT and TNT in the headspace, 1,2- and 1,3-dinitrobenzene (DNB), 1,3,5-trinitrobenzene (TNB), the various isomers of DNT and TNT were also reported detection in GC-ECD as shown in Figure 9-3 [97].

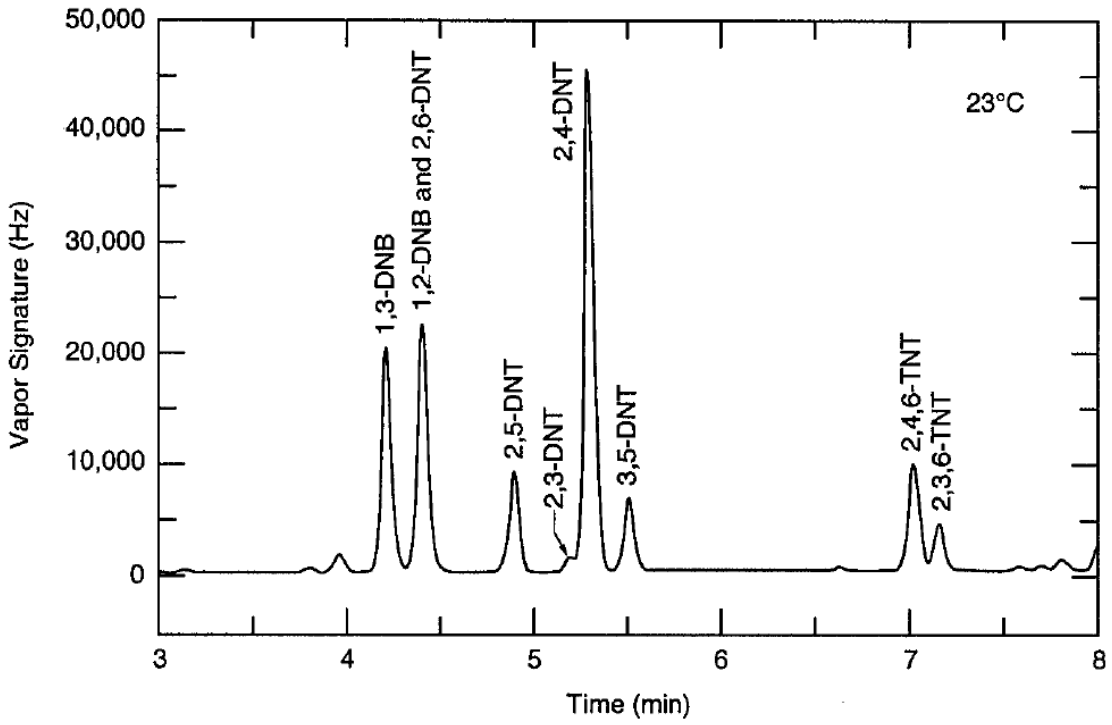

Figure 9-3 Vapor signature of 1966 military-grade TNT as determined by GC-ECD [97]

9.3.1.5 Plastic explosives

Plastic-bonded explosive, or PBX, is a fairly recent development in the military arena. The mixture of high-brisance explosives, such as RDX or HMX, and curable or polyadditive plastics, such as polysulfides, polybutadiene, acrylic acid, polyurethane, can be cured into a desired shape. They have advantages of high mechanical strength, high detonation velocity, excellent stability, and insensitivity to shock and high temperatures. Plastic explosives cover a wide range of formulations, usually containing some ingredients from the list of RDX, PETN, HMX, aluminum, binders and a plasticizer. Two of the best known plastic explosives are C-4 (91 % RDX/9 % plasticizer) and SEMTEX (RDX/PETN) [34,96].

As plastic explosives are composed of explosives with extremely low vapor pressure, in 1996, Congress passed the Anti Terrorism Bill that requires the addition of detection taggants to plastic explosive compounds and the ban of sale or import of plastic explosives that do not contain a detection agent [94]. A detection taggant is a solid or liquid vapor emitting substance added to an explosive material to facilitate discovery before detonation. The international Civil Aviation Organization (ICAO) has designated four compounds in concentration by mass as the detection taggants: 0.5 % 2-nitrotoluene (2-NT), 0.5 % 4-nitrotoluene (4-NT), 0.1 % 2,3-dimethyl-2,3-dinitrobutane (DMNB), and 0.2 % ethylene glycol dinitro (EGDN). The four compounds mentioned above were chosen because they are not commonly found in nature, they do not hinder the explosive properties, they continue to release vapors at a steady rate for 5 to 10 years, they do not

present a significant environmental hazard, and they do not readily adhere to common substances they may come in contact with [71].

9.3.2 Materials and Methods

In this research, all the military explosives were provided by a local airforce base which include NG, EGDN, ETN, PETN, RDX, TNT, and C4. Among the 7 different explosives, NG and EGDN were in the liquid form and thus kept in a small plastic bottle in plastic containers (3 quart) (Figure 9-4 (a)). ETN, PETN and RDX were in the solid form and about 0.5 g of the explosives were weighed on watch glasses and placed in plastic containers (2.5 quart and 3 quart) (Figure 9-4 (b)) and placed in a vented hood in which were given 1 hour to 3 hours equilibrium in the container followed by CMV device dynamic sampling of 1 min and/or 3 min. For TNT and C4 explosives, only wrappers of the explosives were obtained and sealed in Ziploc bags for 24 hours for equilibrium before sampling (Figure 9-4 (c) and (d)). After equilibrium, the Ziploc bag was open and a CMV device was inserted into the bag for dynamic sampling of 1 min. All the CMV devices were then sealed in a piece of aluminum foil and transported to the lab for analysis using the method optimized in Chapter 9.1.

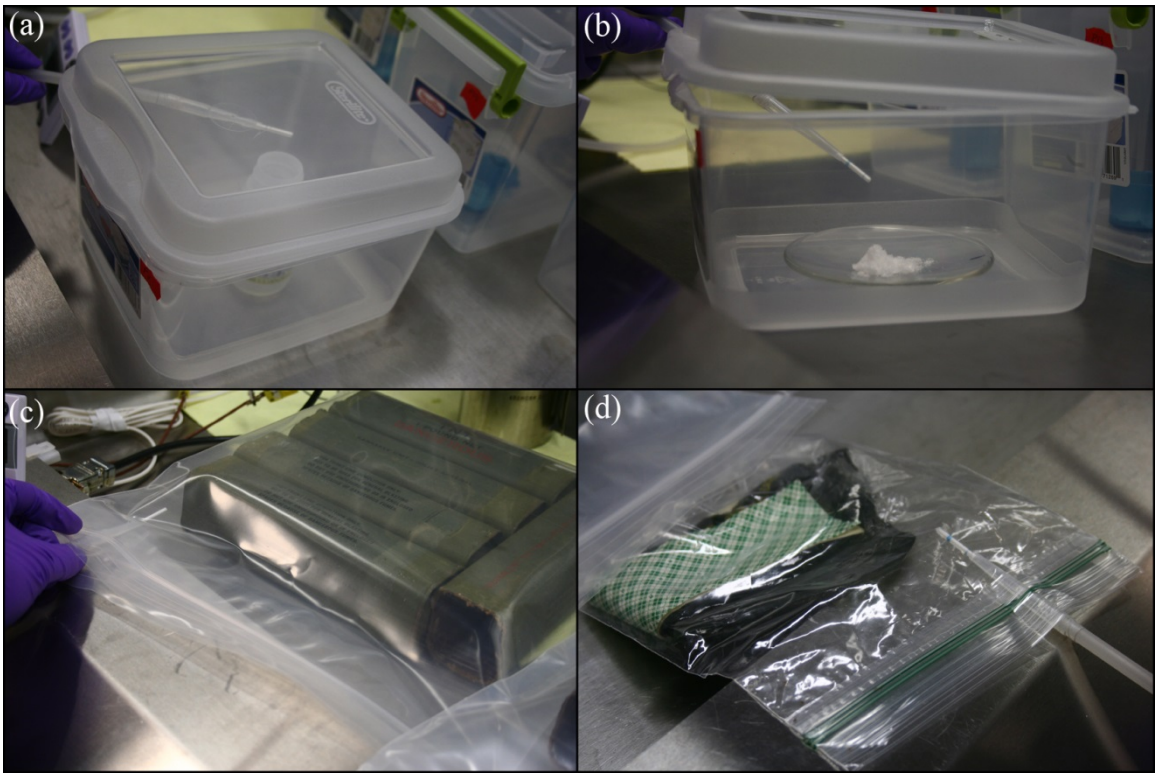

Figure 9-4 Military explosives sampling using dynamic CMV devices (a) NG in a plastic bottle in a 3 quart plastic container (b) ETN on a watch glass in a 3 quart plastic container (c) TNT wrappers sealed in a Ziploc bag (d) C4 wrappers sealed in a Ziploc bag

9.3.3 Results

9.3.3.1 NG, EGDN and ETN

The high vapor pressure of NG and EGDN resulted detection in the headspace with high sensitivity. When the CMV devices were thermally desorbed in the GC-MS, NG showed two peaks in the chromatogram as shwon in Figure 9-5. The one at retention time of 7.3 min matched to the NG mass spectrum in the library, and the one at retention time of 4.2 min was identified as 1,3-propanediol, dinitrate in the library. The two peaks were also found in the μECD shown in Figure 9-6 which can be used as a confirmation for compounds that is high electronegativity. Nitroglycerin mass spectrum was shown in

Figure 9-7 and 1,3-propanediol, dinitrate mass spectrum was shown in Figure 9-8. Both compounds have similar mass spectrum in the electron ionization mode, the only difference is the ratio between m/z 30 and m/z 76. There weren't any research shown that 1,3-propanediol, dinitrate was one of the signature volatile compounds in the headspace of NG; thus, it should be the thermal decomposition products when the CMV device was introduced into the injector.

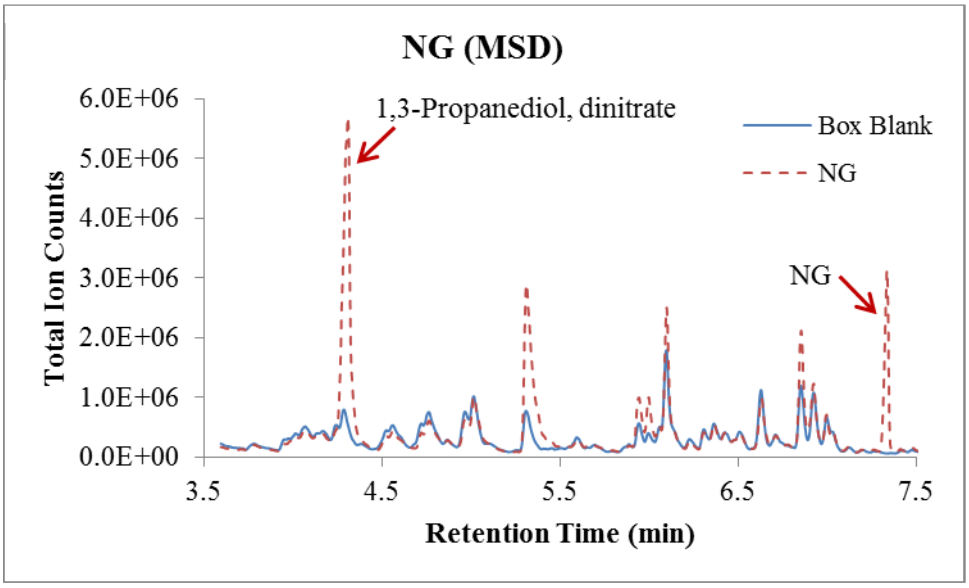

Figure 9-5 Chromatogram of GC-MS after thermally desorbing a CMV device that was used to sample the headspace of NG for 1 min

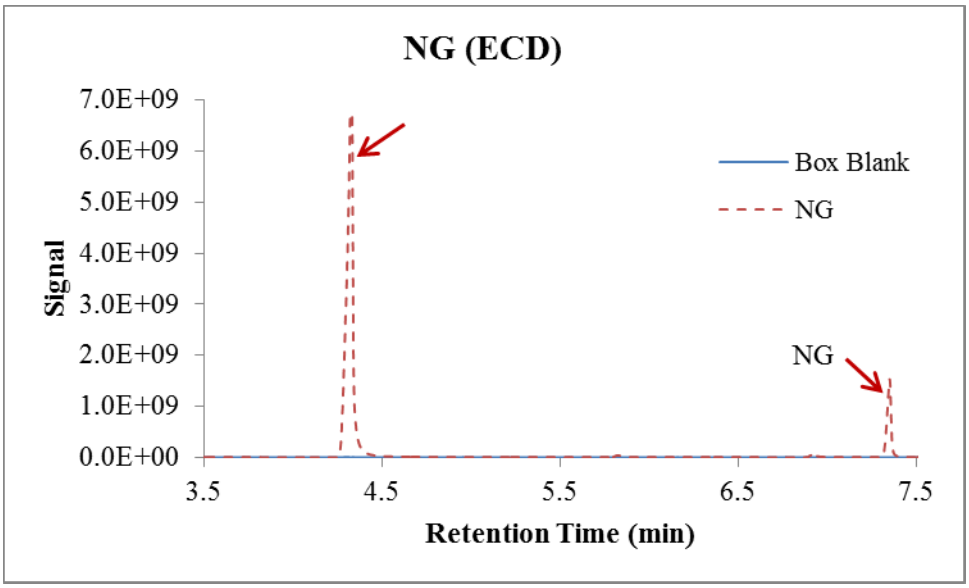

Figure 9-6 Chromatogram of GC-ECD for 1 min dynamic sampling of the headspace of NG with a CMV device

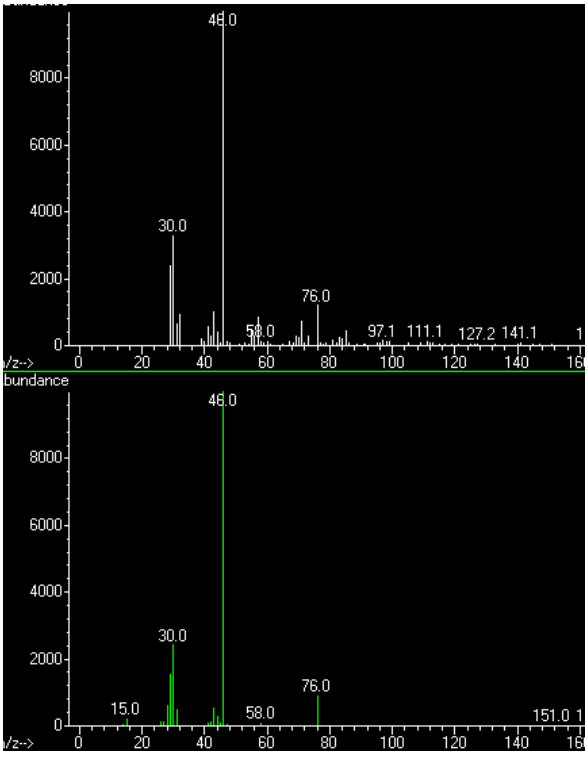

Figure 9-7 Nitroglycerin mass spectrum obtained from the headspace of NG (up) compared to the mass spectrum in the library (down)

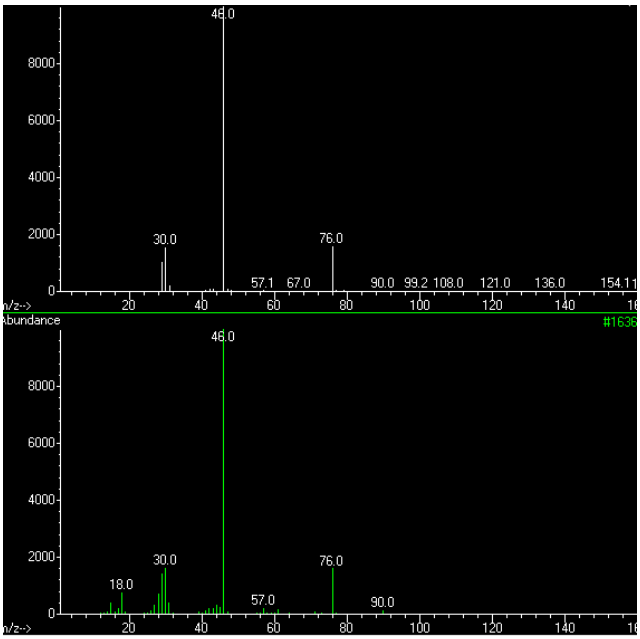

Figure 9-8 1,3-propanediol, dinitrate mass spectrum obtained from the headspace of NG (up) compared to the mass spectrum in the library (down)

The detection of EGDN was even easier than NG because of the high vapor pressure at room temperature (2.8×10^{-2} torr). The CMV device was saturated with the vapors from EGDN and further saturated the detector (Figure 9-9). The peak of retention time at 4.5 min was matched to 1,3-propanediol, dinitrate in the library search and this helped identifying the peak as a thermal decomposition product since NG and EGDN shared the same backbone structure (Table 9-2).

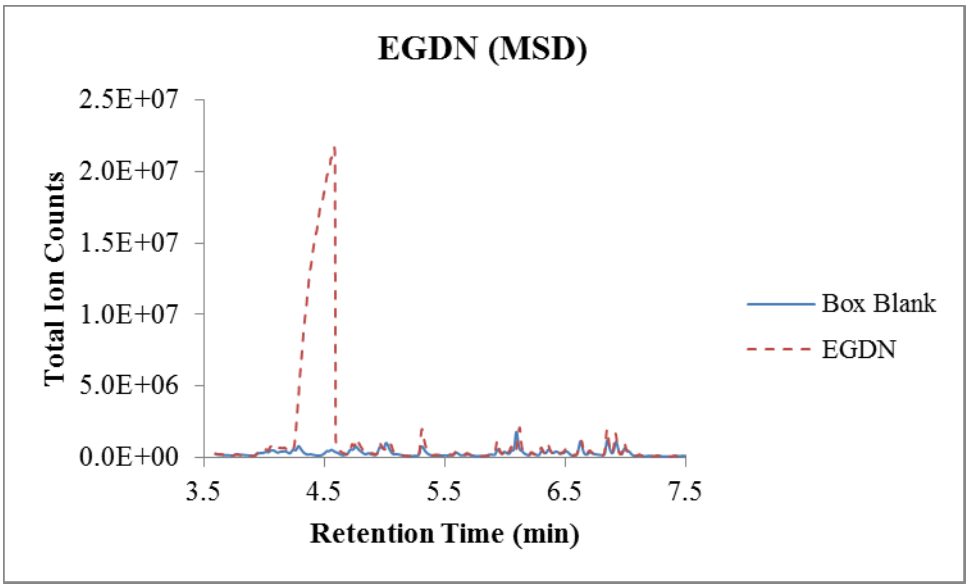

Figure 9-9 GC-MS Chromatogram of EGDN headspace after 1 min dynamic sampling

The detection of ETN was ambiguous (Figure 9-10) which showed the same peak that was present in NG and EGDN. The vapor pressure for ETN is relatively high [95] and the backbone structure is the same as NG and EGDN; thus, the same decomposition product could be present. However, the same peak could also be present because of cross-contamination from high vapor pressure of NG and EGDN. The sampling was accomplished in the same hood with the lid open where the vapor could escape from the containers. As the sampling time and condition was limited, it was impossible to perform additional sampling with no interference to confirm the presence of ETN in the headspace.

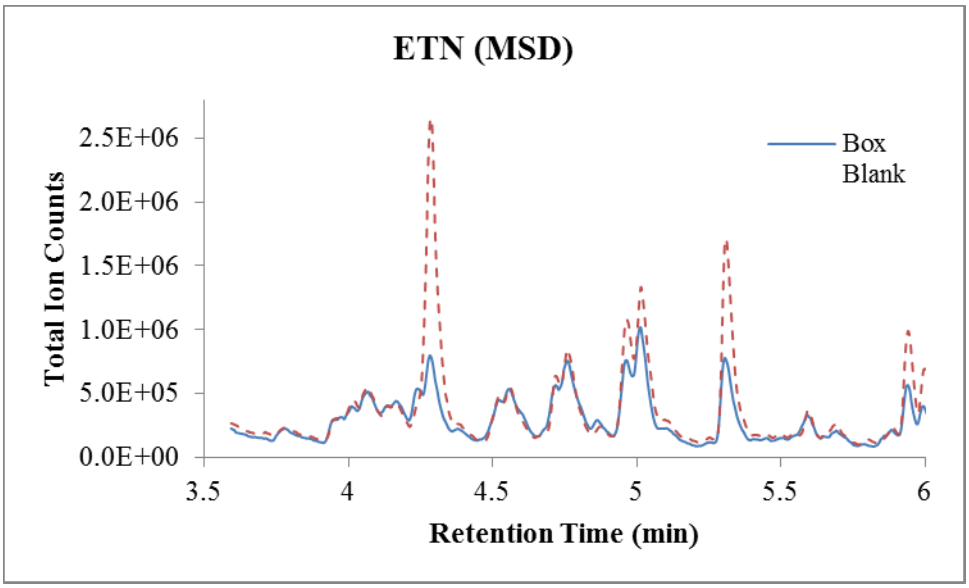

Figure 9-10 GC-MS Chromatogram of ETN after 3 min dynamic extraction using a CMV device

9.3.3.2 PETN and RDX

The other two military explosives, PETN and RDX, have low vapor pressure at room temperature which led to no detection of headspace volatiles. The same peak at 4.5 min retention time was present in both chromatogram of PETN and RDX which was cross-contamination from either NG or EGDN.

PETN and RDX were nitrate ester plastic explosives and their detection in the headspace has been reported with confidence. Most of the detection of the parent explosives were considered as the direct particle transfer instead of the headspace preconcentration owing to the low vapor pressure [18,71].

9.3.3.3 TNT and C4 Wrappers

Because of the limited access to TNT and C4 explosives, only the wrapper for these two explosives were provided as shown in Figure 9-4. The CMV device was inserted into the plastic bag for dynamic sampling of 1 min and 2,4-DNT was found in the TNT headspace while DMNB was found in the C4 headspace.

Composition C4 was composed of RDX and plasticisers. Because of the low vapor pressure of RDX, DMNB (one of the four chemicals added as a marker to plastic and sheet explosives) was used as the taggant and its detection can confirm for detection of these high explosives [18].

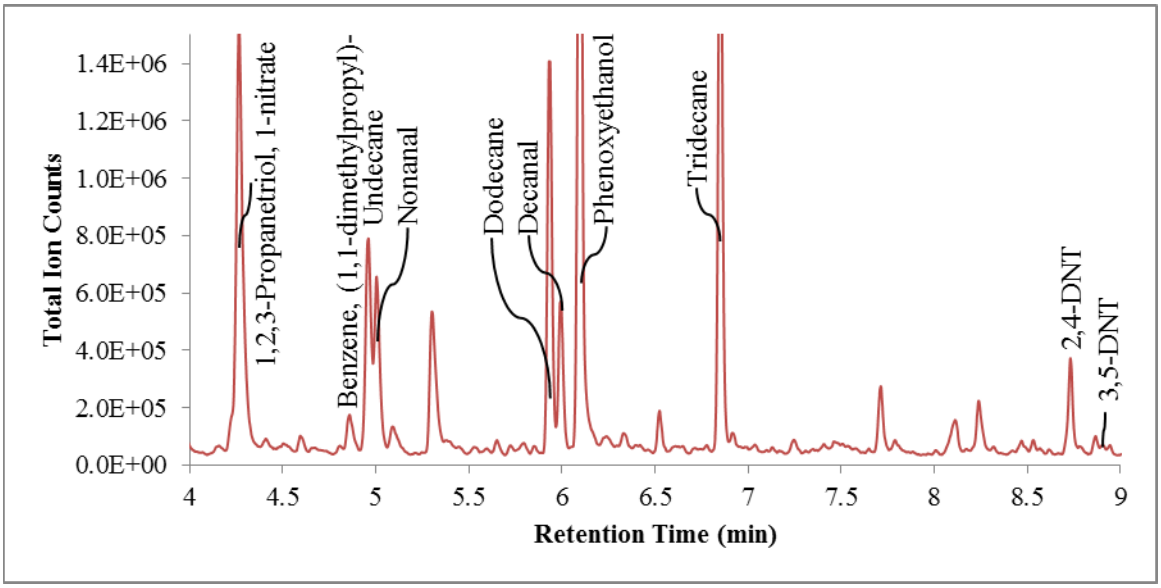

Figure 9-11 Chromatogram of 1 min dynamic headspace of TNT wrappers using GC-MS

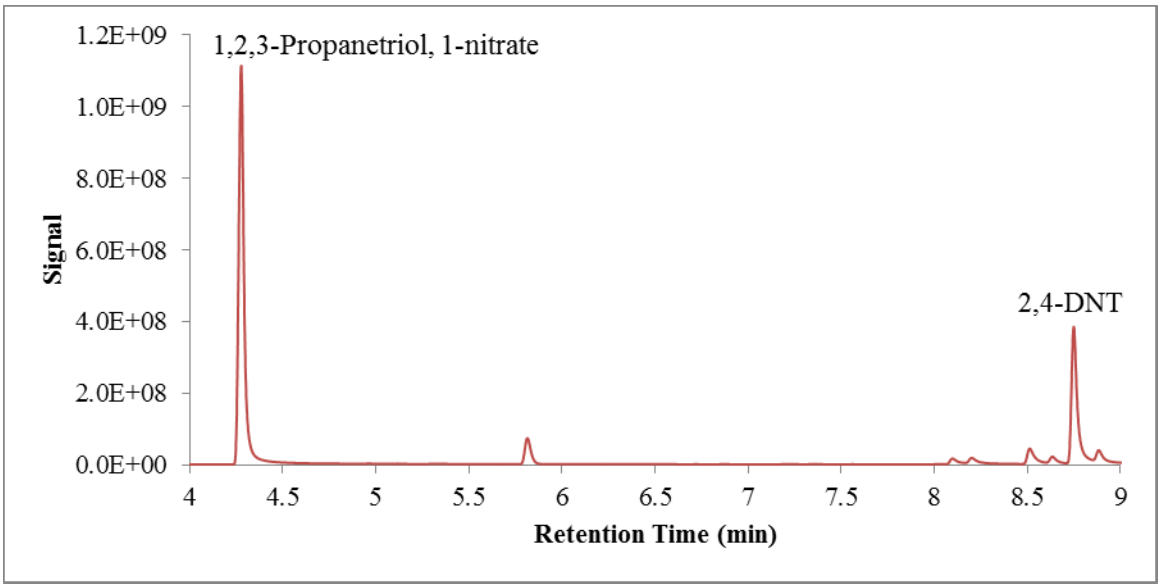

Figure 9-12 Detection of 2,4-DNT in TNT wrappers in GC-µECD after 1 min dynamic headspace sampling using a CMV device

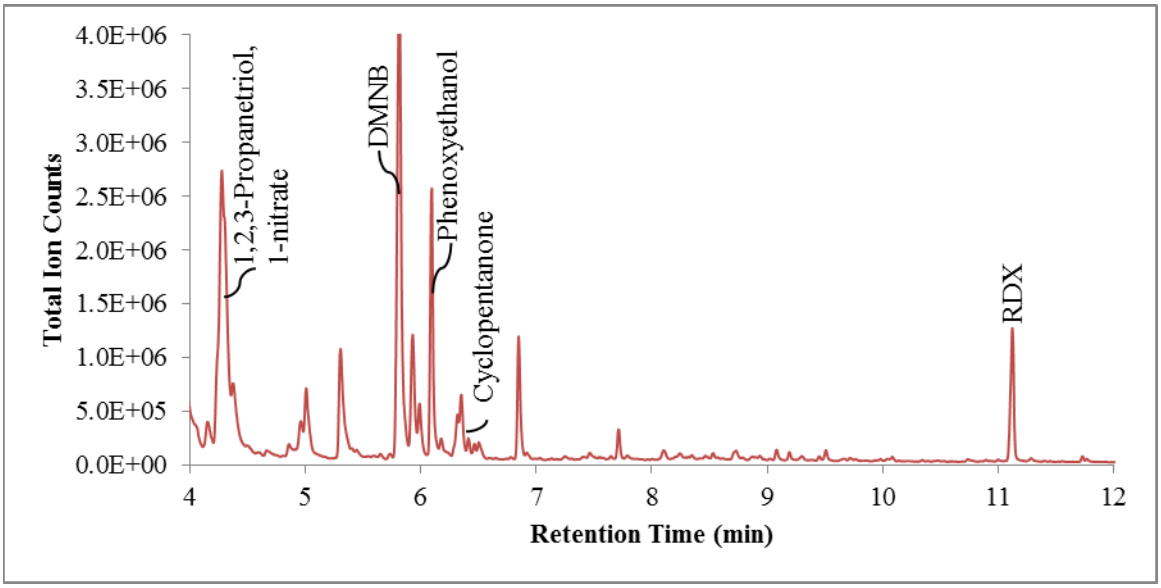

Figure 9-13 Chromatogram of 1 min dynamic headspace of C4 wrappers using GC-MS

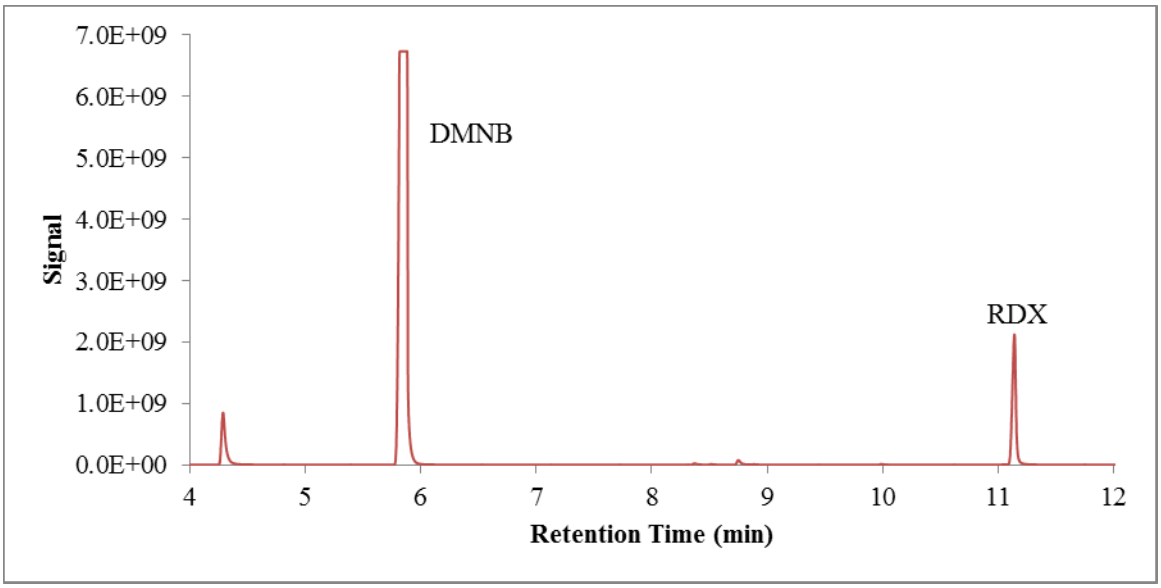

Figure 9-14 Detection of DMNB and RDX in GC-μECD after 1 min dynamic headspace sampling using a CMV device

9.4 Headspace Analysis of Illicit Drugs using CMV-GC-MS

9.4.1 Introduction of Illicit Drugs

Most active compounds in illicit drugs have very low vapor pressures and thus are not easily detected with a trace detector. Many studies have reported that by detecting the volatile compounds in the headspace rather than the parent drugs can improve the detection of illicit drugs [98]. Signature volatile compounds of cocaine, methamphetamine and MDMA were listed in Table 9-3 with their structure.

Table 9-3 Structure of cocaine, methamphetamine and MDMA and their signature volatile compounds in the headspace

Illicit drug	Reported Volatile Chemical Compounds [99,19]
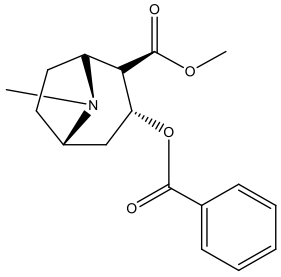 Cocaine	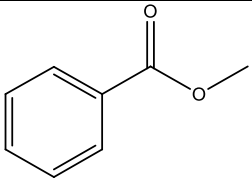 Methyl Benzoate
	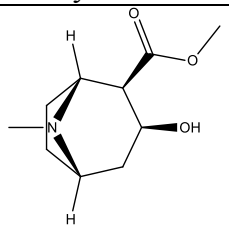 Ecgonine Methyl Ester
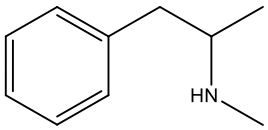 Methamphetamine	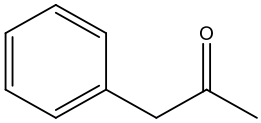 Benzyl Methyl Ketone (P2P)
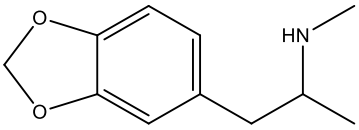 MDMA	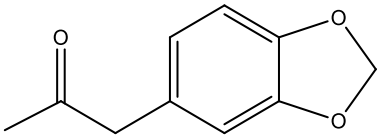 Piperonyl Methyl Ketone (MD-P2P)
	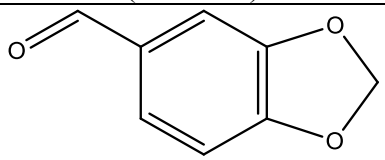 Piperonal

9.4.1.1 Cocaine-Base and Cocaine-HCl

The purities of cocaine base (Coc-Base) and cocaine hydrochloride (Coc-HCl) from the production of illicit cocaine are normally 80-95% and 80-97%, respectively. Pharmaceutical used cocaine can be as pure as 99.5%, but it still has some coca-related

impurities. There are various of impurities could be present in illicit cocaine which include benzoic acid, anhydroecgonine methyl ester, anhydroecgonine, trans-cinnamic acid, ecgonine methyl ester, ecgonine, pseudoecgonine, tropacocaine, benzoylecgonine, norcocaine, beta-truxinic acid, alpha-truxillic acid, cis-cinnamoyl ecgonine methyl ester, trans-cinnamoly ecogonine methyl ester and N-formylcocaine [99]. The quantity and species of impurities can vary from sample to sample and batch to batch. The reported compounds found in the headspace include methyl benzoate, benzoic acid, methyl trans-cinnamate, anhydroecgonine methyl ester, trans-cinnamic acid, and ecgonine methyl ester using Carbowax-DVB SPME fibers [99]. Other SPME fibers (DVB/Carboxen/PDMS and polyacrylate) were also used for profiling the headspace of cocaine and the chromatogram was shown in Figure 9-15 [100].

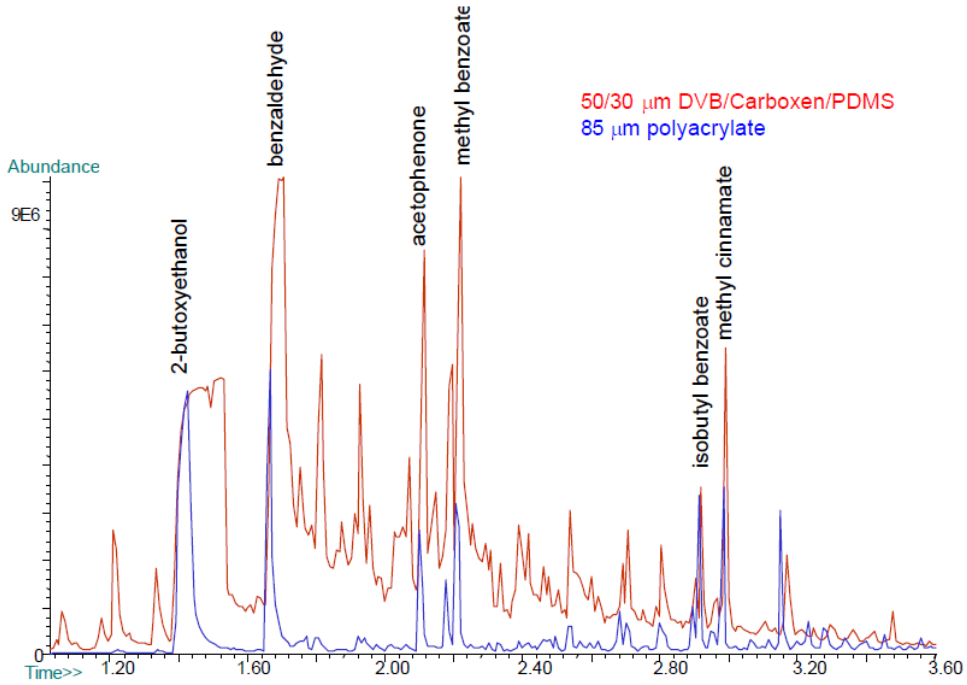

Figure 9-15 Two different SPME fibers were compared for 90 min sampling the headspace of 50 g of Coc-HCl followed by detection in GC-MS [100]

9.4.1.2 Methamphetamine and MDMA

In early studies, methamphetamine was identified as one of the volatile components in the headspace over MDMA and thus the two illicit drugs odor signature studies were relevant. It has been reported that benzaldehyde and ketone 1-phenyl-2-propanon (P2P) in the headspace of seized methamphetamine samples [19].

MDMA is the fifth most identified non-prescription controlled substance in U.S. crime labs and this illicit drug is most often encountered as tablets. MDMA's starting material carries the performed methylenedioxy ring, in the form of safrole, isosafrole or of the derived aldehyde, piperonal [19]. Different synthesis pathways for MDMA were shown in Figure 9-16 and the materials used for the synthesis were also included. Studies has shown detection of acetic acid, camphor (a flavor additive), piperonal (a starting material), isosafrole (a starting material), the intermediate 3,4-methlenedioxyketone (MD-P2P), MD-phenyl-2 propanol and Methamphetamine [19]. Among these compounds, piperonal and MD-P2P are the major headspace composition [98]. Seized MDMA samples were sampled using SPME-GC-MS and the profile of the headspace was shown in Table 9-4 [101].

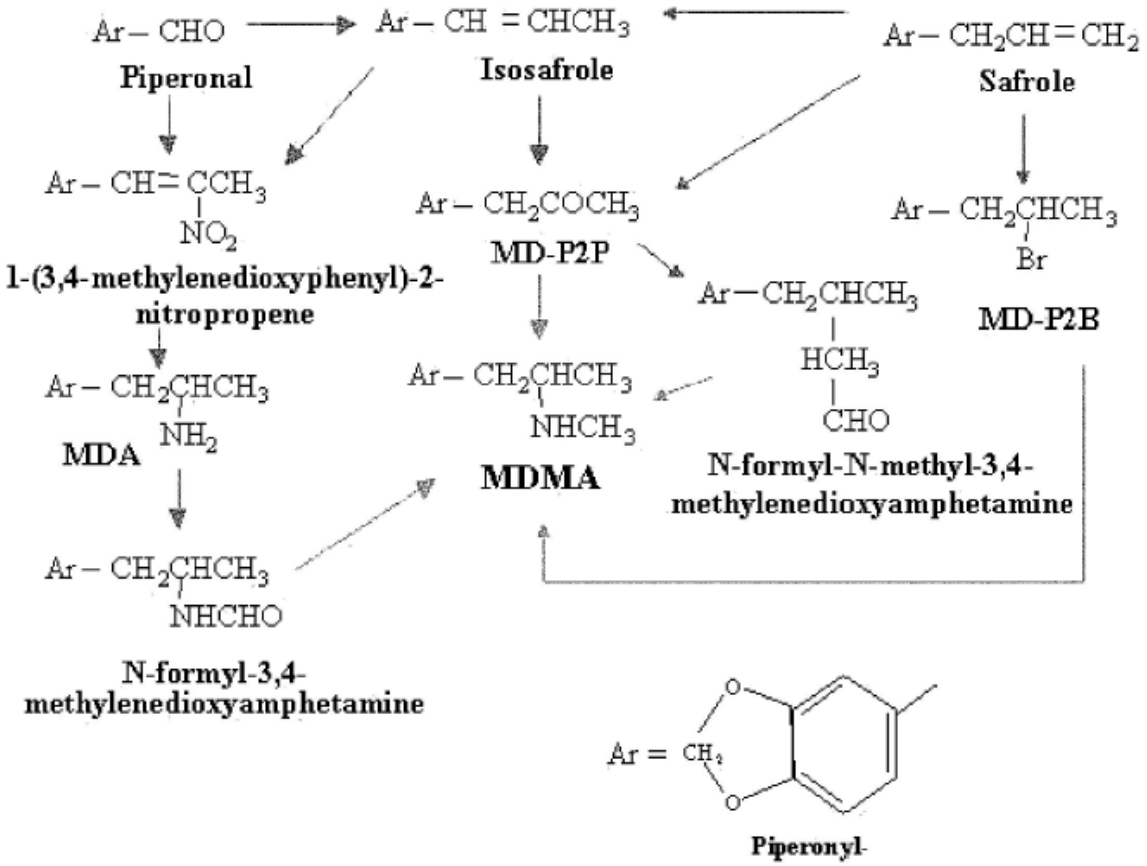

Figure 9-16 Different synthesis pathways of MDMA [19]

Table 9-4 Headspace volatiles detected in the headspace of MDMA [101]

Detected Compound	US K-9	FHP #1	FHP #2	FHP #3	FHP #4
Methamphetamine HCl				X	
Isosafrole			X	X	
Piperonal	X	X	X		X
Piperonyl Alcohol	X				
MDP-2-POH		X	X	X	X
MDP-2-P		X		X	X
MDMA				X	
MDEA				X	

9.4.1.3 Heroin

Headspace studies using SPME-GC-MS study showed detection of propyl acetate, methyl isobutyl ketone, 4-methyl-phenyl ester acetic acid, butylated hydroxytoluene and salicylic acid in the headspace of heroin and pseudo heroin samples (Table 9-5) [101]; yet, the detection is not confident because the signature compounds weren't consistent between samples.

Table 9-5 Headspace compounds detected in heroin and pseudo heroin samples [101]

Headspace Compounds	FHP Heroin	US-K9 Heroin	Commercial Pseudo Heroin	Sigma Pseudo™ Heroin
Acetic Acid	X	X	X	X
Propyl Acetate	X			
Methyl Isobutyl Ketone	X			
4-Methyl-phenyl Ester Acetic acid	X			
Butylated Hydroxytoluene	X	X		
Salicylic Acid			X	

9.4.1.4 Marijuana

While the use of other illicit drugs is a great concern, the abuse of marijuana as a psychoactive drug is still a significant problem. Thus, the detection of the VOCs of marijuana in the headspace is important for the law enforcement officials. The presence of marijuana can be determined using visual examination, color tests, thin layer chromatography, gas/liquid chromatography; however, the preparative steps as well as the analytical procedures are often time consuming [102]. The headspace of marijuana

consists of a volatile fraction (acetone, methanol, acetaldehyde, ethanol, ethylacetate, and isobutylaldehyde), an intermediate volatile fraction (α- and β-pinene, β-myrcene, limonene, ocimene, and β-phellandrene) and a less volatile fraction (β-caryophyllene and β-farnesene) [103]. The psychoactive (Δ^9-tetrahydrocannabinol (Δ^9-THC)) and related compounds indigenous to marijuana are nonvolatile and were not found in the headspace vapors as shown from headspace composition studies of marijuana at 65 °C and essential oil of marijuana using an electronic "sniffer" as shown in Table 9-6 [103].

Table 9-6 Comparison of the composition of headspace vapors of Marijuana with the composition of essential oil of Marijuana [103]

	Composition (%)	
Component	Head-space	Essential Oil
α-Pinene	55.5	3.9
Camphene	0.9	0.7
β-Pinene	16.4	2.2
2-Methyl-2-heptene-6-one	0.4	0.6
Δ^3-Carene	0.6	0.1
Myrcene	8.3	1.0
α-Terpinene	<0.1	<0.1
Limonene/β-Phellandrene	5.4	1.0
cis-Ocimene	1.2	0.2
trans-Ocimene	3.2	0.7
γ-Terpinene	<0.1	<0.1
Terpinolene	0.8	0.6
p-Cymene	—	0.1
Linalool	<0.1	0.5
Fenchyl Alcohol	—	0.1
Borneol	—	<0.1
trans-α-Bergamotene	0.7	8.0
β-Caryophyllene	3.4	37.5
β-Farnesene	0.8	9.8
α-Terpinenol	—	1.0
β-Humulene	0.7	13.9
α-Selinene	—	2.2
β-Bisabolene	—	3.2
Curcumene	—	1.4
Caryophyllene oxide	—	7.4
Total identified components	98.3	96.0

9.4.2 Materials and Methods

Six different illicit drugs (Cocaine-Base, Cocaine-HCl, Methamphetamine, MDMA, Heroin, and Marijuana) were obtained from Drug Enforcement Administration (DEA) in 1 lbs package and each illicit drug was then packaged into controlled odor mimic permeation system (COMPS) bags with 3 g and 25 g materials for future dog training use in Dr. Kenneth Furton's research laboratory. During the packaging process performed by the students, the headspace over the illicit drugs in the open air was sampled for 1 min and 3 min. One 3 g package and two 25 g packages were obtained and sealed in quart sized cans for 3 hours to develop headspace. The equilibrium time was limited to a short time because of the possession of the illicit substance was limited. After the equilibrium time, the CMV device was used to sample the quart can at the hole pre-made on the lid of the can for 1 min with one 25 g package and 3 min with the 3 g package and the other 25 g package. Again, because of the limited access of the substances, all the samples can only be analyzed once.

9.4.3 Results

Five different conditions were analyzed in this study which include (a) 1 min open air sampling, (b) 3 min open air sampling, (c) 3 min dynamic sampling over the headspace of 3 g of illicit substances, (d) 1 min dynamic sampling over the headspace of 25 g of illicit substances, and (e) 3 min dynamic sampling over the headspace of 25 g of illicit substances. Since the headspace did not reach the equilibrium state after such a short time and all the samples were only analyzed once, the condition was not optimized and the headspace analysis results weren't consistent. In the results presented below, the

tables were labeled in two different shades. The darker shade label compounds were detected at least twice in the five conditions and the lighter shade were only detected once in the five conditions. Besides, because Cocaine-Base and Heroin samples were in the powder form, the substances can be floating in the environment and stick to the CMV devices and caused cross-contamination.

9.4.3.1 Cocaine-Base

Chromatogram of the headspace analysis of cocaine-based was shown in Figure 9-17 and the compounds detected in the five conditions were listed in Table 9-7. Among all the compounds, methyl benzoate, methyl cinnamate, benzaldehyde, acetophenone and methylecgonidine were reported previously [99]. Cocaine was also seen in the GC-MS; however, the vapor pressure of cocaine was low and thus the detection of cocaine can only be particle stick to the CMV device and not in the headspace.

Table 9-7 Volatile compounds detected in the headspace of cocaine-base

Illicit Drug	Headspace Volatiles	Reported Previously
Cocaine-Base	Methyl benzoate	✓
	Cocaine	
	2-Ethylhexanol	
	Ethyl benzoate	
	Methyl cinnamate	✓
	Benzaldehyde	✓
	Acetophenone	✓
	Diethyl Phthalate	
	(Z)-13-Docosenamide	
	Methylecgonidine	✓
	2,6-Di-tert-butylphenol	
	Phthalic acid	
	2-ethylhexyl salicylate	

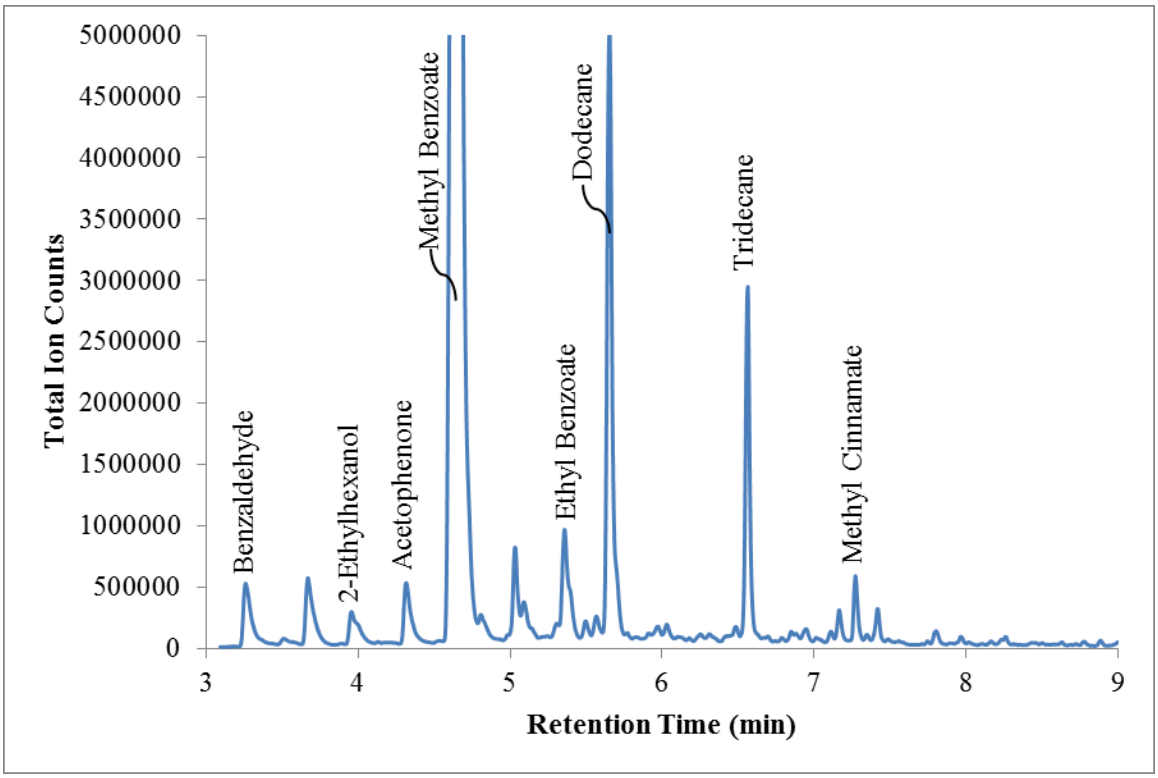

Figure 9-17 GC-MS Chromatogram of 3 g of Cocaine-Base sampled by a CMV device for 3 min in a quart can

9.4.3.2 Cocaine-HCl

There were less volatile compounds in the headspace of Cocaine-HCl samples compared to Cocaine-Base. The chromatogram was shown in Figure 9-18 and the compounds were listed in Table 9-8. Similar to Cocaine-Base, benzaldehyde, acetophenone and methyl benzoate were previously reported. Cocaine was also detected in the Cocaine-HCl sample which was caused by cross-contamination since the Cocaine-HCl was in a rocky form.

Table 9-8 Compounds detected in the headspace of Cocaine-HCl

Illicit Drug	Headspace Volatiles	Reported Previously
Cocaine-HCl	Benzaldehyde	✓
	Cocaine	
	2-Ethylhexanol	
	Acetophenone	✓
	Methyl benzoate	✓
	2,6-Di-tert-butylphenol	
	(Z)-13-Docosenamide	

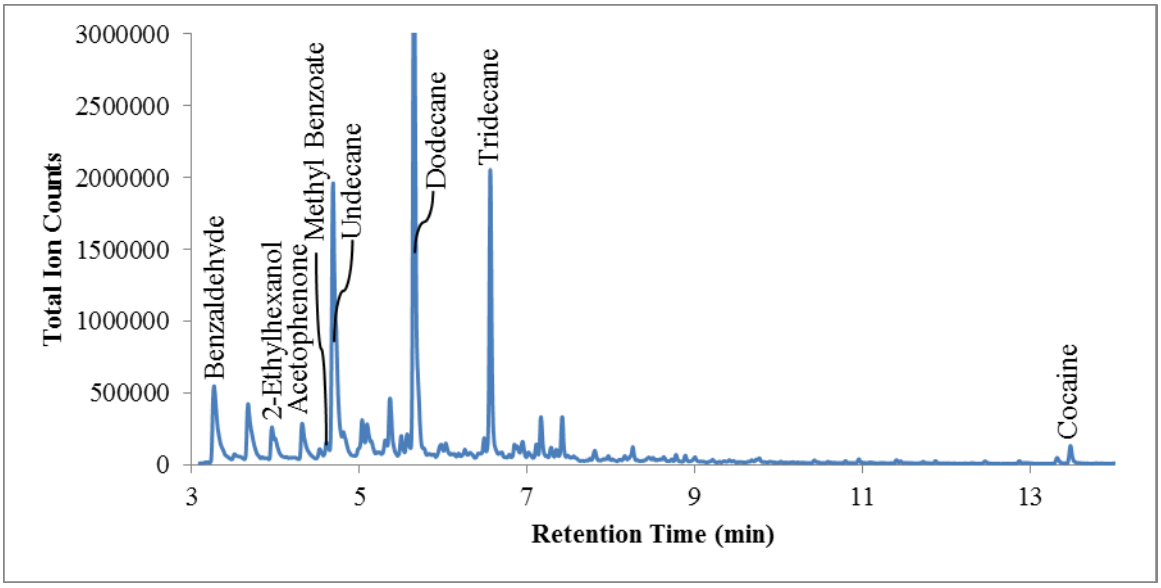

Figure 9-18 GC-MS Chromatogram of 3 min dynamic headspace sampling of 3 g of Cocaine-HCl in a quart can

9.4.3.3 Methamphetamine

Different from what was reported previously, methamphetamine headspace showed more volatile compounds as seen in Figure 9-19 and the detailed list was in Table 9-9. Benzyl methyl ketone, known as P2P, one of the signature compounds in the headspace of methamphetamine was detected. Besides the previously reported compounds, 1-phenyl-2-propanol, methamphetamine, benzeneacetic acid, ethyl ester and benzylideneacetone

were also found in the headspace; however, without further experiments to confirm the consistency of these preliminary results, it is too early to use these compounds as the signature compounds for methamphetamine.

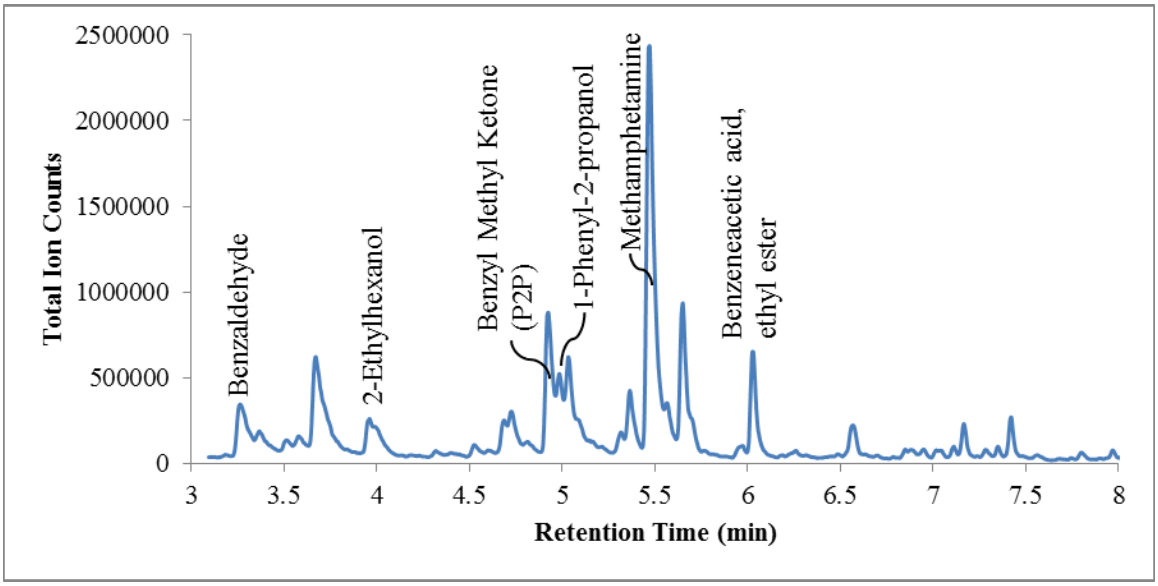

Figure 9-19 GC-MS Chromatogram of 3 min dynamic headspace sampling of 25 g Methamphetamine using a CMV device

Table 9-9 Volatile compounds detected in the headspace of methamphetamine

Illicit Drug	Headspace Volatiles	Reported Previously
Methamphetamine	Benzaldehyde	✓
	2-Ethylhexanol	
	Benzyl methyl ketone	✓
	1-Phenyl-2-propanol	
	Methamphetamine	
	Benzeneacetic acid, ethyl ester	
	Benzylideneacetone	
	Acetophenone	
	Benzyl butyl phthalate	

9.4.3.4 MDMA

As stated before, acetic acid, camphor, piperonal, isosafrole), 3,4-methlenedioxyketone (MD-P2P), MD-phenyl-2-propanol and methamphetamine were previously found in the headspace of MDMA [19]. And among these compounds, piperonal and MD-P2P are the major headspace composition [98]. In this study, piperonal was not detected in all the fiver conditions; however, piperonyl methyl ketone (MD-P2P) was found both times when 3 min dynamic sampling was used for the sealed quart cans (Table 9-10, Figure 9-20). MDMA was in the tablet form which could limit the odor release into the headspace and the previously reported detection was generated with a long equilibrium time and a much longer extraction time; thus, future experiment should definitely increase the two parameters.

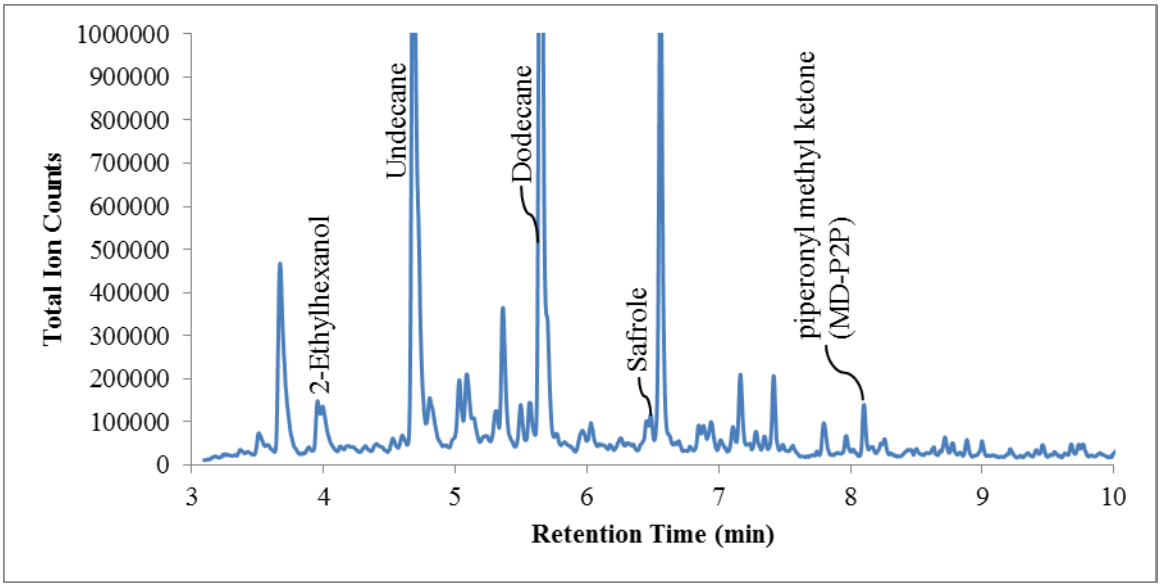

Figure 9-20 GC-MS Chromatogram of 3 min dynamic headspace sampling of 3 g of MDMA in a quart can

Table 9-10 Volatile compounds detected in the headspace of MDMA tablets

Illicit Drug	Headspace Volatiles	Reported Previously
MDMA	piperonyl methyl ketone	✓
	2-Ethylhexanol	
	Safrole	
	2,4-Di-tert-butylphenol	
	Diethyl Phthalate	

9.4.3.5 Heroin

Diacetylmorphine was found in the chromatogram; however, the low vapor pressure of the compound excluded the possibility of detection in the headspace. The detection may be caused by the direct transfer of small particles onto the CMV device. Other than diacetylmorphine, butylated hydroxytoluene was also detected in the headspace which was reported once previously [101]. The chromatogram was shown in Figure 9-21 and the volatile compounds were listed in Table 9-11.

Table 9-11 Volatile compounds detected in the headspace of Heroin

Illicit Drug	Headspace Volatiles	Reported Previously
Heroin	2-Ethylhexanol	
	Butylated hydroxytoluene	✓
	2,6-Di-tert-butylphenol	
	Diacetylmorphine	
	1,2-Benzenedicarboxylic acid	
	butyl cyclohexyl ester	
	3,5-di-tert-Butyl-4-hydroxybenzald	
	2-ethylhexyl salicylate	
	Ethylhexyl benzoate	

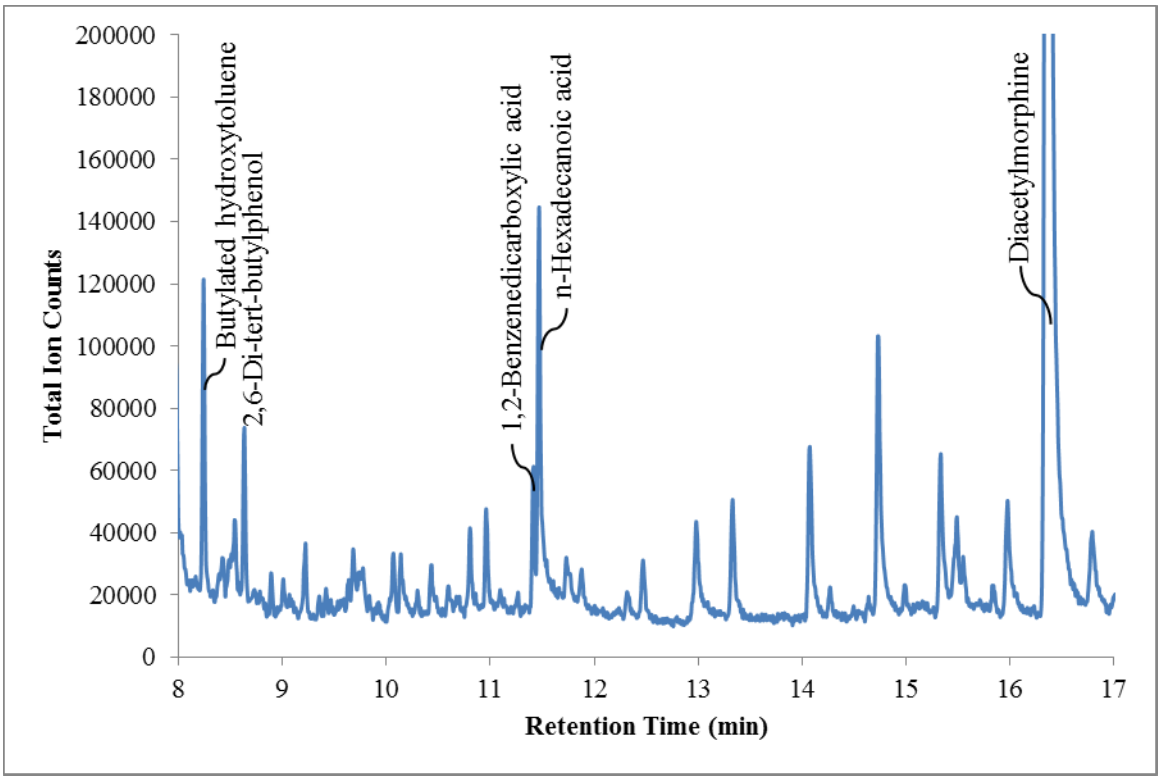

Figure 9-21 GC-MS Chromatogram of open air sampling of Heroin headspace for 1 min using a CMV device

9.4.3.6 Marijuana

There were a lot of volatile compounds reported previously in the headspace of marijuana and majority of the compounds were found in this study (Figure 9-22). Besides these compounds, 2-norbornanol, (±)-4-acetyl-1-methyl cyclohexene, α-Guaiene, γ-Cadinene, δ-Guaiene, Selina-3,7(11)-diene, and Valencen were also found in the headspace as shown in Table 9-12.

As mentioned above, the headspace of marijuana consists of three fractions which are volatile, intermediate volatile and less volatile [103]. The detected compounds were

mainly in the intermediate volatile and less volatile fractions which include β-pinene, β-myrcene, limonene, β-phellandrene (intermediate) and β-caryophyllene (less volatile).

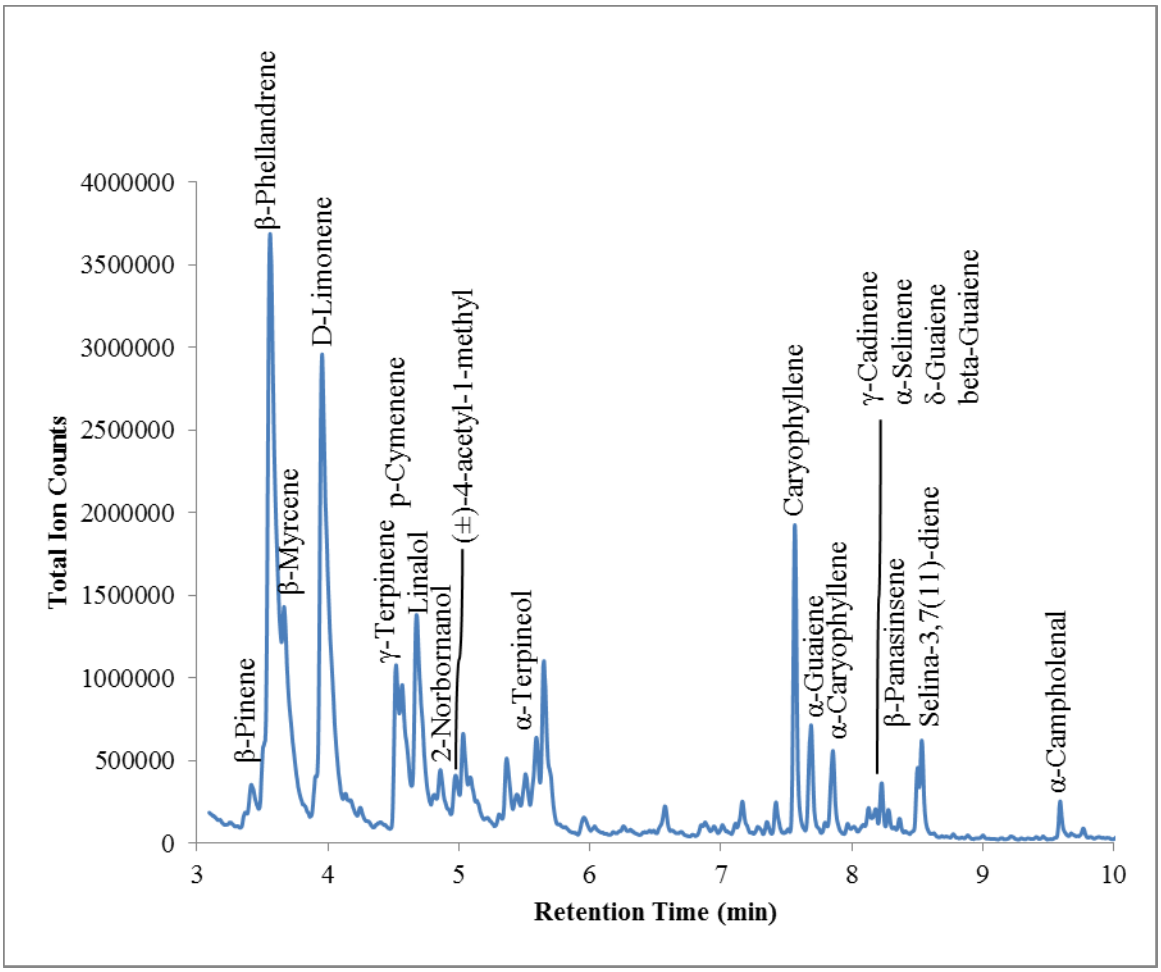

Figure 9-22 GC-MS Chromatogram of 25 g of Marijuana in a quart can sampled with a CMV device for 3 min

Table 9-12 Volatile compounds in the headspace of Marijuana

Illicit Drug	Headspace Volatiles	Reported Previously
Marijuana	β-Pinene	✓
	β-Myrcene	✓
	D-Limonene	✓
	3-Carene	✓
	γ-Terpinene	✓
	p-Cymenene	✓
	2-Norbornanol	
	(±)-4-acetyl-1-methyl cyclohexene	
	α-Terpineol	✓
	Caryophyllene	✓
	α-Guaiene	
	α-Caryophyllene	✓
	γ-Cadinene	
	α-Selinene	✓
	δ-Guaiene	
	Selina-3,7(11)-diene	
	Valencen	
	β-Phellandrene	✓
	Linalol	✓
	β-Guaiene	
	β-Panasinsene	
	α-Campholenal	
	(+)-4-Carene	
	(Z)-13-Docosenamide	
	2-Ethylhexanol	
	Alloaromadendrene	

9.5 Summary

Headspace analysis in the shipping facility did not show detection of any suspicious compounds, only the organic compounds commonly seen in the daily life. For military explosives, the sampling was easy for NG and EGDN because of the high volatility; however, RDX and PETN weren't detected using CMV devices which could be caused by the short equilibrium time and short sampling time. The wrappers for TNT and C4

explosives only contained trace amount of explosives and with 1 min dynamic sampling, 2,4-DNT was found in the TNT wrappers and DMNB was found in C4 wrappers. Illicit drugs headspace profiling gave very rich information, some of the volatile compounds detected were consistent with the previously reported signatures and some of the volatile compounds might become the new signatures for these illicit substances.

The CMV devices were successfully applied to different application using dynamic headspace analysis. From the previously reported results, the analysis of military explosives, illicit drugs, and shipping containers was achieved using conventional SPME fibers with different fiber chemistry, different GC column chemistry, different instrumental setup as well as extensively long extraction times. In this dissertation, all the applications were accomplished using sol-gel PDMS as the preconcentration matrix, DB-5 as the separation column and a commercially available thermal desorption probe. The setup was easy and the sampling can be accomplished at most 5 min to achieve detection of low volatility compounds.

Chapter 10 CMV-GC-MS Biomedical Application

The novel dynamic preconcentration technique was also used to sample the headspace of *Pseudomonas aeruginosa* bacteria which could lead to lethal infection for cystic fibrosis patients. Analyzing the signature volatile compounds in the headspace of the bacteria may serve as a diagnostic tool for infections in breath analysis.

10.1 Introduction of *Pseudomonas aeruginosa* (*P. aeruginosa*)

Breath analysis is a potential revolution in disease diagnostics (especially lung diseases) since the collection of exhaled breath is a safe, non-invasive, easy and simple procedure and each individual can provide breath that contains information regarding their own internal state [104,105].

Cystic Fibrosis (CF) is the most common genetic disorder in the white population which affects 1 in 3300 live Caucasian births [106,107]. This genetic disorder disables a transmembrane chloride conductance regulator (CFTR) that regulates the balance of salts in epithelia cells that exist in many of the glands [106] which affects multiple systems which include lung, pancreas and gastrointestinal systems. In lung disease, deficiency in CFTR causes obstraction of submucosal glands and distal airways with thick tenacious secretions against bacterial infection [108]. Bacteria that most often colonize and infect the lungs of people with CF are *Haemophilus influenza*, *Staphylococcus*, and *Pseudomonas aeruginosa (P. aeruginosa)* and among these three, *Pseudomonas* family has a reputation of being particularly dangerous which correlates with declining lung function and high mortality rates [109,107].

Pseudomonas aeruginosa is a Gram negative bacterium that produces an odor (grape-like) which has been identified as 2-aminoacetophenone (2-AA) by Mann in 1966 [107]. This compound was once detected in the headspace of *Escherichia coli (E. coli)* cultures, but not in any other respiratory pathogens and thus was used as a volatile biomarker for infection and/or colonization in the lung [110]. However, 2-AA was also found in the breath samples of uninfected individuals shortly after eating certain foods (corn, dairy, honey products and wine) Other than 2-AA, 2-nonanone, 2,4-dimethyl-1-heptene, 1-heptene, isopentanol and Limonene were also found in the headspace of spontaneously expectorated sputum towards *P. aeruginosa* [111]. The previously reported volatile compounds that detected in the headspace were listed in Table 10-1 with their chemical structure.

Table 10-1 Potential biomarkers for *Pseudomonas aeruginosa*

Chemical Name:	Mol. Wt.: ($g\ mol^{-1}$)	Chemical Structure	Ref.
2-Aminoacetophenone	135.163	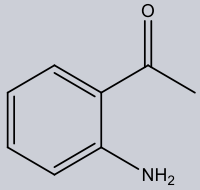	[107]
2-Nonanone	142.239	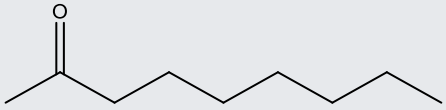	[111]
2,4-dimethyl-1-heptene	126.239	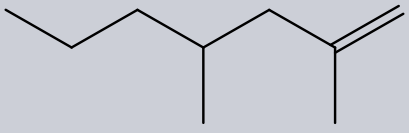	[111]
1-Heptene	98.186	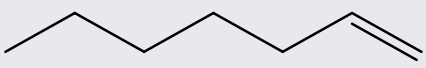	[111]

1-Butanol-3-methyl (Isopentanol)	88.148	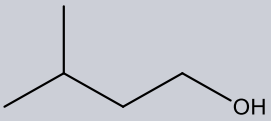	[111]
Limonene	136.234	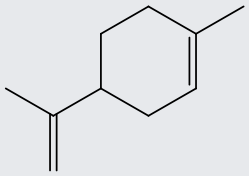	[111]
Hydrogen Cyanide	27.025		[112]

10.2 Materials and Methods

In this research, all the headspace analysis was accomplished only using bacteria cultural plates which included *Pseudomonas aeruginosa, Bacillus* strain, *Chromobacterium violaceum, Escherichia coli,* and *Serratia marcescen*. The bacteria strains used in this study were listed in Table 10-2. For *P. aeruginosa*, not only the laboratory modified strains, but also two clinical isolated strains were obtained to study the difference. The other bacteria strains were used as negative controls for profiling the signature volatile compounds for *P. aeruginosa* strains.

Table 10-2 Bacteria strains used in headspace analysis of *Pseudomonas aeruginosa*

Blind ID	Strain ID	Strain	Relevant characteristics	Source
	Pseudomonas aeruginosa			
GDT1		PAO1	Prototypic wild type	[113]
GDT165	PKM315	PAOΔ*ampR*	In-frame deletion of *ampR* (*PA4109*)	[114]
GDT61	PKM900	PAOΔ*mifS*	In-frame deletion of *mifS* (*PA5512*)	Mathee Lab
GDT33	PKM901	PAOΔ*mifR*	In-frame deletion of *mifR* (*PA5511*)	Mathee Lab
GDT34	PKM902	PAOΔ*mifSR*	In-frame deletion of *mifSR* (*PA5511-PA5512*)	Mathee Lab
GDT170	PDO300	PDO300	PAO*mucA22*	[115]
GDT 163	GDT 163	PKM900(pMifS)	PAO1Δ*mifS* (pMifS); *mifS* ORF on pPSV37-Gm moved into PAO1Δ*mifS*; IPTG-inducible; Gm^R	Mathee Lab

GDT 132	GDT 132	PKM901 (pMifR)	PAO1Δ*mifR* (pMifR); *mifR* ORF on pPSV37-Gm moved into PAO1Δ*mifR*; IPTG-inducible; Gm^R	Mathee Lab
GDT 152	GDT 152	PKM902(pMifSR)	PAO1Δ*mifSR* (pMifSR); *mifSR* ORF on pPSV37-Gm moved into PAO1Δ*mifSR*; IPTG-inducible; Gm^R	Mathee Lab
466		CDN 107	Clinical isolate from Nigeria	Mathee Lab
469		CDN 118	Clinical isolate from Nigeria	Mathee Lab
	***Bacillus* strain**			
GDT172	ATCC 35866	*B. thuringiensis* HD-73	NRRL B4488 [HD73]	ATCC
GDT175	ATCC 23857	*B. subtilis*	*ind- tyr+*	M. Yoshinaga; Rosen Lab
GDT173	ATCC 14581	*B. megaterium*		M. Yoshinaga; Rosen Lab
GDT174	ATCC 53522	*B. cereus* UW85		
	Other strains			
GDT69	CV026	*Chromobacterium violaceum*	Non-pigment production mutant, production restored with AHLs	[116]
GDT5	DH5α	*Escherichia coli*	F^- Φ80*lacZ*ΔM15 Δ (*lacZYA-argF*)U169 *deoR recA1 endA1 hsdR17* (rk^- mk^+) *phoA supE44* λ^- *thi-1 gyrA96 relA1*	New England Biolabs
GDT171	ATCC 13880	*Serratia marcescens*	Isolated from pond water	Mathee Lab

Growth of bacteria was accomplished in 18-ml culture tubes filled with 5 ml LB media shaking at 200 rpm at 37 °C for *P. aeruginosa*, 26 °C for *Serratia marcescens*, *Chromobacterium violaceum* and 30 °C for *Bacillus* strains overnight. Further growth was continued on Luria-Bertani (LB) agar plates.

Preliminary study was performed using *P. aeruginosa*, *Chromobacterium violaceum*, and *Escherichia coli* (Figure 10-1 (a, b, and c)). Two different methods were used for the dynamic sampling using the CMV devices which included over the headspace of LB agar cultural plates (Figure 10-1 (d)) and liquid LB medium in test tubes (Figure 10-1 (e and f)).

For the first set of blind study, different bacteria were given only on LB agar cultural plates with their strain ID and the sampling process was the same as shown in Figure 10-1 (d). The plates were sampled once after obtained from Dr. Mathee's lab in the morning and the plates were left at room temperature under the hood overnight for second day sampling.

For the second set of blind study, 13 different bacteria were given on LB agar cultural plates with their strain ID. Triplicates of the cultural plates were obtained on three consecutive days for quantitative analysis. All the process was the same as the first set of blind study.

Calibration solutions 2-aminoacetophenone were diluted from liquid 2-Aminoacetophenone (Acros Organics, NJ, USA) using Optima Methanol (Fisher Scientific, Fair Lawn, NJ) to 1, 2, 5, 10, 20, and 30 ng μL^{-1}.

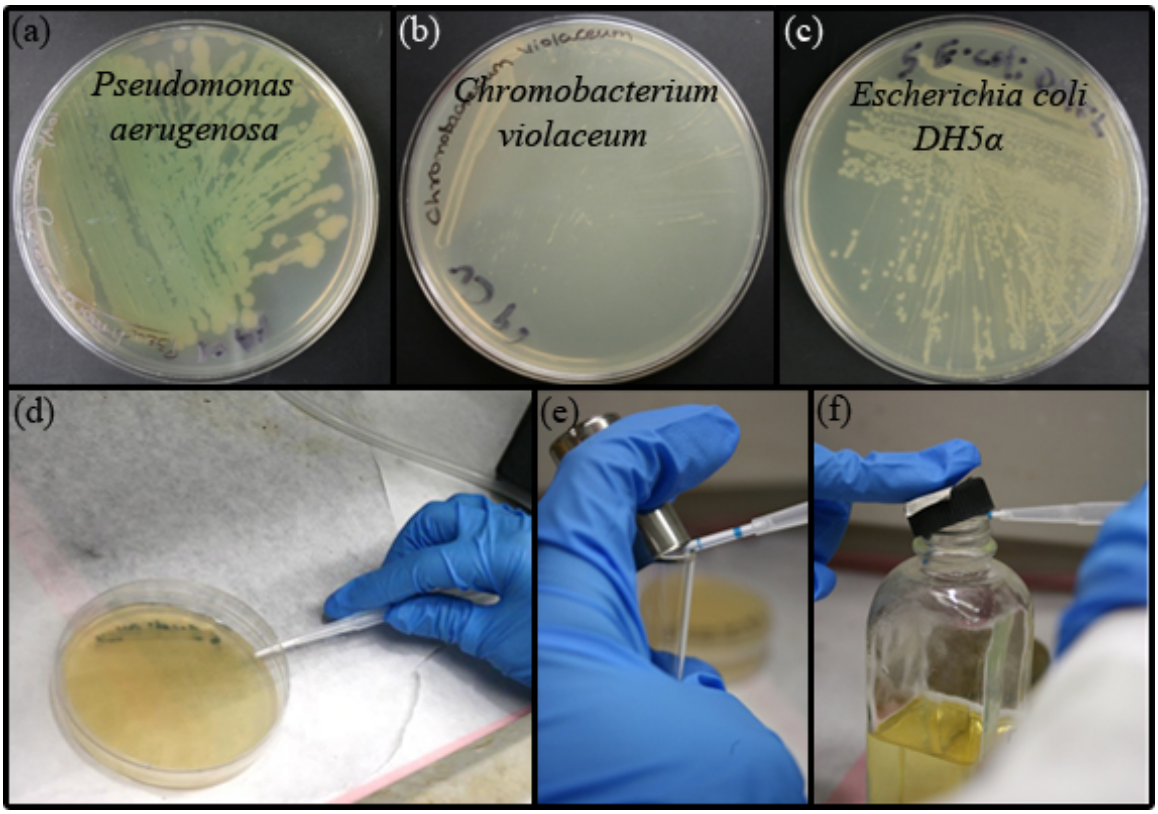

Figure 10-1 The pictures show the three different bacteria used in the study (a) *Pseudomonas aerugenosa*, (b) *Chromobacterium violaceum*, and (c) *Escherichia coli*. Two different methods were used for dynamic sampling with a CMV device over the headspace of (d) a solid LB agar plate, (f) liquid LB medium in a test tube, and (g) liquid Saline medium in a container

10.3 Results

10.3.1 Identification of Volatile Compounds in the Headspace of *P. aeruginosa*

After obtaining the bacteria cultural plates, the headspace of the plates were sampled with CMV devices for only 1 min. And the preliminary results showed detection of undecene and 2-aminoacetophenone only in *P. aeruginosa* and indole in *E. coli* (Figure 10-2) as well as limonene was found in both *P. aeruginosa* and *C. violaceum* plates during the second-day sampling (Figure 10-3).

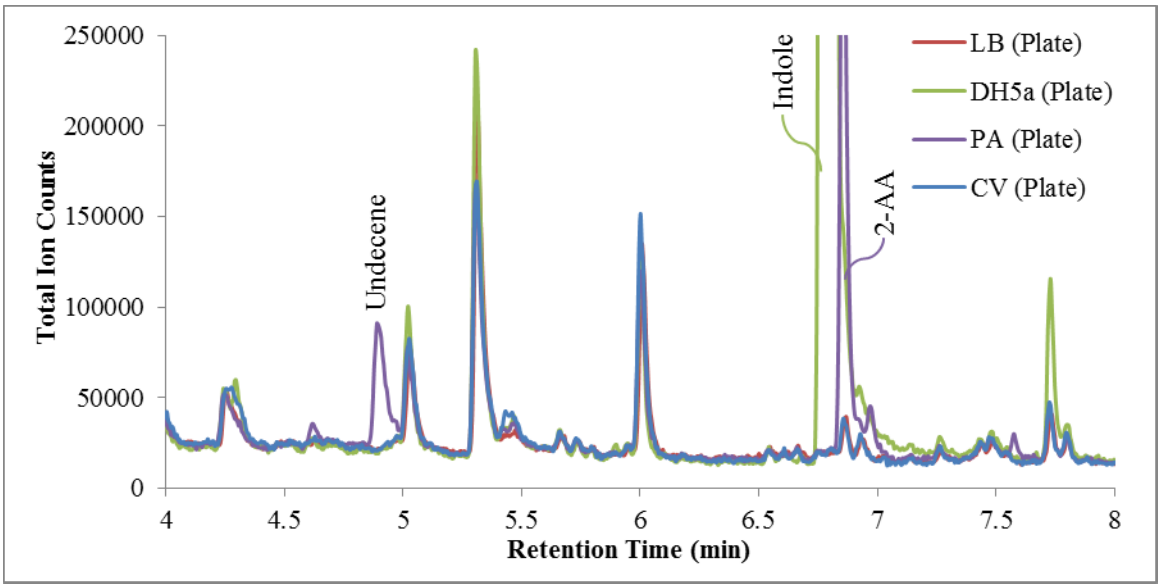

Figure 10-2 1 min dynamic sampling of LB plate, DH5α, PA, CV cultural plate using a CMV device showed detection of Undecene and 2-AA only in the headspace of PA

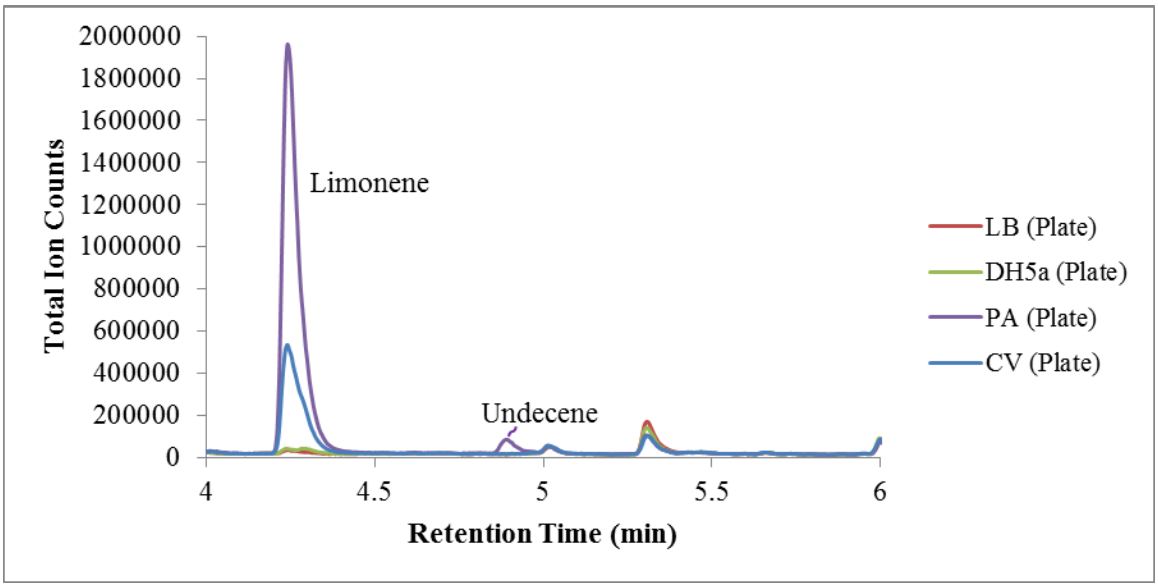

Figure 10-3 Detection of Limonene in PA and CV plate in the second day sampling

The same experiment was also performed using 5 ml liquid bacteria cultural medium in a test tube. The 18 mL test tube did provide larger headspace volume; however, the liquid

medium trapped most of the volatile compounds and a much smaller signal of undecene and 2-AA were observed as shown in Figure 10-4. Accordingly, all the following experiments were accomplished using the solid LB agar cultural plates.

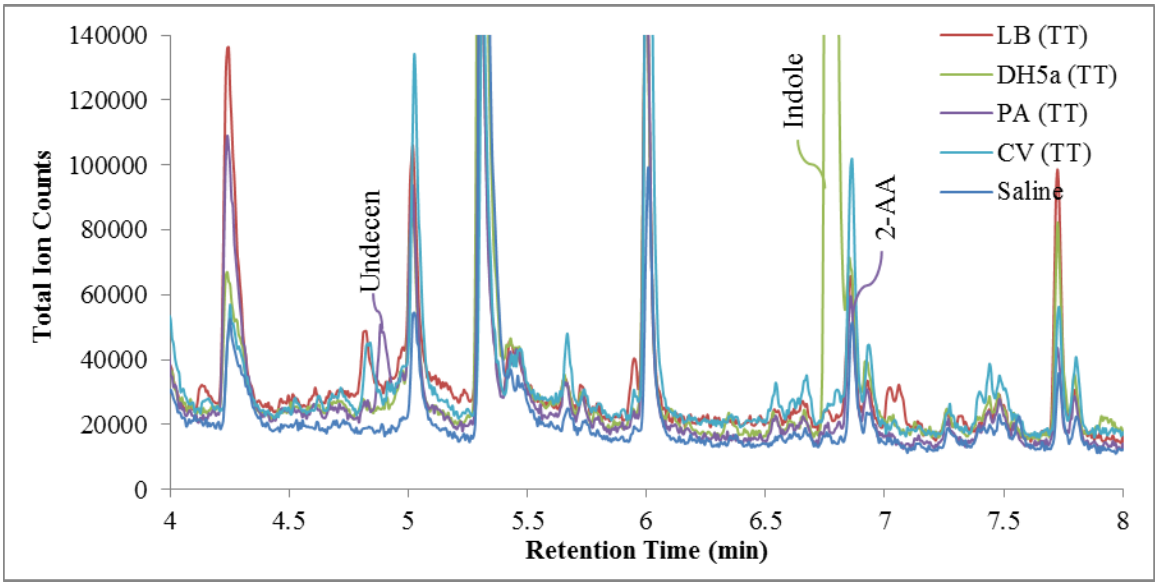

Figure 10-4 1 min dynamic headspace sampling of LB, DH5α, PA, CV and Saline in the liquid cultural solutions in a test tube showed less intensity in headspace volatiles

Based on the preliminary study, limonene and 2-AA were the two compounds consistent with previously published literature as the biomarkers for *P. aeruginosa*. The calibration curve for 2-AA was generated using directly spiking the calibration solutions on the CMV device and then thermally desorbed into the GC-MS (Figure 10-5).

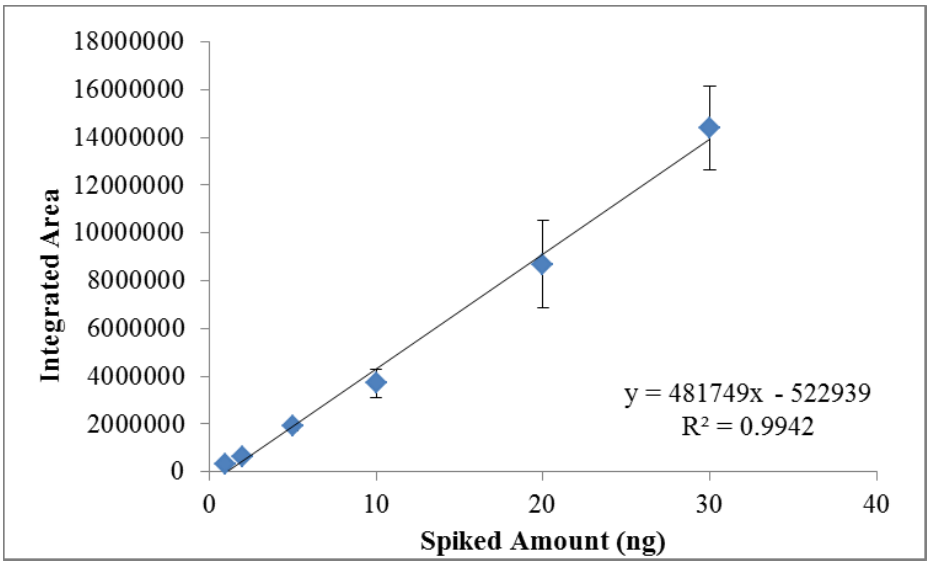

Figure 10-5 Calibration curve for 2-AA

10.3.2 Blind Study to Differentiate Pseudomonas from Other Bacteria

The cultural plates obtained were only labeled with their Blind ID as listed in the second column in the tables and the identity was revealed only after the conclusion was made if the bacteria were *Pseudomonas*. The blind study was done to prove *P. aeruginosa* can be differentiated from other bacteria by using the volatile markers.

The first set blind study simply sampled each cultural plate once after obtained and once after 24 hours. Table 10-3 showed the volatile compounds detected in 10 different plates right after the plates were obtained. The decision was made only using 2-AA as the volatile biomarker since Limonene was present in all the cultural plates. Thus, only GDT33, GDT34, and GDT 61 were correctly identified as *Pseudomonas*. After 24 hours, the same plates were sampled again and the results were shown in Table 10-4. After 24 hours cultural growth at room temperature, GDT1 and PAO were also emitting 2-AA into the headspace and thus were identified as *Pseudomonas*. After the identity of the bacteria

were revealed, there were three more *Pseudomonas* strains weren't correctly classified which were 466, 469, and PA0300. Both 466 and 469 were the clinical isolated strains and PA0300 was genetically modified which possessed the characteristics of the chronic infection strains in CF patients. Another volatile compound that worth mentioning is undecene which was found only in *Pseudomonas* strains and not in other bacteria. If undecene can be confirmed as another volatile compound only presence in the headspace of *P. aeruginosa*, 466, 469, and PA0300 can be successfully classified.

Table 10-3 Volatile compounds detected in the headspace of different cultural plates right after the plates were obtained

Strain	Blind ID	Limonene	Undecene	Acetophenone	2-AA	Indole
Pseudomonas	466	+	+			
Pseudomonas	469	+				
Pseudomonas	PAO	+				
Chromobacterium	GDT69	+				
Escherichia	GDT5	+				+
Pseudomonas	GDT1	+				
Pseudomonas	GDT33	+			+	
Pseudomonas	GDT34	+	+	+	+	
Pseudomonas	GDT61	+	+	+	+	
Pseudomonas	PD0300	+	+			

Table 10-4 Volatile compounds detected in the headspace of different cultural plates after 24 hours

Strain	Blind ID	Limonene	Undecene	Acetophenone	2-AA	Indole
Pseudomonas	466	+	+			
Pseudomonas	469	+	+			
Pseudomonas	PAO	+	+		+	
Chromobacterium	GDT69	+				
Escherichia	GDT5	+				+
Pseudomonas	GDT1	+			+	
Pseudomonas	GDT33	+	+		+	
Pseudomonas	GDT34	+	+		+	
Pseudomonas	GDT61	+	+		+	
Pseudomonas	PD0300	+	+	+		

The second set blind study was not only limited to differentiate *Pseudomonas*, but also quantify the amount of 2-AA present in the headspace. In this set, 13 different bacteria were given in triplicates in three consecutive days; however, the bacteria growth time was not precisely controlled and the colony numbers weren't counted. Consequently, the quantitative analysis still has a lot to be improved. The results of the volatile compounds detected were shown in Table 10-5. Among 13 strains, only 5 of them were *Pseudomonas*. Using 2-AA as the single marker, 5 out of 6 can be successfully classified. The one can not be identified was GDT 170 which is PA0300 in the first set blind study. There were 7 other strains which included 4 *Bacillus*, 1 *Serratia*, 1 *Escherichia*, and 1 *Chromobacterium*. None of these strains were misplaced as *Pseudomonas*. Thus, the differentiation of bacteria strains using CMV-GC-MS was successful. The amount of 2-AA present in different strains were slightly different and the variations were still quite large because the reasons mentioned above. The estimated amount was 3 ng to 5 ng in the headspace. Similar to first set blind study, undecene was very consistent only present in the headspace of *Pseudomonas* strains. More strains should be analyzed before reaching a final conclusion.

Table 10-5 Volatile compounds detected in the headspace of 13 different bacteria with triplicates

Strain	Blind ID	Undecene (4.62 min)	Indole (6.47 min)	2-AA (6.55 min)
Pseudomonas	GDT1	+	-	4.6 ± 2.4 ng
Pseudomonas	GDT165	+	-	4.4 ± 1.5 ng
Pseudomonas	GDT170	-	-	-
Serratia	GDT171	-	-	-
Bacillus	GDT172	-	-	-
Bacillus	GDT173	-	-	-
Bacillus	GDT174	-	-	-
Bacillus	GDT175	-	-	-

Pseudomonas	GDT33	+	-	2.9 ± 1.0 ng
Pseudomonas	GDT34	+	-	4.6 ± 1.4 ng
Escherichia	GDT5	-	+	-
Pseudomonas	GDT61	+	-	4.3 ± 0.8 ng
Chromobacterium	GDT69	-	-	-

10.4 Summary

Beyond forensic analysis, the CMV devices were also brought to the biomedical analysis to differentiate *Pseudomonas aeruginosa* strains from other bacteria strains. The results were promising, showed no false positive classification. The only difficulty was to classify the clinical isolated and clinical-alike strains which do not produce the same signature volatile compounds in the headspace.

In summary, the CMV devices can be considered as a universal preconcentration device that can be applied in various applications when coupling to GC-MS with efficient extractions in a very short time given conclusive results with compounds identification.

Chapter 11 Conclusions

11.1 SPME-GC-MS

The SPME fibers were used to analyze three different smokeless powders: in small containers, detection of volatile odors of smokeless powders can be achieved within 10 min of the extraction time; however, increase in the container's volume with added porous texture, the extraction time increased significantly (2 to 3 hours) which is not ideal in field analysis.

The SPME devices were also used to extract TATP vapors from standard solutions and the recovery showed quantitative results in a GC-MS instrument; however, because of the limited surface area and phase volume, the recovery of TATP reached a maximum of 5% and remained the same with increasing concentration of TATP in the headspace.

As reported in the literatures, SPME fibers can provide quantitative analysis with great sensitivity; however, in my dissertation, headspace extractions with SPME fibers were too long to be applied in the field because of the limitation in the small surface area and phase volume and its fragility.

11.2 PSPME-IMS

The PSPME devices were proven to have increased surface area (0.15 m^2) and phase volume (300 mm^3) in comparison to the traditional SPME fibers with the ability to couple to different IMS system without further modification. Headspace analysis using PSPME with IMS detectors allowed for fast preconcentration and detection of solid peroxide

explosives (TATP and HMTD), standard solution of peroxide explosives (TATP and HMTD), and headspace profiling of twenty-four different smokeless powders.

The peroxide explosive headspace analysis was achieved by preconcentrating TATP from the headspace of solid explosives and standard solutions using PSPME devices followed by detection in the IMS. With only 30 s extraction time for both static and dynamic headspace analysis over the solid explosives, TATP can be detected in the IMS system and the reactant ion peak was fully depleted. For HMTD, the sampling took much longer (2 to 16 hours extraction times) and the plasmagraphs were similar to the results obtained from SPME extractions with unidentified peaks. When compared to SPME-GC-MS analysis for standard solutions extraction, the recovery of PSPME increased as the amount of the sample increased (5 % to 15 %) while the SPME recovery remained the same (5%) which showed the privilege of a larger surface area and phase volume in PSPME preconcentration devices.

When using PSPME to profile twenty-four different smokeless powders, both static mode and dynamic mode were used and resulted in similar volatile compound profiles; however, signal intensities observed for dynamic extractions were significantly lower than that of the static extractions and breakthrough was observed in dynamic sampling mode. Accordingly, modifications still need to be made for dynamic PSPME devices to avoid breakthrough.

The PSPME-IMS performance was also evaluated using a double blind study in which one hundred different solutions were prepared by one researcher and spiked into the can by a second researcher randomly chosen a solution. Without knowing the identity of the

solution, the sampling was done by myself and the detection results were collected from the IMS system. Even though the previous experiments have demonstrated the high throughput on-site detection capability, the double blind study showed one disadvantage of the PSPME-IMS system which is high false alarm rates when strong interferences were present. In the research, most of the solvents (1-butanol, CS_2, 2-propanol, and hexane) interfered with the targeted compounds which included NG, 2,4-DNT, DPA and TATP and caused a high false alarm rate.

In summary, PSPME improved the sampling throughput by introducing a higher surface area and phase volume along with the dynamic sampling option and the ruggedness of the devices allowed for portability for field sampling; however, the identification capability became a disadvantage since the devices can only be coupled to IMS systems which has limited resolution and lacks identification capability. Thus, for complex matrix, a detector that allows selective recognition of the separated compounds is needed.

11.3 CMV-GC-MS

The CMV preconcentration device was the novel design using sol-gel PDMS as the preconcentration matrix for fast dynamic headspace sampling that can be fitted into a thermal desorption unit that can be easily coupled to a GC injector for thermal desorption the extracted compounds into the GC-MS for unknown compounds separation and identification.

The CMV devices maintain a high surface are (0.05 m^2) and phase volume (50 mm^3) from the PSPME devices which can provide high preconcentration capacities that is lacking from SPME fibers. Besides that, the modified geometry also allows dynamic

headspace analysis that improves the sampling throughput, along with the increased preconcentration capacity, the extraction time was shortened from 30 min using a SPME fiber to only 1 min extraction with a CMV device to achieve the same recovery percentage. The recovery of CMV devices is close to 1 % for NG, 2,4-DNT and DPA with only one minute extraction and the recovery increased as the extraction time extended.

When coupling to GC-MS, the CMV devices overcame two disadvantages present in PSPME-IMS: no breakthrough was observed in CMV devices even after 1 hour long extraction time that showed efficient preconcentration and retention capability of the technique and coupling to GC-MS as the detector, complex matrices can be analyzed with identification of individual compounds preconcentrated on the device.

The CMV-GC-MS technique were also proven to not only perform quantitative analysis in a semi-closed system with great precision, but also provide quantitative results in an open system which suggests that the method can be applied to sampling open environment. Because of limited sample loss in the semi-closed setup, not only greater precision was observed, the recovery was also increased in about 2 times.

Besides excellent preconcentration efficiency, the CMV devices also offered portability where the devices can be sealed in clean aluminum foil after sampling the headspace for at least 72 hours and retained 70 % of the original accumulated materials. The portability of the CMV devices allowed for many applications such as shipping facility, military explosives and illicit drugs to be performed on-site, sealed and transported the CMV

devices back to the laboratory for analysis. The results showed detection of the signature volatiles reported in other literatures, even after a delayed analysis of 3-4 days.

Other than the traditional forensic analysis applications using CMV devices, the novel preconcentration devices were also taken into the biomedical research application for headspace analysis of *Pseudomonas aeruginosa* which is one of the causes for cystic fibrosis, a lethal disease that commonly seen in children. The CMV devices identified 2-amonioacetophenone and undecene over the headspace of different strains of *Pseudomonas aeruginosa* strains and both compounds were not found in other bacteria strains provided.

In summary, the CMV devices combined the advantages from both SPME and PSPME and achieved the ultimate goal in preconcentration technique development to provide high throughput quantitative analysis with high recovery and exclusive identification of compounds in the headspace.

11.4 Future Directions

The CMV devices have been proven to be an efficient dynamic headspace sampling technique; further performance evaluation should be completed and the applications can be widely expanded.

The next step to evaluate the performance of the CMV devices is to generate receiver operating characteristics (ROC) curves to show the true positive rate against the false positive rate to reveal both precision and accuracy of the technique. Besides doing large amount of replicates of the experiments, a double blind study is still recommended

because no bias on the presence of a compound since all the information of the prepared solutions is unknown. Unlike the results concluded from double blind study in this dissertation, GC-MS should provide better differentiation and less interferences; thus, different solvents that caused high false negative alarms can still be used in the study.

Besides evaluating the performance, other developments can be considered for the CMV devices. The coating used for the preconcentration matrix is sol-gel based PDMS and this matrix is only great for preconcentration of non-polar compounds; however, modification can be made to develop different coating chemistry like the commercialized SPME fibers to expand the number of compounds that can be preconcentrated at the same time when packing different coating glass filters into one capillary tube.

Proof-of-concept studies performed in this dissertation were only preliminary tests with limited sources that showed successful detection of the signature volatiles over the headspace. Analysis using CMV-GC-MS should be explored for other analytical applications to determine headspace volatile compounds as well as new signature odors which still remain unknown.

List of References

1. Shareefdeen Z, Singh AK (2005) Biotechnology for Odor and Air Pollution Control. Springer-Verlag Berlin Heidelberg,

2. Popiel S, Sankowska M (2011) Determination of chemical warfare agents and related compounds in environmental samples by solid-phase microextraction with gas chromatography. J Chromatogr A 1218 (47):8457-8479. doi:http://dx.doi.org/10.1016/j.chroma.2011.09.066

3. Pérez Pavón JL, Herrero Martín S, García Pinto C, Moreno Cordero B (2008) Determination of trihalomethanes in water samples: A review. Anal Chim Acta 629 (1–2):6-23. doi:http://dx.doi.org/10.1016/j.aca.2008.09.042

4. Demeestere K, Dewulf J, De Witte B, Van Langenhove H (2007) Sample preparation for the analysis of volatile organic compounds in air and water matrices. J Chromatogr A 1153 (1–2):130-144. doi:http://dx.doi.org/10.1016/j.chroma.2007.01.012

5. Jeleń HH, Majcher M, Dziadas M (2012) Microextraction techniques in the analysis of food flavor compounds: A review. Anal Chim Acta 738 (0):13-26. doi:http://dx.doi.org/10.1016/j.aca.2012.06.006

6. Muñoz-González C, Rodríguez-Bencomo J, Moreno-Arribas MV, Pozo-Bayón MÁ (2011) Beyond the characterization of wine aroma compounds: looking for analytical approaches in trying to understand aroma perception during wine consumption. Anal Bioanal Chem 401 (5):1501-1516. doi:10.1007/s00216-011-5078-0

7. Ridgway K, Lalljie SPD, Smith RM (2007) Sample preparation techniques for the determination of trace residues and contaminants in foods. J Chromatogr A 1153 (1–2):36-53. doi:http://dx.doi.org/10.1016/j.chroma.2007.01.134

8. Gołębiowski M, Boguś M, Paszkiewicz M, Stepnowski P (2011) Cuticular lipids of insects as potential biofungicides: methods of lipid composition analysis. Anal Bioanal Chem 399 (9):3177-3191. doi:10.1007/s00216-010-4439-4

9. Liu DQ, Sun M, Kord AS (2010) Recent advances in trace analysis of pharmaceutical genotoxic impurities. J Pharm Biomed Anal 51 (5):999-1014. doi:http://dx.doi.org/10.1016/j.jpba.2009.11.009

10. Ulrich S (2000) Solid-phase microextraction in biomedical analysis. J Chromatogr A 902 (1):167-194. doi:http://dx.doi.org/10.1016/S0021-9673(00)00934-1

11. Pragst F (2007) Application of solid-phase microextraction in analytical toxicology. Anal Bioanal Chem 388 (7):1393-1414. doi:10.1007/s00216-007-1289-9

12. Kintz P (2007) Bioanalytical procedures for detection of chemical agents in hair in the case of drug-facilitated crimes. Anal Bioanal Chem 388 (7):1467-1474. doi:10.1007/s00216-007-1209-z

13. Stadler S, Stefanuto P-H, Brokl M, Forbes SL, Focant J-F (2012) Characterization of Volatile Organic Compounds from Human Analogue Decomposition Using Thermal Desorption Coupled to Comprehensive Two-Dimensional Gas Chromatography–Time-of-Flight Mass Spectrometry. Anal Chem 85 (2):998-1005. doi:10.1021/ac302614y

14. Dogs In Search & Rescue. http://www.ussartf.org/dogs_search_rescue.htm. Accessed 2013-07-08

15. International K-9 Search and Rescue Services for Missing People and Pets. http://www.k9sardog.com/. Accessed 2013-07-08

16. Moore CH, Pustovyy O, Dennis JC, Moore T, Morrison EE, Vodyanoy VJ (2012) Olfactory responses to explosives associated odorants are enhanced by zinc nanoparticles. Talanta 88 (0):730-733. doi:http://dx.doi.org/10.1016/j.talanta.2011.11.024

17. Furton KG, Myers LJ (2001) The scientific foundation and efficacy of the use of canines as chemical detectors for explosives. Talanta 54 (3):487-500. doi:http://dx.doi.org/10.1016/S0039-9140(00)00546-4

18. Harper RJ, Almirall JR, Furton KG (2005) Identification of dominant odor chemicals emanating from explosives for use in developing optimal training aid combinations and mimics for canine detection. Talanta 67 (2):313-327. doi:http://dx.doi.org/10.1016/j.talanta.2005.05.019

19. Lorenzo N, Wan T, Harper R, Hsu Y-L, Chow M, Rose S, Furton K (2003) Laboratory and field experiments used to identify Canis lupus var. familiaris active odor signature chemicals from drugs, explosives, and humans. Anal Bioanal Chem 376 (8):1212-1224. doi:10.1007/s00216-003-2018-7

20. Mandy M, Cornelia F, Malgorzata L, Oliver S, Achim S, Dorothee S (2012) Volatile organic compounds (VOCs) in exhaled breath of patients with breast cancer in a clinical setting. Ginekol Pol 83 (10):730-736

21. Chen X, Xu F, Wang Y, Pan Y, Lu D, Wang P, Ying K, Chen E, Zhang W (2007) A study of the volatile organic compounds exhaled by lung cancer cells in vitro for breath diagnosis. Cancer 110 (4):835-844. doi:10.1002/cncr.22844

22. Pawliszyn J (1997) Solid Phase Microextraction: Theory and Practice. Wiley-VCH,

23. Snow NH, Slack GC (2002) Head-space analysis in modern gas chromatography. TrAC, Trends Anal Chem 21 (9–10):608-617. doi:http://dx.doi.org/10.1016/S0165-9936(02)00802-6

24. Guerra-Diaz P, Gura S, Almirall JR (2010) Dynamic Planar Solid Phase Microextraction-Ion Mobility Spectrometry for Rapid Field Air Sampling and Analysis of Illicit Drugs and Explosives. Anal Chem 82 (7):2826-2835. doi:10.1021/ac902785y

25. Gura S, Guerra-Diaz P, Lai H, Almirall JR (2009) Enhancement in sample collection for the detection of MDMA using a novel planar SPME (PSPME) device coupled to ion mobility spectrometry (IMS). Drug Test Anal 1 (7):355-362. doi:10.1002/dta.81

26. Fan W, Young M, Canino J, Smith J, Oxley J, Almirall J (2012) Fast detection of triacetone triperoxide (TATP) from headspace using planar solid-phase microextraction (PSPME) coupled to an IMS detector. Anal Bioanal Chem 403 (2):401-408. doi:10.1007/s00216-012-5878-x

27. Technologies A (2011) Agilent G4381A Thermal Separation Probe User Guide.

28. Saferstein R (2002) Forensic Science Handbook. vol v. 1. Prentice Hall PTR,

29. Wang Y, McCaffrey J, Norwood DL (2008) Recent Advances in Headspace Gas Chromatography. Journal of Liquid Chromatography & Related Technologies 31 (11-12):1823-1851. doi:10.1080/10826070802129092

30. de Barry Barnett E (1919) Explosives. D. Van Nostrand Company,

31. Yinon J, Zitrin S (1993) Modern methods and applications in analysis of explosives. Wiley,

32. Sovova K, Dryahina K, Spanel P, Kyncl M, Civis S (2010) A study of the composition of the products of laser-induced breakdown of hexogen, octogen, pentrite and trinitrotoluene using selected ion flow tube mass spectrometry and UV-Vis spectrometry. The Analyst 135 (5):1106-1114

33. Diaz P (2010) Improved sampling, pre-concentration, and detection of hidden explosives and illicit drugs by a novel solid phase microextraction geometry coupled to ion mobility spectrometry.

34. Beveridge A (2011) Forensic Investigation of Explosions, Second Edition. Taylor & Francis,

35. Oxley JC, Smith JL, Shinde K, Moran J (2005) Determination of the Vapor Density of Triacetone Triperoxide (TATP) Using a Gas Chromatography Headspace Technique. Propellants Explos Pyrotech 30 (2):127-130. doi:10.1002/prep.200400094

36. Oxley JC, Smith JL, Luo W, Brady J (2009) Determining the Vapor Pressures of Diacetone Diperoxide (DADP) and Hexamethylene Triperoxide Diamine (HMTD). Propellants Explos Pyrotech 34 (6):539-543. doi:10.1002/prep.200800073

37. West C, Baron G, Minet JJ (2007) Detection of gunpowder stabilizers with ion mobility spectrometry. Forensic Sci Int 166 (2-3):91-101. doi:10.1016/j.forsciint.2006.04.004

38. Goktas O, Toker H (2010) Effects of the Traditional Turkish Art of Marbling (Ebru) Techniques on the Adhesion, Hardness, and Gloss of Some Finishing Varnishes. Forest Products Journal 60 (7-8):648-653

39. Munzel T, Gori T (2013) Nitrate therapy and nitrate tolerance in patients with coronary artery disease. Curr Opin Pharmacol 13 (2):251-259. doi:10.1016/j.coph.2612.12.008

40. Jedrzkiewicz S, Parker JD (2013) Acute and Chronic Effects of Glyceryl Trinitrate Therapy on Insulin and Glucose Regulation in Humans. Journal of Cardiovascular Pharmacology and Therapeutics 18 (3):211-216. doi:10.1177/1074248412467693

41. Hoelscher HE, Chamberlain DF (1950) Vapor Phase Condensation of Aniline to Diphenylamine. Industrial & Engineering Chemistry 42 (8):1558-1562. doi:10.1021/ie50488a028

42. Robatscher P, Eisenstecken D, Sacco F, Pöhl H, Berger J, Zanella A, Oberhuber M (2012) Diphenylamine Residues in Apples Caused by Contamination in Fruit Storage Facilities. J Agric Food Chem 60 (9):2205-2211. doi:10.1021/jf204477c

43. Kreiner JG, Warner WC (1969) The identification of rubber compounding ingredients using thin-layer chromatography. J Chromatogr A 44 (0):315-330. doi:http://dx.doi.org/10.1016/S0021-9673(01)92543-9

44. Oxley JC, Smith JL, Chen H (2002) Decomposition of a Multi-Peroxidic Compound: Triacetone Triperoxide (TATP). Propellants Explos Pyrotech 27 (4):209-216. doi:10.1002/1521-4087(200209)27:4<209::aid-prep209>3.0.co;2-j

45. Beveridge A (1998) Forensic investigation of explosions. Taylor & Francis,

46. Schulte-Ladbeck R, Kolla P, Karst U (2003) Trace Analysis of Peroxide-Based Explosives. Anal Chem 75 (4):731-735. doi:10.1021/ac020392n

47. Schulte-Ladbeck R, Kolla P, Karst U (2002) A field test for the detection of peroxide-based explosives. Analyst 127 (9):1152-1154

48. Oxley JC, Smith JL, Chen H, Cioffi E (2002) Decomposition of multi-peroxidic compounds: Part II. Hexamethylene triperoxide diamine (HMTD). Thermochim Acta 388 (1-2):215-225

49. Wikipedia List of terrorist incidents. http://en.wikipedia.org/wiki/List_of_terrorist_incidents. Accessed 10-02-2013

50. Kotz D (2013) Injury toll from Marathon bombs reduced to 264. http://www.bostonglobe.com/lifestyle/health-wellness/2013/04/23/number-injured-marathon-bombing-revised-downward/NRpaz5mmvGquP7KMA6XsIK/story.html. Accessed 2013-08-30

51. Wikipedia 7 July 2005 London bombings. http://en.wikipedia.org/wiki/7_July_2005_London_bombings. Accessed 09-09-2013

52. FBI Terror Hits Home: The Oklahoma City Bombing. http://www.fbi.gov/about-us/history/famous-cases/oklahoma-city-bombing. Accessed 09-09-2013

53. Bennett B, Serrano RA, Dilanian K (2013) Sophistication of Boston bombing explosive devices found to be 'similar to what you might find on a battle field'. http://www.sott.net/article/261359-Sophistication-of-Boston-bombing-explosive-devices-found-to-be-similar-to-what-you-might-find-on-a-battlefield. Accessed 2013-08-30

54. Sheryll S, Mallonee S, Stephens-Stidham S (1998) Summary of Reportable Injuries In Oklahoma. http://web.archive.org/web/20080110063748/http://www.health.state.ok.us/PROGRAM/injury/Summary/bomb/OKCbomb.htm. Accessed 09-09-2013

55. Wikipedia 1993 World Trade Center bombing. http://en.wikipedia.org/wiki/1993_World_Trade_Center_bombing#Bomb_characteristics. Accessed 09-09-2013

56. FBI (2003) A Byte Out of History - Solving a Complex Case of International Terrorism. http://www.fbi.gov/news/stories/2003/december/panam121903. Accessed 09-09-2013

57. Wikipedia Pan Am Flight 103. http://en.wikipedia.org/wiki/Pan_Am_Flight_103#Investigation. Accessed 09-09-2013

58. Techniques CREPSED, Technology BCS, Studies DEL, Council NR (2004) Existing and Potential Standoff Explosives Detection Techniques. National Academies Press,

59. Robards K, Haddad PR, Jackson PE (1994) Principles and Practice of Modern Chromatographic Methods. Elsevier/Academic Press,

60. Handley AJ, Adlard ER (2001) Gas Chromatographic Techniques and Applications. Sheffield Academic Press,

61. Günzler H, Williams A (2001) Handbook of analytical techniques. vol v. 2. Wiley-VCH,

62. Hoffmann E, Stroobant V (2007) Mass spectrometry: principles and applications. J. Wiley,

63. Jennings W (2012) Analytical Gas Chromatography. Elsevier Science,

64. Kolb B, Ettre LS (2006) Static Headspace-Gas Chromatography: Theory and Practice. Wiley,

65. Message GM (1984) Practical aspects of gas chromatography/mass spectrometry. Wiley,

66. Technologies A Thermal Separation Probe (TSP) Training.

67. Eiceman GA, Karpas Z (2005) Ion Mobility Spectrometry. 2nd edn. CRC Press, Boca Raton

68. PNNL (2010). http://www.technet.pnl.gov/sensors/chemical/projects/ES4_IMS.stm. Accessed Oct 3rd, 2010

69. Magin DF (1979) Variable All-glass Effluent Splitter for Dual-detector Operation and Collection of GC Fractions. Industrial Research & Development 21 (10):C6-+

70. Eiceman GA, Nazarov EG, Stone JA (2003) Chemical standards in ion mobility spectrometry. Anal Chim Acta 493 (2):185-194

71. Perr JM, Furton KG, Almirall JR (2005) Solid phase microextraction ion mobility spectrometer interface for explosive and taggant detection. J Sep Sci 28 (2):177-183. doi:10.1002/jssc.200401893

72. Pawliszyn J, Chemistry RSo (1999) Applications of Solid-phase Microextraction. Royal Soc. of Chemistry,

73. McComb ME, Oleschuk RD, Giller E, Gesser HD (1997) Microextraction of volatile organic compounds using the inside needle capillary adsorption trap (INCAT) device. Talanta 44 (11):2137-2143. doi:http://dx.doi.org/10.1016/S0039-9140(97)00093-3

74. Harger RN, Bridwell EG, Raney BB An aerometric method for the rapid determination of alcohol in water and body fluids. In: Am. Soc. Biol. Chem. , 1939.

75. Bovijn L, Pirotte J, Berger A Determination of Hydrogen in water by means of Gas Chromatography. In: Gas Chromatography Symposium, Amsterdam, 1958. Butterworths, London,

76. Arthur CL, Pawliszyn J (1990) Solid phase microextraction with thermal desorption using fused silica optical fibers. Anal Chem 62 (19):2145-2148. doi:10.1021/ac00218a019

77. Zlatkis A, Lichtenstein HA, Tishbee A (1973) Concentration and analysis of trace volatile organics in gases and biological fluids with a new solid adsorbent. Chromatographia 6 (2):67-70. doi:10.1007/bf02270540

78. Theis AL, Waldack AJ, Hansen SM, Jeannot MA (2001) Headspace Solvent Microextraction. Anal Chem 73 (23):5651-5654. doi:10.1021/ac015569c

79. Guerra P, Lai H, Almirall JR (2008) Analysis of the volatile chemical markers of explosives using novel solid phase microextraction coupled to ion mobility spectrometry. J Sep Sci 31 (15):2891-2898. doi:10.1002/jssc.200800171

80. Pawliszyn J (1999) Applications of solid phase microextraction. Royal Society of Chemistry,

81. Koning S, Janssen H-G, Brinkman UT (2009) Modern Methods of Sample Preparation for GC Analysis. Chromatographia 69 (1):33-78. doi:10.1365/s10337-008-0937-3

82. Urbanowicz M, Zabiegała B, Namieśnik J (2011) Solventless sample preparation techniques based on solid- and vapour-phase extraction. Anal Bioanal Chem 399 (1):277-300. doi:10.1007/s00216-010-4296-1

83. Musshoff F, Lachenmeier DW, Kroener L, Madea B (2002) Automated headspace solid-phase dynamic extraction for the determination of amphetamines and synthetic designer drugs in hair samples. J Chromatogr A 958 (1–2):231-238. doi:http://dx.doi.org/10.1016/S0021-9673(02)00317-5

84. Joshi M, Delgado Y, Guerra P, Lai H, Almirall JR (2009) Detection of odor signatures of smokeless powders using solid phase microextraction coupled to an ion mobility spectrometer. Forensic Sci Int 192 (1-3):135-135

85. Joshi M, Rigsby K, Almirall JR (2011) Analysis of the headspace composition of smokeless powders using GC-MS, GC-[mu]ECD and ion mobility spectrometry. Forensic Sci Int 208 (1-3):29-36. doi:DOI: 10.1016/j.forsciint.2010.10.024

86. Stott WR, Nacson S, Eustatiu GI (2006) Chemical identification of peroxide-based explosives.

87. Oxley JC, Smith JL, Kirschenbaum LJ, Marimganti S, Vadlamannati S (2008) Detection of explosives in hair using ion mobility spectrometry. J Forensic Sci 53 (3):690-693. doi:10.1111/j.1556-4029.2008.00719.x

88. Buttigieg GA, Knight AK, Denson S, Pommier C, Bonner Denton M (2003) Characterization of the explosive triacetone triperoxide and detection by ion mobility spectrometry. Forensic Sci Int 135 (1):53-59. doi:Doi: 10.1016/s0379-0738(03)00175-0

89. Marr AJ, Groves DM (2003) Ion mobility spectrometry of peroxide explosives TATP and HMTD. International Journal for Ion Mobility Spectrometry 6 (2):59-62

90. Ewing RG, Waltman MJ, Atkinson DA (2011) Characterization of Triacetone Triperoxide by Ion Mobility Spectrometry and Mass Spectrometry Following Atmospheric Pressure Chemical Ionization. Anal Chem:null-null. doi:10.1021/ac200466v

91. Technologies A Capillary Flow Technology - Splitter.

92. Mózes G (1983) Paraffin Products. Elsevier Science,

93. Sun Y (2010) Field Detection Technologies for Explosives. ILM Publications,

94. Perr J (2005) Improved sampling and detection of ignitable liquid residues and explosives by mass spectrometry and ion mobility spectrometry. Florida International University, Miami, FL

95. Oxley JC, Smith JL, Brady JE, Brown AC (2012) Characterization and analysis of tetranitrate esters. Propellants Explos Pyrotech 37 (1):24-39

96. Meyer R, Köhler J, Homburg A (2008) Explosives. Wiley,

97. Jenkins TF, Leggett DC, Ranney TA (1999) Vapor Signatures from Military Explosives. Part 1. Vapor Transport from Buried Military-Grade TNT. DTIC Document,

98. Lai H, Corbin I, Almirall J (2008) Headspace sampling and detection of cocaine, MDMA, and marijuana via volatile markers in the presence of potential interferences by solid phase microextraction–ion mobility spectrometry (SPME-IMS). Anal Bioanal Chem 392 (1):105-113. doi:10.1007/s00216-008-2229-z

99. Furton KG, Hong Y-c, Hsu Y-L, Luo T, Rose S, Walton J (2002) Identification of Odor Signature Chemicals in Cocaine Using Solid-Phase Microextraction-Gas Chromatography and Detector-Dog Response to Isolated Compounds Spiked on U.S. Paper Currency. J Chromatogr Sci 40 (3):147-155. doi:10.1093/chromsci/40.3.147

100. Vu D, Nicholas P, Erikson C (2010) Characterization of Volatiles Using Solid-Phase Microextraction/Gas Chromatography-Mass Spectrometry (SPME/GC-MS). US Customs and Border Protection, Laboratory Bulletin 10 (1)

101. Macias MS (2009) The development of an optimized system of narcotic and explosive contraband mimics for calibration and training of biological detectors.

102. Clement RE, Siu KWM, Hill HH (1992) Instrumentation for Trace Organic Monitoring. Lewis Publishers,

103. Hood L, Dames M, Barry G (1973) Headspace volatiles of marijuana.

104. Čepelak I, Dodig S (2007) Exhaled breath condensate: a new method for lung disease diagnosis. Clinical Chemistry & Laboratory Medicine 45 (8):945-952. doi:10.1515/cclm.2007.326

105. Gary WH, Raed AD (2008) Applied breath analysis: an overview of the challenges and opportunities in developing and testing sensor technology for human health monitoring in aerospace and clinical applications. Journal of Breath Research 2 (3):037020

106. Hopkin K (1998) Understanding Cystic Fibrosis. University Press of Mississippi,

107. Scott-Thomas A, Syhre M, Pattemore P, Epton M, Laing R, Pearson J, Chambers S (2010) 2-Aminoacetophenone as a potential breath biomarker for Pseudomonas aeruginosa in the cystic fibrosis lung. BMC Pulmonary Medicine 10 (1):56

108. Horsley A, Cunningham S, Innes A (2010) Cystic Fibrosis. Oxford University Press,

109. Orenstein DM, Spahr JE, Weiner DJ (2012) Cystic Fibrosis: A Guide for Patient and Family. Wolters Kluwer Health,

110. Groenewold GS, Scott JR, Rae C (2011) Recovery of phosphonate surface contaminants from glass using a simple vacuum extractor with a solid-phase microextraction fiber. Anal Chim Acta 697 (1-2):38-47. doi:10.1016/j.aca.2011.04.034

111. Savelev SU, Perry JD, Bourke SJ, Jary H, Taylor R, Fisher AJ, Corris PA, Petrie M, De Soyza A (2011) Volatile biomarkers of Pseudomonas aeruginosa in cystic fibrosis and noncystic fibrosis bronchiectasis. Lett Appl Microbiol 52 (6):610-613. doi:10.1111/j.1472-765X.2011.03049.x

112. Francis JG, Cyrus R, Webb AK, Andrew MJ, Patrik Š, David S, Warren L (2012) An investigation of suitable bag materials for the collection and storage of breath samples containing hydrogen cyanide. Journal of Breath Research 6 (3):036004

113. Stover CK, Pham XQ, Erwin AL, Mizoguchi SD, Warrener P, Hickey MJ, Brinkman FSL, Hufnagle WO, Kowalik DJ, Lagrou M, Garber RL, Goltry L, Tolentino E, Westbrock-Wadman S, Yuan Y, Brody LL, Coulter SN, Folger KR, Kas A, Larbig K, Lim R, Smith K, Spencer D, Wong GKS, Wu Z, Paulsen IT, Reizer J, Saier MH, Hancock REW, Lory S, Olson MV (2000) Complete genome sequence of Pseudomonas aeruginosa PAO1, an opportunistic pathogen. Nature 406 (6799):959-964

114. Balasubramanian D, Schneper L, Merighi M, Smith R, Narasimhan G, Lory S, Mathee K (2012) The Regulatory Repertoire of Pseudomonas aeruginosa AmpC beta-Lactamase Regulator AmpR Includes Virulence Genes. PLoS ONE 7 (3). doi:e34067

10.1371/journal.pone.0034067

115. Mathee K, Ciofu O, Sternberg C, Lindum PW, Campbell JIA, Jensen P, Johnsen AH, Givskov M, Ohman DE, Molin S, Hoiby N, Kharazmi A (1999) Mucoid conversion of Pseudomonas aeruginosa by hydrogen peroxide: a mechanism for virulence activation in the cystic fibrosis lung. Microbiology-Sgm 145:1349-1357

116. McClean KH, Winson MK, Fish L, Taylor A, Chhabra SR, Camara M, Daykin M, Lamb JH, Swift S, Bycroft BW, Stewart G, Williams P (1997) Quorum sensing and Chromobacterium violaceum: exploitation of violacein production and inhibition for the detection of N-acylhomoserine lactones. Microbiology-Uk 143:3703-3711

Appendices

Copyright clearance from Journal of Analytical and Bioanalytical Chemistry

SPRINGER LICENSE
TERMS AND CONDITIONS
Oct 07, 2013

This is a License Agreement between Wen Fan ("You") and Springer ("Springer") provided by Copyright Clearance Center ("CCC"). The license consists of your order details, the terms and conditions provided by Springer, and the payment terms and conditions.

All payments must be made in full to CCC. For payment instructions, please see information listed at the bottom of this form.

License Number	3243680151016
License date	Oct 07, 2013
Licensed content publisher	Springer
Licensed content publication	Analytical and Bioanalytical Chemistry
Licensed content title	Fast detection of triacetone triperoxide (TATP) from headspace using planar solid-phase microextraction (PSPME) coupled to an IMS detector
Licensed content author	Wen Fan
Licensed content date	Jan 1, 2012
Volume number	403
Issue number	2
Type of Use	Thesis/Dissertation
Portion	Full text
Number of copies	1
Author of this Springer article	Yes and you are the sole author of the new work
Order reference number	
Title of your thesis / dissertation	IMPROVED DYNAMIC HEADSPACE SAMPLING AND DETECTION USING CAPILLARY MICROEXTRACTION OF VOLATILES COUPLED TO GAS CHROMATOGRAPHY MASS SPECTROMETRY
Expected completion date	Dec 2013
Estimated size(pages)	230

Total 0.00 USD

Terms and Conditions

Introduction
The publisher for this copyrighted material is Springer Science + Business Media. By clicking "accept" in connection with completing this licensing transaction, you agree that the following terms and conditions apply to this transaction (along with the Billing and Payment terms and conditions established by Copyright Clearance Center, Inc. ("CCC"), at the time that you opened your Rightslink account and that are available at any time at http://myaccount.copyright.com).

Limited License
With reference to your request to reprint in your thesis material on which Springer Science and Business Media control the copyright, permission is granted, free of charge, for the use indicated in your enquiry.

Licenses are for one-time use only with a maximum distribution equal to the number that you identified in the licensing process.

This License includes use in an electronic form, provided its password protected or on the university's intranet or repository, including UMI (according to the definition at the Sherpa website: http://www.sherpa.ac.uk/romeo/). For any other electronic use, please contact Springer at (permissions.dordrecht@springer.com or permissions.heidelberg@springer.com).

The material can only be used for the purpose of defending your thesis, and with a maximum of 100 extra copies in paper.

Although Springer holds copyright to the material and is entitled to negotiate on rights, this license is only valid, subject to a courtesy information to the author (address is given with the article/chapter) and provided it concerns original material which does not carry references to other sources (if material in question appears with credit to another source, authorization from that source is required as well).

Copyright clearance from Journal of Analytical and Bioanalytical Chemistry

SPRINGER LICENSE
TERMS AND CONDITIONS
Nov 08, 2013

This is a License Agreement between Wen Fan ("You") and Springer ("Springer") provided by Copyright Clearance Center ("CCC"). The license consists of your order details, the terms and conditions provided by Springer, and the payment terms and conditions.

All payments must be made in full to CCC. For payment instructions, please see information listed at the bottom of this form.

License Number	32644630246458
License date	Nov 08, 2013
Licensed content publisher	Springer
Licensed content publication	Analytical and Bioanalytical Chemistry
Licensed content title	High-efficiency headspace sampling of volatile organic compounds in explosives using capillary microextraction of volatiles (CMV) coupled to gas chromatography-mass spectrometry (GC-MS)
Licensed content author	Wen Fan
Licensed content date	Jan 1, 2013
Type of Use	Thesis/Dissertation
Portion	Full text
Number of copies	1
Author of this Springer article	Yes and you are the sole author of the new work
Order reference number	
Title of your thesis / dissertation	IMPROVED DYNAMIC HEADSPACE SAMPLING AND DETECTION USING CAPILLARY MICROEXTRACTION OF VOLATILES COUPLED TO GAS CHROMATOGRAPHY MASS SPECTROMETRY
Expected completion date	Dec 2013
Estimated size(pages)	230
Total	0.00 USD

Terms and Conditions

Introduction

The publisher for this copyrighted material is Springer Science + Business Media. By

clicking "accept" in connection with completing this licensing transaction, you agree that the following terms and conditions apply to this transaction (along with the Billing and Payment terms and conditions established by Copyright Clearance Center, Inc. ("CCC"), at the time that you opened your Rightslink account and that are available at any time at http://myaccount.copyright.com).

Limited License
With reference to your request to reprint in your thesis material on which Springer Science and Business Media control the copyright, permission is granted, free of charge, for the use indicated in your enquiry.

Licenses are for one-time use only with a maximum distribution equal to the number that you identified in the licensing process.

This License includes use in an electronic form, provided its password protected or on the university's intranet or repository, including UMI (according to the definition at the Sherpa website: http://www.sherpa.ac.uk/romeo/). For any other electronic use, please contact Springer at (permissions.dordrecht@springer.com or permissions.heidelberg@springer.com).

The material can only be used for the purpose of defending your thesis, and with a maximum of 100 extra copies in paper.

Although Springer holds copyright to the material and is entitled to negotiate on rights, this license is only valid, subject to a courtesy information to the author (address is given with the article/chapter) and provided it concerns original material which does not carry references to other sources (if material in question appears with credit to another source, authorization from that source is required as well).

VITA

WEN FAN

Born, Harbin, Heilongjiang, China

2005-2008	B.S., Honors Program (Life Science) China Agricultural University Beijing, China
2008-2009	Technician Research Assistant National Institute of Biological Sciences, Beijing Beijing, China

PUBLICATIONS

Fan, W.; Young, M.; Canino, J.; Smith, J.; Oxley, J.; Almirall, J., Fast detection of triacetone triperoxide (TATP) from headspace using planar solid-phase microextraction (PSPME) coupled to an IMS detector. Anal. Bioanal. Chem. 2012, 403 (2), 401-408.

Fan, W.; Almirall, J., High Efficiency Headspace Sampling of Volatile Organic Compounds in Explosives Using Capillary Microextraction of Volatiles (CMV) Coupled to Gas Chromatography – Mass Spectrometry (GC-MS). Anal. Bioanal. Chem. 2013 (Accepted)

PRESENTATIONS

Wen Fan, Mimy Young and Jose Almirall, Fast Detection of Peroxide Explosives Using Planar Solid Phase Microextraction (PSPME) Coupled to Ion Mobility Spectrometers (IMS), 2013 Florida International University Scholarly Forum, Miami, FL, Mar 2013

Wen Fan, Mimy Young and Jose Almirall, Fast Detection of Peroxide Explosives Using Planar Solid Phase Microextraction (PSPME) Coupled to Ion Mobility Spectrometers (IMS), Second Annual Forensic Science Symposium, Miami, FL, Mar 2013

Wen Fan, Mimy Young and Jose Almirall, Fast Detection of Peroxide Explosives Using Planar Solid Phase Microextraction (PSPME) Coupled to Ion Mobility Spectrometers (IMS), International Society of Ion Mobility Spectrometry Conference, Orlando, FL, July 2012

Wen Fan, Mimy Young and Jose Almirall, Headspace Profiling of Volatile Compounds from Explosives Using Planar Solid Phase Microextraction (PSPME) Followed by Ion Mobility Spectrometer (IMS) Detection , 2012 Florida International University Scholarly Forum, Feb 2012

Mimy Young, Wen Fan and Jose Almirall, Analysis of Gunshot Residue (GSR) from Discharged Firearms by Laser Induced Breakdown Spectroscopy (LIBS), NASLIBS, Clearwater, FL, Aug 2011

Wen Fan, Mimy Young and Jose Almirall, Headspace Profiling of Volatile Compounds from Explosives Using Planar Solid Phase Microextraction (PSPME) Followed by Ion Mobility Spectrometer (IMS) Detection, Gordon Research Conferences, Lucca, Italy, Jun 2011

Mimy Young, Wen Fan and Jose Almirall, Detection of Explosives in Large Volumes Using Planar Solid Phase Microextraction (PSPME) Followed by IMS, International Society of Ion Mobility Spectrometry Conference, Albuquerque, NM, Jul 2010

PATENT

Capillary Microextration of Volatiles (CMV), Serial No. 61/779,690, submitted Mar 13, 2013

AWARDS

Dissertation Evidence Acquisition Fellowship, summer 2013

3rd place in oral presentation in Forensics and Crime at 2013 Florida International University Scholarly Forum

2nd place in poster presentation in Physics, Chemistry, and Biochemistry at 2012 Florida International University Scholarly Forum

Presidential Fellowship, 2009-2012

PROFESSIONAL DEVELOPMENTS

SBIR/STTR Phase I Proposal Preparation Workshop, Miami, FL, Feb 2013

Workshop on Fundamentals of Explosives, Kingston, RI, May 2012

Short Course on Ion Mobility Spectrometry, Albuquerque, NM, Jul 2010

ACTIVITIES

Treasurer of Chemistry Graduate Student Organization at Florida International University, 2010-2011

President of Chemistry Graduate Student Organization at Florida International University, 2012-2013